Radiofluorinations in Homo- and Heteroaromatic Systems with Application in Two New Types of Metabolic PET-Tracers

DISSERTATION

der Mathematisch-Naturwissenschaftlichen Fakultät
der Eberhard Karls Universität Tübingen

zur Erlangung des Grades eines
Doktors der Naturwissenschaften
(Dr. rer. nat.)

vorgelegt von

Noeen Malik
aus Sargodha (Pakistan)

Tübingen
2011

Diese Arbeit wurde im Zeitraum von April 2008 bis Mai 2011 in den Abteilungen für Radiopharmazie des Universitätsklinikums der Eberhard-Karls-Universität Tübingen sowie des Universitätsklinikums Ulm unter Anleitung von **Herrn Prof. Dr. H.-J. Machulla** durchgeführt.

Acknowledgements

First of all, praise is to *Almighty Allah* for granting me His blessings as well as strength and firm determination to pursue this project successfully. Then, I would like to express my sincere gratitude to my supervisors **Prof. Dr. Wolfgang Voelter** and **Prof. Dr. Hans-Jürgen Machulla** to whom I am deeply indebted because of their stimulating suggestions, continuous encouragement, extensive motivation, and at last but not the least, their trust in my abilities to complete the project. It was indeed an honour and privilege to have such supervisors.

Particularly, among many other people, I would like to warmly acknowledge Dr. Sven N Reske, Dr. Christoph Solbach and Dr. Gerald Resichl for their vital scientific assistance and systematic guidance through all stages of my work. I am also grateful to Higher Education Pakistan (HEC, Pakistan)- Deutscher Akademischer Austausch Dienst (DAAD, Germany) for providing me this golden opportunity to study abroad on scholarship and thereby, giving me an invaluable chance to learn new developments in science and technology.

A very special recognition needs to be given to Bettina Mahren, Jens Bertram, Anette Warkentin, Dr. Almut Walte, Wolfgang Scheel, Felix Arndt, and Mathias Fiebig for the daily production of $[^{18}F]$fluoride and technical support. Along with, I am thankful to Bin Shen, Dirk Löffler, Ehab Al Momani, Gordon Winter, and Sophie Schneefeld for being very friendly and thus, creating a very pleasant and healthy atmosphere to work in. I would also like to convey my gratitude and love for my dear friends as they have never made me feel lonely.

In addition, I am extremely obliged to my mother, aiman, and hamza for their unconditional love, pure affection, and enormous moral support throughout my life and beyond.

To My Mother

Rizwana Yasmin

Zusammenfassung

Fluor-18 ($T_{1/2}$ = 110 min) ist an medizinischen Zyklotrons einfach und in sehr hohen Ausbeuten ohne Träger-Zusatz, d.h. praktisch ohne Isotopen-Verdünnung durch Fluor-19, herstellbar. Daher können [^{18}F]-markierte Tracer in hohen spezifischen Aktivitäten synthetisiert werden. Die Konzentrationen können im nano- bis picomolaren Bereich liegen und ermöglichen somit PET-Messungen im Körper, so dass Stoffechselprozesse praktisch ohne konzentrationsbedingte Veränderungen *in vivo* untersuchbar sind.

Aromatische [^{18}F]-Aminosäuren wie [^{18}F]Tyrosin oder [^{18}F]DOPA werden seit langem klinisch als PET-Tracer angewandt, können jedoch über elektrophile Radiofluorierungen verfahrensbedingt nur in niedrigen Aktivitätsmengen und geringen spezifischen Aktivitäten hergestellt werden. Ein Verfahren zur einfachen nukleophilen [^{18}F]-Fluorierung direkt am Benzolring existiert bisher nicht. Bei der betreffenden Verbindungsgruppe handelt es sich um elektronenreiche Aromaten, die einer nukleophilen Substitution (S_NAr) nicht unmittelbar zugänglich sind. Im Gegensatz zur „klassischen" organischen Chemie fehlten grundlegende Arbeiten zu S_NAr, so dass wir in Tübingen mit entsprechenden Untersuchungen vor einigen Jahren begonnen hatten. Diese Arbeiten werden im Grundlagenteil dieser Dissertation an substituierten Benzolen weitergeführt und auf Pyridine ausgedehnt. Im zweiten Teil sind Radiosynthesen für zwei neue [^{18}F]-Verbindungen als PET-Tracer für hypoxisches Tumorgewebe sowie als PSMA-Ligand für Prostata-Tumore mit neuartigen radiopharmazeutischen Konzepten entwickelt worden.

Zur Realisierung von S_NAr in elektronenreichen Aromaten sind elektronenziehende Substituenten notwendig. Bisher war die Substitution der quaternären Ammoniumgruppe praktisch nicht untersucht, lediglich war in dem Reaktionssystem die Bildung von [^{18}F]CH$_3$ als dominierende Nebenreaktion bekannt. Die Experimente an verschieden substituierten Benzaldehyden zeigen keine Nebenreaktion und auch hohe radiochemische Ausbeuten, wenn die quaternäre Ammoniumgruppe in *ortho* Position lokalisiert ist. Erwartungsgemäß entsprechen Substitutionsausbeuten im übrigen denjenigen der Nitrogruppe. Für [^{18}F]-Markierungsstrategien bietet die quaternäre Ammoniumgruppe jedoch den in der Praxis wichtigen Vorteil der schnellen und effizienten Abtrennung vom [^{18}F]-Produkt.

Die grundlegenden Arbeiten zur S_NAr mittels [^{18}F]-Fluorid wurden auf Pyridine ausgedehnt, und führten u.a. zum prinzipiellen Resultat, dass [^{18}F]-Pyridin-Derivate als Surrogate für Benzol bzw. als prosthetische Gruppe z.B. zur [^{18}F]-Markierung geeignet sind. In Hinblick auf [^{18}F]-Markierungsreaktionen ist es von großer Bedeutung, dass die S_NAr an Pyridinderivaten in der Regel mit Ausbeuten von über 80% verläuft und im Gegensatz zu den korrespondierenden Benzolderivaten die Effekte von +M-Substituenten deutlich schwächer ausgeprägt sind. Die z.T. unerwarteten Ergebnisse der Dissertation liefern substantielle Informationen zu weitergehenden systematischen Anwendungen in der Entwicklung neuartiger Radiopharmaka für die *Molekulare Bildgebung*.

Abstract

[^{18}F]fluoride is easily produced at medical cyclotrons in very high yields and without addition of carrier. Therefore, [^{18}F]-labelled tracers can be synthesized with high specific activities. Although aromatic amino acids such as 6-[^{18}F]fluoro-L-DOPA, 2-[^{18}F]Fluoro-L-tyrosine and 6-[^{18}F]fluorophenylalanine are clinically well accepted since quite a while, yet easy and efficient radiofluorinations at benzene ring are still remained to be highly desirable. Since such amino acids possess electron rich aromatic ring, [^{18}F]-labelling by S_NAr has to be facilitated by means of an auxiliary group (EWG) that must be removed at EOS. However, in order to eliminate this additional step, an interesting alternative is the use of substituted pyridines in which nitrogen atom acts as an electron-withdrawing group (EWG).

In present study, the rate of radiofluorinations in various substituted pyridines was studied. When compared to 2-nitrobenzaldehyde, the labelling yield of 2-nitropyridine (84±3%, 20 min) was almost similar to that of 2-nitrobenzaldehyde (83±1%, 20 min) at 140°C. In addition, [^{18}F]-labelling reactions were also carried out in pyridines substituted in *ortho* position by electron-donating groups such as –CH$_3$ and –OCH$_3$. It was observed that pyridines having –NO$_2$ as a leaving group showed almost 90% RCYs at all temperatures (140°C to 60°C) irrespective of being substituted by –OCH$_3$ or –CH$_3$ groups in *ortho* position. Energies of activations (E$_a$) were calculated for the substituted 2-nitropyridines. In case of all compounds, energies of activation were found in the range of 4-25 kJ / mol. Contrary to 2-nitrobezaldehyde (24 kJ / mol) and nitrobenzene (63.5 kJ / mol), E$_a$ for 2-nitropyridine was clearly lower (6.5 kJ / mol).

Another important aspect in [^{18}F]-labelling is the protection of –OH. For this, the hydrolysis of new substituted benzyloxy protected groups for hydroxyl was carried out by acidic as well as catalytic transfer hydrogenation. Time and temperature dependent analysis showed that 2,4-dimethyl benzyl and *p*-xylyl groups can be easily cleaved at 120°C within 10 min after hydrolysis with 32% HCl by giving almost 80% RCYs. In addition, *p*-xylyl was hydrolysed under mild conditions with ca 75% of RCY at 70°C at 10 min by using ammonium formate as a hydrogenating reagent.

[^{18}F]-labelling was carried out in order to develope the new precursors for PET-imaging of hypoxia ([^{18}F]FNT) and prostate cancer ([^{18}F]FPy-DUPA-Pep). Hypoxia radiotracer ([^{18}F]FNT) is a new compound that can utilize the amino acid transporter system to enter the hypoxic tissues and hence, its uptake can be expectedly enhanced for PET imaging. At EOS, 40±1% (decay uncorrected) of [^{18}F]FNT was synthesized with radiochemical purity of > 98% within 90 min. For radiosynthesis *via* S_NAr of a PSMA (prostate-specific membrane antigen) targeting ligand ([^{18}F]Py-DUPA-Pep), the method involves one step radiosynthesis of prosthetic group [(^{18}F)FPy-TFP] itself and one step for coupling with peptide. At the end of synthesis, 48±0.9% (decay uncorrected) of [^{18}F]FPy-DUPA-Pep was synthesised with radiochemical purity of > 98% within 50 min. Hence, an efficient method of radiosynthesis for [^{18}F]FNT and [^{18}F]FPy-DUPA-Pep has been developed. Thus, both of these radiotracers can be used for PET imaging in clinical applications.

IV

Contents

VI

Abbreviations

3-D	Three dimensional
$\boldsymbol{\beta^{-}}$	Beta minus (electron emission)
$\boldsymbol{\beta^{+}}$	Beta plus (Positron emission)
δ	Chemical shift (ppm)
χ	Electronegativity (chi)
μ	micro
$\boldsymbol{e^{+}}$	Positron
γ-rays	Gamma rays
$\boldsymbol{\bar{\nu}}$	Wave number
A°	Angstrom (10^{-10} meter)
AcOH	Acetic acid
ACPI	Advanced configuration and power interface (LC/MS)
ca	Circa
c.a.	Carrier-added
CDCl$_3$	Deuterium chloroform
1,4-CHD	1,4-Cyclohexadiene
CT	Computed tomography
d	Doublet (NMR spectra)
DAST	Diethylaminosulfur trifluoride
DCM	Dichloromethane
DEAD	Diethyl azodicarboxylate
DEE	Diethylether
DMF	*N,N*-Dimethylformamide
DMSO	Dimethylsulfoxide
DMSO-d$_6$	Deuterium dimethylsulfoxide
DNA	Deoxyribonucleic acid
DUPA	2-[3-(1,3-dicarboxypropyl)ureido]pentanedioic acid
E$_a$	Energy of activation
EDG	Electron-donating group
EOS	End of synthesis
EtOAc	Ethylacetate
EtOH	Ethanol
EWG	Electron-withdrawing group
FAB	Fast atomic bombardment (mass spectroscopy)
[^{18}F]FAMT	[^{18}F]fluoro-α-methyltyrosine
[^{18}F]FAZA	[^{18}F]Fluoroazomycin arabinoside
[^{18}F]FET	[^{18}F]fluoroethyltyrosine
[^{18}F]FDG	3,4-dihydroxy-6-[^{18}F]Fluoro-L-phenylalanine
6-[^{18}F]fluoro-L-DOPA	6-[^{18}F]fluoro-L-DOPA
[^{18}F]FLT	3'-[^{18}F]Fluoro-3'-deoxythymidine
[^{18}F]F-m-Tyr	6-[^{18}F]fluoro-*m*-tyrosine
[^{18}F]FMISO	[^{18}F]Fluoromisonidazole
[^{18}F]FTyr	2-[^{18}F]Fluoro-L-tyrosine
[^{18}F]SFB	*N*-succinimidyl 4-[^{18}F]fluorobenzoate
h	Hour
Hist	Histidine
HPLC	High pressure liquid chromatography

HRMS	High resolution mass spectroscopy
I+	Inductive effect
i-PrOH	iso-Propanol
IR	Infrared spectroscopy
J	Coupling constant (NMR spectra)
J/K mol	Joule per Kelvin per mol
k'	rate constants, min^{-1}
k´	Selectivity (HPLC)
K_d	Dissociation constant
kcal	killocalorie
keV	killoelectronvolt
K222 (kryptofix-222)	4,7,13,21,24-hexaoxa-1, 10-diazabicyclo[8.8.8]-hexacosane
LAT	Large neutral amino acid transporter
LC/MS	Liquid chromatography mass spectroscopy
Leu	Leucine
LG	Leaving group
LNCaP	Prostate cancer cell line
M+	Mesomeric effect
MBq	Megabecquerel
MeCN	Acetonitrile
MeI	Iodomethane
MeOH	Methanol
Met	Methionine
MeV	Megaelectronvolt
m	Multiplet (NMR spectra)
mCi	millicurie (radiation)
MHz	Megahertz
min	Minute
m.p.	Melting point (°C)
MPLC	Middle pressure liquid chromatography
MRI	Magnetic resonance imaging
MRT	Magnetic resonance tomography
MS-EI	Mass spectroscopy-Electron impact
m/z	Mass to charge ratio (mass spectra)
NADPH	Nicotinamide adenine dinucleotide phosphate
NaOMe	Sodium methoxide
n.c.a.	No-carrier-added
NOTA	1,4,7-Triazacyclononane-*N*,*N'*,*N''*-triacetic acid
NMR	Nuclear magnetic resonance
ODS	Octadecyl silane
OI	Optical imaging
OTsCl	*p*-Tosylchloride
PBS	Phosphate buffer saline
PCC	Pyridinium chlorochromate
Pd	Palladium
PE	Petroleum ether
PET	Positron emission tomography
pg	picogram

Ph	Phenyl
Phe	Phenylalanine
pmol	picomol
ppm	Parts per million
PSMA	Prostate-specific membrane antigen
PTC	Phase transfer catalyst
R^2	Regression coefficient
R_f	Retention factor (TLC)
R_t	Retention time (HPLC)
RCYs	Radiochemical yields
RNA	Ribonucleic acid
RT	Room Temperature
s	Singlet
S_NAr	Nucleophilic aromatic substitution reaction
SD	Standard deviation
SPECT	Single photon emission computed tomography
t	Triplet (NMR spectra)
$TBA-HCO_3$	Tetrabutylammonium hydrogen carbonate
TFA	Trifluoroacetic acid
2TFP-Py	2,3,5,6-Tetrafluorophenyl-6-(2,3,5,6-tetrafluoriphenoxy)nicotinate
THF	Tetrahydrofuran
TIS	Triisopropyl silane
TLC	Thin layer chromatography
TMA	Trimethylammonium
TOF	Time of flight
Trp	Tryptophan
UI	Ultrasouund imaging
UV	Ultraviolet
Val	Valine

1. INTRODUCTION

1.1 Radiopharmacy

Radiopharmacy is the area handling the methods and procedures for development, research and production of tracers to be used as radiopharmaceuticals in clinical applications. Those tracers mainly are biological compounds labelled with an appropriate radionuclide allowing to study physiological and biochemical processes directly within the body. Those radionuclides emit γ-radiation penetrating the body barrier and, for probing, nuclear medical imaging techniques such as Single Photon Emission Computed Tomography (SPECT) and Positron Emission Tomography (PET) can be applied in clinical diagnostics. In principle, it is a really unique feature of PET to assess metabolic functions in a selective and even quantitative way as turnover rates of the metabolic pathway of interest can be determined *in vivo*. Moreover, the concentrations of a tracer applied in diagnostic application are in the range of a few μmoles and picomoles so that metabolic processes remain unchanged.

This diagnostic approach was first published by George Hevesy in 1924 and was termed as the *"tracer method"*. Therein, he applied this method for studying absorption, distribution and elimination of bismuth in rabbits[1]. In 1943, he was awarded the Nobel Prize for his remarkably important contribution to medicine. Since then, his method is one of the essential tools in medical research. Interestingly, within the past ten years, PET-applications of tracers as radiopharmaceuticals received a particular enhancement by a fast technological development of the different imaging modalities such as Ultrasouund Imaging (UI), Computed Tomography (CT), Magnetic Resonance Tomography (MRT or MRI), Optical Imaging (OI), and SPECT and PET[2] both of which are combined with CT as hybrid scanning systems.

Principally, the PET system detects the pairs of gamma rays (γ-rays) emitted indirectly by a positron-emitting radionuclide (Table 1-1)[3-4] incorporated in the tracer. Afterwards, the images reflecting the tracer concentrations in different tissues in the 3-dimensional space within the body are reconstructed by computer programmes with suitable algorithms.

In order to conduct a scan, a short-lived radioactive tracer is injected into the living subject and a registration of the tracer concentration is made as the radioactive tracer decays. In case of a positron decay (positive beta decay), the radioisotope emits a positron (e^+) which travels in the tissue for a short distance of a few millimeters or centimeters, during which it loses its kinetic energy, and interacts with an electron forming the positronium (β^+)[5-9]. This encounter annihilates by producing a pair of photons of 511 keV moving in opposite directions (180°). The detection of these γ-rays is carried out by PET that consists of a circular arrangement of scintillation detectors. In these rings of detectors, pairs of opposite detectors are connected for coincidence measurements. As a result, the two γ-rays of the annihilation process hit both of the opposite detectors and are detected within the time frame of a few nanoseconds. Thus, a burst of light is created that is detected by photomultiplier tubes.

The visual field is defined by the central area covered by areas of coincidence. Hence, this technique basically depends on the simultaneous i.e. the coincident registration of the pair of photons moving in opposite directions. Alternatively, the time of γ-photons can be measured as it depends on the distance between the point of annihilation and the two opposite detectors i.e. the time of flight (TOF) of γ-photons is registered and, thus, the 3-D information is obtained.
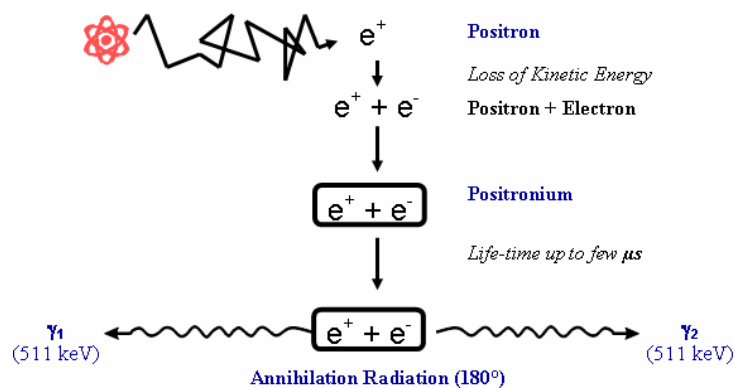
Fig 1.1 Positron emission and annihilation[10]

The most recent development includes PET/MRI[2, 11] for simultaneous registration by both imaging modalities. MRI is known to provide exquisite structural details while PET gives the information about the biochemical process that a radiotracer follows within the body. Due to the instability of photomultipliers within strong magnetic fields of MRI, the PET-technology was developed in a new way by using silicon avalanche photodiode detector that is a highly sensitive semiconductor electronic device having functional analogy to photomultipliers (Fig 1.2)[11].
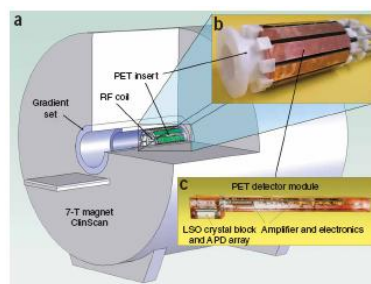
Fig 1.2 Combination of PET/MRI (a) drawing of PET/MR (b) MRI compatibale PET detector modules (c) single PET detector module[11]

Examples of the molecular mechanism underlying PET measurements are receptor binding, metabolism, transport across the cell membrane, and binding to several kinds of macromolecules (DNA, RNA, proteins). Thus, for interesting PET applications, a variety of criteria are to be met generally such as lipophilicity (logP ≤ 1.5-2) and high binding affinity (low K_d) together with a high specificity of the target molecule[12].

1.2 PET Radionuclides

Positron emitting radionuclides are neutron deficient and can only be produced by acceleraters for which the medical cyclotrons are typical examples. The range of the path, in which β-particles lose energy by collisions, is specific for the employed radionuclide. Various PET-radionuclides produced at a cyclotron are shown in Table 1-1.

Table 1-1 Positron emitters[13] used for PET

Nuclide	Half-Life	Decay Mode (%)	$E_{\beta+, max}$ (keV)
^{11}C	20.4 min	β^+ (99.8), EC (0.2)	960
^{13}N	9.96 min	β^+ (100)	1190
^{15}O	2.03 min	β^+ (99.9), EC (0.1)	1720
^{30}P	2.5 min	β^+ (99.8), EC (0.2)	3250
^{18}F	109.6 min	β^+ (97), EC (3)	635
^{75}Br	98 min	β^+ (75.5), EC (24.5)	1740
^{76}Br	16.1 h	β^+ (57), EC (43)	3900
^{73}Se	7.1 h	β^+ (65), EC (35)	1320
^{120}I	1.35 h	β^+ (64), EC (36)	4100
^{124}I	4.18 d	β^+ (25), EC (75)	2140
^{38}K	7.6 min	β^+ (100)	2680
^{55}Co	17.5 h	β^+ (77), EC (23)	1500
^{60}Cu	23.4 min	β^+ (93), EC (7)	3920
^{61}Cu	3.32 h	β^+ (62), EC (38)	1220
^{62}Cu	9.7 min	β^+ (98), EC (2)	2930
^{64}Cu	12.7 h	β^+ (18), β^- (37), EC (45)	655
^{66}Ga	9.45 h	β^+ (57), EC (43)	4153
^{68}Ga	68.3 min	β^+ (90), EC (10)	1900
^{82m}Rb	6.3 h	β^+ (26), EC (74)	780
^{82}Rb	1.3 min	β^+ (96), EC (4)	3350
^{86}Y	14.7 h	β^+ (34), EC (66)	1300
^{83}Sr	32 h	β^+ (24), EC (76)	1150
^{45}Ti	3.1 h	β^+ (86), EC (14)	1040
^{94m}Tc	52 min	β^+ (72), EC (28)	2470
^{72}As	26 h	β^+ (88), EC (12)	2515
^{89}Zr	78.4 h	β^+ (22), EC (78)	900

Among all isotopes of the organic elements, only a very few exist and are characterized by short half-lives. Another important aspect is the fact that very small masses of those radionuclides that are used for the PET registration (Table 1-2)[11].

In PET measurements, 37 MBq to 370 MBq are the typical amounts of radioactivity. The mass can be calculated by the following mass-activity-equation of the radioactive decay, the mass (m) can be calculated for the different radionuclides (Table 1-2).

$$m = \frac{A.w}{\lambda . N_A}$$

In this mass-activity equation:

A = Total radioactivity

w = Atomic weight / Molecular weight

λ = Decay constant

N_A = Avogadro's number, 6.02 x 10^{23}

Half-life ($t_{1/2}$) is calculated from the decay constant (λ):

$$t_{1/2} = \frac{\ln 2}{\lambda}$$

For comparison, ^{14}C is added in Table 1-2 because it is a neutron rich radionuclide and has a long half-life. That emits β^--particles exclusively resulting in a complete absorption within the tissue and, hence, any registration outside the body is not possible by means of the nuclear medical techniques. Moreover, due to the long half-life, the mass of an activity of 37 MBq is equal to 0.224 mg. In contrast, in case of ^{11}C, the activity of 37 MBq gives rise to a mass of only 1.19 pg.

Table 1-2 Radionuclides of the organic elements suited for PET-registration[11]

Element	Radionuclides (Neutron-deficient)	Half-Life	Mass 37 MBq = ?g
O	^{15}O (β^+)	2.03 min	1.62 x 10^{-13} g
N	^{13}N (β^+)	9.96 min	6.9 x 10^{-13} g
C	^{11}C (β^+)	20.4 min	1.19 x 10^{-12} g
P	^{30}P (β^+)	2.5 min	3.97 x 10^{-13} g
H	-	-	-
F for 'H', 'OH'	^{18}F (β^+)	109.6 min	1.05 x 10^{-11} g
For Comparison (Neutron-rich)			
C	^{14}C (β^-)	5730 a	2.24 x 10^{-4} g

1.3 [^{18}F]-Labelled Radiopharmaceuticals

Among all, the remarkability of fluorine-18 as a positron emitter can be attributed to its physical as well as nuclear properties such as its sterically similar size (1.35 A$^{°}$) to hydrogen (1.20 A$^{°}$) and the high electronegative character (χ: 3.98). In addition, the almost complete positron decay (97%, by emission of β^+) and the low energy of the positron [635 keV (maximum), 2.3 mm mean range in matter] are particularly advantageous in terms of resolution of PET-images[12]. It can also be produced reliably in a routine way on a large scale (> 100 GBq), and its relatively long half-life ($t_{1/2}$=109.6 min) opens the possibility that [^{18}F]-radiopharmaceuticals can be synthesized in nuclear medicine facilities without a cyclotron. Moreover, the direct distribution of [^{18}F]-radiopharmaceuticals to the neighbouring PET centers, which do not have a cyclotron, allows the use of PET in the clinical environment. It is important to note that the incorporation of fluorine-18 can enhance the biochemical specificity of the tracer molecule with high sensitivity. This further facilitates the imaging and quantification of a biochemical processes *in vivo*[14-15] (Table 1-3).

Table 1-3 [^{18}F]-labelled PET-tracers interesting for clinical use[14-15]

[^{18}F]-Labelled Radiotracer	Radiosynthesis	Clinical Application
2-Deoxy-2-[^{18}F]fluoro-D-glucose *(2-[^{18}F]FDG)*	Nucleophilic fluorination	Glucose metabolism
3-Deoxy-3-[^{18}F]fluoro-D-glucose *(2-[^{18}F]FDG)*	Nucleophilic fluorination	Glucose transport
6-[^{18}F]FluoroDOPA	Fluorodematallation	Dopamine metabolism
6-[^{18}F]Fluorodopamine	Nucleophilic fluorination	Cardiac sympathetic innervations
2-[^{18}F]Fluoro-L-tyrosine *([^{18}F]FTyr)*	Fluorodestannylation	Dopamine metabolism
6-[^{18}F]Fluoro-L-*m*-tyrosine *([^{18}F]F-m-Tyr)*	Fluorodestannylation	Dopamine metabolism
[^{18}F]Fluoroethyltyrosine *([^{18}F]FET)*	*O*-alkylation with [^{18}F]fluoroethyltosylate	Tumor imaging
[^{18}F]Fluoro-α-methyltyrosine *([^{18}F]FAMT)*	Electrophilic fluorination with [^{18}F]AcOF	Tumor imaging
6-[^{18}F]Fluorophenylalanine	Electrophilic fluorination with [^{18}F]AcOF	Neutral amino acid transport
[^{18}F]Fluoromisoindazole *([^{18}F]FMISO)*	*N*-alkylation with [^{18}F]epifluorohydrin	Hypoxia imaging
1-(5-[^{18}F]Fluoro-5-deoxy-α-D-arabinofuranosyl)-2-nitroimidazole *([^{18}F]FAZA)*	Fluorodetosylation	Hypoxia imaging
3'-deoxy-3'-[^{18}F]Fluorothymidine *([^{18}F]FLT)*	Nucleophilic fluorination	DNA synthesis
[^{18}F]Fluorocholine	Nucleophilic fluorination	Lipid synthesis
[^{18}F]Fluoroacetate	Nucleophilic fluorination	Lipid synthesis
(-)-6-[^{18}F]Fluoronorepinephrine	Nucleophilic fluorination	Cardiac sympathetic innervations
16α-[^{18}F]Fluoro-17ß-estradiol	Nucleophilic displacement of aliphatic cyclic sulfone	Estrogen receptor positive tumors
2-[^{18}F]Fluoro-4-boronophenylalanine	Electrophilic fluorination with [^{18}F]AcOF	Neutron capture therapy titration
6-[^{18}F]Altanserin	Nucleophilic aromatic substitution	5HT$_{2A}$ receptors
[^{18}F]Fluoroethylspiperone	N-alkylation with [^{18}F]fluoroethyltosylate	D$_2$ receptor
[^{18}F]Fleroxacin	Nucleophilic displacement of mesylate	Antibiotic pharmacokinetics
5-[^{18}F]Fluorouracil	Electrophilic fluorination	Tumor imaging
2-β-Carbomethoxy-3-β-(4-[^{18}F]fluorophenyl)tropane *([^{18}F]CFT)*	Fluorodestannylation	Dopamine transport

For studies of metabolic pathways, the concept of *"blocked metabolism"* plays an important role for which [^{18}F]FDG is the classical example. The fact behind *"blocked metabolism"* is the reversible sequence of the biochemical cycles. 2-[^{18}F]FDG and 3-[^{18}F]FDG have been synthesized and clinically evaluated in the past. Among these two analogues, 2-[^{18}F]FDG is widely used as a clinical research tool and as a diagnostic agent in oncology and neurology. Though both analogues of glucose can be transported across the cellular membrane efficiently but once entered, their way of further

cellular metabolism describes the preference of 2-[^{18}F]FDG over 3-[^{18}F]FDG (Fig 1.3)[16]. The priniciple behind the mechanism of 2-[^{18}F]FDG in clinical studies is the missing –OH group at C-2 that is needed for glycolysis. So, the [^{18}F]-substituent at C-2 blocks further phosphorylation because of the high energy of the C-F bond. Thus, 2-[^{18}F]FDG remains trapped in the second metabolic step in the form of 2-[^{18}F]FDG-6-phosphate after reaction with hexokinase. As a result, the distribution of 2-[^{18}F]FDG provides a good index of cellular turnover of glucose within the tumor or the organ of interest. In addition, its efficient radiosynthesis from high activities of [^{18}F]fluoride ion ensures its availability to the imaging centres within a few half-lives of transport time[17-20].
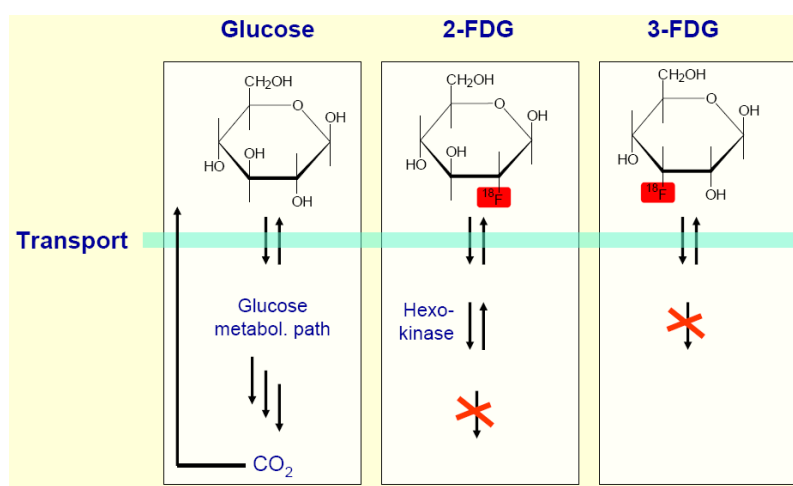
Fig 1.3 Metabolic pathways of glucose and its radio-analogues[16]

Among amino acids used in preclinical and clinical research, the most frequently discussed include 6-[^{18}F]fluoro-L-DOPA, 6-[^{18}F]fluoro-*m*-tyrosine ([^{18}F]F-m-Tyr), 2-[^{18}F]Fluoro-L-tyrosine ([^{18}F]FTyr) and 6-[^{18}F]fluorophenylalanine[21-27]. 6-[^{18}F]fluoro-L-DOPA is one of the few established radiopharmaceuticals having extensive applicability in neurology for diagnosis of central motor disorders such as Parkinson's disease and schizophrenia[28]. As far as [^{18}F]FTyr is concerned, it was reported[29] that this radiotracer could be used as an index of protein synthesis for oncology. Later studies showed that though [^{18}F]FTyr accumulated in tumors, the actual process being measured was the one of the neutral amino acid transporters rather than that of protein synthesis[30]. In addition to these amino acids, the clinical utility of 6-[^{18}F]fluorophenylalanine to assess neutral amino acid transport both in normal human brain and tumor tissues was also investigated[31].

Two tyrosine analogues such as [^{18}F]fluoroethyltyrosine ([^{18}F]FET) and [^{18}F]fluoro-α-methyltyrosine ([^{18}F]FAMT) have been studied for imaging brain tumors[32-33]. Imaging results for [^{18}F]FET in a series of patients with suspected primary or recurrent intracerebral tumors were comparable to [^{11}C]methionine[34]. Similarly, [^{18}F]FAMT exhibited tumor-to-background ratios significantly higher than [^{18}F]FDG in brain tumor[35].

1.3.1 [^{18}F]Fluoride Production

Fluorine-18 may be produced by several methods (Table 1-4)[36], but by far, the most useful one is at a cyclotron via proton irradiation of ^{18}O-enriched water [^{18}O (p, n)^{18}F (E_p = 16 ⟶ 3 MeV][36] and fluorine-18 is obtained as a solution of [^{18}F]Fluoride in the irradiated target water**.** Thus, this method ensures the production of 70 GBq and even more from a single irradiation whereas only 5-15 mCi (0.185 GBq to 0.55 GBq) of radiotracer is needed to be injected into a human subject for a single PET examination. Another attractive feature of this method of production is that fluorine-18 is obtained in a "no-carrier-added" form (n.c.a.). This means that the [^{18}F]fluoride ion has a very high specific activity (i.e., ratio of [^{18}F]fluoride ion radioactivity to the mass of carrier or total fluoride ion). Typically, the specific activity exceeds 185 GBq/μmol (5 Ci/μmol). Theoretically, the maximum value of specific activity of fluorine-18 ($t_{1/2}$:109.6 min) is 63,000 GBq/μmol (1.7 x 10^6 Ci/mmol). Such a high specific activity also enables radiotracers to be administered to human subjects in low mass doses (less than 1-10 nmol) generally without toxic or pharmacological effects.

Table 1-4 [^{18}F]Fluorine production pathways[36]

Nuclide	^{18}O(p, n)^{18}F	^{16}O(^{3}He, p)^{18}F	^{20}Ne(d, α)^{18}F	^{18}O(p, n)^{18}F
Target	$H_2{}^{18}O^a$	H_2O	Ne (200 μmol F_2)^b	$^{18}O_2$, Kr (50 μmol F_2)^c
Particle Energy	16 ⟶ 3	36 ⟶ 0	14 ⟶ 0	16 ⟶ 3
Main Product Form	^{18}F$^-_{aq}$	^{18}F$^-_{aq}$	[^{18}F]F_2	[^{18}F]F_2
Exp. Yield [GBq/μAh]	2.22	0.26	0.40	1.0
Specific Activity [MBq/μmol]	≈600.103	≈50.103	≈100	≈600

^{a}Ti-target with Ti window ^{b}passivated Ni target ^{c}two step process, Al target

Among other methods, the ^{3}He-irridiation of ^{16}O is of minor importance because the nuclear reaction ^{6}Li (n, α) ^{3}H/^{16}O (^{3}H, n) ^{18}F only allows activity productions of < 1 GBq and also causes ^{3}H waste problems[37]. That process had some importance when cyclotrons were rare and nuclear power plants were accessible.

For radiofluorinations *via* electrophilic substitution reactions, [^{18}F]F_2 is required. For this purpose, ^{20}Ne and ^{18}O gas targets are used. The major problem in both cases is the fact that fluorine-18 gets absorbed on target walls so that an addition of elemental fluorine to the target gas is mandatory and, thus, high specific activities can not principally be attained[37]. Since two consecutive irradiations are essential with the $^{18}O_2$-target for saving enriched material, the ^{20}Ne (d, α) ^{18}F-reaction is the most practical and widely used process for the production of electrophilic fluorine-18.

As an alternative, proton irradiation of ^{18}O-oxygen gas is brought into use because the nuclear data of the ^{18}O (p, n) ^{18}F-reaction exhibited higher production yields (from threshold 3 MeV up to 30 MeV proton energy)[38]. In addition, the saturation integral yield encourages irradiation up to about $E_p \leq$ 20 MeV.

1.3.2 [^{18}F]Fluorination Methods

The chemical reactions commonly used for radiosynthesis of [^{18}F]-labelled radiopharmaceuticals fall into the following two categories:
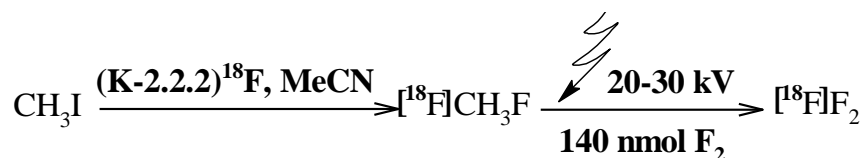
1. electrophilic fluorination,
2. nucleophilic fluorination.

1.3.2.1 Electrophilic [^{18}F]Fluorination

This method utilizes the electrophilic form of ([^{18}F]F$_2$) for labelling of organic molecules. However, due to high reactivity and desctructive property of ([^{18}F]F$_2$, numerous fluorinating reagents have been synthesized from fluorine gas. Such reagents included acetyl hypofluorite, xenon difluoride, diethylaminosulfurtrifluoride, perchloryl fluoride (ClO$_3$F), nitrosyl fluoride, *N*-fluoro-*N*-alkylsulfonamides, *N*-fluoro-2-pyridone, and *N*-fluoropyridinium triflates etc. As all of these reagents are produced in a carrier-added method, therefore, all electrophilic fluorinations are principally carrier-added and finally result in radiotracers with low specific activities. This disadvantage is a serious limitation in the utility of this method.

Another major drawback is that the maximum achievable radiochemical yield (RCY) is only 50% as in reactions with [^{18}F]F$_2$ only one of the two fluorine atoms is incorporated into the product. Despite the drawbacks such as low specific activity, reduced radiochemical yields (RCYs), and poor regioselectivity, this method has been the choice for radiosynthesis of clinically important [^{18}F]-labelled radiopharmaceuticals such as 6-[^{18}F]fluoro-L-DOPA.

Several attempts were made to reduce the amount of fluorine-19 carrier in the synthesis of electrophilic ^{18}F-labelled tracers. Hence, higher molar specific activities of about 30 GBq/µmol of [^{18}F]F$_2$ were tried to be obtained *via* electric gaseous discharge of [^{18}F]methylfluoride prepared by n.c.a. nucleophilic substitution (Scheme 1-1)[39], yet the method was not brought into a general application.

$$CH_3I \xrightarrow{\textbf{(K-2.2.2)}^{18}\textbf{F, MeCN}} [^{18}\text{F}]CH_3F \xrightarrow[\textbf{140 nmol F}_2]{\textbf{20-30 kV}} [^{18}\text{F}]F_2$$

Scheme 1-1 Electrophilic [^{18}F]fluorine generated by electric gaseous discharge[39]

1.3.2.2 Nucleophilic [^{18}F]Fluorination

Unlike electrophilic [^{18}F]fluorinations, the specific activities are higher in this method of labelling. This is due to the fact that [^{18}F]fluoride as a nucleophile can be obtained in a n.c.a. form. Moreover, [^{18}F]fluoride can be produced in an easy and an efficient way by a medical cyclotron. Following irradiation of a [^{18}O]water target, the [^{18}F]fluoride ion is obtained in an aqueous solution that makes it unreactive for further reaction as water molecules mask the free [^{18}F]fluoride ion by solvation.

Therefore, removal of water is essential and is primarily carried out by azeotropic distillation with acetonitrile (MeCN) along with the addition of a cationic counterion. This is achieved by using some soft metal ions such as potassium, rubidium or caesium complexed by a cryptand such as kryptofix-222 (PTC), or tetraalkylammonium salts. However, addition of these salts also leads to the addition of another anion to the reaction mixture. For this purpose, non-nucleophilic anions are selected such as carbonates since these do not compete with [^{18}F]fluoride ion during reaction. After addition of a base such as K_2CO_3 along with K222, water is evaporated in order to activate the anion (^{18}F$^-$) towards n.c.a. [^{18}F]fluorination (Fig 1.4)[15].
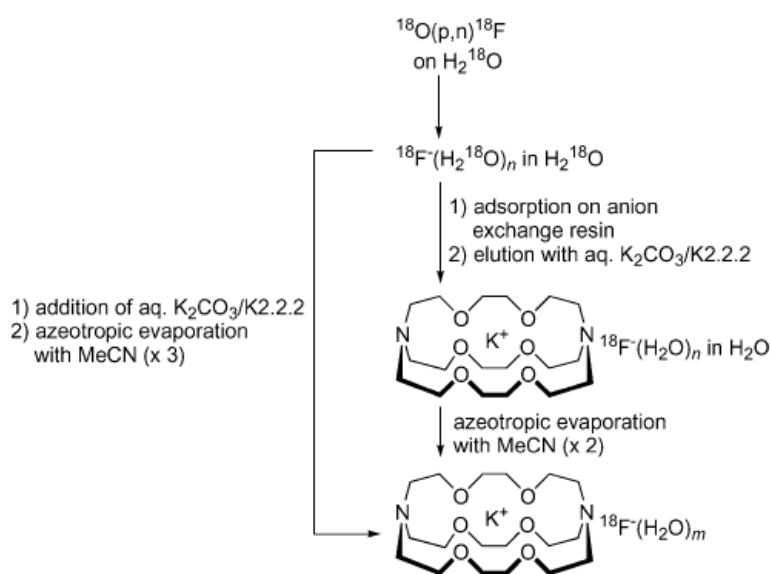
Fig 1.4 Flow chart showing the structure of [^{18}F]KF-K222 complex and its preparation from cyclotron-irradiated [^{18}O]water by two alternative processes[15]

To the dried residue of activated [^{18}F]KF-K222 complex, precursor dissolved in dipolar aprotic solvent is added. Solvents such as dimethylsulfoxide (DMSO) and *N,N*-dimethylformamide (DMF) are usually used as these solvents not only dissolve the organic precursors but also solubilize the [^{18}F]KF-K222 complex.

Although the use of "ionic" (polar protic) is generally thought to be impossible for nucleophilic substitution, *tert.*BuOH as a solvent along with cesium fluoride (CsF) was successfully implemented for this purpose by Kim *et al.* in 2007[40]. It was reported that the rate of fluorination increased with increasing bulk of the alcohol (reaction rates followed the order: *tert.*BuOH > i-PrOH > EtOH > MeOH; or simply: tertiary > secondary > primary alcohol)[40]. The reason was that the tertiary alcohols do not coordinate so tightly with fluoride ion, and hence, flexibility is exhibited between solvent and nucleophile (Fig 1.5)[40]. This breakthrough has proved the tolerance of nucleophilic substitution reactions for water up to 20% in reaction media. The use of such "ionic" liquids has been extended for the radiosynthesis of clinically important tracers such as [^{18}F]FDG and [^{18}F]FLT[41-42].

Fig 1.5 Reactivity-enhancing effects of tert-alcohol on nucleophilic fluorination reaction[40]

1.3.3 Nucleophlic Aromatic [^{18}F]Fluorination

To facilitate [^{18}F]-labelling of aromatic compounds such as tyrosine or phenylalanine, an appropriate leaving group must be present together with an auxiliary group in *ortho* or *para* position to the leaving group, both with strong electron-withdrawing properties. In various studies, the utility of such an approach has been shown[43-46].

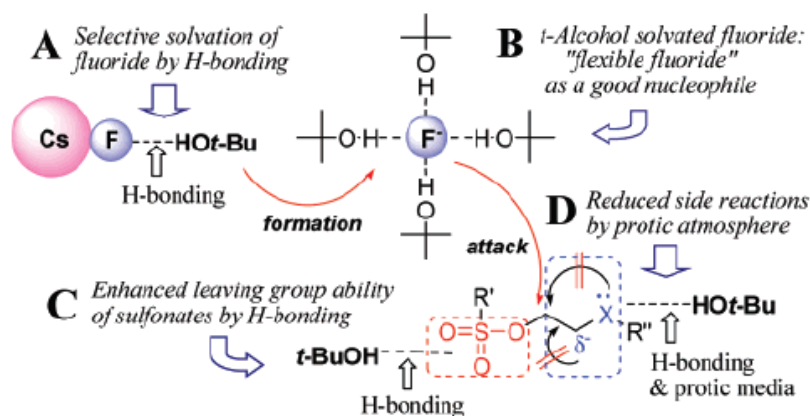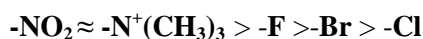A good leaving group is mandatory. Among all leaving groups, the nitro (-NO$_2$) and trimethylammoniumtriflate [-N$^+$(CH$_3$)$_3$ SO$_3$CF$_3$$^-$] groups account for an efficient radiosynthesis of [^{18}F]aryl fluorides resulting in high RCYs. However, halogens are used less frequently. The order of reactivity of leaving groups towards nucleophilic aromatic substitution (S$_N$Ar) reactions in dependence on increasing RCY is as follows:

$$-NO_2 \approx -N^+(CH_3)_3 > -F > -Br > -Cl$$

Isotopic exchange of ^{19}F by ^{18}F, despite of resulting in high RCYs, has not been in the focus of interest since the specific activities to be achieved are thought to be unattractively low due to the presence of ^{19}F-carrier (c.a.). However, as reported earlier[47-49], this type of radiofluorination showed distinct advantages because the ratio of the rate constants of the ^{18}F/^{19}F exchange (k$_E$) exceeded those for the displacement of other halogens (k$_D$) up to 10^3.

In order to reduce the electron density of benzene ring and to enhance its reactivity towards S$_N$Ar, an auxiliary group such as -NO$_2$, cyano (-CN) or carbonyl group is required. These groups are particularly of choice due to their highly positive values of Hammett constants [σ (para): +0.78 (-NO$_2$), +0.66 (-CN)]. Among all, the most feasible and favourable is the aldehyde group (-CHO) since it can be removed easily by means of catalytic decarbonylation by using Wilkinson's catalyst[43, 50].

The use of diphenyliodonium salts (Ar-I$^+$-Ar$_1$) has the distinct advantage that it eliminates the need of an auxiliary group on benzene ring[51-54]. In this case, the more electron deficient ring is preferably attacked by the [^{18}F]fluoride ion. However, it has limited applicability due to the unwanted radioactive by-products (Scheme 1-2)[53].

X = Cl, Br, I, OTs, ClO$_4$, CF$_3$SO$_3$
R or R$_1$ = H, Cl, Br, I, NO$_2$, CH$_3$, OCH$_3$

Scheme 1-2 General procedure of [^{18}F]-labelling *via* diaryliodonium salts[53]

For the synthesis of radiotracers such as 6-[^{18}F]-L-DOPA *via* nucleophilic aromatic substitution reaction, it is necessary to protect the –OH groups. For this purpose, usually, the –CH$_3$ group is used. However, –OCH$_3$ strongly inactivates the benzene ring towards S$_N$Ar *via* electron-donating mesomeric effect (M+) and, thus, decreases the RCY. Hence, it was essential to study the impact of –OCH$_3$ groups on the rate of radiofluorination via S$_N$Ar in substituted benzaldehydes. Bin *et al.* carried out a systematic study in methoxy-substituted *ortho* nitrobenzaldehydes[55]. It was found that 4-methoxy-2-nitrobenzaldehyde **(i)**, 4,5-dimethoxy-2-nitrobenzaldehyde **(ii)** and 3,4-dimethoxy-2-nitrobenzaldehyde **(iii)**, potential precursors for synthesis of [^{18}F]-labelled tyrosine or DOPA, gave maximum RCYs of > 85%. Even the precursors substituted with three **(iv)** and four **(v)** –OCH$_3$ groups showed good RCYs[55] (Fig 1.6).
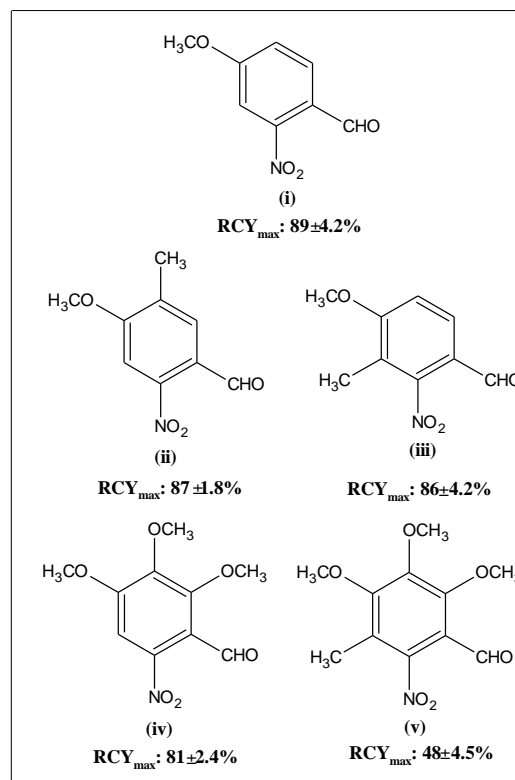

Fig 1.6 Methoxy substituted 2-nitrobenzaldehydes[55]

For enhancing nucleophilc aromatic substitution, an interesting alternative is the heteroatom within the hetroaromatic system, for which pyridine is the leading example. The *ortho* position of the nitrogen is known to be well suited for a nucleophilic substitution reaction. Labelling with fluorine-18, however, was only studied in a few cases for which ^{18}F-substituted purines[56] and nicotinic acid amides[57] are typical examples (Table 1-5). Dolci *et al.* (1999) evaluated the scope of nucleophilic aromatic fluorinations of 2-substituted pyridine rings using the activated [^{18}F]KF-K222 complex (Scheme 1-3)[58-59]. This is of particular interest since in case of substituted benzenes without an auxiliary group, a nucleophilic substitution is thought to be almost impossible to occur.

LG = -N(CH$_3$)$_3$$^+$, -NO$_2$, -Br, -Cl
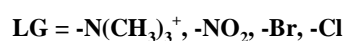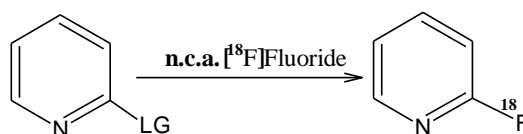
Scheme 1-3 [^{18}F]-labelling of 2-substituted pyridines[58-59]

The main advantage of using the pyridine system for radiosyntheses of radiopharmaceuticals is the lack of one additional step i.e. the removal of activating group (such as removal of –CHO by Wilkinson's catalyst) after the radiosyntheses.
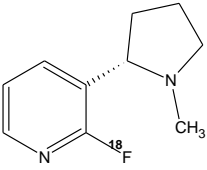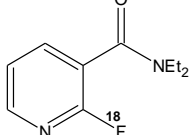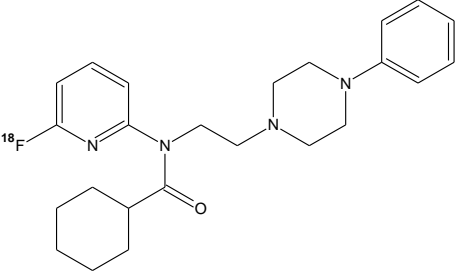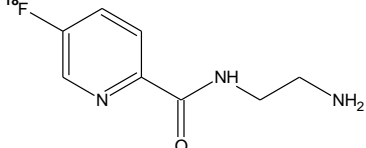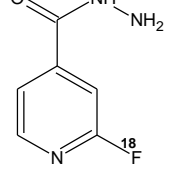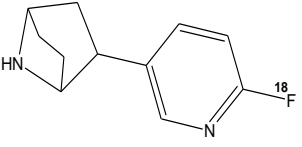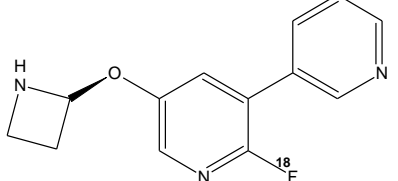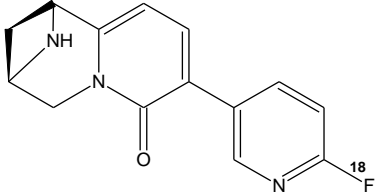
However in the pyridine system, it is almost impossible to get good RCYs when radiofluoriation *via* S$_N$Ar is to be performed in *meta* position. This is due to the fact that the *meta* position is not activated towards S$_N$Ar by an electron-withdrawing mesomeric effect of the N-atom. For the first time, *meta* position in pyridines was labelled by [^{18}F]fluoride by S$_N$Ar using diaryliodonium salts (Scheme 1-4)[60].
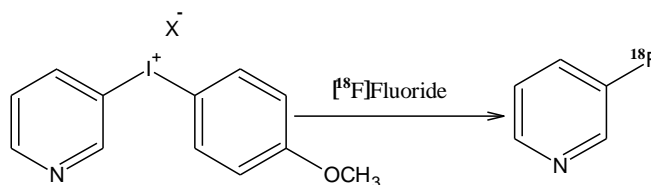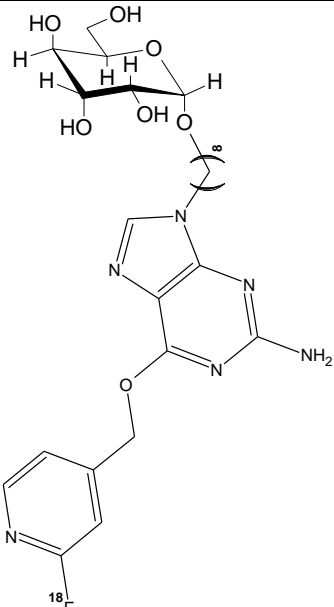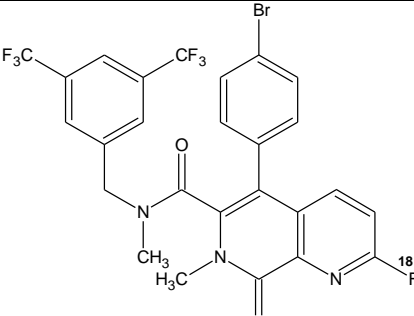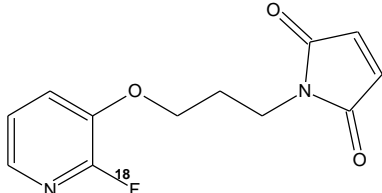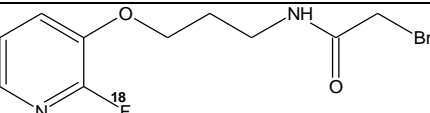
Scheme 1-4 [^{18}F]-labelling in *meta* position in pyridines via diaryliodonium salts[60]

In this case, electron density is lower in *meta* position of pyridine ring than in benzene substituted by –OCH$_3$ group in *para* position. This particular fact assured a very selective radiofluorination in the pyridine ring, and nevertheless, the RCYs so obtained were as high as 55-63% after 30 min of reaction time.

Table 1-5 Examples of [^{18}F]fluorinated heteroaromatic radiopharmaceuticals[58]

Radiotracers	Structural Formuals
2-[^{18}F]Fluoronicotinic acid diethylamide	
2-[^{18}F]Fluoronicotine	
[6-Pyridinyl-^{18}F]fluoro-WAY-100635	
N-(2-Aminoethyl)-5-[^{18}F]fluoropyridine-2-carboxamide	
2-[^{18}F]Fluoroisonicotinic acid hydrazide	
Nor-chloro[^{18}F]fluoroepibatidine	
[^{18}F]NIDA52158	
(-)-9-(2-[^{18}F]Fluoropyridinyl)cytisine	

2-Amino-6-(2-[¹⁸F]fluoropyridin-4-ylmethoxy)-9-(octyl-*β*-D-glucosyl)-purine	
***N*-[3,5-bis(Trifluoromethyl)benzyl]-*N*-methyl-5-(4-bromophenyl)-2-[¹⁸F]fluoro-7-methyl-8-oxo-7,8-dihydro-[1,7]naphthyridine-6-carboxamide**	
1-[3-(2-[¹⁸F]Fluoro-pyridin-3-yloxy)-propyl]-pyrrole-2,5-dione	
***N*-[3-(2-[¹⁸F]Fluoropyridin-3-yloxy)propyl]-2-bromoacetamide**	

1.3.4 Indirect [¹⁸F]Fluorination

In some cases, indirect [¹⁸F]-labelling methods are applied. These procedures imply a two step of radiosynthesis in which the primary step is the [¹⁸F]-labelling of a prosthetic group or a synthon that is coupled in a secondary step with another molecule to form the final product. Important procedures *via* prosthetic groups are the [¹⁸F]fluoroalkylation, [¹⁸F]fluoroacylation, and the [¹⁸F]fluoroamidation (Scheme 1-5)[61-62].

The various [¹⁸F]fluorinated synthons used for direct [¹⁸F]-labelling mehods include [¹⁸F]fluorobenzylhalides, aceto-4-[¹⁸F]fluorophenone, 2- or 4-[¹⁸F]fluoroaniline, 4-[¹⁸F]fluoro phenyl lithium, 1-[¹⁸F]fluoro-4-haloarenes, 4-cyano-1-[¹⁸F]fluorobenzene, 4-[¹⁸F]fluorophenol and 4-[¹⁸F]fluorobenzaldehyde[62].

X, Y = Br, I, OTs, OTf
Z = N, O, S
R = Alkyl, Aryl
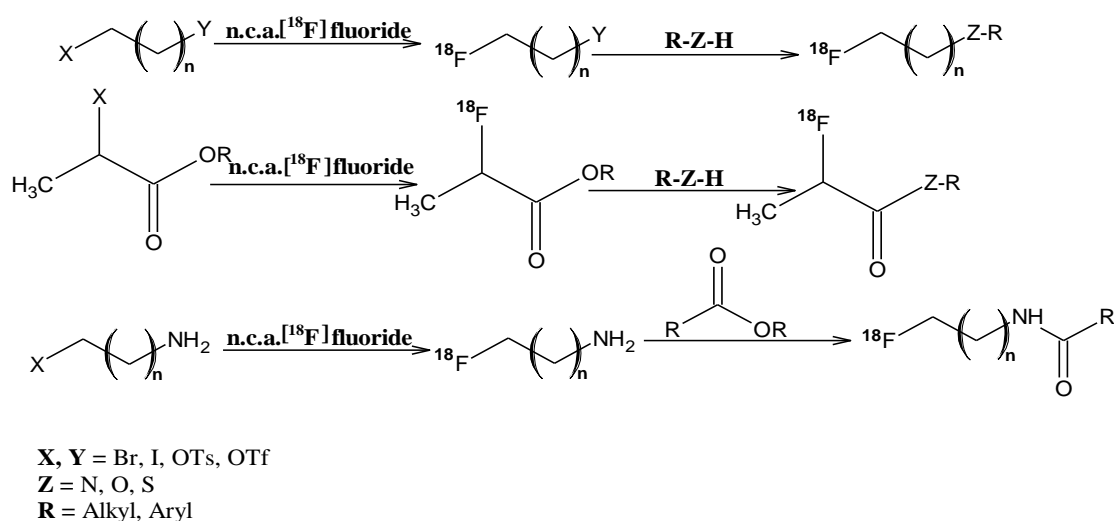
Scheme 1-5 [^{18}F]-labelling *via* [^{18}F]-labelled prosthetic group[61-62]

1.4 Radiopharmaceuticals for PET Imaging of Hypoxia

For PET imaging of hypoxia, a probe was needed that could compete directly with intracellular O_2 when supply of O_2 was inadequate to accommodate the electrons produced by the electron-transport chain (Fig 1.7)[63]. Aiming at this purpose, Chapman[64] used ^{14}C-labelled derivatives of *N*-alkyl-2-nitroimidazoles that were trapped successfully in hypoxic cells but still showed electron-transport activity.
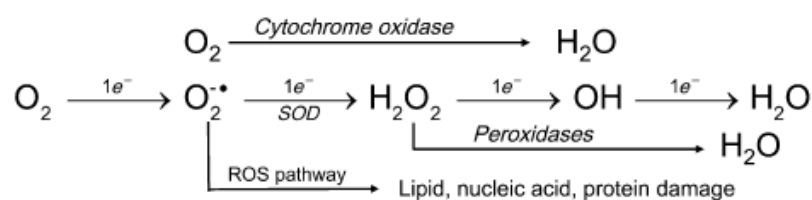
Fig 1.7 Pathway of electron-transport chain in absence of adequate cellular oxygen[63]

The reason was the fact that 2-nitroimidazole possesses the ideal capability to follow intracellular metabolism depending on the oxygen concentration within the tissues. As a first step, the nitro group traps electrons produced from respiratory cycle and forms a radical anion i.e. $-NO_2^{-\bullet}$ (Fig 1.8). If O_2 is sufficiently high in cells, it will compete with the nitro group in trapping electrons from $-NO_2^{-\bullet}$ and, hence, nitroimidazole radical will return to its parent state. On the other hand, if cells are deficient in O_2, then, nitroimidazole radical is reduced to an amine-derivative that further reacts with intracellular macromolecules leading to irreversible trapping. The reduction process is usually catalyzed by reductases such as xanthine oxidase, lipogenases, and NADPH oxidases. This reduction process occurs on the flavin site and results in transferring a single electron to the heteroaromatic $-NO_2$ group, and thus, converts it to the hydroxylamine[64-66].
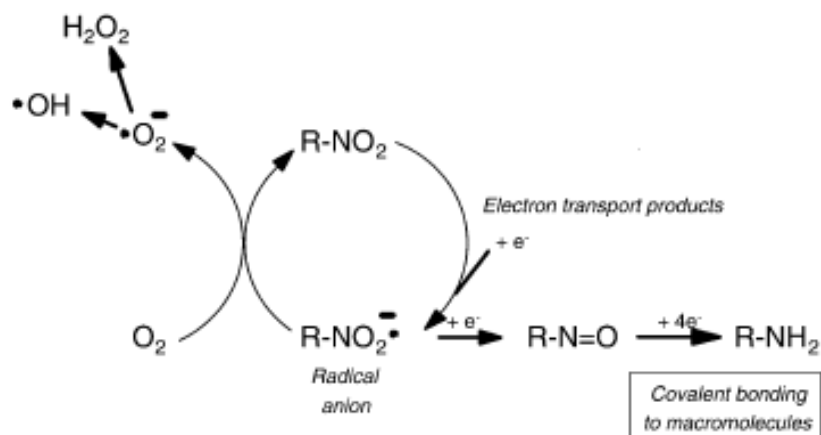
Fig 1.8 Cyclic pathway showing intrecellular metabolism of –NO$_2$ of 2-nitroimidazole[63]

Upto now, many radiotracers, containing 2-nitroimidazole rings, have been synthesized for PET-imaging of hypoxia (Fig 1.9). Among all, [^{18}F]FMISO and [^{18}F]FAZA are the most widely used ones[67-68]. For radiofluorination of hypoxia precursors such as [^{18}F]FMISO, two basic strategies have been used that involve a one step or a two step radiosynthesis involving nucleophilic substitution reaction:

a) direct [^{18}F]-labelling approach by nucleophilic substitution,

b) coupling of a pre [^{18}F]-labelled precursor with 2-nitroimidazole.
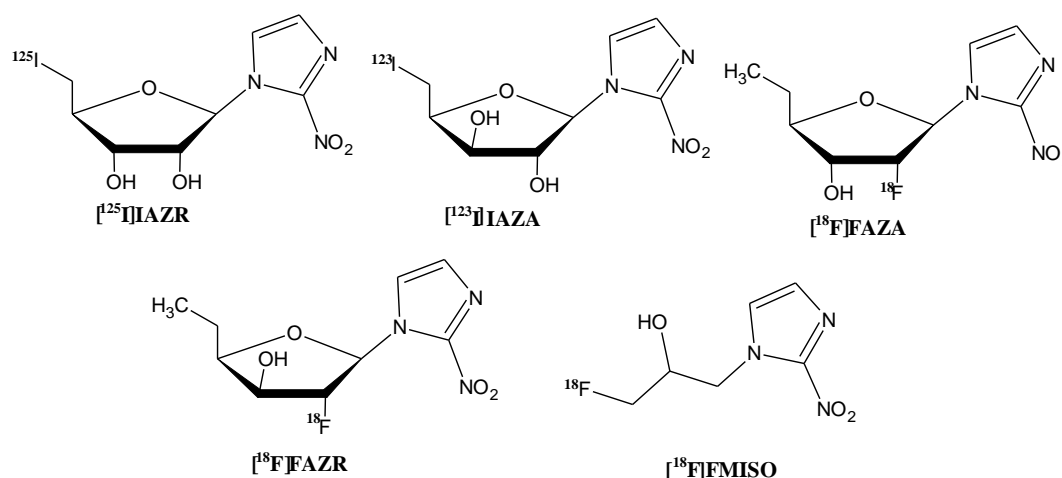
Fig 1.9 Molecular structures of some widely discussed hypoxia tracers

For uptake in the cells, many transport systems of cell membrane are utilized by radiotracers. As far as transportation of amino acids is concerned, numerous amino acid transport systems have been characterised including L, y$^+$L, A, ASC, asc, b$^{o,+}$, B$^{o,+}$ and x$^-$, Gly, n and T[69]. Among all, system L is a major one as it transports large neutral amino acids in a Na$^+$-independent manner and it includes two isoforms i.e. LAT1 and LAT2 (L-type amino acid transporter1 and 2)[69-70] (Fig 1.10). LAT1 transports large neutral amino acids such as Leu, Val, Phe, Tyr, Trp, Met, and Hist.
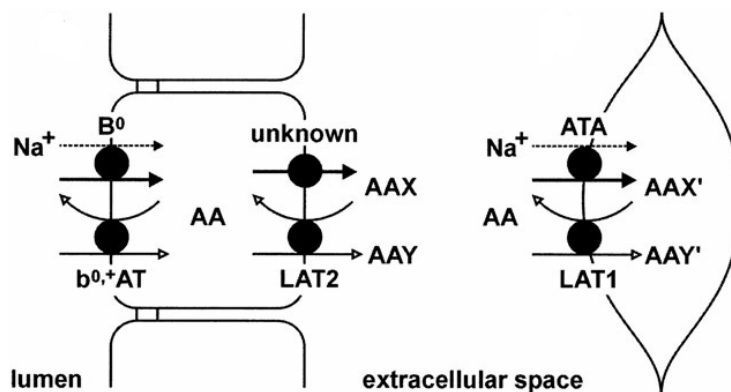
Fig 1.10 Schematic illustration of the role played by LAT1 and LAT2[70]

As a new concept, a bifunctional hypoxia tracer having both 2-nitroimidazole and *p*-tyrosine with propane as a linker was to be synthesized as it might be transported hypothetically into the cells *via* amino acid transporter system (LAT1). For this purpose, methyl *N*-[(benzyloxy)carbonyl]-*O*-[2-{[(4-methylphenyl)sulfonyl]oxy}-3-(2-nitro-1*H*-imidazol-1-yl)propyl]tyrosine (*see 3.3.1,* **e**) was chosen for radiosynthesis of *O*-[2-[^{18}F]fluoro-3-(2-nitro-1*H*-imidazol-1-yl)propyl]tyrosine ([^{18}F]FNT], **i**) (Fig 1.11).
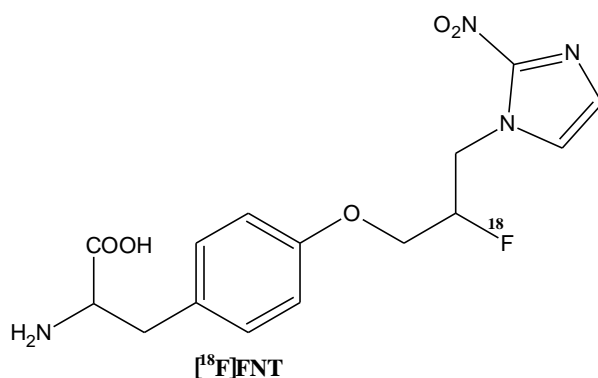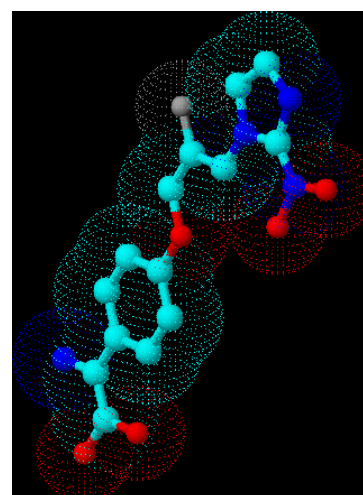
(a)   (b)

Fig 1.11 (a) Structural formula of [^{18}F]FNT; (b) Three dimensional structure of [^{18}F]FNT

1.5 [^{18}F]Fluorination of PSMA Targeting Ligands

The targeting of glutamate carboxypeptidase II, also known as prostate-specific membrane antigen (PSMA) is one of the most favourable approach because of its presence in prostate epithelium. As a dimeric, type II integral membrane-glycoprotein, it consists of a large, globular extracellular localized domain (ED, amino acids 45-750), a hydrophobic transmembrane domain (TM, amino acids 20 to 44) and an endocytic intracellular targeting motif (CD, amino acids 1 to 19, binding site)[71] (Fig 1.12).
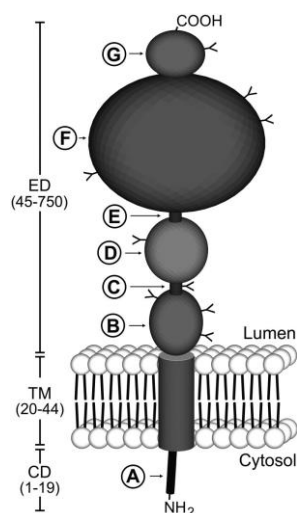
Fig 1.12 Integral structure of prostate specific membrane antigen (PSMA)[71]

It over-expresses only in localized and metastatic prostate cancer. Its expression level increases with increase of tumor growth. It is considered as the most suitable protein for LNCaP-targeting drug delivery studies because of its internalization through clathrin-coated pits[72] (Fig 1.13).
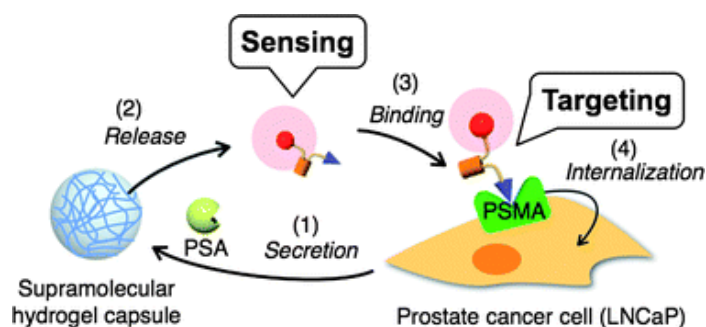
Fig 1.13 Schematic illustration of PSA-DUPA binding by PSMA in LNCaP cells[72]

Due to the specificity of over expression of PSMA exclusively in prostate cancer (PCa) and related cell lines (e.g. LNCaP, LNCaP C4-2), numerous PSMA-specific tracers have been synthesized and evaluated until now[72-74]. Among all those ligands, [^{99m}Tc]-labelled analogues of 2-[3-(1,3-dicarboxypropyl)ureido]pentanedioic acids (DUPA, a well-known high affinity inhibitor of PSMA) with 7 to 16 atom spacers have shown high specificity and selective tumor uptakes with very little accumulation in other tissues except kidney[73]. Especially, the linking of DUPA to 8-aminooctanoic acid followed by two phenylalanine residues (for maximal interaction with hydrophobic pockets of the protein) created an imaging ligand with excellent potential for clinical studies[74].

However, to label tracers, such as DUPA or DUPA analogues, the suitable prosthetic group is required that can be labelled with fluorine-18 with high yields along with 95-96% of purity. So, the ^{18}F-labelled prosthetic group can be coupled with proteins in high radiochemical yields (RCYs) and, thus, yielding > 98% pure radiotracer for further biological analysis. For this purpose, the most commonly used prosthetic group is *N*-succinimidyl 4-[^{18}F]fluorobenzoate ([^{18}F]SFB)[75-77]. Recently, an

automated radiosynthesis of [^{18}F]SFB has been optimized[77] using synthetic routes proposed by Scott *et al.*. The main drawback was that the radiosynthesis of [^{18}F]SFB is performed through multiple steps.

Another approach has been reported[78] to label larger peptides (such as NOTA-octreotide) by using Al^{18}F. However, the disadvantage of this method was the formation of two interchangeable diastereoisomers (R_t = 17.4 and 19.8 min) that could not be separated even after HPLC purification. Alternatively, direct one-step [^{18}F]-labelling[79] of peptides was performed *via* nucleophilic aromatic substitution using –CN or –CF$_3$ as electron-withdrawing groups in *ortho* position to the trimethylammonium group (TMA) as leaving group. This method showed promising results for labelling peptides, however, the approach is incompatible with non-protected side chains of amino acids.

Upto now, the most promising prosthetic group for labelling peptides is 6-[^{18}F]fluoronicotinic acid 2,3,5,6-tetrafluorophenyl ester ([^{18}F]FPy-TFP), first reported by Olberg *et al.*[80]. It involves one step radiosynthesis of prosthetic group itself and then, after simple cartridge purification, one step for coupling with peptide. The other advantage of using this prosthetic group for labelling peptides lies in the fact that [^{18}F]FPy reduces the lipophilicity of resulting peptide by many folds as compared to [^{18}F]SFB because the calculated lipophilicity of [^{18}F]FPy-DUPA-Pep (logP: 2.32±0.95) is clearly lower than that of [^{18}F]FB-DUPA-Pep (logP: 3.12±0.93)[81-82].

The goal of this work was the radiosynthesis of the new [^{18}F]-labelled DUPA conjugate ([^{18}F]FPy-DUPA-Pep) suitable for PSMA-specific imaging of prostate tumors. For labelling, 2,3,5,6-tetrafluorophenyl 6-[^{18}F]-fluoronicotinate ([^{18}F]FPy-TFP) was used as a prosthetic group (Fig 1.14).

(a)

[^{18}F]FPy-DUPA-Pep

(b)
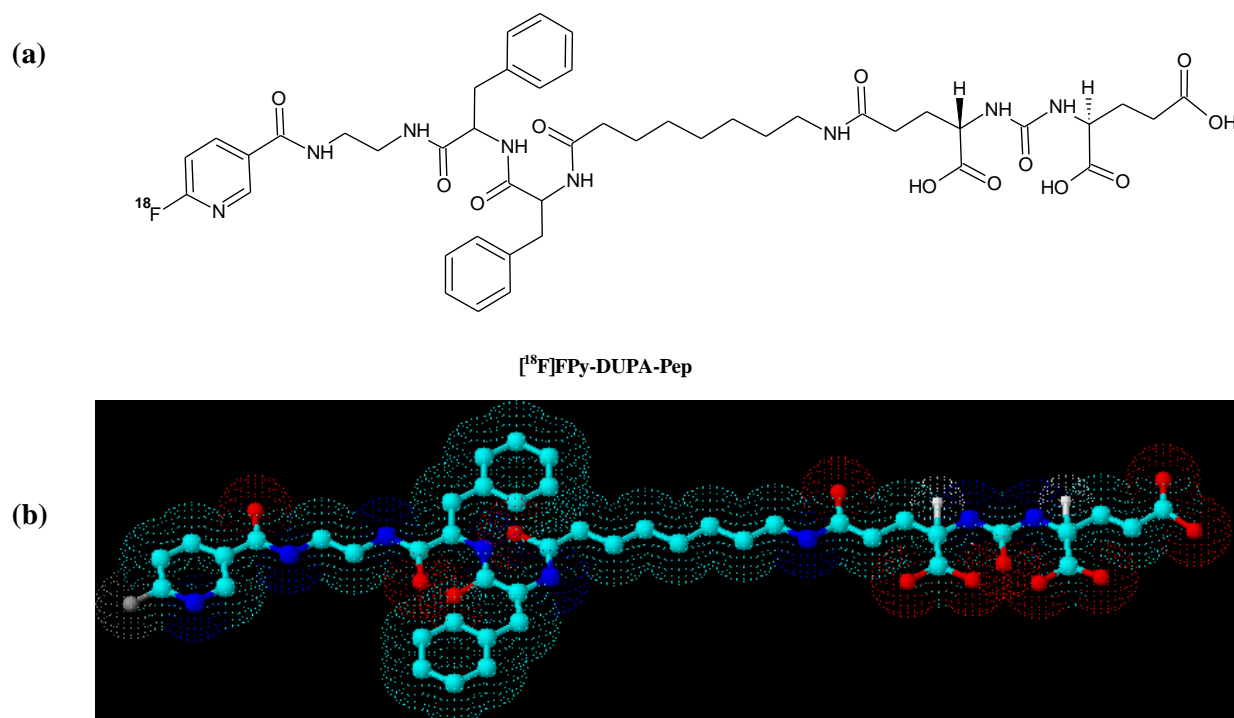
Fig 1.14 (a) Structural formula of [^{18}F]FPy-DUPA-Pep; (b) Three dimensional structure of [^{18}F]FPy-DUPA-Pep

1.6 Automated Modules for Synthesis of Radiotracers

Automated radiosyntheses have been one of the most important aspects for production of PET radiopharmaceuticals in a reliable, cost-effective and most efficient way. Basically, the design of automated radiotracer synthesis is according to the general organic synthesis. An automatic module constitutes laboratory unit operations (LUO) with a feedback controlling system that usually comprises of sensors[83]. LUO are the same as organic synthetic steps, such as addition of reagents, evaporation of solvents, regulation of temperature, and cartridge purifications (solid phase extraction).

However, the development of automated modules is quite different from the automated machines used for organic synthesis. The difference lies in the fact that radiosynthesis is usually carried out at micro scale (concentrations: mg or μg/μL or mL) as compared to organic syntheses (concentrations: mg or g/mL or L). Other important factors are the time limitations (due to half-lives of the radioactive isotopes) and the shielding requirements in order to avoid the exposure to radiations. These limitations are thought to make automatic radiochemical processes quite difficult to perform.

Since 1980, there has been a great evolution regarding development as well as utilization of automated radiosynthesis because of the possibility of using high starting activities (> 10 GBq). The earliest automated modules included hard-wired automatic syntheses of [^{11}C]glucose[84] and ^{13}NH$_3$[85], automated syntheses of L-[^{13}N]glutamate[86] by microprocessor-based system, and syntheses of [^{75}Br]-labelled radiopharmaceuticals[87] by automated production modules. Later in 1990, the interest of using automated systems highly increased due to the successful one-pot synthesis of [^{18}F]FDG[88] by a stereospecific route *via* nucleophilic substitution that became possible only after development of new cyclotron targets for the production of [^{18}F]fluoride ion from H$_2$^{18}O[89]. At present, due to the high demands of automated modules for routine synthesis of PET radiopharmaceuticals, technological problems have been overcome by applying new engineering strategies, such as in case of syntheses of 6-[^{18}F]fluoro-L-DOPA *via* electrophilic fluorodestannylation[90] and [^{11}C]flumazenil using Anatech RB-86 robot system[91]. In addition, the automatic production as well as the handling of PET radiotracers is also important in clinical studies for drug application both *in vivo* and *in vitro*. For this purpose, many modules have been built that include new features such as automated quality control of the final labelled compound in order to assure its purity[92], infusion systems for automated injection of radiopharmaceuticals[93], automated dose dispensing systems having calibrated dose delivery system that functions automatically according to the intended injection times[94]. Another interesting development was the automated delivery systems having pneumatic transporter system [95] that includes PLC (programmable logic controller), a small control box and a new loading station in order to avoid exposure to radiations.

The most important step towards final formulation of a radiotracer involves the purification either by solid phase extraction or by radio HPLC semipreparative separation. Afterwards, it is highly desirable to get rid of the excessive volumes of eluents that can be possibly achieved by evaporation.

Hence, in modern automation technology[96], these modifications have been incorporated in order to get the final product with high RCY, specific activity and chemical purity ($\geq 99\%$).

2. PROBLEM

Among all positron-emitting radioisotopes, fluorine-18 is most widely used. For synthesis of [^{18}F]-labelled radiotracers such as 6-[^{18}F]-L-FDOPA for PET, most commonly used pathway is electrophilic substitution using [^{18}F]F$_2$ and [^{18}F]acetylhypofluorite as reagents. However, this methodology results in the low specific activity of the radiotracer and thus, its utility for radiofluorination is limited. Contrarily, radiopharmaceuticals with high specific activities can be obtained by nucleophilic substitution using n.c.a. [^{18}F]fluoride ion produced efficiently at cyclotron. But to introduce ^{18}F$^-$ ion directly at aryl carbons is almost impossible resulting because of high electron density of benzene ring. To overcome this, usually, S$_N$Ar reactions are performed on aromatic systems that are highly activated towards attack of nucleophile (^{18}F$^-$ ion). This ring activation is achieved by substituting benzene ring by an additional electron-withdrawing group such as aldehyde (–CHO).

In addition to the auxiliary group, a suitable leaving group, bearing electron-withdrawing properties, must also be present on benzene ring. Among leaving groups, –NO$_2$ and –N$^+$(CH$_3$)$_3$ are thought to be the best that give relatively high RCYs when compared to halogens (–F, –Br, –Cl). Along with, S$_N$Ar has to be performed in the presence of electron-donating groups such –OCH$_3$ (for –OH protection) and –CH$_3$ (for linking glycine moiety). Such groups are known to decrease S$_N$Ar very strongly when present in *para* or in *ortho* position to the leaving group. Thus, it appeared highly desirable to study the impact of such groups on the rates of radiofluorinations *via* S$_N$Ar. However, upto now, the effect on S$_N$Ar was studied only in substituted 2-nitrobenzaldehydes[55] and no data has been reported for –N$^+$(CH$_3$)$_3$.

For this purpose, various –OCH$_3$ and –CH$_3$ substituted benzaldehydes bearing quaternary ammonium salt [–N$^+$(CH$_3$)$_3$] as leaving group have been designed in order to study the kinetics of S$_N$Ar by [^{18}F]fluoride (Fig 2.1).

LG = N$^+$(Me)$_3$CF$_3$SO$_3^-$
R$_1$, R$_3$, R$_4$ = H, **R$_2$** = CHO
R$_1$ = CH$_3$, **R$_2$** = CHO, **R$_3$, R$_4$** = H
R$_1$, R$_3$ = H, **R$_2$** = OCH$_3$, **R$_4$** = CHO
R$_1$, R$_2$ = H, **R$_3$** = OCH$_3$, **R$_4$** = CHO
R$_1$ = H, **R$_2$, R$_3$** = OCH$_3$, **R$_4$** = CHO
R$_1$ = CH$_3$, **R$_2$, R$_3$, R$_4$** = H
R$_1$, R$_4$ = CH$_3$, **R$_2$, R$_3$** = H
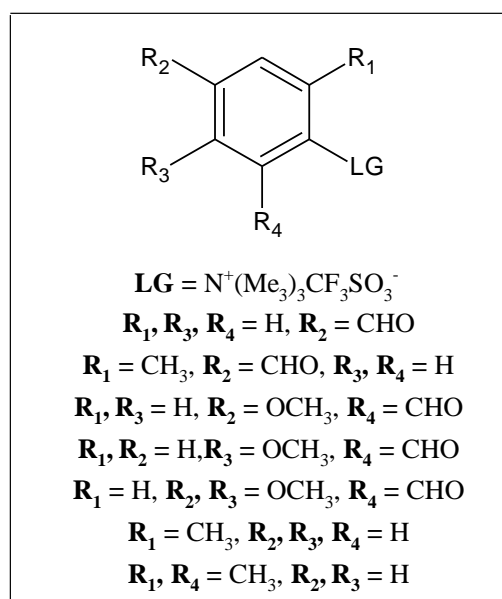
Fig 2.1 Homoaromatic model compounds having –N$^+$(CH$_3$)$_3$ as a leaving group

After radiolabelling, auxiliary group (e.g. –CHO) can be removed easily by decarbonylation using Wilkinson's catalyst[43]. In order to avoid the use of an activating group, an interesting alternative is pyridine ring in which the nitrogen atom acts as an electron-withdrawing group. Recently, [^{18}F]-labelling was performed on 2-substituted pyridines *via* S_NAr, and unexpectedly very high RCYs were reported[58-59]. However, the model compounds so studied[58-59] were without electron-donating substituents (EDG), such as –OCH$_3$ (use for –OH protection prior to labelling) and –CH$_3$ (used for linking glycine moiety). Hence, it appeared very important to study the impact of such subsituents on kinetics of radiofluorination. For this purpose, various model compounds are selected in the present study (Fig 2.2). Additionally, energies of activations (E$_a$) will be calculated by Arrhenius plots for comparison with homoaromatic analogues (substituted benzaldehydes).

LG = NO$_2$, F, Br, Cl
R$_1$, R$_2$ = H; 2-substituted pyridines
R$_1$ = CH$_3$, **R$_2$** = H; model compound for azaphenylalanine
R$_1$ = OCH$_3$, **R$_2$** = H; 3-methoxy-2-substituted pyridines
R$_1$ = OCH$_3$, **R$_2$** = CH$_3$; model compound for azatyrosine
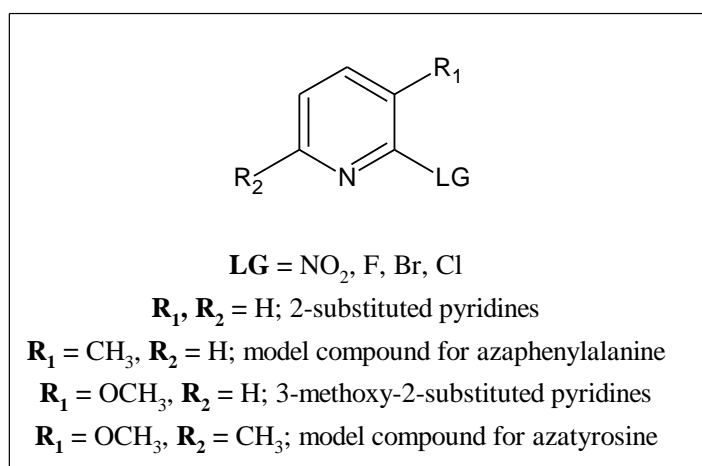
Fig 2.2 Heteroaromatic model compounds for radiofluorinations

Another important way of radiofluorinations is S_NAr by isotopic exchange (^{18}F/^{19}F) but this method is rarely performed as the specific activities to be achieved are usually very low due to the presence of ^{19}F-carrier (c.a.). Thus, in present work, [^{18}F]-labelling will be carried out in dependence on the substrate concentrations for 2-[^{18}F]-fluoropyridine as it may be of practical importance both for preclinical and clinical applications.

In [^{18}F]-labelling, the protection of –OH substituent is another important aspect and it is usually carried out by using –CH$_3$ group. But the hydrolysis conditions utilized for this purpose are very harsh such as 150°C and HBr that make hydrolysis highly incompatible with the automatic modules because of the corrosive effects on walls, fittings, tubings, and valves. Hence, it becomes necessary to find new protecting groups that can be hydrolysed under mild experimental conditions. For this purpose, various *O*-protecting groups have been selected such as benzyl (–OBn), 3-methylbenzyl (–*m*-xylyl), 4-methylbenzyl (–*p*-xylyl), 3,5-dimethylbenzyl, and 2,4-dimethylbenzyl (Fig 2.3) and the cleavage will be performed by acidic as well as catalytic transfer hydrogenation in order to develop a new approach towards protection/deprotection of –OH group.

R = -CH₃, -Bn, -p-xylyl,
m-xylyl, 3,5-dimethylbenzyl,
2,4-dimethylbenzyl
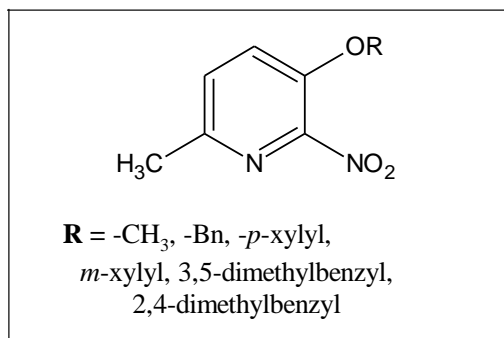
Fig 2.3 Model compounds having different *O*-protecting groups for hydrolysis studies

Along with amino acids, radiotracers for PET imaging of hypoxia are also of high clinical importance. Till now, among all hypoxic radiotracers, [¹⁸F]FMISO and [¹⁸F]FAZA are most widely used. Among these, [¹⁸F]FAZA is more efficient as it utilizes the nucleoside transporter system for entering the cells. However, as another alternative to increase the uptake of [¹⁸F]-labelled hypoxic tracer in cells, a bifunctional PET-radiotracer has been designed ([¹⁸F]FNT) as a new approach in which *p*-tyrosine is coupled to 2-nitroimidazole (Fig 2.4). Hypothetically, it can utilize an amino acid transporter system (such as LAT1[69-70]) to enter the cells. In present work, its organic as well as radiosynthesis *via* nucleophilic aliphatic substitution reaction will be performed.
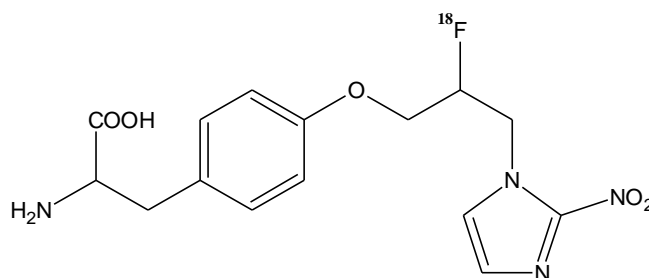
Fig 2.4 Structure of hypoxic radiotracer ([¹⁸F]FNT)

In addition, a new PSMA (prostate-specific membrane antigen) targeting ligand ([¹⁸F]Py-DUPA-Pep) will be synthesized. This new radiotracer is supposed to enhance the PSMA specific imaging of prostate tumors. In it, DUPA is linked *via* 8-aminooctanoic acid to two phenylalanine rings that may increase the binding with hydrophobic pits of the membrane. Radiofluorinations will be carries out *via* prosthetic group [(¹⁸F)FPy-TFP] Fig 2.5.
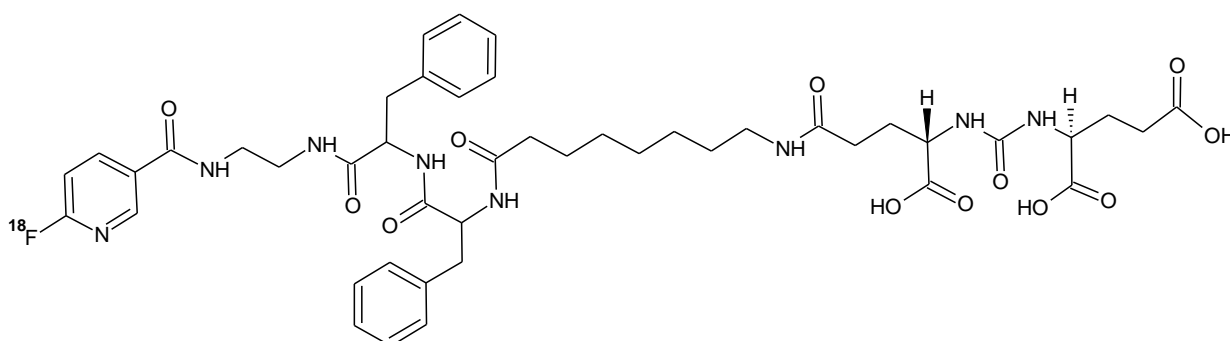
Fig 2.5 Structure of a new PSMA targeting ligand ([¹⁸F]FPy-DUPA-Pep)

3. RESULTS AND DISCUSSIONS

3.1 Nucleophilic Aromatic Substitution

For nucleophilic aromatic substitution, an auxiliary group is required in *ortho* or *para* position to the leaving group. Most widely used leaving groups are $-NO_2$, $-N^+(Me_3)_3$, and halogens (-F, -Br, -Cl). Theoretically, for these leaving groups, increasing order of RCY is $-N^+(Me_3)_3 \approx -NO_2 > -F > -Br > -Cl$. For an auxiliary group, an electron-withdrawing group is used. Commonly used electron-withdrawing groups are cyanide (-CN), nitro ($-NO_2$) and carbonyl groups. The dependence of RCY on auxiliary groups can be seen (Fig 3.1) clearly as RCY is only $1\pm0.1\%$ in case of nitrobenzene. However, it increases fast (> 80%) for the compounds, where $-NO_2$ **(c)** and $-CHO$ **(d)** groups are present as electron-withdrawing groups in *para* position to the leaving group ($-NO_2$).
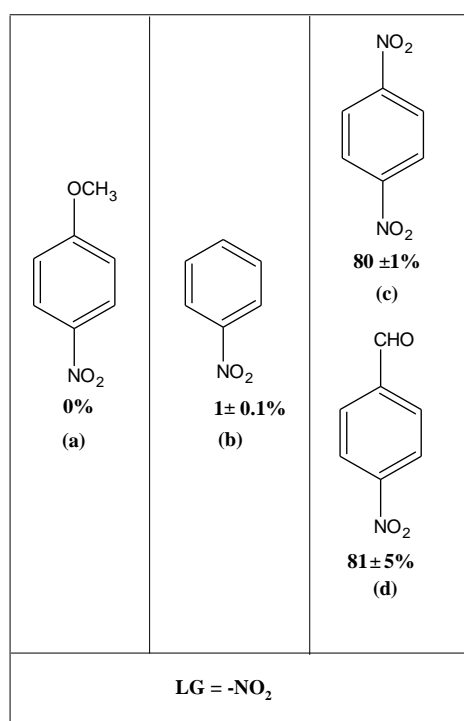
Fig 3.1 Dependence of the radiochemical yields (RCYs) of radiofluorinations on auxiliary group in substituted nitrobenzenes[97]

The most convenient auxiliary group used so far[43-44, 50] is aldeyhde (-CHO) because of its feasible removal. The decarbonylation reaction can be performed by using Wilkinson's catalyst $[RhCl(PPh_3)_3]$ or a palladium/carbon catalyst. Recently, it was reported that Wilkinson's catalyst has several advantages with respect to reaction rates and mild conditions over palladium/carbon catalyst[43-44]. The mechanistic scheme of decarbonylation by Wilkinson's catalyst is as follows:

Wilkinson's Catalyst
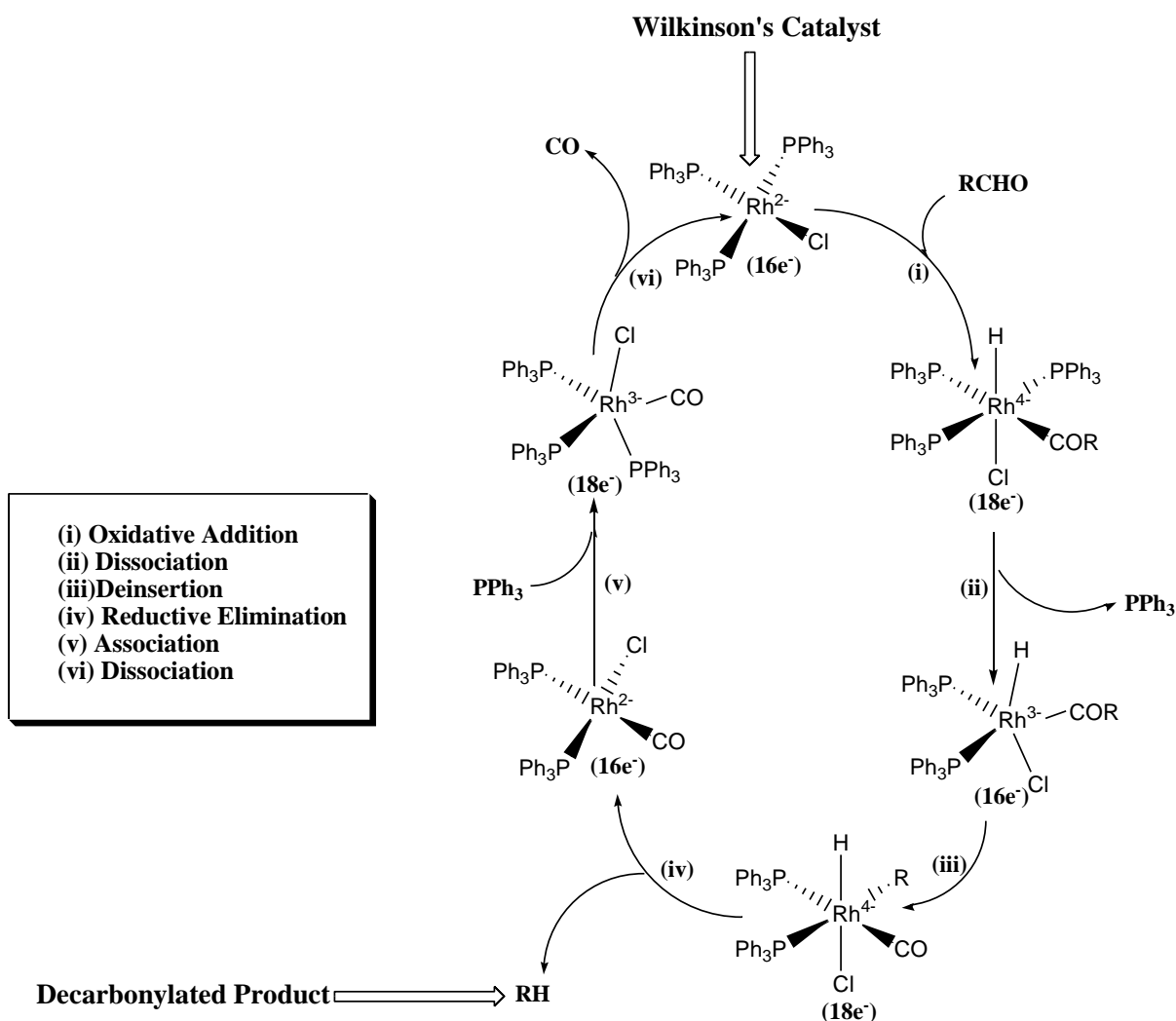
Fig 3.2 Mechanism of decarbonylation by rhodium catalyst (Wilkinson's catalyst)[50]

Because of the easy and fast decarbonylation, –CHO is usually used as an auxiliary group in order to reduce the electron density of benzene ring and, thus, to activate it towards S_NAr. Among leaving groups, the kinetics of –NO_2 in radiolabelling of benzaldehydes substituted by –OCH_3 groups has been reported previously[55]. But in benzaldehydes having –$N^+(Me_3)_3$, the effect of electron donating groups such as –OCH_3 (+M) or –CH_3 (+I) on radiofluorinations was yet to be studied. For this purpose, various homoaromatic model compounds were synthesized throughout this work (*see 3.1.1*).

On the contrary, in order to avoid this additional step (removal of –CHO) in radiosyntheses, an interesting alternative appeared to be the use of substituted pyridines. Because of the presence of N-atom within the ring, pyridine resembles benzene having strong electron-withdrawing groups. This specific characteristic of pyridine is evident by the following two examples i.e. amination by sodium amide, known as the *"Chichibabin reaction"* and alkylation or arylation by organolithium compounds (Fig 3.3).
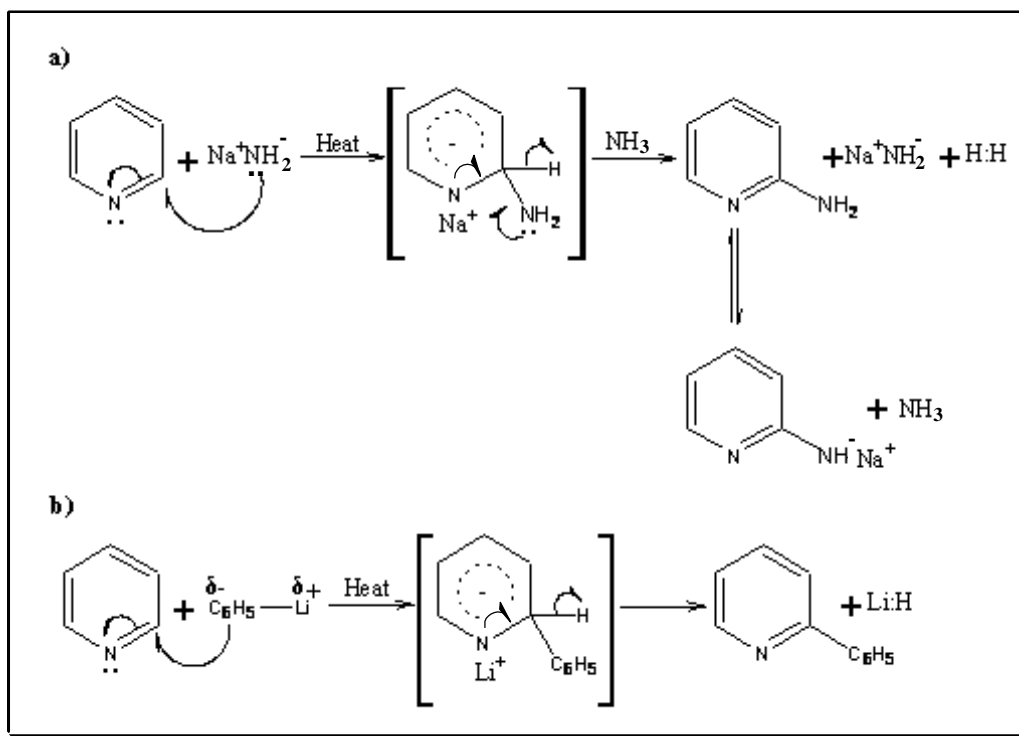
Fig 3.3 S$_N$Ar by (a) Chichibabin reaction b) Arylation using organolithium compound

The above two examples have shown that the reactivity of pyridine towards nucleophilic substitution is so great that even the powerfull basic hydride ion (–H$^-$) can be displaced. In comparison to benzene, this fast kinetics is reflected by the relatively higher chemical shift values of ^{1}H-NMR (8.54 ppm) as well as ^{13}C-NMR (150 ppm) of C-atom adjacent to the highly electronegative N-atom of the ring (Fig 3.4).
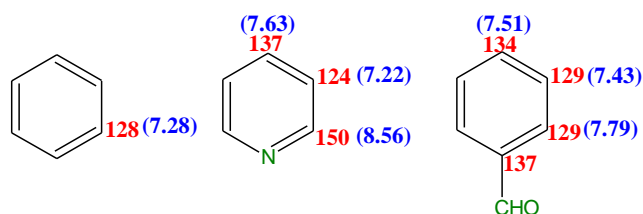
Fig 3.4 Comparison of ^{1}H-NMR (values in brackets, blue colour) and ^{13}C-NMR (red colour) chemical shift values (δ, ppm) in benzene, pyridine and benzaldehyde

For studying the kinetics of radiofluorinations in pyridines substituted by electron-donating groups such as –OCH$_3$ or –CH$_3$ group, different heteroaromatic model compounds (*see 3.1.2*) were designed comprising of different leaving groups (–NO$_2$, –F, –Br, –Cl).

3.1.1   Homoaromatic Model Compounds

Among homoaromatics, different compounds having quaternary salt [–N$^+$(CH$_3$)$_3$] as a leaving group were selected (Fig 3.5) because that had not been studied in case of S$_N$Ar until now. Compound (**2**) corresponds to be the model compound for synthesis of phenylalanine with –CH$_3$ representing the position for the glycine moiety. Furthermore, the compounds (**3**), (**4**) and (**5**) were tested to study the

influence of –OCH$_3$ groups on [^{18}F]fluorination as hydroxyl groups are usually protected as –OCH$_3$ e.g. in case of [^{18}F]-L-tyrosine and [^{18}F]FDOPA. Compounds (**6**) and (**7**) were labelled in order to check the kinetics of –N$^+$(Me$_3$)$_3$ group as a leaving group even without the presence of an auxiliary group.

Another model compound (**8**) was designed having –CHO and –CH$_3$ groups both in *ortho* position to the leaving group. Two synthetic pathways [Scheme-5: route (a) and (b)] were followed but instead of the desired product, some by-products were obtained as confirmed by NMR and mass spectra.

With -CHO in *para*

With -CHO in *para* or in *ortho* and -CH$_3$ in *ortho*

With -CHO in *ortho* and -OCH$_3$ in *para* or *meta*

With -CH$_3$ in *ortho*

LG = -N$^+$(Me$_3$)$_3$CF$_3$SO$_3$$^-$
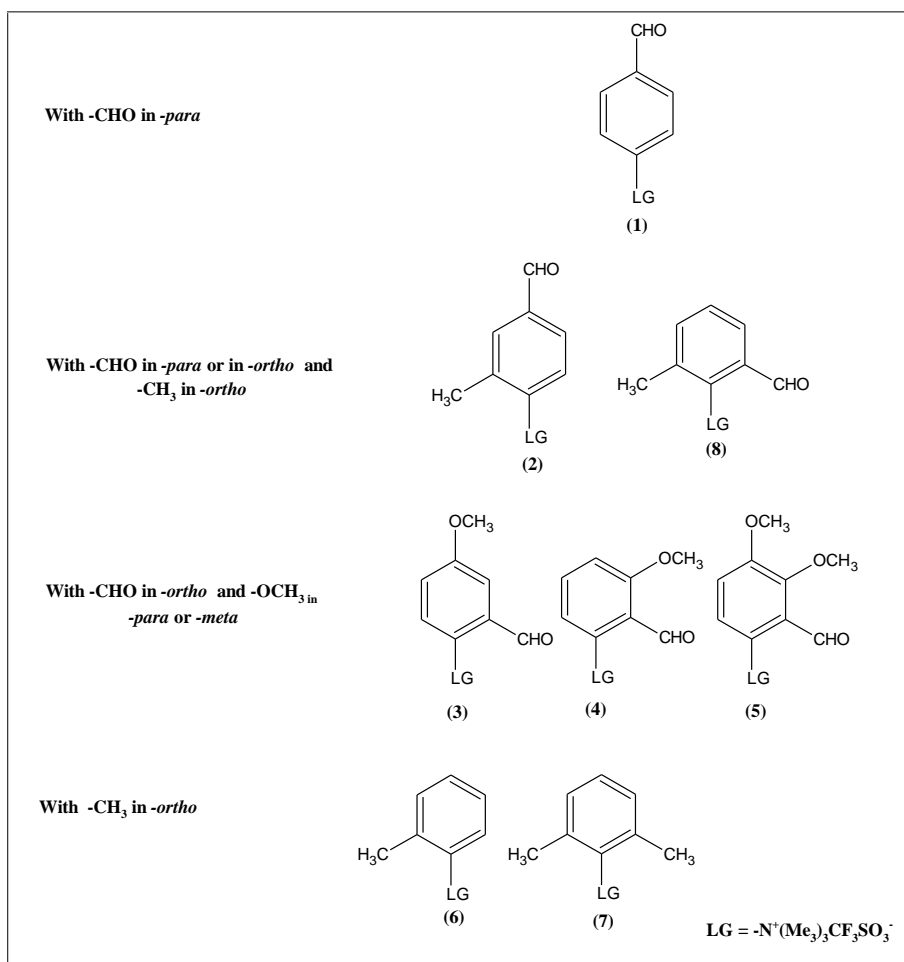
Fig 3.5 Substituted benzaldehydes having quaternary ammonium salt as a leaving group

3.1.1.1 Organic Synthesis

Above mentioned homoaromatic model compounds were synthesized by the following pathways (*see 5.2*):

Scheme-1

Methyltrifluoromethane sulfonate
(1.75 eq)

DCM, RT
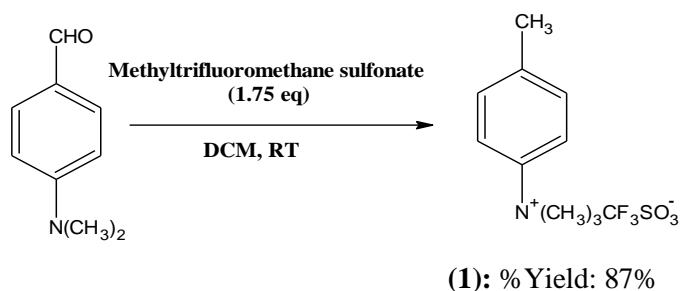
(**1**): % Yield: 87%

Organic synthesis was carried out by one step. Precursor (**1**) was directly synthesized from commercially available starting compound using methane trifluoromethane sulfonate in DCM at RT.

Scheme-2
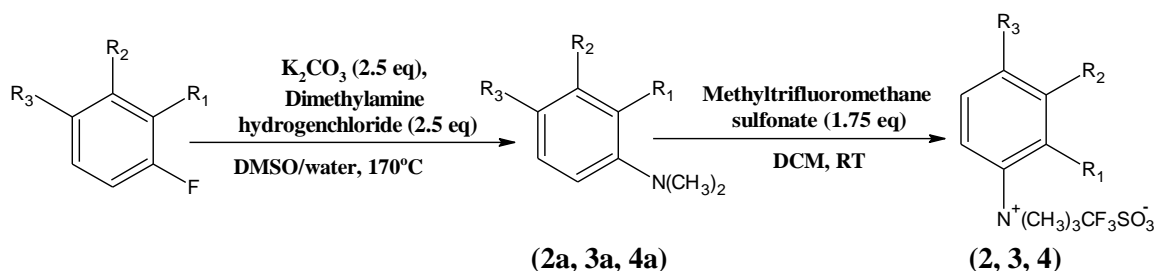
(**2**): R_1= CH_3; R_2=H; R_3=CHO (%Yield: 80%)

(**3**): R_1=CHO; R_2= H; R_3= OCH_3 (%Yield: 81%)

(**4**): R_1= CHO; R_2= OCH_3; R_3= H (%Yield: 85%)

Organic synthesis was carried out *via* two steps. First step was the formation of *N,N*-dimethylamine by substitution of the fluoro group using dimethylamine hydrogenchloride in the presence of K_2CO_3 as a base. A DMSO/water mixture was used as a solvent system and the reaction was carried out at 170°C. Final precursors (**2, 3, 4**) were synthesized from intermediates (**2a, 3a, 4a**) by using methane trifluoromethane sulfonate in DCM at RT.

Scheme-3
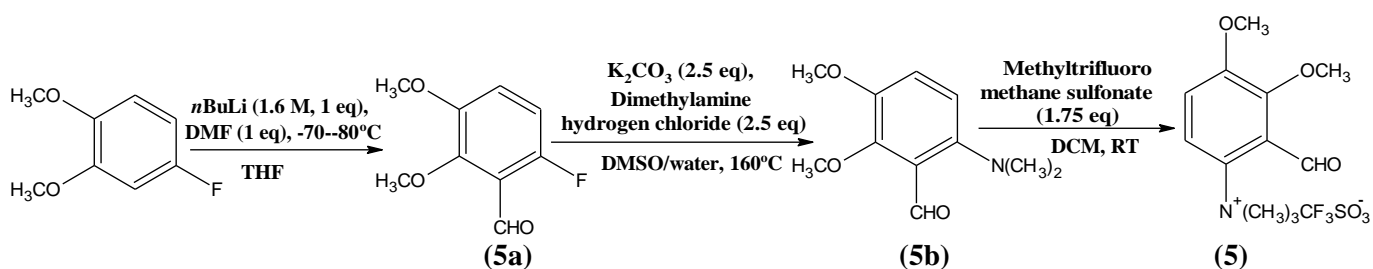
(%Yield: 75%)

Compound (**5**) was synthesized by a three-step synthesis. First step was a formylation for introducing the –CHO group in *ortho* position to the fluoro group using *n*-BuLi along with DMF at -70 to -80°C in THF as solvent. Substitution of the fluoro group by *N,N*-dimethylamine was carried out at 160°C by dimethylamine hydrogenchloride in presence of K_2CO_3 as base producing the intermediate (**5b**) and using methane trifluoromethane sulfonate in DCM at RT yielding the precursor (**5**).

Scheme-4

Organic synthesis of compound (**8**) was carried out by two routes. But from each route, instead of the expected product, several by-products were formed. The structure of the by-product formed *via* route (b) was confirmed by NMR as well as mass spectra.

Route (a)

(8a)   **(8b)**   **(8c)**
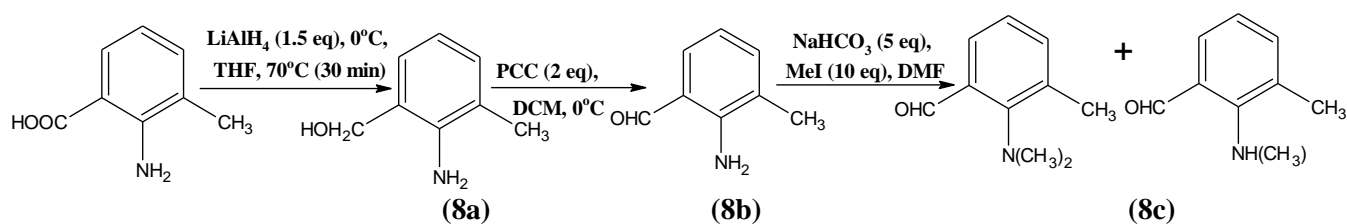
Note: Always a mixture of monomethylamine and dimethylamine was obtained instead of only **(8c)** which couldn't be separated because of the same retention factors on TLC and same retention times on HPLC, therefore, the synthetic route was changed to route (b).

Route (b)

(8a)   **(9a)**

PCC (2 eq), DCM, 0°C

NMR showed
1,8-dimethyl-1,4-dihydro-2H-3,1-benzoxazine
as the main product

(9b)

Scheme-5

(6a, 7a)   **(6, 7)**
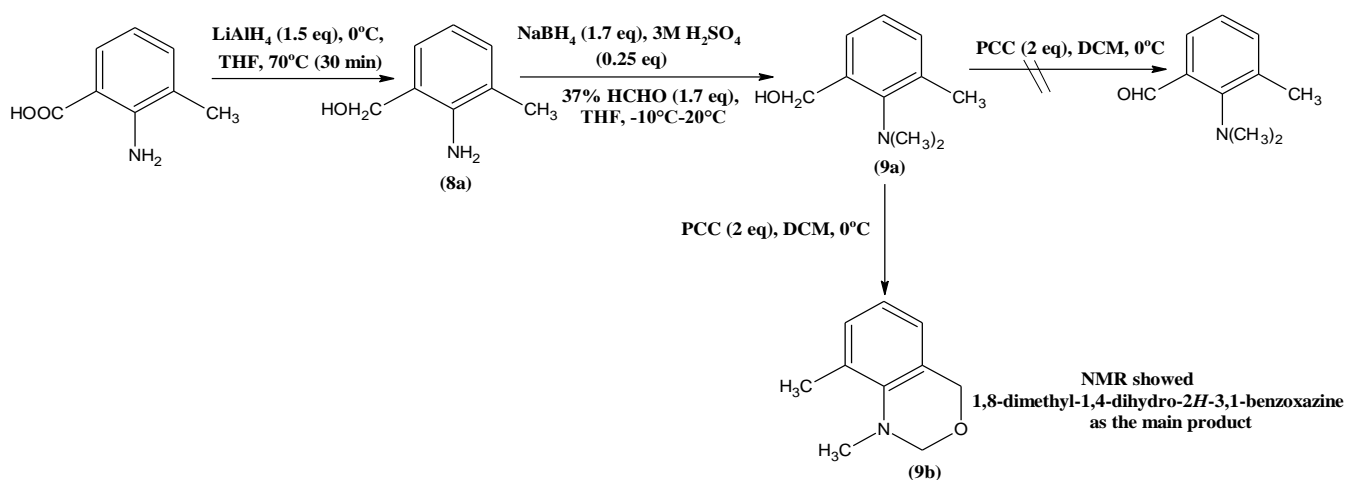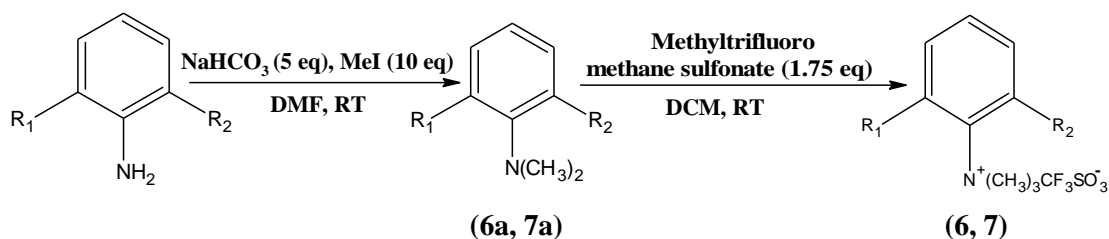
(6): R_1=H; R_2=CH_3 (% Yield: 80%)

(7): R_1= CH_3; R_2=CH_3 (% Yield: 77%)

The organic synthesis was carried out *via* two steps. At first, the methylation of –NH_2 group was performed by using $NaHCO_3$ as a base and iodomethane (MeI) as an alkylating reagent. Reaction was carried out at room temperature (RT) in DMF as a solvent. Secondly, the precursors **(6, 7)** were synthesized from intermediates **(6a, 7a)** by using methane trifluoromethane sulfonate in DCM at RT.

3.1.2   Heteroaromatic Model Compounds

For enhancing nucleophilc aromatic substitution, an interesting alternative is the heteroatom within the hetroaromatic system, for which pyridine is the leading example. The neighbouring position

of the nitrogen is known to be well-suited for a nucleophilic substitution reaction (*see Fig 3.3*). Labelling with fluorine-18, however, was only studied in a few cases for which ^{18}F-substituted purines[56] and nicotinic acid amides[57] are typical examples. Dolci *et al.* (1999) evaluated for the first time the scope of nucleophilic aromatic fluorinations of 2-substituted pyridine rings using the activated [^{18}F]FK-K222 complex (carbonated Kryptofix system)[58-59]. However, the effect of electron-donating substituents on nucleophilic substitution has not been studied until now. That is of particular interest, since in case of substituted benzenes without an auxiliary group, a nucleophilic substitution is thought to be almost impossible to occur. So, different compounds were selected comprising of nitro or halopyridines substituted by –CH$_3$ or –OCH$_3$ or by both groups or by –CHO group in *ortho* position to the leaving group (Fig 3.6).
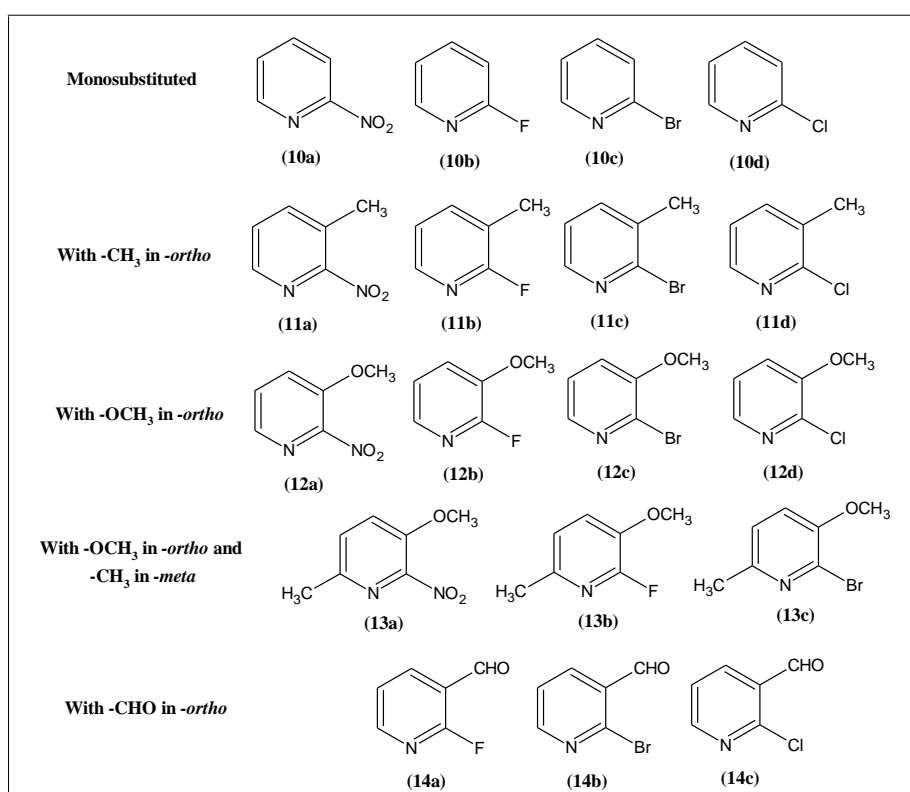
Fig 3.6 Model compounds of substituted pyridines for studies of heteroaromatic S$_N$Ar

3.1.2.1 Organic Synthesis

Most of the compounds were commercially available. The rest were synthesized as described in the following.

Scheme-7
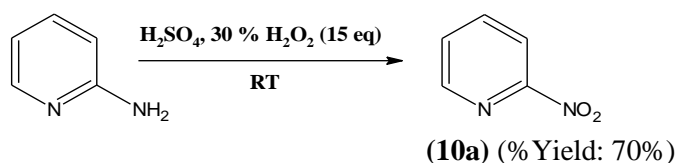
Compound **(10a)** was synthesized by direct oxidation of amino (-NH$_2$) group into –NO$_2$ group in acidic media (H$_2$SO$_4$) in the presence of 30% H$_2$O$_2$ at RT.

Scheme-8
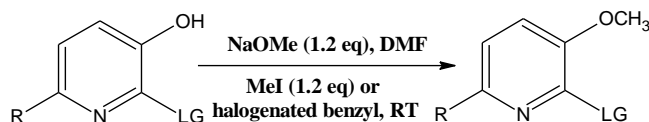
(12d): R=H; LG=Cl (% Yield: 80%)

(13a): R=CH$_3$; LG= NO$_2$ (% Yield: 81%)

(13c): R= CH$_3$; LG= Br (% Yield: 85%)

Simple methoxylation was carried out for preparation of compounds **(12d, 13a, 13c)** in the presence of base (NaOMe) in DMF using MeI at RT.

Scheme-9 (Synthesis of Reference Standards)
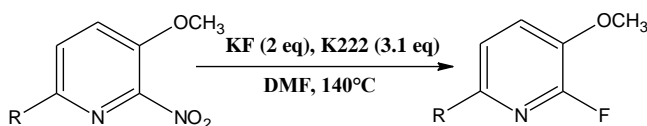
(12b): R=H (% Yield: 60%)

(13b): R=CH$_3$ (% Yield: 56%)

Standards **(12b, 13b)** were prepared from precursors **(12a, 13a)** by nucleophilic aromatic substitution using KF in presence of K222 and DMF at 140°C.

3.1.3 Analytical Assay of the [^{18}F]-Labelled Product

In analytical radiochemistry, the identity and purity of [^{18}F]-labelled products is checked precisely mainly by radio-TLC and radio-HPLC. For all [^{18}F]-labelling experiments, three analytical protocols were applied.

3.1.3.1 Method 1

Aliquots from the reaction mixture after radiofluorination are spotted on TLC plates along with a spot for the standard (marked under UV by spotting the [^{18}F]fluoride activity). These TLC plates are analysed by means of a phosphor imager. In addition, HPLC analytics was also carried out by using a NaI (TI)-scintillation detector for highly volatile [^{18}F]-labelled products and because of low resolution of TLC. Peaks of [^{18}F]-labelled products were identified in radio-HPLC by comparing the UV signals shown by non radioactive standards with the radioactive signal. Furthermore, the peaks of final [^{18}F]-labelled compounds were collected and activity was additionally measured by a γ-counter and, thus, RCY was calculated by relating the activity of the product peak to the total activity injected in the HPLC-system.

3.1.3.2 Method 2

In order to apply LC/MS analysis, carrier-added nucleophilic fluorinations were performed in the presence of a K^{19}F (spray-dried) as a carrier (c.a. reaction). In these experiments, K^{19}F is added to increase the mass of fluorinated product because the mass of ^{18}F-labelled product is too low to be

detected by LC/MS. Such c.a. experiments may lead to poor RCY but allow the characterization of ^{18}F-labelled products by finding the mass of [^{19}F]-product the within the fraction collected by HPLC of specific retention time.

3.1.3.3 Method 3
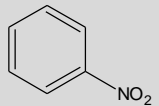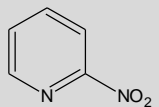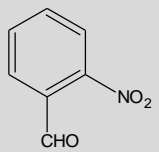
By this method, identification was carried out by comparing the retention times (R_t, HPLC) and R_f values (TLC) of the [^{18}F]-labelled product resulting after hydrolysis of different precursors.

3.2 Factors Effecting [^{18}F]Fluorination by S_NAr

3.2.1 Effect of Electron-Withdrawing Group (EWG)

In case of homoaromatic compounds with a quaternary ammonium group, the maximum RCY (89±0.6%) was observed for compound (**1**) after a reaction time of 10 min. This high yield is caused by the presence of formyl group (-CHO) as an electron-withdrawing substituent in *para* position to the leaving group. But as discussed above, the –CHO group has to be removed after a labelling step. In order to eliminate that additional step, the interesting alternative is the use of pyridine instead of benzene as the nitrogen atom present in the ring acts as an auxiliary group and has an unambiguous effect in enhancing RCYs as can be seen in case of 2-nitropyridine exhibiting a radiochemical yield of 84±3% at a temperature of 140°C after 20 min as also reported in the literature[59] (Table 3-1; Appendix-1).

Table 3-1 Radiochemical yields (RCYs) at different temperatures and reaction times for 2-nitropyridine, nitrobenzene and 2-nitrobenzaldehyde.

Compound	μmoles/mL	Temperature (°C)	n	% RCY		
				7 min	20 min	30 min
(nitrobenzene)	81.2	140°C	4	-	-	1±0.1
(2-nitropyridine)	81	140°C	4	76±1.1	84±3 (90±3)*	88±1
		60°C	3	65±2	79±2	80±3
(2-nitrobenzaldehyde)	66.2	140°C	5	84±0.4	83±1	82±3.6
		60°C	3	57±3	61±3.5	62±3.6
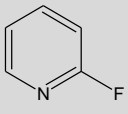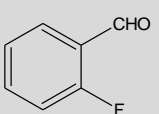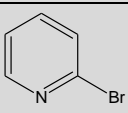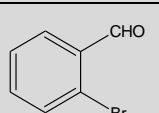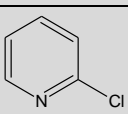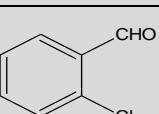
Labelling conditions (for all compounds): Precursor (10 mg), DMF (1 mL), Kryptofix 2.2.2 (15 mg), 3.5 % K$_2$CO$_3$ (100 μL), *****Analysis by HPLC

When compared to nitrobenzene[97] and 2-nitrobenzaldehyde[97], the labelling yield of 2-nitropyridine (84±3%, 20 min) was almost similar to that of 2-nitrobenzaldehyde (83±1%, 20 min) at

140°C, but for both compounds, the labelling yield is reduced by one third after 7 min at lower temperatures e.g. 60°C. However, 2-nitropyridine still remained to be substituted in a yield of 80% at 30 min at 60°C (Table 3-1).

For halogens as leaving groups, $^{18}F/^{19}F$ isotopic exchange resulted in relatively high RCYs as compared to –Br and –Cl. In case of 2-fluoropyridine, RCY was found to be 83±1.5% at 140°C after a reaction time of 20 min (Appendices-2, 3, 4; Table 3-2).

Table 3-2 Radiochemical yields (RCYs) at different temperatures and reaction times of 2-halopyridines and 2-halobenzaldehydes.

2-Halo pyridines	μmoles/mL	% RCY (20 min)	2-Halo Benzaldehydes[97]	μmoles/mL	% RCY (30 min)
(2-fluoropyridine)	103	83±1.5 (90±2)*	(2-fluorobenzaldehyde)	81	75±1
(2-bromopyridine)	63.3	56±3 (66±3)	(2-bromobenzaldehyde)	54	74±0.7
(2-chloropyridine)	88	57±3 (61±2)	(2-chlorobenzaldehyde)	71	69±1.1

Labelling conditions (for all compounds): Precursor (10 mg), DMF (1 mL), Kryptofix 2.2.2 (15 mg), 3.5 % K_2CO_3 (100 μL), ***Analysis by HPLC

When at 140°C the labelling of 2-fluoropyridine and that of 2-fluorobenzaldehyde[97] were compared, 2-fluoropyridine was labelled in a RCY of 83±1.5% within 20 min but 2-fluorobenzaldehyde showed a RCY of 75±1% within 30 min (Table 3-2). Interestingly, the RCY observed in case of 2-bromopyridine (56±3%) and 2-chloropyridine (57±3%) were quite lower than their corresponding benzaldehydes (Table 3-2).

From the above results, it can be concluded that the electron-withdrawing efficiency of the heteroatom in pyridine appears to be stronger than that of the aldehyde group in benzene and, thus, high RCYs can be obtained within short reaction times when using –NO_2 as a leaving group.

3.2.2 Effect of Electron-Donating Groups (EDGs)

In case of benzenes, the introduction of a methyl group increases the electron density of the aromatic ring (+I-effect) and, thus, the reactivity towards nucleophilic attack is reduced. A methoxy group exhibits an even stronger electronic effect (+M-effect), and hence, the nucleophilic substitution is less facilitated. Thus, it was necessary to study the effect of such groups on the overall RCY, because for the syntheses of radiopharmaceuticals, model compounds are usually designed having electron-donating substitutents on aromatic rings. Methoxy (–OCH_3, for –OH protection) and methyl

(–CH$_3$, linker for glycine moiety) are two such substituents that may be involved to the synthesis of final radiotracers.

3.2.2.1 Effect in Homoaromatics

Among homoaromatics, model compounds (**2, 3, 4, 5, 6** and **7**) were synthesized for this purpose. In case of compound **(2)** having methyl group in *ortho* position to the leaving group [-N$^+$(CH$_3$)$_3$] and in *meta* position to the –CHO group, RCY was 69±1% at 3 min and decreased to 53±1.1% after 30 min. In addition, for compounds **(6, 7)**, ca 2% of RCYs were obtained at 3 min. These very low RCY values were due to the absence of an auxiliary group (-CHO) on the benzene ring (Appendix-5; Fig 3.7).
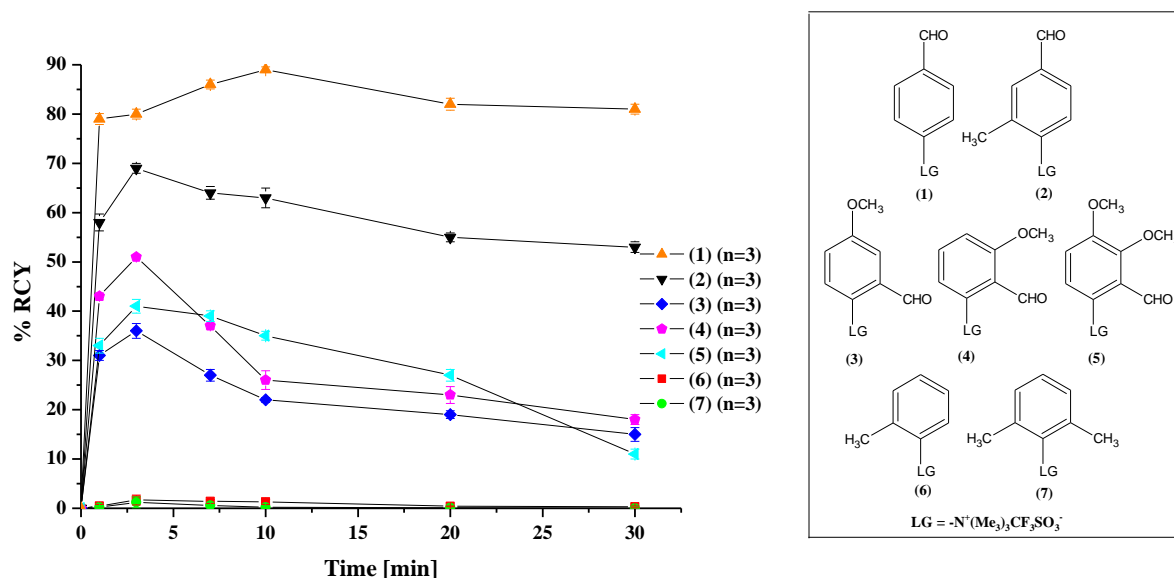
Fig 3.7 Dependence of the RCYs on reaction time at 140°C for S$_N$Ar by [^{18}F]fluoride

As all reactions were performed at 140°C, the maximum decrease in RCY (36±1.5%, 3 min) was observed in case of compound **(3)** in which the electron-donating effect (+M) of –OCH$_3$ group was very strong because of being present in *para* position to the leaving group. For compound **(4)**, this mesomeric effect was minimal (RCY: 51±0.4%, 3 min) as –OCH$_3$ is present in *meta* position to the –N$^+$(CH$_3$)$_3$. In case of compound **(5)** bearing two methoxy groups, in *para* and *meta* position to the leaving group, the maximum RCY was 41±1.4% at a reaction time of 3 min. However, in all above mentioned compounds **(3, 4, 5)**, the RCY decreased down to ca 10% at 30 min (Fig 3.7).

That decrease in RCY was due to the dominant competing demethylation resulting in the formation of ^{18}F-CH$_3$. In addition, the kinetics of forming by-products such as ^{18}F-CH$_3$ and *N,N*-dimethylaminobenzaldehyde became fast with passage of time[98] (Fig 3.8).
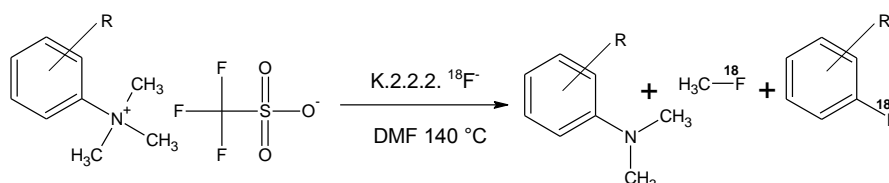
Fig 3.8 Demethylation after [^{18}F]fluorination

3.2.2.2 Effect in Heteroaromatics

Model compounds composed of pyridine rings with –CH$_3$ or –OCH$_3$ substituents in *ortho* position to leaving groups were used for [^{18}F]fluorination by S$_N$Ar. For 3-methyl-2-nitropyridine **(11a)**, the labelling yield was the highest at 140°C (89±1%, 30 min). Compared to 3-methyl-2-nitrobenzaldehyde (48±5%, 7 min)[97], the labelling yield was higher (84±2%, 7 min) for 3-methyl-2-nitropyridine at 140°C (Table 3-3). In case of 3-methyl-2-nitrobenzaldehyde **(11a)**, it may be recalled that the lower yield was due to the formation of a by-product by a condensation reaction[97] (Fig 3.9).

R = H or OCH$_3$
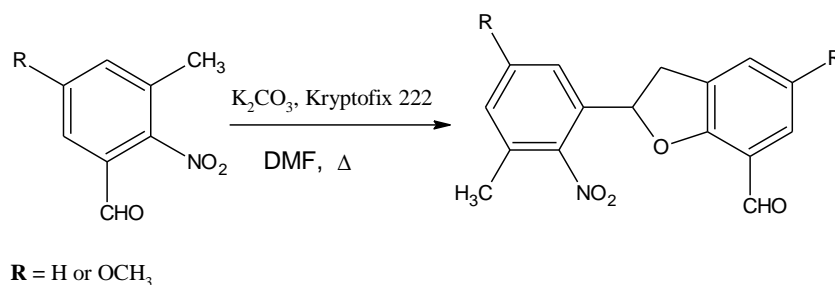
Fig 3.9 Condensation reaction for precursors containing *o*-nitrotoluene structure[97]

In case of 3-methoxy-2-nitropyridine **(12a)** at 140°C after 1 min of reaction time, 88±1% RCY was obtained. When compared to 3-methoxy-2-nitrobenzaldehyde (66.5±4, at 30 min)[97], labelling yields were higher for 3-methoxy-2-nitropyridine (91±0.4, at 30 min) at 140°C (Table 3-3). For 3-methoxy-6-methyl-2-nitropyridine **(13a)** at 30 min of reaction time, a high yield of 81±1% was obtained at 140°C.

The attack of nucleophile (^{18}F$^-$) to substitute –NO$_2$ group in 3-methoxy-2-nitropyridine **(12a)** can be explained by the following resonating structures of the corresponding substituted 2-nitropyridines (Fig 3.10).
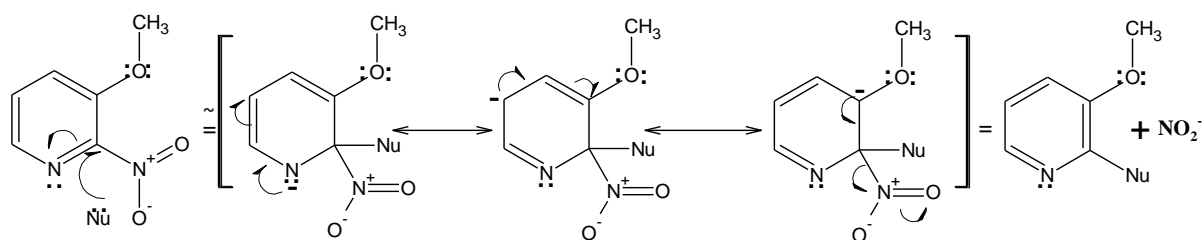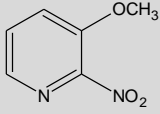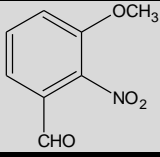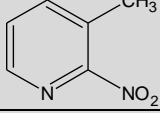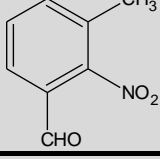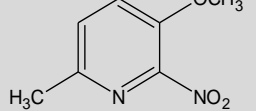
Fig 3.10 Resonance structures for S$_N$Ar in 3-methoxy-2-nitropyridine (Nu = nucleophile)

It strongly reflects the electron deficiency at C-2 and C-6 due to the electron-withdrawing effect of the nitrogen atom of pyridine and, thus, it highly activates the ring for S$_N$Ar. The value of ^{13}C-NMR chemical shift value (148 ppm) shows higher electrophilicity of C-atom bearing –NO$_2$ group in case of 3-methoxy-2-nitropyridine than in corresponding analogue (3-methoxy-2-nitrobenzaldehyde, 137 ppm). This fact is also evident in 3-methyl-2-nitropyridine in which high RCYs at 140°C can be attributed to higher electrophilicity (158 ppm) as compared to that of 3-methoxy-2-nitrobenzaldehyde (148 ppm).

Table 3-3 RCY at 140°C for 2-nitropyridines and 2-nitrobenzaldehydes[97] substituted by electron-donating groups (EDG).

EDG	Compound	μmoles/mL	n	% RCY		
				7 min	20 min	30 min
-OCH₃	(3-methoxy-2-nitropyridine)	65	5 (2)*	90±0.1	90±0.4	91±0.4 (87±1.4)*
	(3-methoxy-2-nitrobenzaldehyde, CHO)	55.2	4	70.1±3	67±3	66.5±4
-CH₃	(3-methyl-2-nitropyridine)	72.4	5 (2)*	84±2	88±1	89±1 (87±3)*
	(3-methyl-2-nitrobenzaldehyde, CHO)	61	6	48±5	45.6±4.9	45±4.5
-CH₃ & -OCH₃	(6-methyl-3-methoxy-2-nitropyridine)	59.5	4	79±1.6	81±0.6	81±1
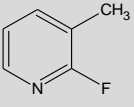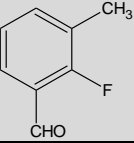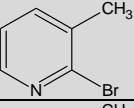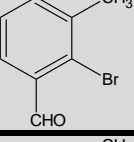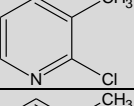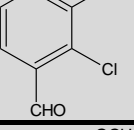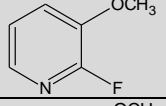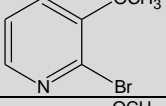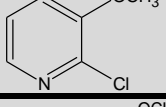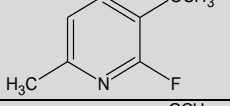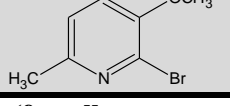
Labelling conditions (for all compounds): Precursor (10 mg), DMF (1 mL), Kryptofix 2.2.2 (15 mg), 3.5 % K_2CO_3 (100 μL), *Analysis by HPLC

When comparing the methyl substituent with the methoxy group, interestingly, the methoxy and methyl group in *ortho* position to the leaving group showed only a small effect on the labelling reaction. The observation is even more evident in case of 2-nitropyridine substituted by both groups i.e. methoxy (in *ortho* position to –NO₂) and methyl (in *meta* position to –NO₂).

Among halogens, the effect of electron-donating substituents such as –OCH₃ and –CH₃ was more pronounced in –Cl and –Br substituted pyridines than in pyridines having –F as leaving group (Table 3-4). In case of 3-methyl-2-fluoropyridine **(11b)**, 3-methoxy-2-fluoropyridine **(12b)** and 6-methyl-3-methoxy-2-fluoropyridine **(13b)**, high RCYs of 80±1%, 78±1%, and 55±3%, respectively, were obtained at 140°C. The results showed that in 2-fluoropyridines, substitution by a methyl (80±1%) or a methoxy (78±1%) group resulted in almost the same RCY at 140°C after 30 min.

Comparison of 3-methyl-2-fluoropyridine **(11b)** and 3-methyl-2-fluorobenzaldehyde[97] showed that both compounds have high and almost similar RCYs of 80±1% (30 min) and 79±3% (3 min), respectively (Table 3-4).

Table 3-4 RCYs for radiofluorinations of 2-halopyridines and 2-halobenzaldehydes[97] substituted by electron-donating groups (EDG).

Substituent	Compound	μmoles/mL	n	% RCY±SD (30 min)
-CH$_3$	(pyridine, CH$_3$, N, F)	90	4	80±1
	(benzaldehyde, CH$_3$, F, CHO)	72.4	4	61±1.4 (79±3)[b]
	(pyridine, CH$_3$, N, Br)	58	4	47±1.6
	(benzaldehyde, CH$_3$, Br, CHO)	50	5	50±5
	(pyridine, CH$_3$, N, Cl)	78	4	13.6±1
	(benzaldehyde, CH$_3$, Cl, CHO)	65	5	61±8
-OCH$_3$	(pyridine, OCH$_3$, N, F)	79	5	78±1
	(pyridine, OCH$_3$, N, Br)	53	4	41±3 (39±1.4)*
	(pyridine, OCH$_3$, N, Cl)	70	3	20±0.7 (25±3)*
-CH$_3$ & -OCH$_3$	(pyridine, OCH$_3$, H$_3$C, N, F)	71	4	55±3
	(pyridine, OCH$_3$, H$_3$C, N, Br)	49.5	3	20±0.6%

Labelling conditions (for all compounds): 140°C, Precursor (10 mg), DMF (1 mL), *Analysis by HPLC, [b]Maximum RCY at 3 min.

In case of 2-bromo-3-methylpyridine **(11c)**, 2-bromo-3-methoxypyridine **(12c)** and 2-bromo-3-methoxy-6-methylpyridine **(13c)**, the maximum RCYs obtained after 30 min of reaction time were 47±1.6%, 41±3%, and 20±0.6%, respectively (Table 3-4). The RCY for 2-bromo-3-methyl-pyridine **(11c)** was almost similar to 2-bromo-3-methylbenzaldehyde[97] (50±5%) at 30 min at 140°C (Table 3-4).

Among the halogen derivatives, RCYs were the lowest for $-CH_3$ and $-OCH_3$ substituted 2-chloropyridines. Even at 140°C, the maximum RCYs for 2-chloro-3-methylpyridine and 2-chloro-3-methoxypyridine were around 20% at a reaction time of 30 min (Table 3-4). Contrarily, RCY obtained for the corresponding 2-chloro-3-methylbenzaldehyde was 61±8% (30 min).

In summary, the effect of electron-donating groups was more pronounced at lower temperature. However, methoxy- and methyl- substituted pyridines can efficiently be substituted by [^{18}F]fluoride at reaction temperatures > 100°C within a reaction time between 10 and 30 min. In addition, pyridines having a $-NO_2$ leaving group showed RCYs of almost 90% irrespective of being substituted by $-CH_3$ or $-OCH_3$ group in *ortho* position. Among halogens, RCYs remained as high as 80% at 140°C for methyl- or methoxy- substituted 2-fluoropyridines. But the reason of the low yield of labelling of 6-methyl-3-methoxy-2-fluoropyridine **(13b)** may be attributed to unknown side-reactions. In addition, in case of methyl substituted 2-chloro- and 2-bromopyridines, electron-donating effects were stronger in reducing RCYs as compared to the corresponding methyl substituted benzaldehydes. Also, the lower RCY obtained in case of 2-halo-3-methoxypyridines in comparison to that of 2-halo-3-methylpyridines indicated a significant impact of the $-OCH_3$ over the $-CH_3$ group on the radiofluorination reaction.

3.2.3 Effect of Temperature

In radiofluorinations *via* S_NAr reactions, the effect of temperature on RCYs in dependence on reaction time is usually very significant, and hence, it was essential to study the [^{18}F]-labelling for all precursors at different temperatures (30°C to 140°C) as well as at different reaction times (1, 3, 7, 10, 20, 30 min). For all precursors, fast kinetics of radiofluorinations were observed at high temperature such as 140°C, whereas there was a rapid decrease in RCYs when decreasing the temperature to 30°C.

For simple 2-substituted pyridines, 2-nitropyridine **(10a)** showed 79±0.5%, 84±3% and 88±1% at 140°C after 10, 20 and 30 min, respectively. At 60°C, 65±2%, 79±2% and 80±3% were obtained at 10, 20 and 30 min of reaction time, respectively (Appendix-1; Fig 3.11). Even, at 30°C, the maximum RCY still was 63±0.8% after 30 min.
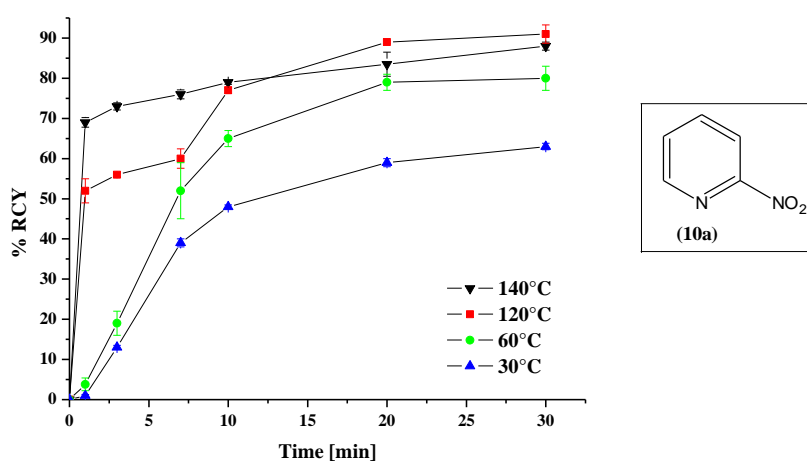
Fig 3.11 Dependence of RCY on time and temperature for 2-nitropyridine (10a) in S_NAr

In case of 2-fluoropyridine **(10b)**, the RCY was around 80% at 140°C at 20 min, and it decreased slightly to 68±0.8% (20 min) at 120°C. This effect of temperature was more pronounced at 60°C where RCYs of 19±1.6% were observed after 30 min of reaction time (Appendix-2; Fig 3.12).
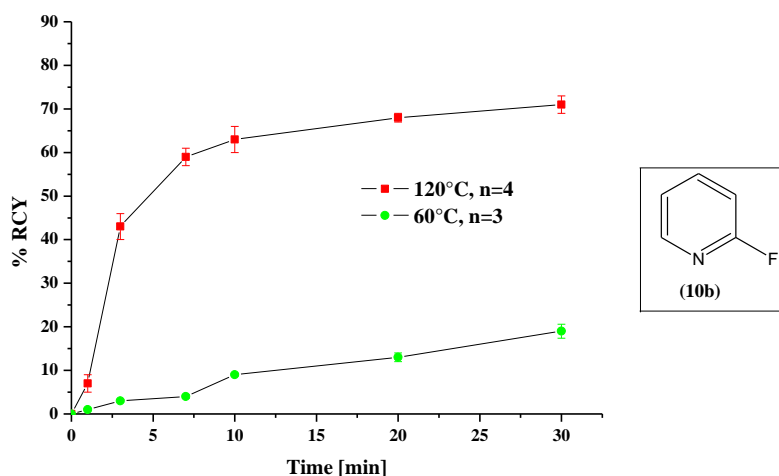
Fig 3.12 Dependence of RCY on time and temperature 2-fluoropyridine (10b) for ^{18}F/^{19}F exchange

For 2-bromopyridine **(10c)** and 2-chloropyridine **(10d)**, RCYs were as low as 40-50% even at 140°C after 20 min of reaction time. However, at 120°C and at 60°C, the RCYs for **(10c)** and **(10d)** were around 15% and 3%, respectively, after a reaction time of 30 min (Appendices-2,3; Fig 3.13).
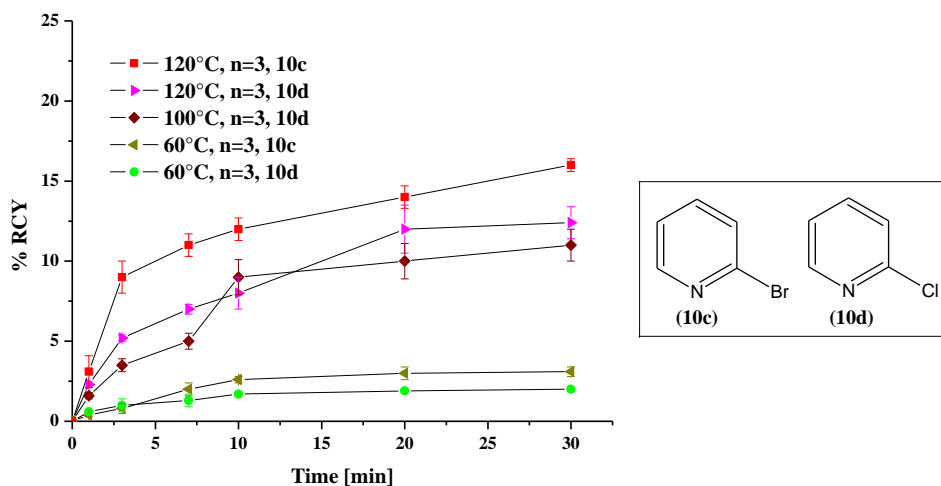
Fig 3.13 Dependence of RCY on time and temperature for 2-bromo (10c) and 2-chloropyridine (10d) for the substitution of halogen by [^{18}F]fluoride

In case of 2-nitropyridines substituted by –CH_3 or –OCH_3 group, maximum RCYs were in the range of 81-90% at 140°C at 30 min of reaction time. For 3-methyl-2-nitropyridine **(11a)**, even at 1 min, 72±2% RCY was obtained at 140°C and it increased to 87±1.5% at 10 min of reaction time. But at 120°C after 30 min, maximum RCY of 72±3 % was obtained while at 60°C it decreased to 51±1.4% after 30 min (Appendix-1; Fig 3.14).
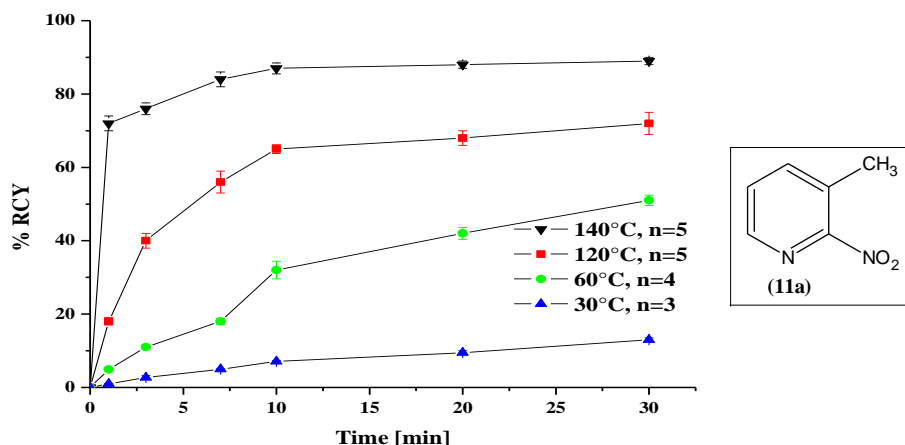
Fig 3.14 Dependence of RCY on time and temperature for 3-methyl-2-nitropyridine (11a) in case of –NO$_2$ substitution by [^{18}F]fluoride

When going down to 30°C, the RCY decreased to 13±0.5%. The great difference was due to the formation of a [^{18}F]-labelled by-product. The TLC analysis (R$_f$: 0.48) illustrated that 60% of this [^{18}F]-labelled by-product formation occurred at 30°C, while it was only 3% at 140°C (Fig 3.15).
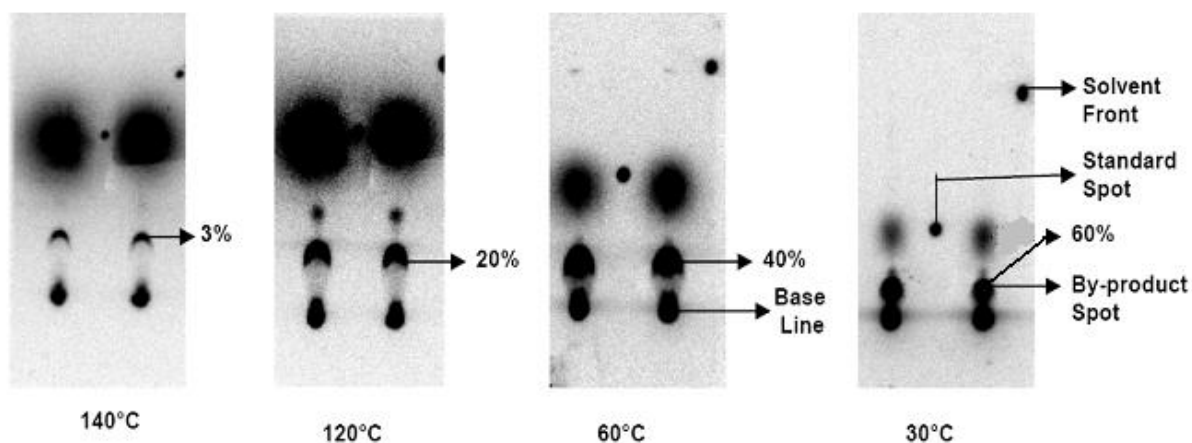
Fig 3.15 Radio-TLC plates monitoring the S$_N$Ar of 3-methyl-2-nitropyridine (11a) by [^{18}F]fluoride at 30°C, 60°C, 120°C and 140°C after 30 min (Eluent: PE/EtAc: 3/1)

For 3-methoxy-2-nitropyridine (**12a**), after 30 min at all temperatures, maximum yields were in the range of 88-91% (Appendix-1; Fig 3.16). At 120°C, 86±1% and 90±0.6% RCYs were observed at reaction time of 10 and 30 min, respectively. Even at 60°C and 30°C, labelling yields of 77±1.5% and 49±0.9% were found after 10 min, respectively. However, the highest RCY (88±2%) at 60°C was obtained at 30 min. But at 1 min, RCYs were as low as 14.6±3% at 60°C and 33±4% at 120°C.
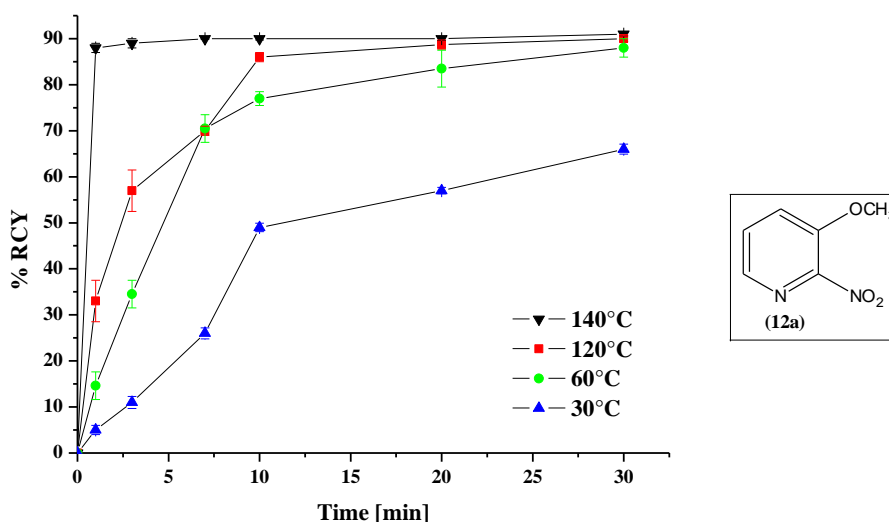
Fig 3.16 Dependence of RCY on time and temperature for the reaction of 3-methoxy-2-nitropyridine (12a) with [^{18}F]fluoride

For 3-methoxy-6-methyl-2-nitropyridine **(13a)**, even at 1 min at 140°C, 57±3% RCY was observed that increased to 79±1.6% at 7 min. At 120°C after 10 min of reaction time, RCY was 79±1.3%. However, when going down to lower temperatures such as 60°C and 30°C, maximum RCYs (30 min) were 70±1% and 22±1%, respectively (Appendix-1; Fig 3.17).
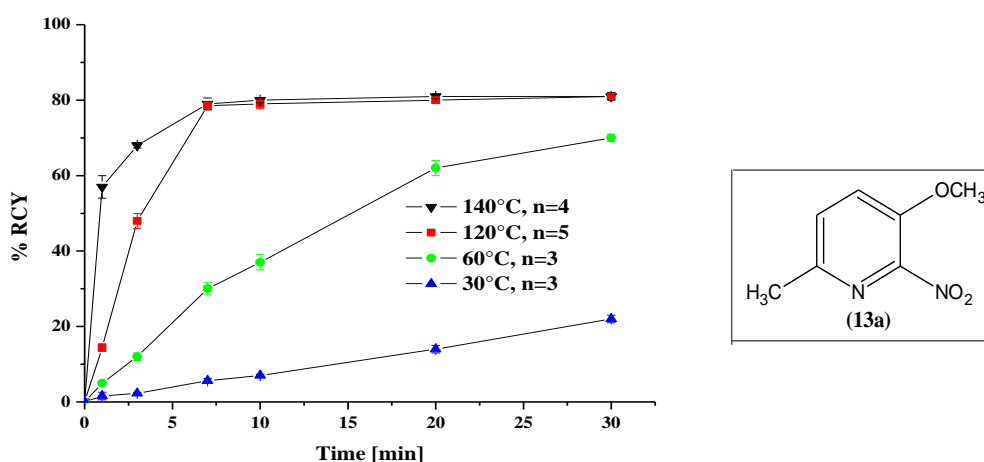
Fig 3.17 Dependence of RCY on time and temperature for 3-methoxy-6-methyl-2-nitropyridine (13a) in case of –NO$_2$ substitution by [^{18}F]fluoride

For substituted 2-fluoropyridines, the highest RCY (80±1%, 30 min) was obtained for 2-fluoro-3-methylpyridine. However, in case of 2-fluoro-3-methoxypyridine, RCYs were 74±0.8% and 78±0.6% at 10 min and 30 min, respectively. The important role of temperature in enhancing the yield of nucleophilic substitution reactions was particularly illustrated by decreasing the reaction temperature to 120°C where RCYs were 59±2%, 49±1% and 46±2%, respectively, for compounds **(11b, 12b, 13b)** after a reaction time of 30 min (Appendix-2; Fig 3.18).
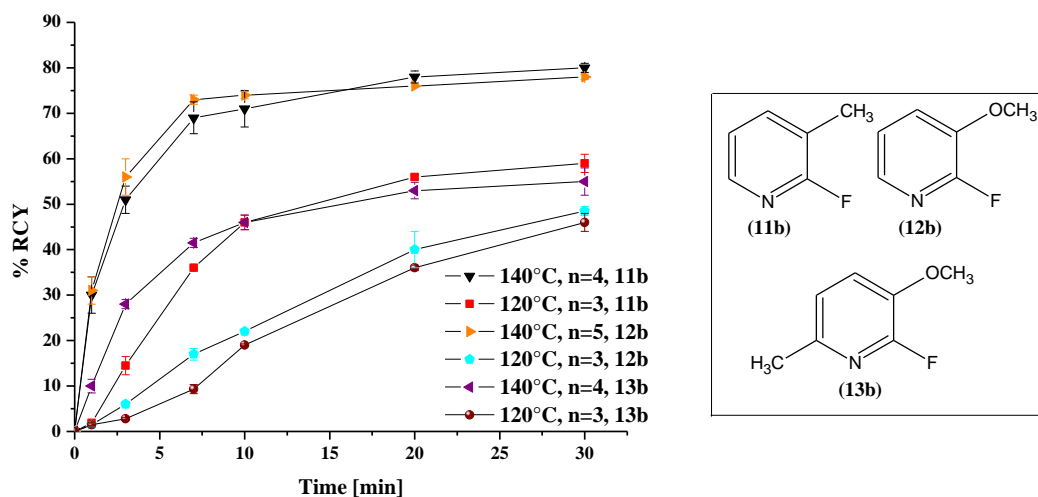
Fig 3.18 Dependence of RCY on time and temperature for substituted 2-fluoropyridines *via* [18]F/^{19}F exchange

In case of 2-bromo-3-methylpyridine (**11c**) and 2-bromo-3-methoxypyridine (**12c**), 47±1.6% and 41±3% of RCYs, respectively, were obtained at 140°C after 30 min of reaction time. However, the RCY for both compounds decreased to 20% when lowering the temperature to 120°C. For 2-bromo-3-methoxy-6-methypyridine (**13c**), 28±1.1% (30 min) RCY was observed at 140°C (Appendix-3; Fig 3.19).
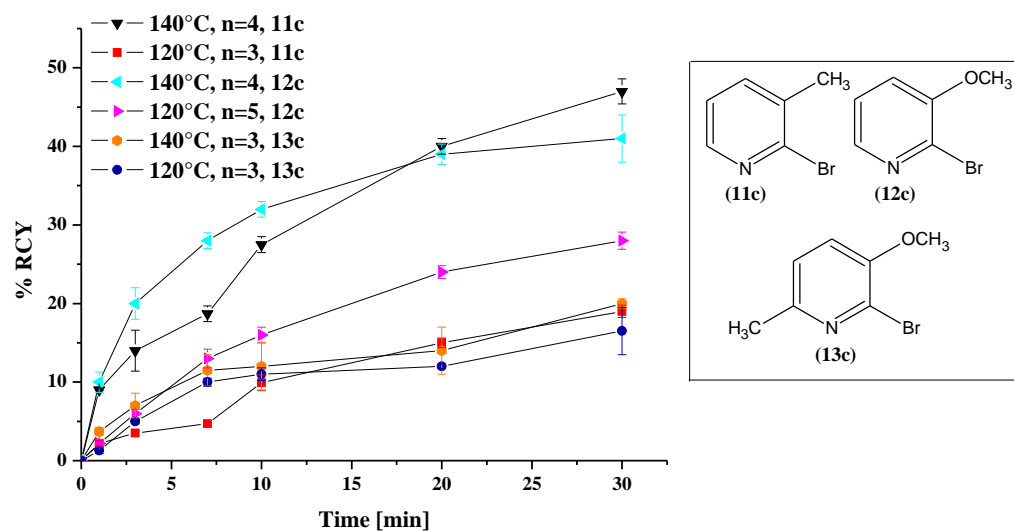
Fig 3.19 Dependence of RCY on time and temperature for substituted 2-bromopyridines in case of –Br substitution by [^{18}F]fluoride

For 2-chloro-3-methylpyridine (**11d**) and 2-chloro-3-methoxypyridine (**12d**), RCYs were around 10% even at 140°C at 30 min of reaction time. However, the RCYs for both compounds decreased to 2% when lowering down the temperature to 120°C (Appendix-4; Fig 3.20).
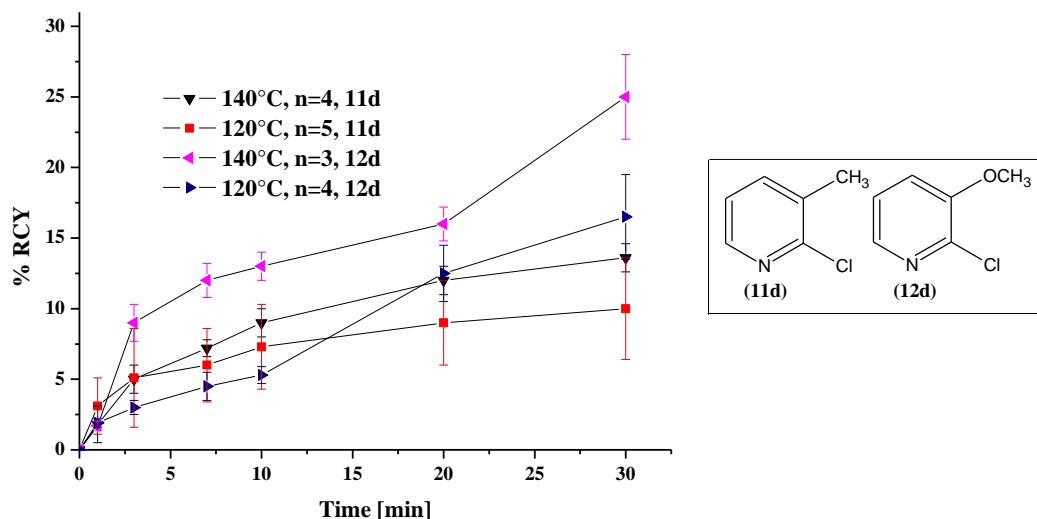
Fig 3.20 Dependence of RCY on time and temperature for substituted 2-chloropyridines *via* S$_N$Ar

For 2-fluoropyridine substituted by –CHO (EWG) in *ortho* position to the leaving group, the highest RCY (77±1.3%) was obtained at 1 min of reaction time while it decreased to 8±1.5% at 30 min. Similarly, at 60°C, the highest RCY (75±0.6%) was observed at 1 min but decreased to 54±3% after 30 min. However, the reduction in RCY was more pronounced at high temperature (140°C) than at lower one (60°C) (Appendix-2; Fig 3.21).
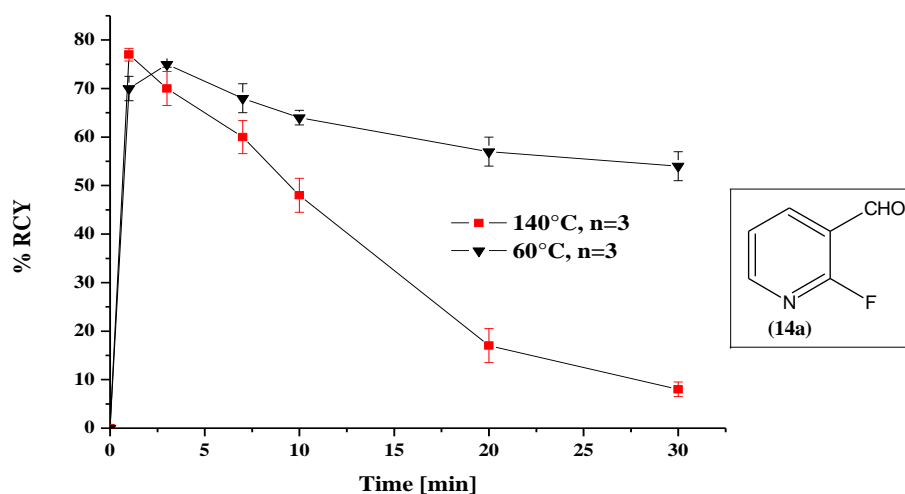
Fig 3.21 Dependence of RCY of radiofluorination on time and temperature for 2-fluoro-3-nicotinaldehyde (14a)

In case of 2-bromo-3-nicotinaldehyde **(14b)**, 84±4% and 85±1% of RCYs were obtained at 140°C and at 100°C, respectively, after 3 min of reaction time. Thereafter, the RCY decreased to 50% at 30 min. At 60°C, also a high yield of 79.5±1% of RCY was obtained at 20 min, after which it decreased to 76±1% at 30 min. However, the RCY at 30°C was 50±7% after 30 min. Hence, the curve showed a slow but steady increase in RCYs with the passage of time at 60°C and 30°C (Appendix-3; Fig 3.22).
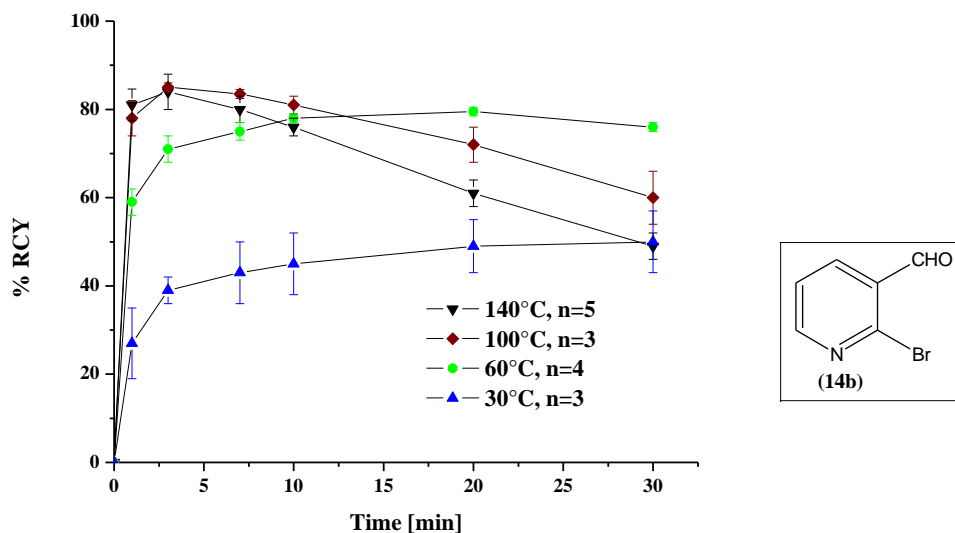
Fig 3.22 Dependence of RCY on time and temperature for 2-bromo-3-nicotinaldehyde (14b) after radiofluorinations

For 2-chloro-3-nicotinaldehyde (**14c**), the maximum RCY so obtained was around 75% at 140°C (1 min) and at 60°C (30 min). At 100°C, maximum RCY was 70±2.5% after 1 min of reaction time but it decreased rapidly to 1.5±0.4% at 30 min (Appendix-4; Fig 3.23).
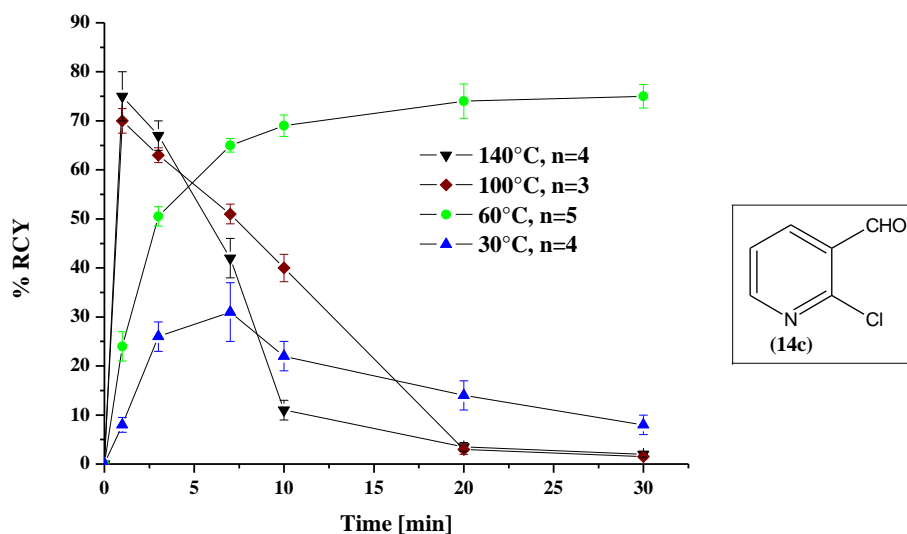
Fig 3.23 Dependence of RCY on time and temperature for 2-chloro-3-nicotinaldehyde (14c) for –Cl substitution by [¹⁸F]fluoride

These results showed that at lower temperatures, the dependency of RCY on time was more pronounced as compared to at 140°C, especially in case of substituted 2-nitropyridines. Further, fast kinetics of radiofluorination *via* S_NAr was observed in case of all precursors. However, among all halopyridines, substituted 2-fluoropyridines showed good RCYs at 140°C. In addition, in case of substituted 2-bromo- and 2-chloropyridines, the RCYs remained < 50% at all temperatures after 30 min of reaction time. However, for 2-halo-3-nicotinaldehydes having –CHO as an electron withdrawing substituent (EWG), RCY was highly dependent on reaction time and also, fast kinetics (RCY≈80%) were observed at high temperatures ≥ 100°C after 3 min but afterwards yields decreased
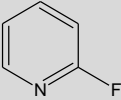
to $\leq 50\%$ at 30 min of reaction time because of the strong dominating decomposition reaction. But at low temperatures $\leq 60°C$, labelling yields were increasing with time, being maximum ($\approx 70\%$) at 30 min.

3.2.4 Specific Activities in Isotopic Exchange ($^{18}F/^{19}F$)

In case of homoaromatic systems such as [^{18}F]FDOPA, radiofluorinations are mainly performed *via* electrophilic substitution by means of [^{18}F]F_2 containing high amount of carrier. Hence, specific activities typically are in the range between 4 MBq/µmol and 20 MBq/µmol. Contrarily, high attainable specific activities are possible *via* S_NAr by [^{18}F]fluoride (n.c.a.) produced by cyclotrons. Although in isotopic exchange, specific activity is assumed to be low, ^{18}F-labelling was studied in dependence on the substrate concentrations for 2-[^{18}F]-fluoropyridine (Table 3-5).

Specific activities ranged from 0.524 GBq/µmole at the substrate concentration of 103 µmoles/mL to 11.65 GBq/µmol for 1.03 µmoles/mL (Table 3-5). Although, the higher specific activity was obtained at a lower RCY of 20%, it could be of practical importance both for preclinical and clinical applications. The reason is that very high amounts of [^{18}F]fluoride can be produced at commonly used medical cyclotrons (> 120 GBq in 1 h) and so, in spite of lower radiochemical yields, high amounts of the product are obtained.

Table 3-5. Specific activities of isotopic exchange in 2-fluoropyridine by [^{18}F]fluoride.

Amount [mg]	µmoles/mL	% RCY±SD*	[a]Specific Activity [EOS, GBq/µmol]
10	103	90±2	0.524
5	51.5	68±1	0.792
1	10.3	59±3	3.44
0.5	5.15	45±2	5.24
0.1	1.03	20±2	11.65

Labelling conditions: DMF (1 mL), 140°C, 20 min , *Analysis by HPLC, [a]Specfic activity at end of synthesis (EOS) after application of an aliquot of a 60 GBq [^{18}F]fluoride batch obtained after irradiation for 60 min with a current of 35 µA.

In conclusion, the results showed that $^{18}F/^{19}F$ isotopic exchange in 2-fluoropyridine is an efficient labelling technique resulting in radiochemical yields up to 80% in short reaction times even if 2-fluoropyridine is substituted by an electron-donating group. Moreover, this labelling technique can be of high practical value since specific activities can be a factor of 100 and much better than electrophilic radiofluorinations.

3.2.5 Leaving Group Tendency in Pyridines

In the light of all results as shown above, the following tendency was observed in the order of increasing RCY among all leaving groups in case of substituted pyridines:

$$-NO_2 > -F > -Br > -Cl$$
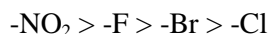
Hence, it became clear that $[^{18}F]$fluorodenitration demonstrates the fast kinetics even at temperature as low as 60°C and even in presence of electron-donating substituents. Furthermore, the isotopic exchange ($^{18}F/^{19}F$) also showed high RCYs but in strong dependence on time and temperature.

3.2.6 Energy of Activation (E_a)

Rate constants (k', min^{-1}) can be determined from time and temperature dependent curves of RCYs, and hence, by utilizing the vlues of k', the activation energies (E_a)[99] of radiofluorinations can be calculated by Arrhenius plots. Theoretically, a labelling reaction is assumed to follow the pseudo-first-order kinetics because concentration of precursor is always much higher than the corresponding n.c.a. $[^{18}F]$fluoride. For the kinetics of such reaction, the rate is equivalent to the following differential equation:

$-d[^{18}F^-]/dt = k'[^{18}F^-]$

By separating variables:

$-d[^{18}F^-]/[^{18}F^-] = k'dt$

Integrating this equation (boundary conditions $C_o \longrightarrow C$ and $0 \longrightarrow t$) gives:

$-\ln ([^{18}F^-]_t/[^{18}F^-]_o) = k't$

$\ln[^{18}F^-]_o - \ln[^{18}F^-]_t = k't$

$\ln([^{18}F^-]_o/[^{18}F^-]_t) = k't$

Incorporating $[^{18}F^-]_t = [^{18}F^-]_o$-RCY:

$\ln([^{18}F^-]_o/[^{18}F^-]_o$-RCY$) = k't$ *or* $\ln(1$-RCY$/[^{18}F^-]_o) = k't$

As the concentration of $[^{18}F^-]_o$ is almost negligible, thus, the above equation will be equal to:

$$\boxed{\ln(1\text{-RCY}) = k't}$$

Hence, a graph of ln(1-RCY) versus reaction time gives a linear function with a slope of $-k'$. The temperature dependency of labelling reactions is shown by the temperature dependency of the rate constant. The rate constant (k') increases exponentially with increasing temperature. This is expressed usually by the following equation:

$k' = Ae^{-b/T}$ (A and b are empirically determined constants)

According to Arrhenius, $-E_a/R$ can substitute the constant "b", where E_a is the activation energy and R is the gas constant (R = 8.314 J/K mol). Therefore, the equation can be written as:

$k' = Ae^{-(E_a/RT)}$

which may be written in natural logarithmic way as:

$\ln k' = \ln A - (E_a/RT)$

Hence, from a plot of lnk' against 1/T (K), a linear function with the slope of -E_a/R is obtained. Thus, for the calculation of activation energy mathematically, at least two rate constants measured at different temperatures for one reaction are used:

For T_1: $\ln k_1 = \ln A - E_a/(RT_1)$ For T_2: $\ln k_2 = \ln A - E_a/(RT_2)$

Subtraction of T_2 from T_1 leads to:

$\ln(k_1/k_2) = E_a/R(1/T_2 - 1/T_1)$

From this equation, the activation energy is equivalent to:

$$E_a = R[T_1 T_2/(T_1 - T_2)]\ln(k_1/k_2)$$

In order to calculate the Arrhenius constants (rate constants, min^{-1}), RCYs of 2-nitropyridine **(10a)**, 3-methyl-2-nitropyridine **(11a)**, 3-methoxy-2-nitropyridine **(12a)**, and 3-methoxy-6-methyl-2-nitropyridine **(13a)** were chosen at different time points (1, 3, 7, 10, 20, and 30 min) and at four different temperatures (140°C, 120°C, 60°C, and 30°C). From these rate constants (k'), energy of activation (E_a) was determined graphically. However, for the above mentioned compounds (**10a, 11a, 12a,** and **13a**), E_a were calculated from the rate constants (k') obtained at 120°C, 60°C and 30°C because at 140°C, maximum RCYs at 7 to 30 min of reaction times were as high as 80-90%. The linearity of all graphs was evaluated by the correlation coefficient R^2. A reliable linear graph would be assumed to have "R^2" in the range of 0.7-1.00. Fig 3.24 (Appendicies-6, 8, 10, 12) shows the calculation of k' from linear functions for substituted 2-nitropyridine.
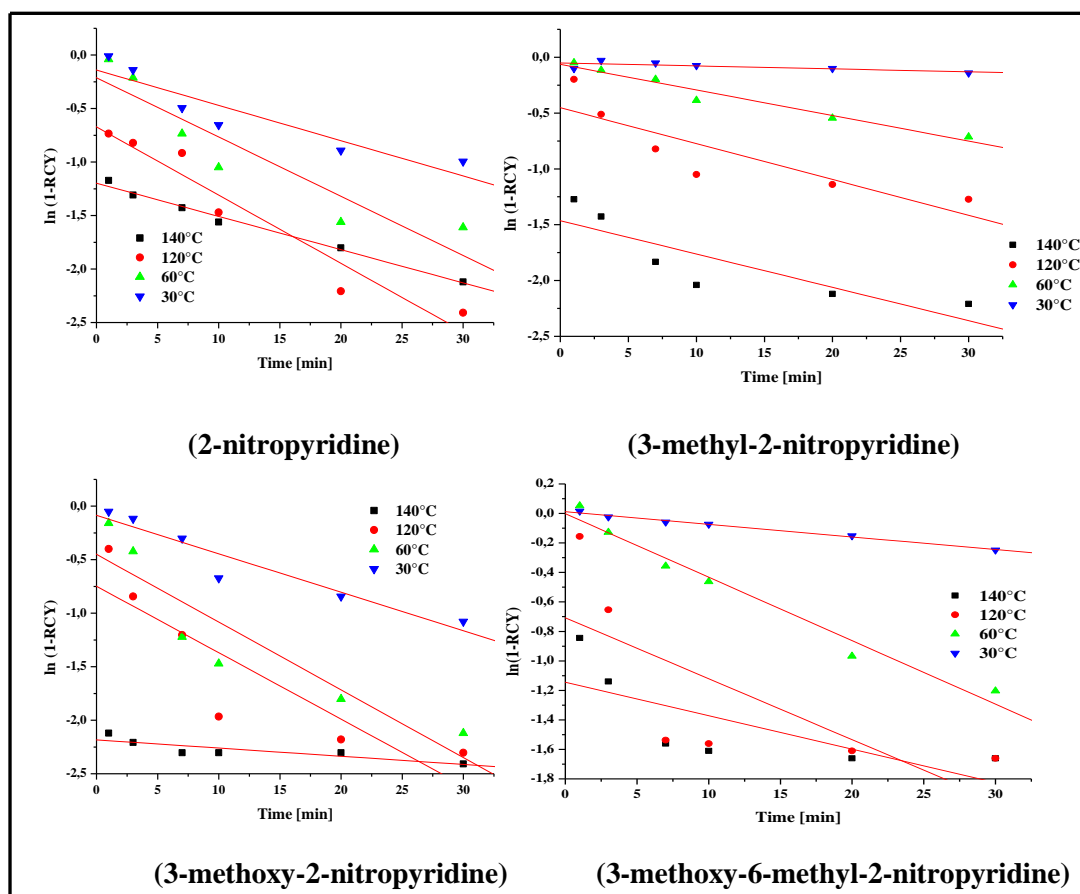
Fig 3.24 Linear functions for determination of k' values for substituted 2-nitro pyridines

Linear functiones obtained from above correlation curves of all four compounds (**10a, 11a, 12a, 13a**) were as follows:

For 2-nitropyridine (10a):

$$T (140°C): \ln (1-RCY/100) = -1.197-0.031*t$$

$$T (120°C): \ln (1-RCY/100) = -0.672-0.064*t$$

$$T (60°C): \ln (1-RCY/100) = -0.213-0.055*t$$

$$T (30°C): \ln (1-RCY/100) = -0.140-0.033*t$$

For 3-methyl-2-nitropyridine (11a):

$$T (140°C): \ln (1-RCY/100) = -1.464-0.0298*t$$

$$T (120°C): \ln (1-RCY/100) = -0.452-0.032*t$$

$$T (60°C): \ln (1-RCY/100) = -0.064-0.023*t$$

$$T (30°C): \ln (1-RCY/100) = -0.051-0.00265*t$$

For 3-methoxy-2-nitropyridine (12a):

$$T (140°C): \ln (1-RCY/100) = -2.183-0.0077*t$$

$$T (120°C): \ln (1-RCY/100) = -0.748-0.062*t$$

$$T (60°C): \ln (1-RCY/100) = -0.450-0.063*t$$

$$T (30°C): \ln (1-RCY/100) = -0.086-0.036*t$$

For 3-methoxy-6-methyl-2-nitropyridine (13a):

$$T (140°C): \ln (1-RCY/100) = -1.145-0.023*t$$

$$T (120°C): \ln (1-RCY/100) = -0.707-0.041*t$$

$$T (60°C): \ln (1-RCY/100) = -0.0021-0.043*t$$

$$T (30°C): \ln (1-RCY/100) = -0.0117-0.0086*t$$

The values of constants (k') were calculated from these above mentioned linear functions obtained graphically by plotting $\ln (1-RCY)$ values against respective time points at different temperatures. These k' values obtained at 120°C, 60°C and 30°C were utilized further in Arrhenius plot of $\ln k'$ versus $1/T*10^{-3}$ values for calculation of E_a for S_NAr (Fig 3.25, Appendicies 7, 9, 11, 13). Energies of activation were calculated from linear functions obtained from Arrhenius plots (Fig 3.23).

For 2-nitropyridine (10a):

$$\ln k' = -0.595-823.02 * 1/T$$

$$E_a = 823.02 \times 8.314 / 1000$$

$$= 6.5 \text{ kJ/mol} = 1.6 \text{ kcal/mol}$$

For 3-methyl-2-nitropyridine (11a):

$$\ln k' = 4.579-3037.99 * 1/T$$

$$E_a = 3037.99 \times 8.314 / 1000$$

$$= 25.3 \text{ kJ/mol} = 6 \text{ kcal/mol}$$

(2-nitropyridine)

(3-methyl-2-nitropyridine)

(3-methoxy-2-nitropyridine)

(3-methoxy-6-methyl-2-nitropyridine)
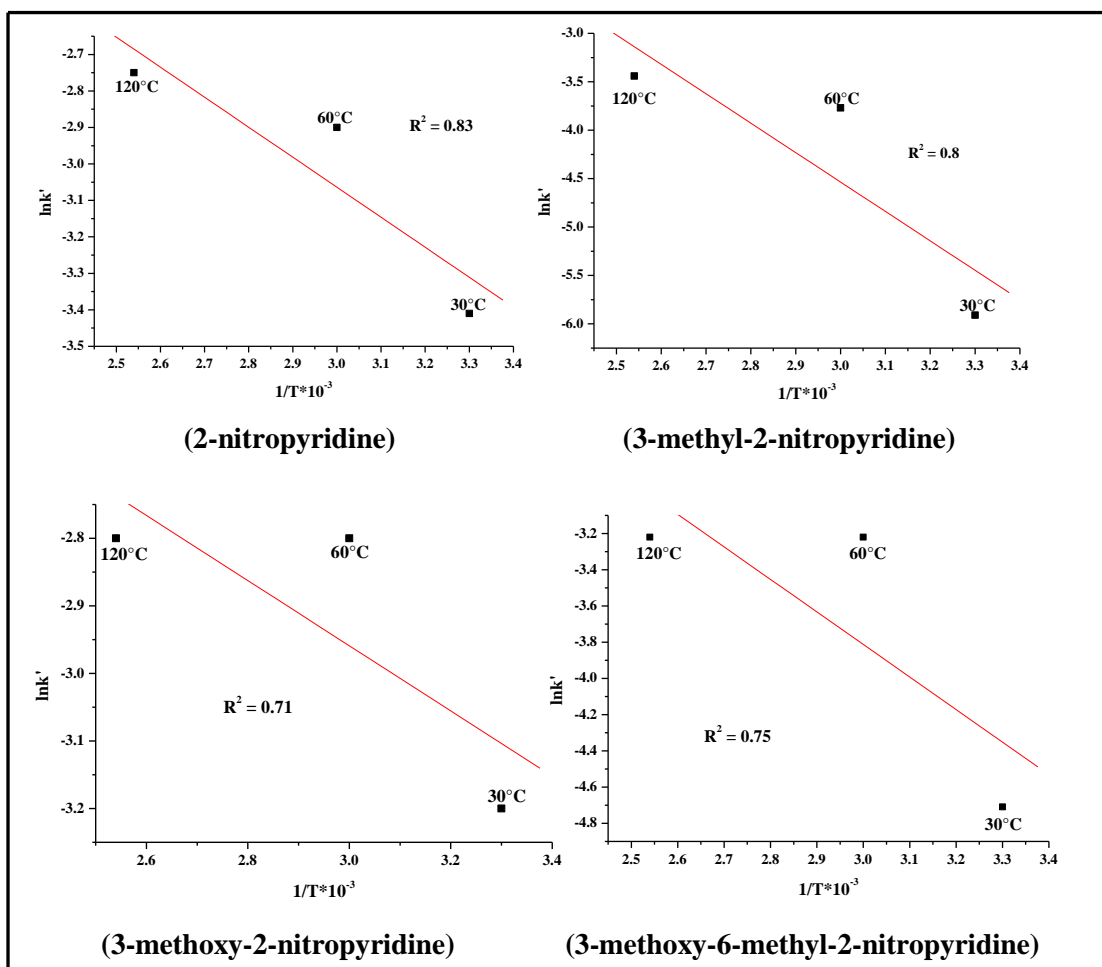
Fig 3.25 Arrhenius plot for substituted 2-nitropyridines for calculation of activation energy

For 3-methoxy-2-nitropyridine (12a):

$$lnk' = -1.512 - 482.26 * 1/T$$

$$E_a = 482.26 \times 8.314 / 1000$$

$$= 4.5 \, kJ/mol = 1.1 \, kcal/mol$$

For 3-methoxy-6-methyl-2-nitropyridine (13a):

$$lnk' = 1.577 - 1796.41 * 1/T$$

$$E_a = 1796.41 \times 8.314 / 1000$$

$$= 14.9 \, kJ/mol = 3.6 \, kcal/mol$$

In case of the compounds **10a**, **11a**, **12a**, and **13a**, energies of activation were found in the range of 4-25 kJ/mol. E_a for 2-nitropyridine was clearly lower (6.5 kJ/mol) than both of 2-nitrobezaldehyde[99] (24 kJ/mol) and nitrobenzene[99] (63.5 kJ/mol). This fact is illustrated by the fast kinetics of radiofluorinations in substituted 2-nitropyridines as compared to the homoaromatic analogues. Moreover, it shows stronger electron-withdrawing ability of the nitrogen atom in pyridine than that of –CHO in benzenes and hence, the pyridine system is highly activated towards S_NAr.

Within the substituted 2-nitropyridines, E_a for 3-methyl-2-nitropyridine (model compound for azaphenylalanine) was higher (25 kJ/mol) than 3-methoxy-2-nitropyridine (4.5 kJ/mol). Such high

value of E_a might be attributed to the formation of radioactive by-product at temperatures < 140°C for 3-methyl-2-nitropyridine (*see 3.4.3*). However, for 3-methoxy-2-nitropyridine (**12a**), the RCYs were high (ca 88%) at all temperatures (except 30°C) at 7 to 10 min of reaction time. Thus, E_a observed in 3-methoxy-2-nitropyridine (4.5 kJ / mol) was almost equal to that of 2-nitropyridine (6.5 kJ / mol).

For 3-methoxy-6-methyl-2-nitropyridine (**13a**), E_a was lower (14.9 kJ / mol) than 3-methyl-2-nitropyridine (25 kJ / mol). This difference could also be due to the strong dominating competing reaction at lower temperatures that decreased the RCY sharply to 51±1.4% at 60°C after 30 min of reaction time whereas for 3-methoxy-6-methyl-2-nitropyridine (**13a**), relatively higher RCY (70±1%) was observed at 60°C at 30 min.

In conclusion, heteroaromatic systems having $-NO_2$ as a leaving group showed lower values of E_a than homoaromatic analogues. Consequently, substituted 2-nitropyridines showed fast kinetics in radiofluorinations by S_NAr.

3.2.7 Selection of Protecting Groups

In case of S_NAr, hydroxylic groups must be protected in order to avoid solvation effects which strongly reduce the reactivity of [^{18}F]-fluoride. For this purpose, usually, methylation of hydroxyl groups is applied (as in compound **13a**). Subsequently, demethylation is typically performed by HBr or HI under elevated temperature such as 150°C and often gives rise to only low deprotection yields. To improve the deprotection yields, Wagner *et al.*[100] and Tierling *et al.*[101] applied benzyl group instead of methyl group for radiosynthesis of 6-[^{18}F]Fluoro-L-DOPA by isotopic exchange (^{18}F$^-$/^{19}F$^-$). Yet, they used HBr at 150 °C for deprotection. Such reaction conditions, however, are poorly suited, e.g., for synthesis of sensitive compounds or for the automated radiosyntheses. In the last case, those harsh conditions led to the corrosive effects on walls, fittings, and tubings as experienced previously[102].

Hence, it was necessary to study new phenolic hydroxyl protecting groups for n.c.a. nucleophilic aromatic radiofluorination aiming at mild deprotection conditions and high deprotection yields. As shown in Fig 3.26, a number of model precursors (for azatyrosine) were synthesized.
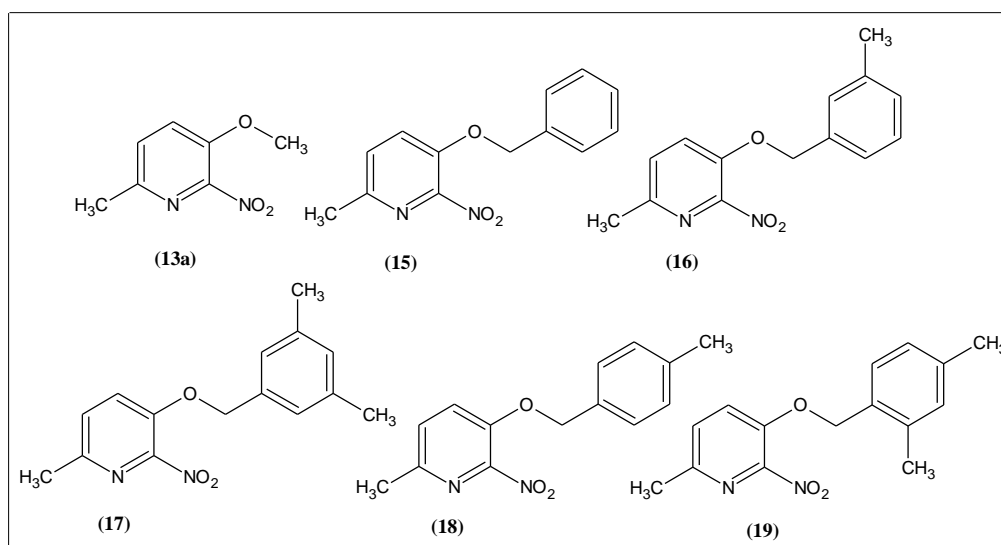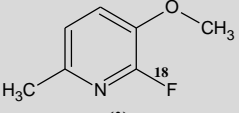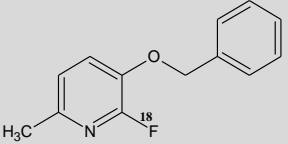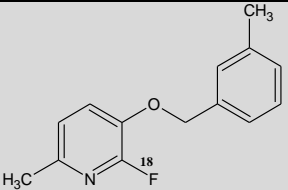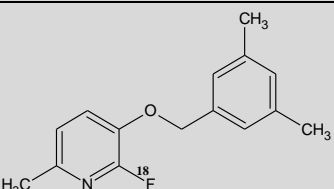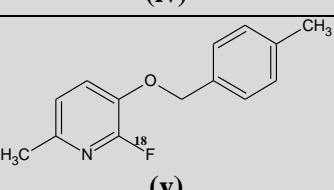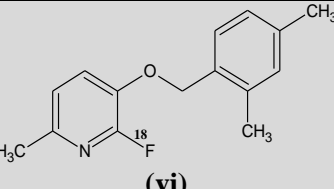
Fig 3.26 Model precursors for studying and optimizing hydrolysis conditions

As a model synthesis, the n.c.a. preparation of 2-[^{18}F]fluoro-3-hydroxy-6-methyl-pyridine from *O*-protected 3-hydroxy-6-methyl-2-nitropyridine was chosen. In addition, different conditions such as acidic hydrolysis and catalytic transfer hydrogenation (catalytic hydrolysis) were applied for cleavage of benzyloxy protecting groups.

3.2.7.1 Acidic Hydrolysis

Deprotection of 2-[^{18}F]fluoro-3-hydroxy-6-methyl pyridine protected with methyl, benzyl, 3-methylbenzyl (*m*-xylyl), 4-methylbenzyl (*p*-xylyl), 3,5-dimethylbenzyl and 2,4-dimethylbenzyl using four different acidic media [HI (NaI/48% HBr), 48% HBr, 32% HCl, and 70% TFA] was studied (Table 3-5).

Table 3-5 RCY after hydrolysis of substituted benzyloxy intermediates at 150°C at 10 min (n=3).

Intermediates	% RCY			
	HI	48%HBr	32%HCl	70%TFA
(i)	58±0.1 (61±0.9)*	51±1.2	29.7±1	22±0.4
(ii)	85±0.3	69±0.5	36±1.5	19±0.5
(iii)	79±0.8	67±1.3	38±1.4	18.5±1
(iv)	77.5±1	71±1.6	55±0.3	33±0.1
(v)	81±0.1 (85±1.8)*	71±0.5 (76±1.3)*	69±0.9 (79±1.6)*	46±1.6 (50±1.5)*
(vi)	82±0.9 (87±2)*	78±2.1 (84±0.7)*	77±1.8 (82±1.1)*	78±0.1 (80±0.3)*

*RCYs calculated from γ-counter in collected peaks after HPLC-separation

At 150°C, good RCYs could be obtained in a reaction time of 10 min. For 2-[^{18}F]fluoro-3-methoxy-6-methylpyridine **(i)**, overall RCY was 58±0.1% when hydrolysed by HI (NaI/48% HBr), whereas hydrolysis with 70% TFA resulted only in a yield of 22±0.4% (Table 3-5).

However, for all studied benzyloxy intermediates, hydrolysis by HI (NaI/48% HBr) gave almost 80% yield of the deprotected product. With 70% TFA, a good RCY (78±0.1%) was also obtained in case of 3-[(2,4-dimethylphenyl)methoxy]-2-[^{18}F]fluoro-6-methylpyridine **(vi)**. Lowest yield after hydrolysis with 70% TFA was observed in case of 2-[^{18}F]fluoro-6-methyl-3-(*m*-tolylmethoxy)pyridine **(iii)** (18.5±1%) and 3-benzyloxy-2-[^{18}F]fluoro-6-methylpyridine **(ii)** (19±0.5%). For deprotection of 2-[^{18}F]fluoro-6-methyl-3-(*m*-tolylmethoxy)pyridine **(iii)** and 3-benzyloxy-2-[^{18}F]fluoro-6-methylpyridine **(ii)** using 48% HBr, the RCYs were ca. 70%. In contrast, after hydrolysis with 32% HCl, RCYs were only about 35% (Table 3-5).

After hydrolysis of 3-[(3,5-dimethylphenyl)methoxy]-2-[^{18}F]fluoro-6-methylpyridine **(iv)** by HI (NaI/48% HBr) and 48% HBr, ca 70% of hydrolysed product was obtained whereas RCYs of hydrolysis decreased to 55±0.3% and 33±0.1% with 32% HCl and 70% TFA, respectively.

In case of 3-[(2,4-dimethylphenyl)methoxy]-2-[^{18}F]fluoro-6-methylpyridine **(vi)** and 2-[^{18}F]fluoro-6-methyl-3-(*p*-tolylmethoxy)pyridine **(v)** (Table-3-5), high RCYs of ca. 80% were obtained with strong acids i.e. HI (NaI/48% HBr), 48% HBr, and 32% HCl. However, hydrolysis of 2-[^{18}F]fluoro-6-methyl-3-(*p*-tolylmethoxy)pyridine **(v)** with 70% TFA, at 150°C after 10 min of reaction time resulted in 46±1.6% of hydrolysed product.

3.2.7.2 Effect of Time and Temperature

In general, a fast reaction was observed within the first 10 min and during this period maximum radiochemical yields (RCYs) were obtained.

In case of 2-[^{18}F]fluoro-6-methyl-3-(*p*-tolylmethoxy)pyridine **(v)**, hydrolysis with 32% HCl at 120°C resulted in RCY of 68±0.4% at 10 min and 57±0.3% at 3 min with full consumption of the protected intermediate. At 60°C, RCY decreased to 47±0.5% at 10 min and at least 5% of the protected intermediate was still present in the reaction media. At room temperature (RT), 45% of the starting material was left along with 39±1% of hydrolysed product (Appendix-14; Fig 3.27).

In contrast, hydrolysis with 70% TFA at 120°C resulted in the RCY of 43±1.4% at 10 min and 35±1.3% at 3 min. Labelled intermediate (unhydrolysed) was almost 51% and 5% at 3 min and 10 min, respectively. At 60°C, RCY decreased to 29±1.9% at 10 min with at least 50% of labelled intermediate still present in reaction media. At RT, labelled reaction intermediate was 70% with hydrolysed product (23±0.2%) (Appendix-14; Fig 3.27).
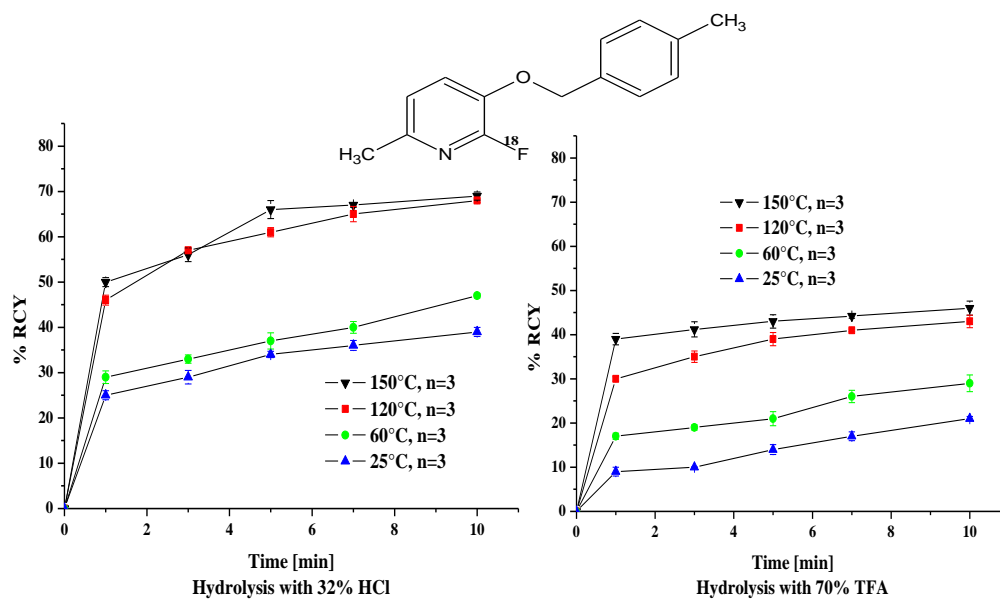
Fig 3.27 Hydrolysis of 2-[^{18}F]fluoro-6-methyl-3-(*p*-tolylmethoxy)pyridine (v) in dependence of RCYs on reaction time at different temperatures

For 2,4-dimethylbenzyl as a protecting group as in 3-[(2,4-dimethylphenyl)methoxy]-2-[^{18}F]fluoro-6-methylpyridine **(vi)**, hydrolysis with 32% HCl at 120°C resulted in RCY of 72±0.7% at 10 min and 57±1% at 5 min with no unhydrolysed intermediate. At 60°C, RCY decreased to 55±0.5% at 10 min with no labelled intermediate. At RT, RCY of hydrolysed product was 39±0.5% at 10 min (Appendix-14; Fig 3.28). The labelled intermediate was completely hydrolysed after 5 min at 120°C, 60°C and RT. Moreover, at 120 °C, hydrolysis with 70% TFA resulted in RCY of 57±0.8% at 10 min and 49±1.1% after 5 min. At lower temperatures (60°C, RT) RCYs decreased to 40 % and less.
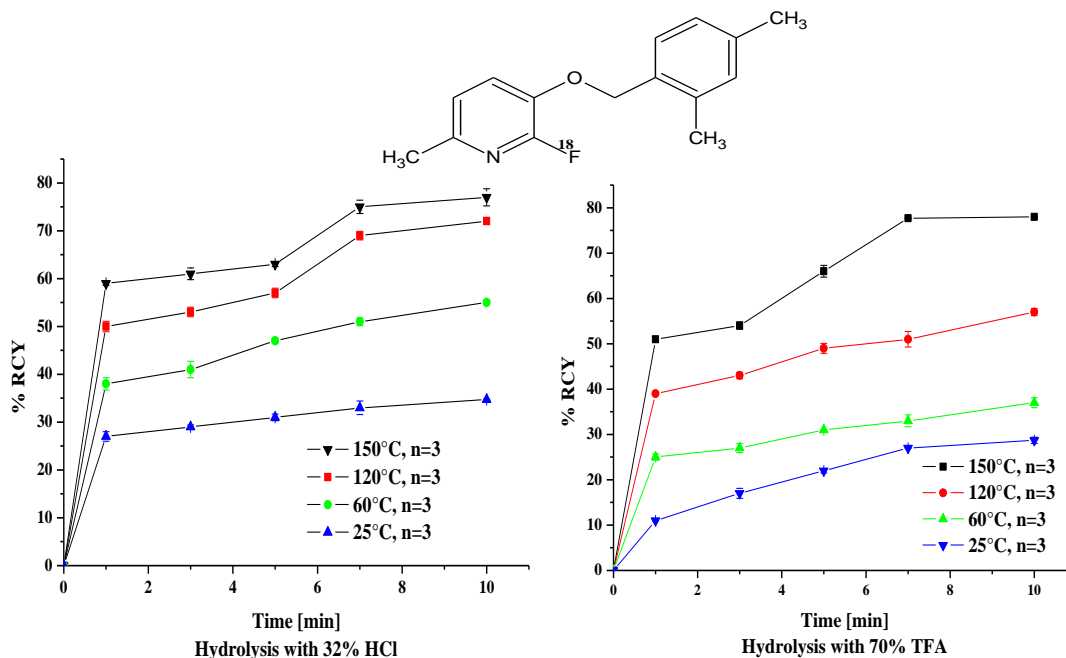
Fig 3.28 Hydrolysis of 3-[(2,4-dimethylphenyl)methoxy]-2-[^{18}F]fluoro-6-methylpyridine (vi) in dependence of RCYs on reaction time at different temperatures

The sum of RCYs of the product (P) and the unreacted intermediate (I) was always lower than 100% (Appendix-13) and radiofluoride as a side product originating from the concomitant hydrolytic cleavage of C–^{18}F-bond was observed in the reaction mixture. Significant quantities of radiofluoride were formed, especially if 70% TFA was used for the deprotection (Appendix-14). In case of 3-[(2,4-dimethylphenyl)methoxy]-2-[^{18}F]fluoro-6-methylpyridine **(vi)**, radiofluoride was the main radioactive product after 7 and 10 min of incubation with 70% TFA at RT and 60°C. The yield of 2-[^{18}F]fluoro-3-hydroxy-6-methylpyridine increased with increasing of reaction temperature and reached 78±0.1% after 10 min of incubation at 150°C. In contrast, if the *p*-xylyl group was used as a protecting group, the significant amount of radiofluoride was observed when applying 70% TFA at 120°C and 150°C for deprotection, thus, only 46% yield of the desired deprotected product could be obtained.

3.2.7.3 Catalytic Transfer Hydrogenation

In addition to acidic hydrolysis, catalytic hydrolysis was also carried out using 10% Pd/C as a catalyst in presence of 1,4-cyclohexadiene (1,4-CHD) or ammonium formate (HCOONH$_4$) as hydrogenating reagents. For 2-[^{18}F]fluoro-6-methyl-3-(*p*-tolylmethoxy)pyridine **(v)**, the rate of catalytic hydrolysis with 1,4-CHD was rather slow and resulted only in 1–3% of the deprotected pyridol in MeOH at 70°C after 3 min of reaction time (Appendix-14; Fig 3.29). RCYs increased to 45.0±1.2% and 57±1% after 7 min and 10 min, respectively, and reached the maximum (68±0.7%) only after 30 min of reaction time.
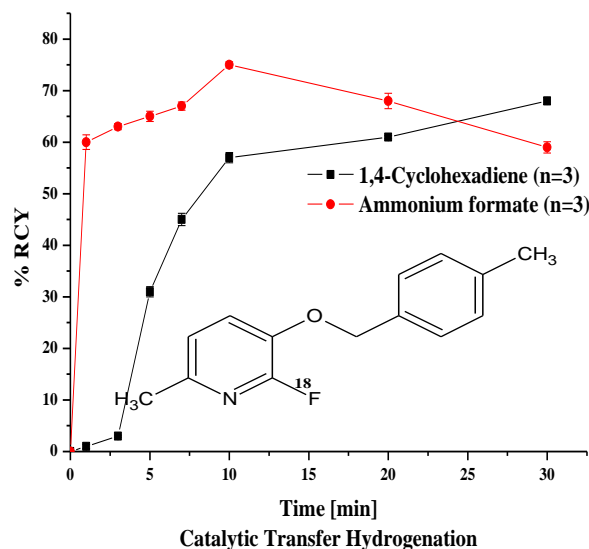
Fig 3.29 Catalytic transfer hydrogenation of 2-[^{18}F]fluoro-6-methyl-3-(*p*-tolylmethoxy)pyridine (v) in dependence of RCYs on time at 70°C

Contrarily, when HCOONH$_4$ instead of 1,4-CHD was used as a hydrogenating reagent, 60.0±1.4% of the deprotected product was obtained under the same reaction conditions already after 1 min of reaction time. The RCY first increased gradually and reached 75.0±0.6% after 10 min. Thereafter, it dropped to about 59±1.1% when the hydrogenation was allowed to run for 30 min, presumably, due to hydrogenolytic cleavage of C–^{18}F bond (Appendix-14; Fig 3.29).

In summary, among the protecting groups so tested, *p*-xylyl (4-methylbenzyl) and 2,4-dimethylbenzyl groups are proven to be the best hydroxyl protecting groups for n.c.a S_NAr radiofluorination. The model deprotection of the respective benzyl ethers with 32% HCl at 120°C gave 2-[^{18}F]fluoro-3-hydroxy-6-methylpyridine in 80% yield already after 10 min of reaction time. Additionally for *p*-xylyl group, the fast and clean cleavage by catalytic transfer hydrogenation using ammonium formate as a hydrogenating agent was demonstrated. Due to the mild deprotection conditions (70°C, 10 min), *p*-xylyl and 2,4-dimethylbenzyl protecting groups are well suited for the automated radiosynthesis.

3.2.8 Correlation of RCYs with ^{13}C-NMR values (δ, ppm)

The total effect of all substituents on the electron density of the carbon atom bearing the leaving group (LG) may be derived from the ^{13}C-NMR chemical shifts (δ, pm) of this carbon position. In the work of Rengan *et al.*[103] and Ding *et al.*[104], a correlation of the RCY with the deshielding of the carbon atom bearing the leaving group was found ($R^2 = 0.53$[103]; $R^2 = 0.87$[104]). However, the correlations of RCYs with ^{13}C-NMR chemical shift values were exclusively limited to structurally similar compounds[55]. Rengan for the first time tried to study this correlation between structurally different compounds ($R^2 = 0.53$) but belonging to the same system (homoaromatic).

Theoretically, the deshielding of the LG-substituted carbon atom is considered to be a measure of its electrophilicity. This suggests that at the reaction centre (where LG is attached) a downfield chemical shift (larger ppm value) indicates a lower electron density and hence, results in a higher radiochemical yield for nucleophilic substitution. Therefore, the labelling yield may additionally be discussed in dependence on the chemical shift of the particular carbon atom.

For this purpose, a correlation curve of ^{13}C-NMR chemical shifts values with RCYs of all substituted pyridines was calculated but the value of the regression coefficient was rather low ($R^2 = 0.57$). Taking out the results for the two compounds **(8, 9)** (Table 3-6), the R^2 value of 0.75 was obtained (Fig 3.30).
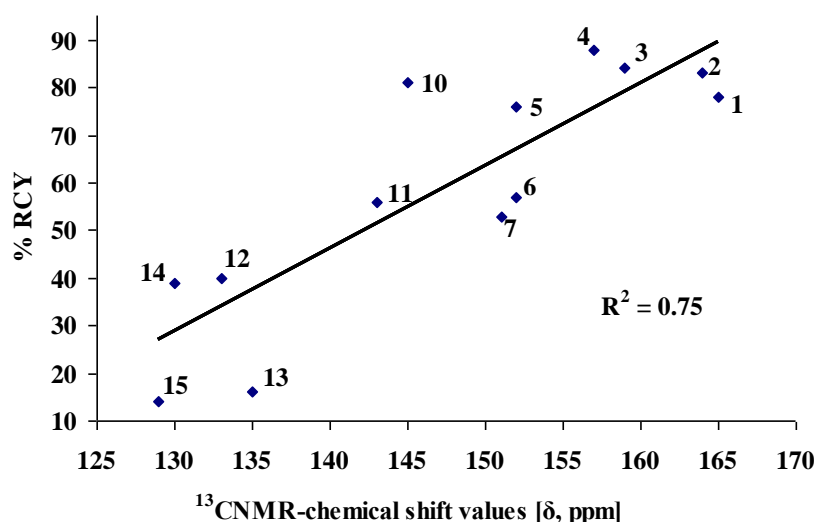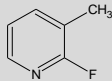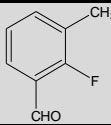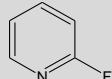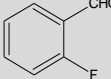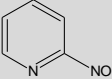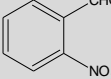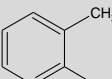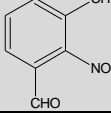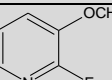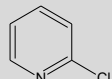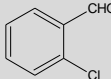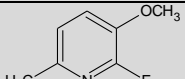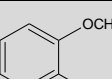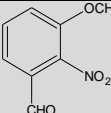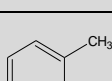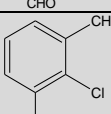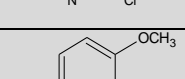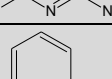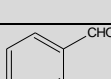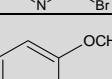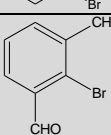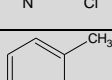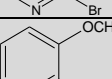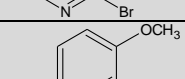
Fig 3.30 Correlation of RCYs versus ^{13}C-NMR chemical shift values

Table 3-6 RCYs and ^{13}C-NMR chemical shift values (δ, ppm) of C-atoms bearing leaving groups in substituted pyridines and substituted benzenes

Nr.	Pyridines	^{13}C-NMR [δ, ppm]	%RCY*	Nr.	Benzenes[97]	^{13}C-NMR [δ, ppm]	%RCY*
1	(2-fluoro-3-methylpyridine)	165	78	16	(2-fluoro-3-methylbenzaldehyde)	164	66
2	(2-fluoropyridine)	164	83	17	(2-fluorobenzaldehyde)	167	75
3	(2-nitropyridine)	159	84	18	(2-nitrobenzaldehyde)	149	83
4	(3-methyl-2-nitropyridine)	157	88	19	(2-methyl-6-nitrobenzaldehyde)	148	46
5	(2-fluoro-3-methoxypyridine)	152	76	-	-	-	-
6	(2-chloropyridine)	152	57	20	(2-chlorobenzaldehyde)	133	65
7	(2-fluoro-3-methoxy-6-methylpyridine)	151	53	-	-	-	-
8	(3-methoxy-2-nitropyridine)	148	90	21	(3-methoxy-2-nitrobenzaldehyde)	137	67
9	(2-chloro-3-methylpyridine)	148	12	22	(2-chloro-6-methylbenzaldehyde)	135	61
10	(3-methoxy-6-methyl-2-nitropyridine)	145	81	-	-	-	-
11	(2-bromopyridine)	143	56	23	(2-bromobenzaldehyde)	127	73
12	(2-chloro-3-methoxypyridine)	135	16	24	(2-bromo-6-methylbenzaldehyde)	125	51
13	(2-bromo-3-methylpyridine)	133	40	-	-	-	-
14	(2-bromo-3-methoxypyridine)	130	39	-	-	-	-
15	(2-bromo-3-methoxy-6-methylpyridine)	129	14	-	-	-	-

*Standard deviations range from 0.1 to 5 for all values of RCYs

The reason for removing these two precursors **(8, 9)** was very high RCY (90%) for 3-methoxy-2-nitropyridine than that of 2-chloro-3-methylpyridine (12%), though chemical shift value of C-atom bearing leaving groups in both cases was same (148 ppm) (Table 3-6).

The study for the correlation of ^{13}C-NMR values versus RCY was also carried out in substituted pyridines and the homoaromatic analogues[97] (Fig 3.31). Therein, a poor correlation was obtained ($R^2 = 0.37$). A reason could be the formation of radioactive/UV-active by-products as it was observed in some of the substituted 2-nitrobenzaldehydes i.e. in case of 3-methyl-2-nitrobenzaldehyde (*see 3.2.2.2*).
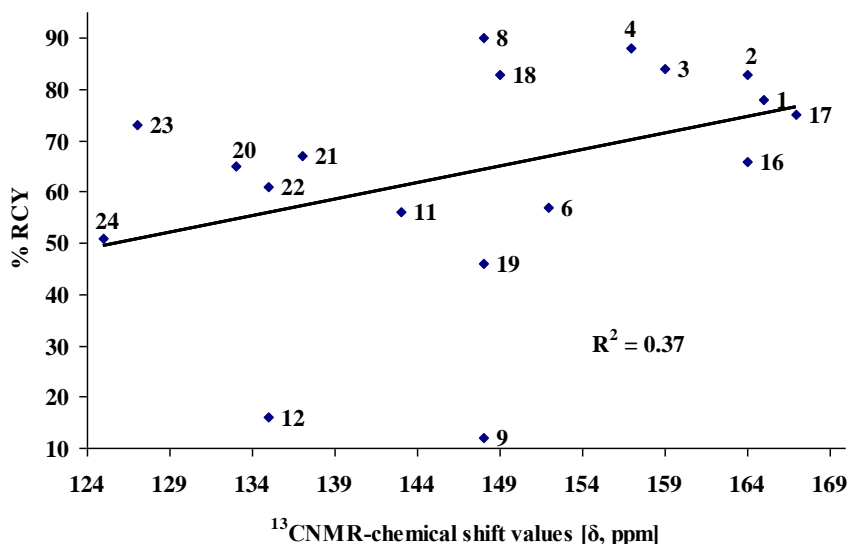
Fig 3.31 Correlation of RCYs versus ^{13}C-NMR chemical shift values

In labelling, these side reactions become more influential by causing the precursor to be less reactive. That is particularly to be taken into consideration because the radioactive compounds are present in low concentrations (μmoles to pmoles) while other components are used in millimolar amounts for the labelling reactions. So, in radiofluorinations, the [Precursor]/[^{18}F]F$^-$ ratios applied are very high. In case, if no side reaction occurs that may consume or deactivate the ^{18}F$^-$ ion, there should be a complete incorporation of ^{18}F$^-$ into the precursor forming the reaction product. Only the time needed for the completion of the reaction should vary according to the electrophilicity of the precursor. This may explain why the low RCYs, observed as a result of side reactions, appeared to have a poor correlation with the ^{13}C-NMR chemical shift values as reactivity parameters.

3.3 A New Class of Hypoxia PET-Tracer: [^{18}F]FNT

As a new concept, a bifunctional hypoxia PET-tracer ([^{18}F]FNT, **i**) having *p*-tyorsine coupled with 2-nitroimidazole was chosen. In [^{18}F]FNT, *p*-tyrosine moiety may hypothetically increase the transportation across the cell by utilizing amino acid transporter system. *O*-[2-[^{18}F]fluoro-3-(2-nitro-1*H*-imidazol-1-yl)propyl]tyrosine ([^{18}F]FNT, **i**) was prepared from methyl *N*-[(benzyloxy)carbonyl]-*O*-[2-{[(4-methylphenyl)sulfonyl]oxy}-3-(2-nitro-1*H*-imidazol-1-yl)propyl]tyrosine **(e)** *via* aliphatic nucleophilic substitution.

3.3.1 Organic Synthesis

Precursor for radiosynthesis of [^{18}F]FNT was synthesized by the synthetic pathway as described in following scheme (*see 5.4.1*).

Scheme-10
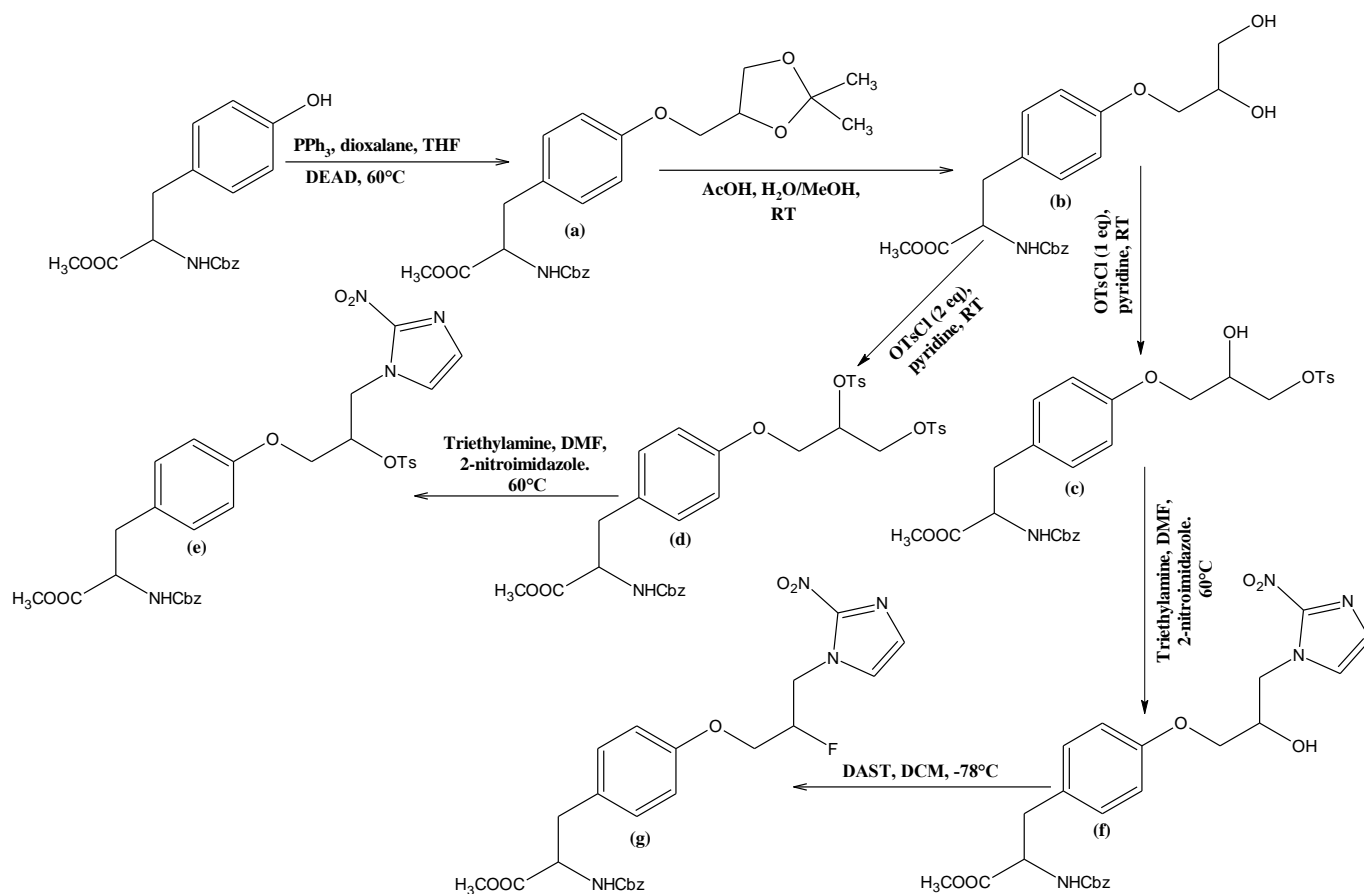
(e): (% Yield: 69%)
(g): (% Yield: 57%)

3.3.2 Radiosynthesysis

Radiosynthesis of [^{18}F]FNT from precursor (**e**) synthesized as shown in Scheme-10, was carried out in following way (*see 5.4.2*).
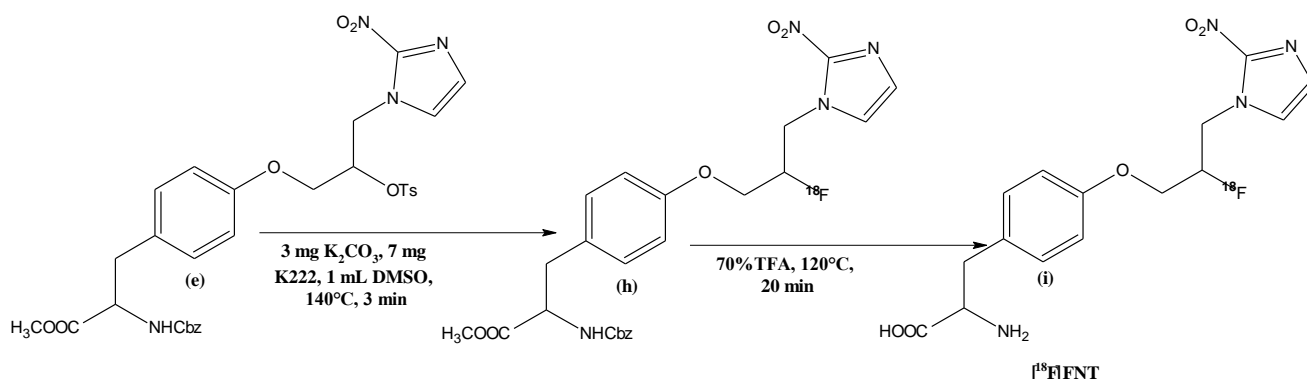
3.3.3 [^{18}F]-Labelling

[^{18}F]-labelling of precursor (**e**) was performed under various sets of experimental conditions in order to increase the RCY and to minimize the by-product formation. For this purpose, different solvents were tried. All labelling experiments were repeated at least three times and were carried out in dependence on time (1, 2, 3, 5, 7, 10, 15, 20 min) and temperature (140°C, 120°C, 110°C). In a first set of experiments, acetonitrile (MeCN) was used with 3.5 mg of K$_2$CO$_3$ and 15 mg of K222. Highest RCY was 29±0.9% (2 min) at 90°C (Appendix-15; Fig 3.32).
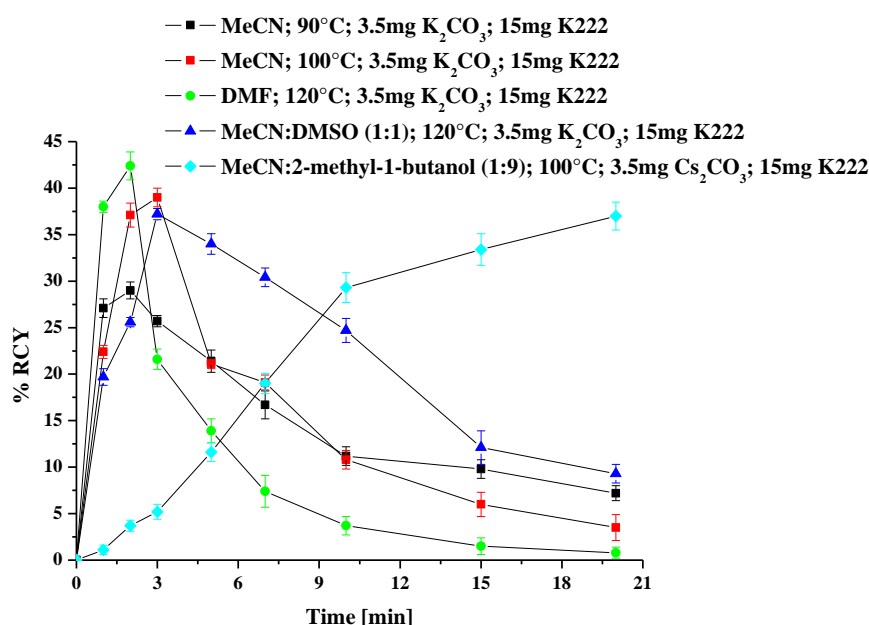
Fig 3.32 RCY of methyl *N*-[(benzyloxy)carbonyl]-*O*-[2-[^{18}F]fluoro-3-(2-nitro-1*H*-imidazol-1-yl)propyl]tyrosine (h) in dependence on time under various experimental conditions

However, increase in temperature (100°C) also increased the RCY (39±1%, 3 min) but there was a sharp decrease in RCYs at both temperatures (90°C, 100°C) with time. Hence, the lowest RCYs

of 7.2±0.8% and 3.5±1.4% were observed after 20 min of reaction time with MeCN at 90°C and 100°C, respectively (Appendix-15; Fig 3.32).

In another set of experiments, MeCN was used in combination with other solvents such as DMSO and amylbutanol. When radiofluorination was performed at 120°C with MeCN/DMSO (1:1), maximum RCY so observed was 37.2±0.6% at 3 min and the minimum was 9.3±1% after 20 min. However, when MeCN/2-methyl-1-butanol (1:9) mixture was used as a solvent system along with 3.5 mg of cesium carbonate (Cs_2CO_3), a slowly increasing trend in RCY was observed with 19±1.1% and 37±1.5% of RCY at 7 and 20 min, respectively. However, when DMF was used as a solvent along with same amounts of base and K222, ca 45% RCY was obtained at 120°C (Appendix-15; Fig 3.32).

Among all solvents, DMSO proved to be the best one. In it, maximum RCY so obtained was ca 50% at 3 min. However, when temperature was lowered to 110°C, the highest RCY (45±1.3%) for formation of [^{18}F]-labelled intermediate (methyl *N*-[(benzyloxy)carbonyl]-*O*-[2-[^{18}F]fluoro-3-(2-nitro-1*H*-imidazol-1-yl)propyl] tyrosine, **h**) was observed after 5 min of reaction time using standard experimental conditions such as 3.5 mg of K_2CO_3 and 15 mg of K222. Further studies for optimization of labelling conditions were carried out in DMSO (Appendix-16; Fig 3.33).

When temperature was increased to 120°C, 56±1.5% of maximum RCY was obtained at 3 min (3.5 mg K_2CO_3, 10 mg of K222). However, almost similar RCY (58±1.3%) was obtained at 120°C when only the amount of K_2CO_3 was reduced to 1.8 mg. By increasing temperature to 140°C, highest RCY (81±0.9%, 3 min) was obtained by using 3 mg of K_2CO_3 and 7 mg of K222. When base was changed to $KHCO_3$ (2 mg) and amount of K222 was further reduced to 2 mg, RCY decreased to 37±1% after 10 min of reaction time (Appendix-16; Fig.3 33).
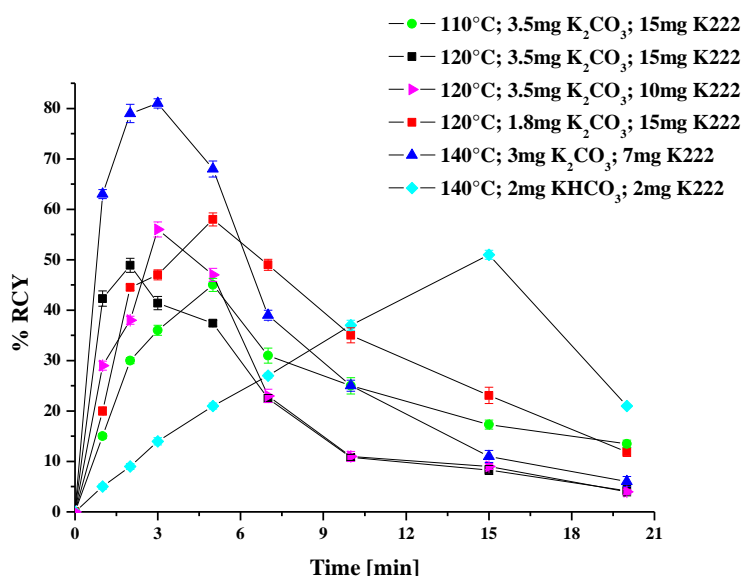
Fig 3.33 RCY of methyl *N*-[(benzyloxy)carbonyl]-*O*-[2-[^{18}F]fluoro-3-(2-nitro-1*H*-imidazol-1-yl)propyl] tyrosine (h) in dependence on reaction time in DMSO

Except in the case of MeCN/2-methyl-1-butanol (1/9; v/v) (Fig 3.32), all reactions showed fast reaction kinetics within 5 min, but thereafter RCYs decreased to sharply to 20% and even less at 20

min (Fig 3.32, 3.33). The reason of the decreasing tendency in RCY with time was the formation of by-products as verified by LC/MS analysis (Fig 3.34). For LC/MS analysis, samples (5 µL) taken directly from the (c.a.) labelling reaction mixtures were injected. The results showed two by-product mass peaks (174 [M+1]$^+$ and 331 [M+1]$^+$) and the mass peak of the product (502 [M+1]$^+$). It appeared to be evident from structures related to the mass peaks that the side reaction was most probably the alkaline hydrolysis catalysed by phase transfer catalyst as previously experienced[80] in the radiosynthesis of [^{18}F]FPy-TFP (*see 3.4.4*). In addition, the results of radiofluorinations in the present study also predicted that the rate of side-reaction was directly proportional to the amount of K222.
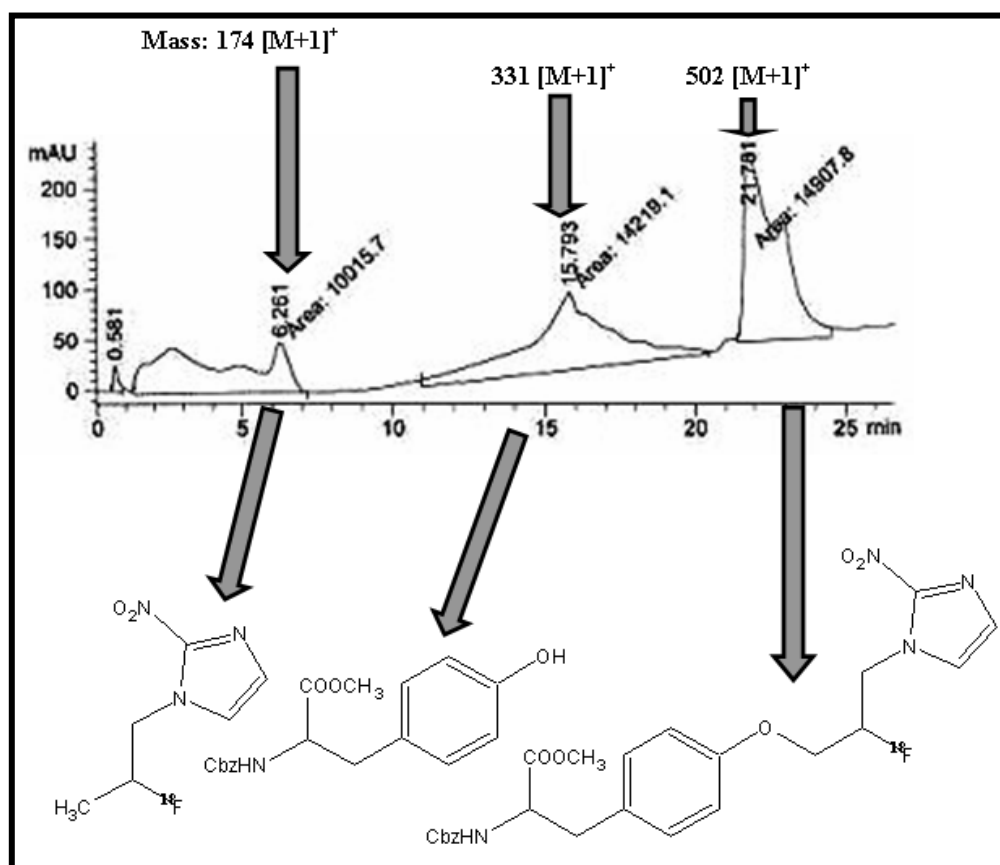
Fig 3.34 LC/MS analysis of reaction mixture after radiofluorinations of precursor (e) HPLC conditions: Column: ODS Hypersil C18, 100 x 2.1 mm, 5µm; Eluent: A = water with 2mM NH$_4$OAc, B = methanol with 2mM NH$_4$OAc; Gradient: 100% A at 0 min to 5 min, from 5 min to 10 min, 100% B; Flow rate: 0.5 mL/min; Injection Volume: 5 µL, Mode: ACPI (+)].

3.3.4 Hydrolysis

Conditions of hydrolysis were examined in acidic media. For this purpose, 70% trifluoroacetic acid (TFA) and 32% hydrochloric acid (HCl) were used at different temperatures (90°C, 120°C, 140°C).Time dependent analysis (10, 15, 20 min) was carried out and all experiments were repeated for three times (n = 3). RCYs were additionally measured by γ-counter.

At all temperatures, maximum RCYs were obtained after 20 min of reaction time. After hydrolysis with 70%TFA at 90°C, only 11±1% of RCY was obtained. However, when temperature

was increased to 120°C, RCY of hydrolysis increased to 56±1.5% (Fig 3.35). But at 140°C, maximum RCY was as low as 36±0.7% because of strong decomposition reaction of [^{18}F]-labelled intermediate **(h)**. In contrast, RCYs after hydrolysis with 32%HCl were around 10-20% at temperatures ranging from 90°C to 120°C (Appendix-17; Fig 3.35).
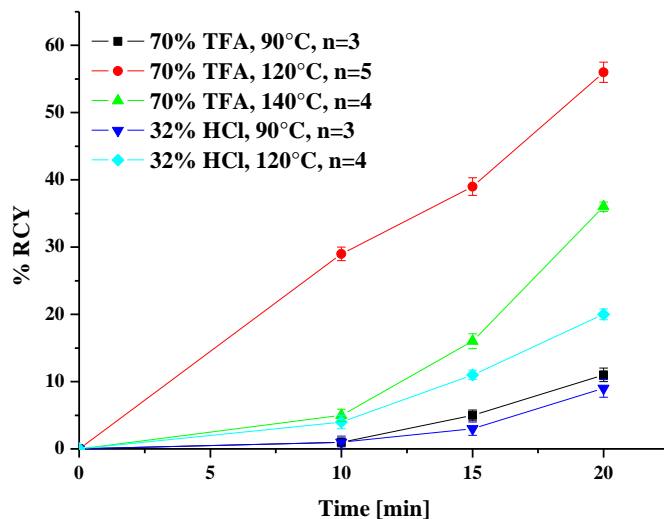
Fig 3.35 RCY of *O*-[2-[^{18}F]fluoro-3-(2-nitro-1*H*-imidazol-1-yl)propyl] tyrosine (i) in dependence on reaction time with 70%TFA and 32%HCl

Hence, maximum RCYs after hydrolysis were obtained after hydrolysis with 70%TFA at 120°C after 20 min of reaction time.

3.3.5 HPLC Purification

After hydrolysis, the product was isolated from the reaction mixture by preparative HPLC with a reversed phase preparative column using gradient elution by MeCN/water (0.1%TFA). Three peaks were observed in HPLC chromatogram (Fig 3.36). First peak at 3.5 min, second one at 6.7 min ([^{18}F]FNT, **i**) and third one at 14.7 min (labelled intermediate with hydrolysis at ester group only).
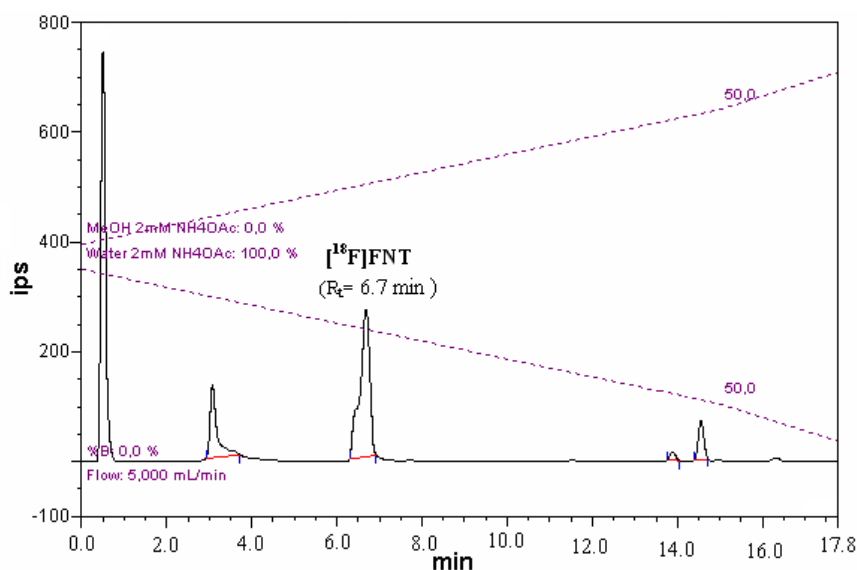
Fig 3.36 HPLC chromatogram for preparative analysis (*see 5.4.2.4*)

Product peak collected from HPLC was passed through a cartridge in order to reduce the volume. At end of synthesis (EOS), quality control of [^{18}F]FNT in final formulation was carried out by using reversed phase analytical column with the same gradient elution as mentioned above for preparative step. HPLC chromatogram showed only one peak at 8.9 min ([^{18}F]FNT, **i**) in radioactive region and no signal in UV (λ:254 nm, 220 nm) (Fig 3.37).
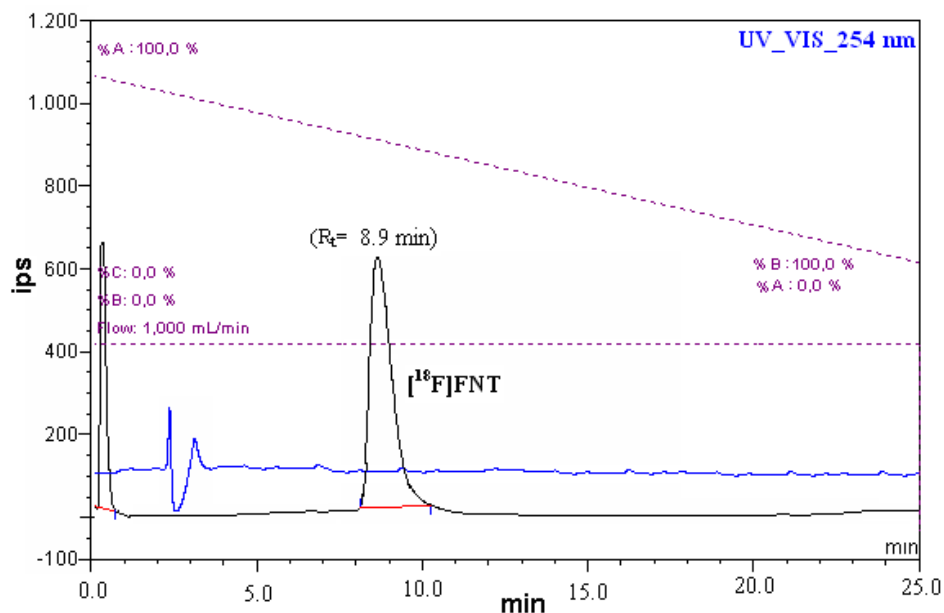
Fig 3.37 HPLC chromatogram for quality control (*see 5.4.2.4*)

3.4 A New PSMA-Targeting Ligand: [¹⁸F]FPy-DUPA-Pep

In this part of the work, a new PSMA (prostate-specific membrane antigen) targeting ligand, DUPA-Pep having DUPA linked *via* 8-aminooctanoic acid to two phenylalanine rings (for maximum binding) was synthesized. Indirect labelling method was chosen using 2,3,5,6-tetrafluorophenyl 6-[¹⁸F]-fluoronicotinate ([¹⁸F]FPy-TFP) as a prosthetic group to be coupled with DUPA-conjugate (DUPA-Pep).

3.4.1 Organic Synthesis

Precursors and standards for radiosynthesis of [¹⁸F]FPy-DUPA-Pep was synthesized by the synthetic pathway as described in following schemes (*see 5.5.1*).

Scheme-11

Synthesis of the prosthetic group (FPy-TFP) was carried out as follows.

(k): (% Yield: 79%)

(l): (% Yield: 37%)
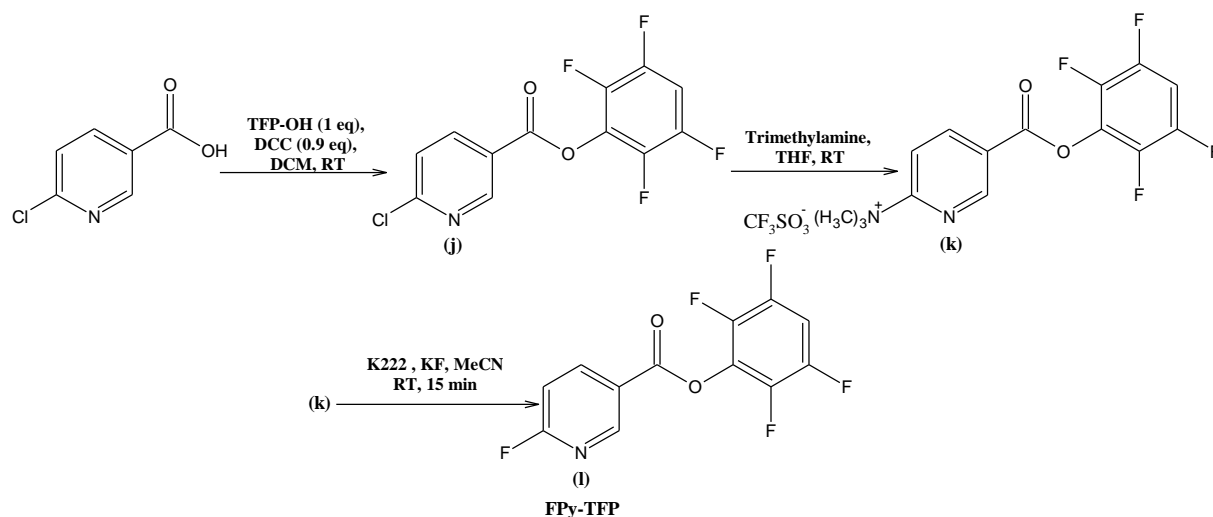
Synthesis of Fmoc-protected peptide was performed as under.
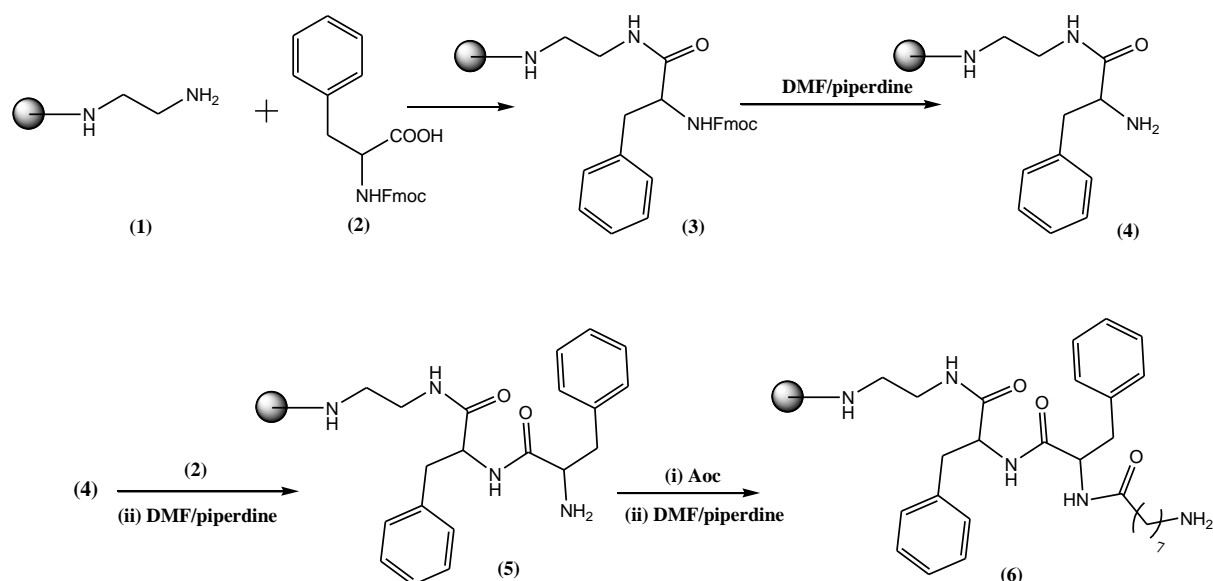
Scheme-12

Synthetic steps of FPy-DUPA-Pep are shown below.

(p)
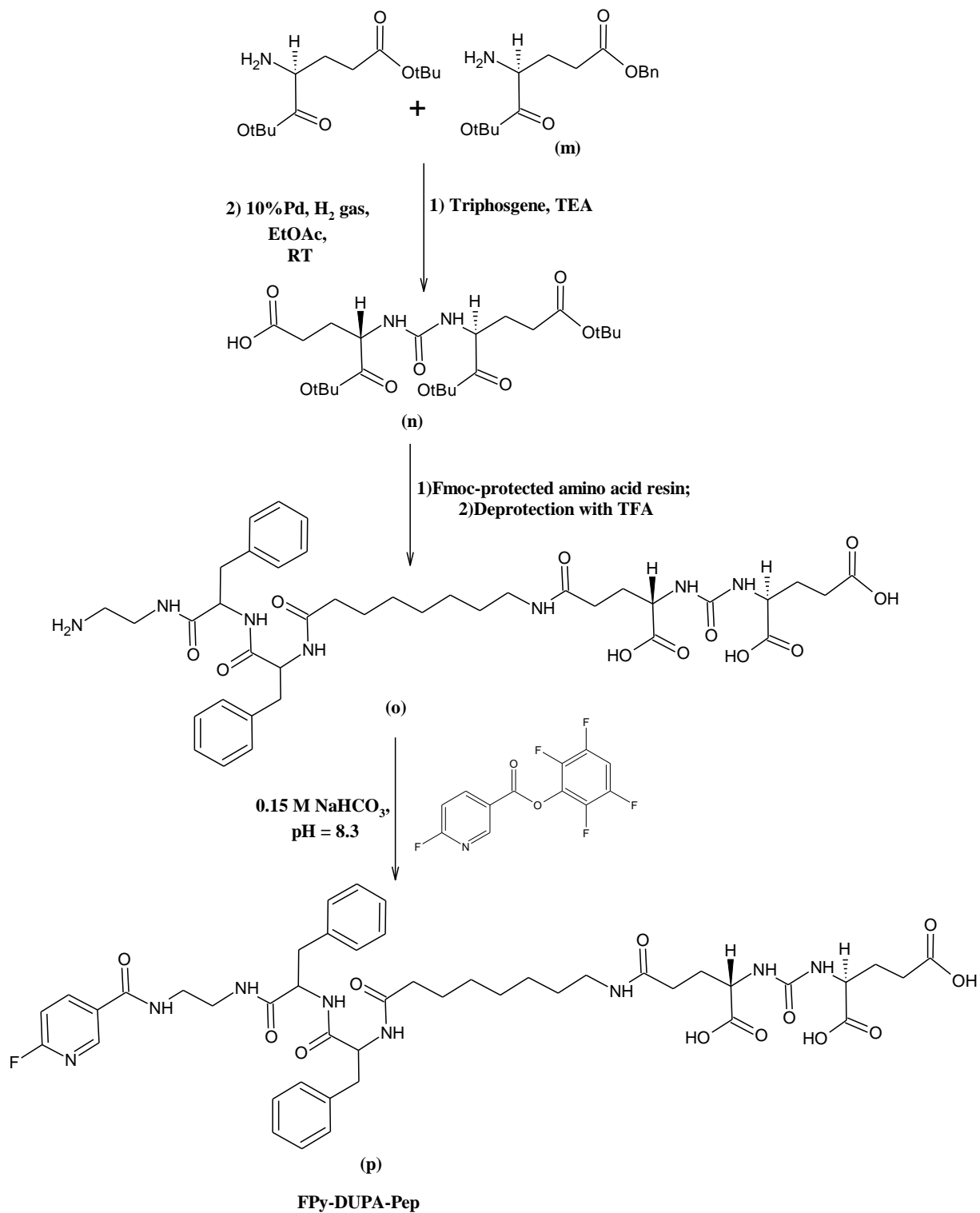
FPy-DUPA-Pep

(t): (%Yield: 67%)

(u): (%Yield: 77%)

3.4.2 Radiosynthesis of [^{18}F]FPy-DUPA-Pep

Radiosynthesis of [^{18}F]FPy-DUPA-Pep was done in following way (*see 5.5.2*).

[^{18}F]FPy-DUPA-Pep
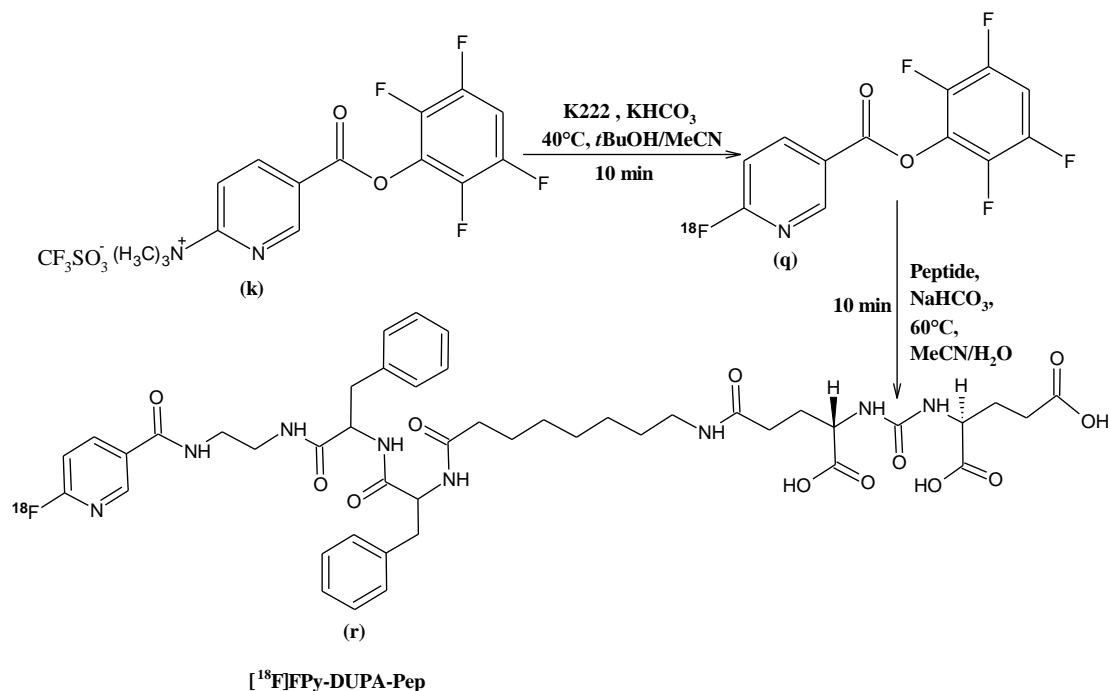
3.4.3 Labelling of [^{18}F]FPy-TFP

[^{18}F]-labelling of the prosthetic group ([^{18}F]FPy-TFP) was performed under various sets of experimental conditions in order to increase the RCY and to minimize the by-products formation. Two main by-products were formed during labelling as reported elsewhere[80]. One of the by-product (2TFP-Py, R_t = 19.5 min under analytical HPLC conditions) was visible in UV$_{254}$ and was formed by substitution of trimethylammonium group with tetrafluorophenylether (TFP) while the other by-product was 6-[^{18}F]fluoronicotinic acid (R_t = 7.5 min under analytical HPLC conditions) formed by basic hydrolysis of precursor. Temperature for all experiments was 40°C as high temperature was reported to increase the formation of 6-[^{18}F]fluoronicotinic acid[80]. All experiments were repeated 2-4 times (Table 3-7,-8).

3.4.4 Effect of Solvent and Base

One set of experiments was carried out using conventional [^{18}F]-labelling conditions such as 10 mg precursor, 3.5 mg K$_2$CO$_3$, 15 mg K222, and 1 mL of DMF at 40°C for 10 min (Table 3-7). Low RCY (19±1%) was observed while the major product so obtained was 6-[^{18}F]fluoronicotinic acid (80±0.8%). In addition, almost 40% of UV-active by-product (2TFP-Py, non radioactive) was also present in the reaction media.

When 2 mg of KHCO$_3$ were used for 7 mg of precursor using 7 mg of K222 in 1 mL of MeCN at 40°C, 72±1.3% of [^{18}F]FPy-TFP was obtained along with 20% of 6-[^{18}F]fluoronicotinic acid. Almost 40% of 2TFP-Py was formed (Table 3-7). So, amounts of precursor and K222 were changed to 8 mg and 2 mg, respectively. The amount of KHCO$_3$ was same as above. Solvent so used in this set of

experiments was MeCN/*t*BuOH (1:4) (Table 3-8). As a result, the maximum RCY (90±0.9%) of [^{18}F]FPy-TFP synthesis was obtained at 20 min. Also, at 10 min of reaction time, RCY was as high as 86% along with very low yield (< 1%) of 6-[^{18}F]fluoronicotinic acid. Although, 85±0.7% of [^{18}F]-labelled product was obtained at 20 min of reaction time after applying same reaction conditions in 1mL of MeCN instead of MeCN/tBuOH. 5% of hydrolysed by-product was observed at this time point. However, at 10 min, product so formed was almost 70% (Table 3-7).

Table 3-7 RCY for the radiosynthesis of [^{18}F]FPy-TFP in 1 mL of solvent

Solvent (mL)	n	Precursor (mg)	K222 (mg)	Base (mg)	Time (min)	RCY [^{18}F]FPy-TFP
DMF	3	10 mg	15 mg	3.5 mg (K$_2$CO$_3$)	10	19±1 (16±0.8)*
MeCN	4	8 mg	2 mg	2 mg (KHCO$_3$)	10	71±1 (69±1.2)*
					15	79±1.4 (75±0.9)*
					20	85±1 (82±0.6)*
	3	7 mg	7 mg	2 mg (KHCO$_3$)	10	72±1.3 (68±1.1)*
	2	3 mg	2 mg	2 mg (KHCO$_3$)	15	79±1.2 (76±0.8)*

*Analysis by TLC

When using 30 μL of 0.8 M TBA-HCO$_3$ as a phase transfer catalyst and as a base instead of K$_2$CO$_3$ along with 9 mg of precursor and 1 mL of MeCN/*t*BuOH (1:4) as a solvent, [^{18}F]FPy-TFP was obtained with a yield of 25±1.1% in 10 min of reaction time. Hydrolysed [^{18}F]-labelled by-product was almost 60%. However, only 5% 2TFP-Py was formed (Table 3-8).

Table 3-8 RCY for the radiosynthesis of [^{18}F]FPy-TFP in MeCN/*t*BuOH (2:8)

n	Precursor (mg)	K222 (mg)	Base (mg)	Solvent (mL or μL)	Time (min)	RCY [^{18}F]FPy-TFP
4	9 mg	30μL of 0.8M TBA-HCO$_3$		1 mL	10	25±1.1 (23±0.5)*
5	8 mg	2 mg	2 mg (KHCO$_3$)	1 mL	10	86±0.3 (81±0.5)*
					15	88±1.4 (85±0.7)*
					20	90±0.9 (89±0.5)*
2	5 mg	2 mg	2 mg (KHCO$_3$)	500μL	15	83±1 (80±1)
2	3 mg	2 mg	1.6 mg (KHCO$_3$)	1 mL	15	90±1 (89±0.7)*
3	3 mg	1.6 mg	1.6 mg (KHCO$_3$)	1 mL	15	82.5±0.7 (81±1.1)*
2	3 mg	1.6 mg	1.6 mg (KHCO$_3$)	500μL	15	81±1.5 (78±0.6)*
3	1.5 mg	1 mg	1 mg (KHCO$_3$)	300μL	15	38±0.4 (33±0.5)*

*Analysis by TLC

Hence, the results of [^{18}F]-labelling with K$_2$CO$_3$ or TBA-HCO$_3$ showed 6-[^{18}F]fluoronicotinic acid as a major product. This indicated the increased rate of alkaline hydrolysis catalysed by phase

transfer catalyst (K222). So, all other experiments were carried out with $KHCO_3$ and very low amounts of K222 (< 5 mg).

By lowering the precursor amount to 3 mg, the highest RCY (90±1.3%) was obtained after using 1.6 mg of $KHCO_3$ and 2 mg of K222 in 1 mL of MeCN/tBuOH (1:4). 6-[^{18}F]fluoronicotinic acid formed under such conditions was only 1.5%. When lowering the precursor amount to 1.5 mg with 1 mg of $KHCO_3$ and 1 mg of K222, a low RCY (38±0.9%) for [^{18}F]FPy-TFP was obtained. Almost 50% of 6-[^{18}F]fluoronicotinic acid was observed under these conditions (Table 3-8).

In short, the best conditions for [^{18}F]-labelling of [^{18}F]FPy-TFP were found with a precursor amount of 8 mg along with 2 mg of K222 and 2 mg of $KHCO_3$ in 1 mL of MeCN/tBuOH (1:4) at 10 min of reaction time.

3.4.5 Cartridge Purification

[^{18}F]FPy-TFP was purified by using Oasis cartridges having both cation exchange and reversed phase properties. The main advantage of using this cartridge was the fact that it retained the positively charged precursor (precursor having quarternary ammonium as a leaving group). So, it became easy to elute the [^{18}F]-labelled products. Different concentrations of MeCN (20%, 40%, 50%, 60% and 65%) were tried as eluents in order to get rid of by-products or to minimize the amount of by-products in eluate. The best purification was observed with 65% MeCN. So, [^{18}F]FPy-TFP was eluted from Oasis cartridge by 2.1 mL of MeCN. Because of larger volumes of solvent (such as 2.1 mL), it was necessary to evaporate the solvent. For this purpose, evaporation was carried out 100°C under argon but there was also a loss of almost 30% of [^{18}F]FPy-TFP because of its hydrolysis into 6-[^{18}F]fluoronicotinic acid. So, in order to reduce the volume, timing, and to avoid hydrolysis, eluate after the first purification was passed through two preconditioned Strata-x cartridges (C18, RP) and product was eluted directly into the vial (containing DUPA-Pep and $NaHCO_3$) by 500 μL of 80% MeCN.

3.4.6 Coupling with DUPA-Pep

Coupling of DUPA-Pep with carried out at 40°C, 50°C and 60°C and analysis was made by dependence on time. For this purpose, 100 μL samples were taken from reaction mixture at 3, 7, 10, 20, and 30 min for HPLC analysis. Product peaks were collected from HPLC and were measured by γ-counter. Highest RCY (95±1.2%) for radiosynthesis of [^{18}F]FPy-DUPA-Pep was observed at 60°C at 10 min of reaction time with 2 mg of peptide and 8 mg of $NaHCO_3$ (Appendix-18; Fig 3.38).

[^{18}F]FPy-DUPA-Pep synthesis was also carried out with 1 mg of peptide and 5.5 mg of $NaHCO_3$ at 60°C, the observed RCY was still as high as 90% within 10 min.
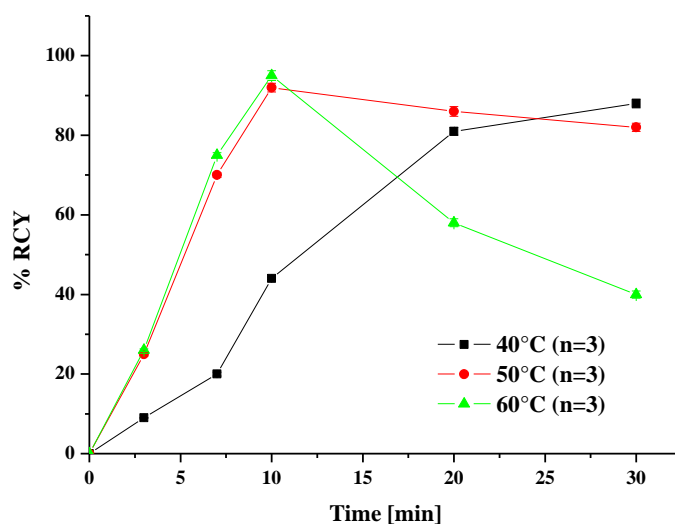
Fig 3.38 RCY of [¹⁸F]FPy-DUPA-Pep at different temperatures in dependence on time

3.4.7 Chemical Stability of [¹⁸F]FPy-DUPA-Pep

Chemical stability of [¹⁸F]Fpy-DUPA-Pep was checked by taking 100 µL as an aliquote from final formulation in EtOH and by adding 100 µL of different chemicals such as isotonic phosphate buffered saline (PBS), 0.1N HCl and 0.2M $NaHCO_3$ for 15 min. It was observed that [¹⁸F]Fpy-DUPA-Pep was stable at all temperatures (RT, 40°C, 60°C) in PBS. Also, when checked at 37°C in 0.1N HCl (pH: 2-3) or in 0.2M $NaHCO_3$ (pH: 8-9), no decomposition or defluorination was observed because only one product peak ([¹⁸F]FPy-DUPA-Pep: R_t = 10.2 min) could be seen in HPLC.

3.4.8 HPLC-Purification

After preparative separation by using isocratic elution (28% MeCN), the product peak ([¹⁸F]FPy-DUPA-Pep, 6.5 min) was subjected to cartridge purification in order to concentrate it in 200 µL of ethanol (EtOH). In order to check the radiochemical purity, analysis for quality control was carried out using gradient system (MeCN/water, 0.1% TFA). HPLC chromatogram showed only one signal in radioactive region and no signal in UV (λ: 254 nm, 220 nm) (Fig 3.39).

In summary, an efficient method for the radiosynthesis of a new PSMA targeting ligand ([¹⁸F]FPy-DUPA-Pep) was developed using [¹⁸F]FPy-TFP as a prosthetic group. 48±0.9% overall RCY (without decay correction) was obtained within 50 min with a radiochemical purity of > 98% at EOS.
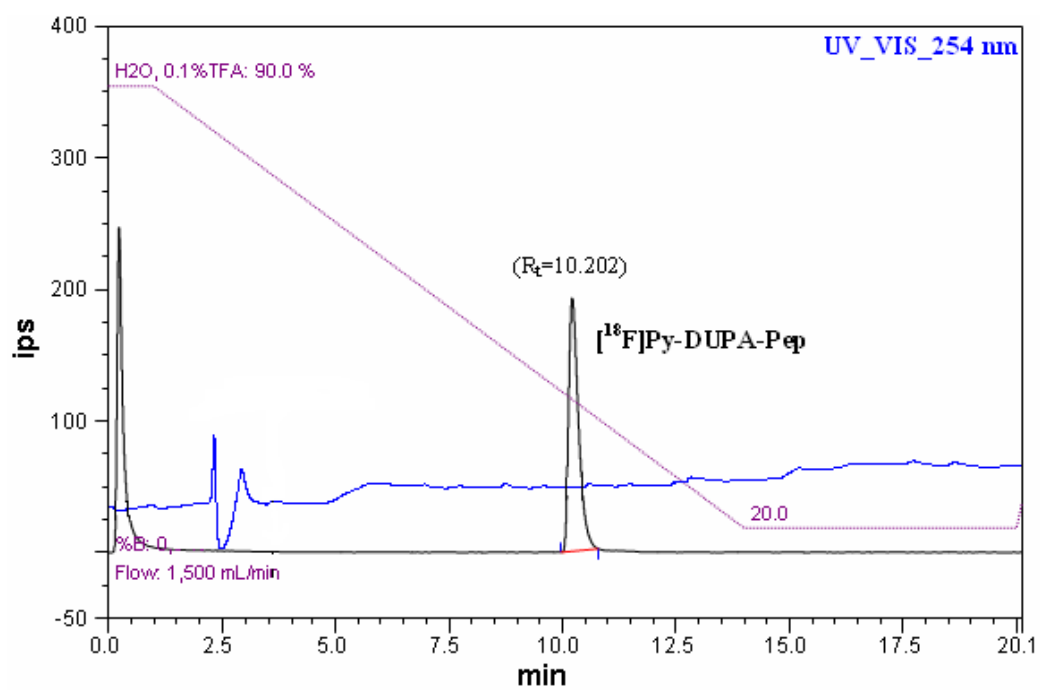
Fig 3.39 HPLC chromatogram for quality control of [^{18}F]FPy-DUPA-Pep (*see 5.5.2.4*)

4. SUMMARY

The main objective of the present study was to develop the most convenient pathway for nucleophilic radiofluorinations to be applied in radiosyntheses of [^{18}F]-labelled aromatic compounds such as 6-[^{18}F]fluoro-L-DOPA, 2-[^{18}F]Fluoro-L-tyrosine and 6-[^{18}F]fluorophenylalanine for clinical PET-imaging. In particular, for [^{18}F]-labelled aromatic amino acids radiofluorinations allowing the direct nucleophilic introduction of [^{18}F]-fluoride do not exist, yet they are needed in order to obtain the [^{18}F]-tracers in high specific activities i.e. in a high ratio of [^{18}F]-labelled compound to the (non radioactive) [^{19}F]-one because that is the prerequisite for following the metabolic pathways without any alterations originated by the high concentrations of the [^{19}F]-isotopomeric compound of the tracer. In order to perform radiofluorinations *via* nucleophilic aromatic substitution (S$_N$Ar) the benzene ring must be substituted by a suitable leaving group and an auxiliary group (e.g. –CHO), both bearing electron-withdrawing properties. Among leaving groups, –NO$_2$ and –N$^+$(CH$_3$)$_3$ are thought to be the best when aiming at high RCYs. Moreover, in the compounds of interest, S$_N$Ar has to be performed in the presence of electron-donating groups such –OCH$_3$ (for –OH protection) and –CH$_3$ (for linking glycine moiety). However, these groups are known to decrease S$_N$Ar very strongly when present in *para* or in *ortho* position to the leaving group. Thus, it appeared highly desirable to study the impact of such groups on the rates of radiofluorinations *via* S$_N$Ar because, upto now, the effect on S$_N$Ar was studied only in substituted 2-nitrobenzaldehydes[55] and no data has been reported for –N$^+$(CH$_3$)$_3$.

For this purpose, various –OCH$_3$ and –CH$_3$ substituted benzaldehydes bearing quaternary ammonium salt [–N$^+$(CH$_3$)$_3$] as leaving group (Compounds: **1-7**) were labelled by [^{18}F]fluoride. A very strong impact of electron-donating groups on RCYs was observed as in compounds (**3, 4, 5**) with one and two –OCH$_3$ groups in *para* or *meta* or in both *meta* and *para* position to the leaving group (RCY: 10% to 80%). The maximum RCY of 69±1% was observed at 3 min in case of compound (**2**) having –CH$_3$ group in *ortho* position to the leaving group. Also, for compound (**5**) having two –OCH$_3$ groups, the highest RCY was 41±1.4% (3 min). In all above mentioned compounds, the RCY decreased fast with reaction time by reaching around 10%. The reason for this reduction in RCYs could be attributed to the competing reaction that became dominant with passage of time as indicated by formation of [^{18}F]-CH$_3$ and *N,N*-dimethyl amino substituted benzenes as by-products. The results proved that electron-donating groups in substituted benzenaminium salts do show strong impact on RCYs but in the presence of good auxiliary group (–CHO), RCYs as high as 50% could be obtained.

After radiolabelling, auxiliary group can be removed easily by decarbonylation using Wilkinson's catalyst[43]. However, in order to eliminate this additional step, an interesting alternative is the use of substituted pyridines in which the nitrogen atom within the ring reduces the electron density of the ring and, thus, makes it highly activated towards S$_N$Ar for which the *"Chichibabin reaction"* is the well known example. In this work, the rate of radiofluorinations in various substituted pyridines (**10-13**) was studied. When compared to 2-nitrobenzaldehyde[97], the labelling yield of 2-nitropyridine (84±3%, 20 min) was almost similar to that of 2-nitrobenzaldehyde (83±1%, 20 min) at 140°C. Also,

in 2-halo pyridines, RCYs were either higher or almost equal to their corresponding homoaromatic analogues (*see 3.2.1*). In addition, [^{18}F]-labelling reactions were also carried out in pyridines substituted in *ortho* position by electron-donating groups such as –CH$_3$ and –OCH$_3$. It was observed that the effect of electron donating substituents was more pronounced in reducing RCYs (80% to 7%) at lower temperatures in substituted halopyridines **(11-13)** that were efficiently substituted at a reaction temperature > 100°C within a reaction time between 10-30 min. In contrast, pyridines having –NO$_2$ as a leaving group showed almost 90% RCYs at all temperatures (60°C to 140°C) irrespective of being substituted by –OCH$_3$ or –CH$_3$ groups in *ortho* position.

Radiofluorinations are rarely performed by isotopic exchange (^{18}F/^{19}F) as the specific activities to be achieved are thought to be unattractively low due to the presence of ^{19}F-carrier (c.a.).Thus, [^{18}F]-labelling was studied in dependence on the substrate concentrations for 2-[^{18}F]-fluoropyridine. The results showed the specific activities ranged from 0.524 GBq/μmole at the substrate concentration of 103 μmoles/mL to 11.65 GBq/μmole for 1.03 μmoles/mL. Although, the higher specific activity was obtained at a lower RCY of 20%, yet it might be of practical importance both for preclinical and clinical applications because very high amounts of [^{18}F]fluoride can be produced at commonly used medical cyclotrons (> 120 GBq/h) and so, in spite of lower radiochemical yields, high amounts of the product are obtained.

Additionally, energies of activations (E$_a$) were determined for the substituted 2-nitropyridines **(10a, 11a, 12a. 13a)** by Arrhenius plots. In case of all compounds, energies of activation were found in the range of 4-25 kJ / mol. Contrary to 2-nitrobezaldehyde[99] (24 kJ / mol) and nitrobenzene[99] (63.5 kJ / mol), E$_a$ for 2-nitropyridine was clearly lower (6.5 kJ / mol). This fact strongly advocates the fast kinetics of radiofluorinations in substituted 2-nitropyridines as compared to their homoaromatic analogues. For substituted 2-nitropyridines, E$_a$ for 3-methyl-2-nitropyridine **(11a)** was greater (25 kJ / mol) than 3-methoxy-2-nitropyridine (4.5 kJ / mol) and 3-methoxy-6-methyl-2-nitropyridine (14.9 kJ / mol). This very high value of E$_a$ for 3-methyl2-nitropyridine **(11a)** might be attributed to the formation of radioactive by-product at temperatures < 140°C (*see 3.4.3*).

Another important aspect in [^{18}F]-labelling is the protection of –OH substituent which is usually carried out by using –CH$_3$ group. But the hydrolysis conditions utilized for this purpose are very harsh such as 150°C and HBr so that an application of the particular labelling procedure in automatic modules becomes difficult because of the corrosive effects on walls, fittings, tubings, and valves[102]. Hence, it was desirable to find new protecting groups that could be hydrolysed under mild experimental conditions. For this purpose, hydrolysis of benzyloxy *O*-protecting groups was performed by acidic as well as catalytic transfer hydrogenation. Results proved 2,4-dimethyl benzyl and *p*-xylyl groups to be the best among all so tested. Time and temperature dependent analysis showed that both protecting groups could easily be cleaved at 120°C within 10 min after hydrolysis with 32% HCl by giving almost 80% RCYs. In addition, *p*-xylyl was hydrolysed under mild conditions with ca 75% of RCY at 70°C at 10 min by using ammonium formate (HCOONH$_4$) as a hydrogenating reagent.

In short, substituted 2-nitropyridines among all above mentioned compounds can be a surrogate of benzenes because of not only efficient radiofluorination by giving ca 90% RCY, but also because of elimination of one additional step (decarbonylation) in radiosynthesis of radiotracers. Thus, no need of electron-withdrawing group is required for [^{18}F]-labelling. In additions, *p*-xylyl can be used as *O*-protecting group in future because of its easy cleavage under mild conditions (70°C, 10 min).

As it has been discussed before[55, 103-104] that ^{13}C-NMR chemical shift values could be correlated to RCYs because these values are direct indicator of electrophilicity of the carbon atom bonded with the leaving group. However, all previous studies[55, 103-104] had to limit their findings only on structurally similar compounds. In the present work, for the first time, a complete correlation was found for those compounds even together with the structurally different heteroaromatic compounds (*see 3.2.8*). That is clearly due to the fact of vey well defined reaction parameters. Contrary to the previous theory, good value of linear regression ($R^2 = 0.7$) was obtained. Hence, it was proved that correlations can be studied among compounds bearing different substituents and irrespective of the substituents present on ring. However, this theory works only when there is no side or competing reaction going on.

[^{18}F]-labelling was carried out in order to develope the new precursors for PET-imaging of hypoxia ([^{18}F]FNT) and prostate cancer ([^{18}F]FPy-DUPA-Pep). Hypoxia radiotracer ([^{18}F]FNT) is a new compound that can utilize the amino acid transporter system to enter the hypoxic tissues and hence, its uptake can be expectedly enhanced for PET imaging. Its radiosynthesis was carried out by two steps; first step being the [^{18}F]-labelling *via* nucleophilic aliphatic substitution and second step being hydrolysis. [^{18}F]-labelled intermediate (**h**) was confirmed by correlating its R_f and R_t values with cold standard whereas [^{18}F]FNT formed after hydrolysis was confirmed by LCMS (353 (100%) [M+1]$^+$. At EOS, 40±1% (decay uncorrected) of [^{18}F]FNT was synthesized with radiochemical purity of > 98% within 90 min.

For radiosynthesis *via* S_NAr of a PSMA (prostate-specific membrane antigen) targeting ligand ([^{18}F]Py-DUPA-Pep), the method involves one step radiosynthesis of prosthetic group [(^{18}F)FPy-TFP] itself and one step for coupling with peptide. This prosthetic group was labelled with high RCYs of almost 90%. Also, the precursor could be easily removed from labelled product by cartridge purification and afterwards, the eluate was directly used for coupling with peptide i.e. DUPA-Pep. The other advantage of using this prosthetic group lies in the fact that [^{18}F]FPy reduces the lipophilicity of resulting peptide by many folds as compared to [^{18}F]SFB because the calculated lipophilicity of [^{18}F]FPy-DUPA-Pep (logP: 2.32±0.95) is clearly lower than that of [^{18}F]FB-DUPA-Pep (logP: 3.12±0.93)[81-82]. At the end of synthesis, 48±0.9% (decay uncorrected) of [^{18}F]FPy-DUPA-Pep was synthesised with radiochemical purity of > 98% within 50 min.

Hence, an efficient method of radiosynthesis for [^{18}F]FNT and [^{18}F]FPy-DUPA-Pep has been developed. Thus, both of these radiotracers can be used for PET imaging in clinical applications.

5. EXPERIMENTAL

5.1 General

All chemicals and solvents for organic synthesis and [^{18}F]-radiochemical synthesis were purchased from the Aldrich (Germany), Fluka (Germany), Riedel-de Haën (Germany), Sigma (Germany), Alfa Aesar (England), ABCR (England), and Merck (Germany). All chemicals and solvents were directly used in the synthesis without purification.

Following precursors for direct [^{18}F]-labelling and reference standards (for radiofluorinations) were purchased commercially: 3-methoxy-2-nitropyridine (12a, Aldrich, 98%), 3-methyl-2-nitropyridine (11a, Synchem OHG, 98%), 2-bromopyridine (10c, Aldrich, 99%), 2-bromo-3-methoxypyridine (12c, Aldrich, 97%), 2-bromo-3-methylpyridine (11c, ABCR, 98%), 2-chloropyridine (10d, Aldrich, 99%), 2-chloro-3-methylpyridine (11d, ABCR, 98%), 2-fluoropyridine (10b, Aldrich, 98%), and 2-fluoro-3-methylpyridine (11b, ABCR, 97%), 4-fluoro-3-methylbenzaldehyde (Aldrich, 97%), 2-fluorotoluene (Aldrich, 98%), 2,6-difluorotoluene (Aldrich, 98%).

5.1.1 Analytical Assay

Analytical assay was carried out by thin-layer chromatography (TLC) with silica gel plates (Polygram® Silica G/UV$_{254}$, 8 x 4 cm, Macherey Nagel, Germany) as stationary phase visualized under UV-lamp (254 nm) for cold synthesis and under phosphor imager (Raytest, FLA3000) for radiosynthesis. In addition, radio high pressure liquid chromatography (HPLC, P680 Dionex) equipped with NaI (TI)-scintillation detector (Raytest, GABI, Raytest, Gemany) and a UV detector (GY-400, 254 nm), was used for further identification of [^{18}F]-labelled products.

For additional measurement of radiochemical yields (RCYs), a γ-counter (1480 Wallac WIZARD 3", Perkin Elmer, USA) was used. However, for purification of intermediates in the organic synthesis, middle pressure liquid chromatography system (MPLC, Büchi, Switzerland) was applied for the purification using columns packed with silica gel 60 (0.040-0.063 mm, Merck) as stationary phase.

Eluents for TLC as well as for MPLC analysis were mixtures of petroleum ether (60/90°C) and ethyl acetate (PE/EtOAc, v/v) while for HPLC, the mixtures were of methanol (MeOH), acetonitrile (MeCN) and water (H$_2$O).

Sep-Pak© plus alumina N (Waters, USA), Sep-Pak© light C18 (Waters, USA), Strata-X (30 mg/mL, Phenomenex), and Sep-Pak© plus oasis (MCX, Waters) catridges were used for purification of [^{18}F]-labelled products.

Analysis by liquid chromatography coupled with mass-spectrometry on a quadrupole LC/MS (Agilent Technologies, Model 1200). Melting points (m.p.) were determined using Gallekamp device (MPG 350, USA).

5.1.2 Spectral Analysis

MS spectra were measured by using Triple Stage Quadrupole TSQ 70 Finnigan MAT-Massenspektrometer (Finnigan-MAT, Bremen, Germany).

^{1}H-NMR and ^{13}C-NMR were carried out on Avance 400 (Bruker, USA) operating at 400 and 100.6 MHz, respectively. [1]H chemical shifts (δ) are reported in ppm relative to residual peaks of deutrated solvent. The observed signal multiplicities are characterized as follows: s = singlet, d = doublet, t = triplet, m = multiplet.[13]C chemical shifts are reported relative to the peaks of solvents. (DMSO-d$_6$: δ = 2.49 in ^{1}H-NMR and δ = 39.5 in ^{13}C-NMR, CDCl$_3$: δ = 7.25 in ^{1}H-NMR and δ = 77.0 in ^{13}C-NMR).

5.2 Synthesis of Homoaromatic & Heteroaromatic Model Compounds (1-18)

5.2.1 2,3-Dimethoxy-6-fluorobenzaldehyde (5a)

n-BuLi (28 mL, 41 mmol, 1.6M, 0.7 g/dm^3) was added dropwise to the solution of 3,4-dimethoxy fluorobenzene (5 mL, 6.4 g, 1.17 g/dm^3, 41 mmol) dissolved in 80 mL of THF under argon at the temperature of -70 to -80°C using acetone/dry ice bath. After 2.5 h, 3.2 mL (41 mmol) of *N,N´*-dimethylformaide (DMF) was added and the reaction mixture was kept stirring at room temperature for 30 min. Afterwards, reaction mixture was quenched by adding 15 mL of acetic acid. Then, it was extracted by diethylether (DEE, 250 mL), washed by brine (250 mL) and water, dried over anhydrous sodium sulfate (Na$_2$SO$_4$), filtered and solvent was evaporated. Crude product was cleaned by using PE/EtOAc (4:1) as a solvent system at a flow rate of 5 mL/min. White solid (5 g, 27 mmol) was obtained as product (%yield: 66%).
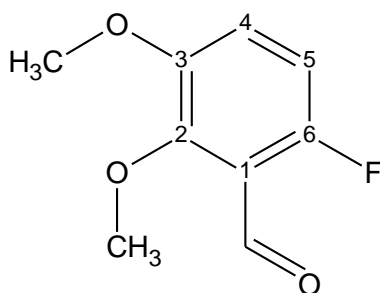
^{1}H-NMR (DMSO-D$_6$, 400.16 MHz):

δ 9.96 (1H, s, CHO), 7.05 (1H$_4$, d, $^3J_{4,5}$ = 7.89 Hz, Ph), 6.8(1H$_5$, d, $^3J_{5,4}$ = 8.79 Hz, Ph), 3.48 (3H, s, OCH$_3$), 3.67 (3H, s, OCH$_3$).

^{13}C-NMR (DMSO-D$_6$, 100.63 MHz):

δ 183 (C-CHO), 164 (C-6), 149 (C-2), 134 (C-3), 119 (C-4, d, $^4J_{4,6}$ = 4 Hz), 116 (C-5, d, $^3J_{5,6}$ = 26 Hz), 56 (C-OCH$_3$), 51 (C-3CH$_3$).

IR $\bar{\nu}$/cm^{-1}(T%):

2944 (90%), 2871 (93%), 2841 (92%), 2762 (97%), 1695 (30%), 1607 (60%), 1587 (72%), 1484 (26%), 1454 (65%), 1442 (65%), 1418 (81%), 1405 (76%), 1390 (52%), 1306 (78%), 1276 (60%),

1251 (22%), 1235 (35%), 1190 (70%), 1157 (83%), 1078 (47%), 1045 (26%), 965 (46%), 940 (75%), 868 (70%), 810 (48%), 777 (50%), 724 (74%), 704 (56%), 671 (77%).

MS-EI (70 eV) *m/z:*

183.7 (100 %) [M-1]$^+$, 153.7 (34 %) [M-CH$_2$O]$^+$, 93.8 (22 %) [M-C$_7$H$_7$]$^+$, 43 (18 %) [M-C$_6$H$_2$FO$_2$]$^+$.

HRMS (EI) m/z measured : 184.05332 [M]$^+$m/z calculated: 184.053556.

m.p.: 112°C. **R$_f$:** 0.14 (PE/EtOAc 1:1).

5.2.2 *General Procedure for Dimethylamine Substitution of Fluoro (2a, 3a, 4a, 5b)*

N,N´-dimethylamine hydrogen chloride (2.5 eq) and potassium carbonate (K$_2$CO$_3$, 2.5 eq) were added to the solution of fluoro precursors in DMSO/water (2.5:1). The reaction mixture was refluxed at 150°C for 4 h. Afterwards, the reaction mixture was poured in water (200 mL), extracted with DEE (250 mL), washed by brine and water, dried over anhydrous Na$_2$SO$_4$, filtered and solvent was evaporated. Crude products were cleaned by MPLC using PE/EtOAc [5:1 **(2a, 3a)**; 4:1 **(4a)**; 2:1 **(5b)**] as a solvent system at a flow rate of 5-6 mL/min. %Yield was 61-63% for all compounds and all of these were in form of pale yellow oil except compound (**4a**, pale yellow solid).

5.2.2.1 *3-Methyl-4-N,N´-dimethylaminobenzaldehyde (2a)*
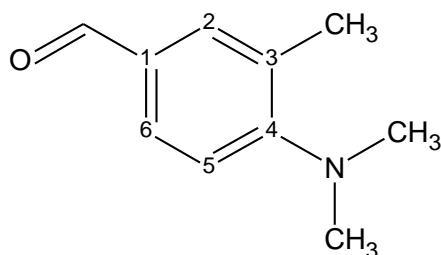
^{1}H-NMR (400.16 MHz, DMSO-D$_6$):

δ 10.1(1H, s, CHO), 7.8 (1H$_{6,5}$, d, $^3J_{6,5}$ = 8.4 Hz, Ph), 7.07 (1H$_2$, s, Ph), 6.54 (1H$_5$, d, $^3J_{5,6}$ = 8.4 Hz, Ph), 2.7 (6H, s, 2CH$_3$), 2.3 (3H, s, CH$_3$).

^{13}C-NMR (100.63 MHz, DMSO-D$_6$):

δ 192.1 (C-CHO), 170 (C-4), 157 (C-2), 132 (C-6), 129 (C-1), 127 (C-3), 117 (C-5), 56 (C-2CH$_3$), 21 (C-CH$_3$).

IR $\bar{\nu}$/cm^{-1}(T%):

2946 (85%), 2834 (83%), 2791 (82%), 2722 (90%), 1679 (29%), 1594 (22%), 1565 (55%), 1500 (45%), 1476 (79%), 1445 (64%), 1418 (76%), 1372 (72%), 1333 (55%), 1313 (58%), 1230 (30%), 1186 (62%), 1156 (56%), 1137 (61%), 1099 (27%), 1053 (66%), 1004 (87%), 956 (43%), 933 (75%), 897(76%), 821 (48%), 778 (51%), 744 (68%), 731 (60%), 703 (80%).

MS-EI (70 eV) *m/z:*

163 (100%) [M]$^+$, 148 (50%) [M-CH$_3$]$^+$, 132 (28%) [M-CH$_3$OH]$^+$, 118 (15%) [M-C$_2$H$_5$O]$^+$, 91 (16%) [C$_7$H$_7$]$^+$.

R$_f$: 0.54 (PE/EtOAc 5:1).

5.2.2.2 5-Methoxy-2-N,N´-dimethylaminobenzaldehyde (3a)
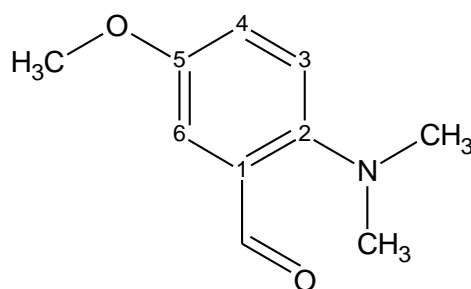
^{1}H-NMR (400.16 MHz, DMSO-D$_6$):

δ 10.1 (1H, s, CHO), 7.1 (1H$_6$, s, Ph), 6.9 (1H$_3$, d, $^3J_{3,4}$ = 8.5 Hz, Ph), 6.84 (1H$_4$, d, $^3J_{4,3}$ = 8.43 Hz, Ph), 3.7 (3H, s, OCH$_3$), 2.7 (6H, s, 2CH$_3$).

^{13}C-NMR (100.63 MHz, DMSO-D$_6$):

δ 192.1 (C-CHO), 152 (C-5), 149 (C-2), 129 (C-1), 123 (C-4), 121 (C-3), 111.5 (C-6), 55.4 (C-OCH$_3$), 46.1 (C-2CH$_3$).

IR $\bar{\nu}$/cm^{-1}(T%):

2944 (85%), 2834 (79%), 2789 (86%), 1676 (32%), 1607 (76%), 1572 (87%), 1494 (25%), 1453 (56%), 1415 (59%), 1381 (61%), 1301 (57%), 1275 (34%), 1234 (45%), 1185 (63%), 1164 (59%), 1151 (44%), 1089 (72%), 1034 (35%), 950 (66%), 937 (65%), 926 (63%), 869 (68%), 822 (57%), 774(55%), 729 (90%), 687 (53%).

MS-EI (70 eV) *m/z:*

179 (100%) [M]$^+$, 163.1(16%) [M-CH$_3$]$^+$, 151 (25%) [M-CO]$^+$, 136 (19%) [M-CH$_3$CO]$^+$, 119 (23%) [M-C$_2$H$_4$O$_2$]$^+$.

R$_f$: 0.43 (PE/EtOAc 1:1).

5.2.2.3 6-Methoxy-2-N,N´-dimethylaminobenzaldehyde (4a)
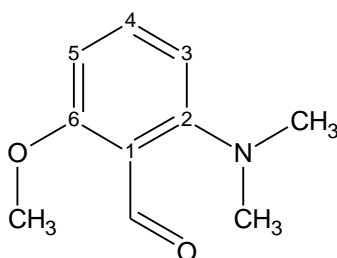
^{1}H-NMR (400.16 MHz, DMSO-D$_6$):

δ 9.5 (1H, s, CHO), 7.30 (1H$_4$, d, $^3J_{4,5}$ =7.67 Hz, Ph), 6.42 (1H$_5$, m, Ph), 6.33 (1H$_3$, d, $^3J_{3,4}$ =7.80 Hz, Ph), 3.83 (3H, s, OCH$_3$), 2.7 (6H, s, 2CH$_3$).

^{13}C-NMR (100.63 MHz, DMSO-D$_6$):

δ 190 (C-CHO), 163 (C-6), 157 (C-2), 135 (C-4), 115 (C-1), 113 (C-3), 106 (C-5), 56 (C-OCH$_3$), 43 (C-2CH$_3$).

IR $\bar{\nu}$/cm^{-1}(T%):

2949 (89%), 2837 (81%), 2788 (81%), 1671 (41%), 1611 (79%), 1571 (87%), 1496 (35%), 1451 (61%), 1420 (57%), 1382 (58%), 1299 (54%), 1271 (31%), 1232 (35%), 1179 (63%), 1169 (49%), 1153 (54%), 1091 (74%), 1027 (32%), 961 (63%), 941 (71%), 916 (57%), 873 (69%), 821 (56%), 770 (65%), 719 (90%), 683 (52%).

MS-EI (70 eV) *m/z:*

179 (100%) [M]$^+$, 162.1 (92%) [M-CH$_3$]$^+$, 150.2 (68%) [M-CHO]$^+$, 147.2 (56%) [M-CH$_4$O]$^+$.

HRMS (EI) m/z measured : 179.09645 [M]$^+$ m/z calculated: 179.094616.

m.p.: 64°C. **R$_f$:** 0.21 (PE/EtOAc 4:1).

5.2.2.4   *2,3-Dimethoxy-6-N,N´-dimethylaminobenzaldehyde (5b)*
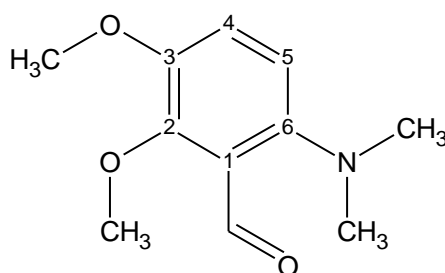
^{1}H-NMR (DMSO-D$_6$, 400.16 MHz):

δ 10.2 (1H, s, -CHO), 7.2 (1H$_4$, d, $^3J_{4,5}$ = 8.22 Hz, Ph), 6.91 (1H$_5$, d, $^3J_{5,4}$ = 9.01 Hz, Ph), 3.85 (6H, s, 2OCH$_3$), 3.45 (3H, s, CH$_3$).

.^{13}C-NMR (DMSO-D$_6$, 100.63 MHz):

δ 189 (C-CHO), 151 (C-2), 148 (C-6), 146 (C-3), 122 (C-4), 119 (C-1), 113 (C-5), 61 (C-OCH$_3$), 56 (C-OCH$_3$), 45 (C-2CH$_3$).

IR $\bar{\nu}$/cm^{-1}(T%):

2961 (87%), 2837 (90%), 1686 (40%), 1608 (75%), 1507 (30%), 1483 (37%), 1453 (47%), 1417 (52%), 1340 (85%), 1304 (81%), 1229 (27%), 1192 (42%), 1149 (47%), 1115 (46%), 1069 (43%), 1045 (37%), 1027 (27%), 951 (35%), 832 (41%), 798 (45%), 765 (43%), 765 (42%), 765 (51%), 708 (52%).

MS-EI (70 eV) *m/z:*

209 (88 %) [M]$^+$, 194 (100 %) [M- CH$_3$]$^+$,166 (27 %) [M-CH$_3$ CO]$^+$, 137 (28 %) [M-C$_4$H$_{10}$N]$^+$, 85.1 (39 %) [C$_5$H$_9$O]$^+$, 43.2 (73%) [CH$_3$CO]$^+$.

HRMS (EI) m/z measured : 209.10534 [M]$^+$ m/z calculated: 209.105176.

R$_f$: 0.45 (PE/EtOAc 2:1).

5.2.3   *General Procedure for Dimethylation of Amino-Group (2a, 3a, 4a, 5b)*

Sodium bicarbonate (NaHCO$_3$, 5 eq) was added to the solution of starting material (methyl anilines) in DMF (7 mL). Afterwards, iodomethane (MeI, 10 eq) was added slowly at 0°C. After 1.5 h, reaction was stopped, and reaction mixture was extracted with DEE (250 mL), washed by brine and

water, dried over anhyd.Na$_2$SO$_4$, filtered and solvent was evaporated. Cleaned products (**6a, 7a**; yellow oil; %yield: 75%) were obtained with chemical purity > 98%.

5.2.3.1 2-N,N´-Dimethylaminotoluene (6a)
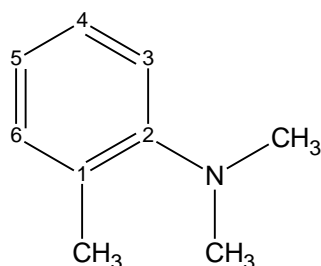
^{1}H-NMR (400.16 MHz, DMSO-D$_6$):

δ 7.03 (2H$_{4,6}$, m, Ph), 6.91 (1H$_3$, d, $^3J_{3,4}$ = 7.99Hz, Ph), 6.83 (1H$_5$, d, $^3J_{5,6}$ = 7.73Hz, Ph), 2.7 (6H, s, 2CH$_3$) 2.19 (3H, s, CH$_3$).

^{13}C-NMR (100.63 MHz, DMSO-D$_6$):

δ 152 (C-2), 131 (C-6), 130 (C-1), 128 (C-4), 122(C-5), 118 (C-3), 44 (C-2CH$_3$), 18 (C-CH$_3$).

IR $\bar{\nu}$/cm^{-1}(T%):

3144 (90%), 1642 (86%), 1396 (69%), 1427 (89%), 1400 (89%), 1249 (17%), 1192 (19%), 1135 (21%), 1069 (68%), 1042 (48%), 1019 (20%), 934 (49%), 847 (47%), 779 (51%), 751 (49%), 710 (79%), 707 (68%), 683 (80%).

MS-EI (70 eV) *m/z*:

134.2 (100%) [M-1]$^+$, 120 (76%) [M-CH]$^+$, 118 (48%) [M-CH$_3$]$^+$, 104 (40%) [M-C$_2$H$_2$]$^+$, 91 (40%) [C$_7$H$_7$]$^+$.

R$_f$: 0.73 (PE/EtOAc 4:1).

5.2.3.2 2-N,N´-Dimethylamino-m-xylene (7a)
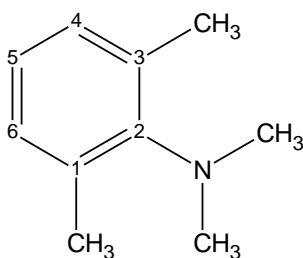
^{1}H-NMR (400.16 MHz, DMSO-D$_6$):

δ 6.83 (3H$_{4,5,6}$, m, Ph), 2.73 (6H, s, 2CH$_3$), 2.29 (6H, s, 2CH$_3$).

^{13}C-NMR (100.63 MHz, DMSO-D$_6$):

δ 149 (C-2), 137 (C-3,1), 129 (C-4,6), 125 (C-5), 42 (C-2CH$_3$), 19 (C-2CH$_3$).

IR $\bar{\nu}$/cm^{-1}(T%):

3110 (90%), 1744 (83%), 1479 (77%), 1419 (75%), 1373 (87%), 1246 (15%), 1219 (29%), 1143 (24%), 1049 (67%), 1018 (11%), 941 (55%), 843 (63%), 789 (43%), 751 (71%).

MS-EI (70 eV) *m/z:*

149 (100%) [M]$^+$, 134 (80%) [M-CH$_3$]$^+$, 118 (60%) [M-C$_2$H$_7$]$^+$, 105 (40%) [M-C$_3$H$_8$]$^+$.

R$_f$: 0.93 (PE/EtOAc 1:1).

5.2.4 General Procedure for Quaternization (1, 2, 3, 4, 5, 6, 7)

Methyltrifluorimethane sulfonate (1.75 eq) was added to the solution of starting material (dimethylamino precursors: **2a, 3a, 4a, 5b, 6a, 7a**) in DCM under argon. After 4 hours, reaction was stopped. DCM was evaporated and the product was crystallized from DCM/DEE (5:1). All products were obtained as white solids (%yields: 75-85%).

5.2.4.1 4-Formyl-N,N,N-trimethylbenzenaminium trifluoromethanesulfonate (1)
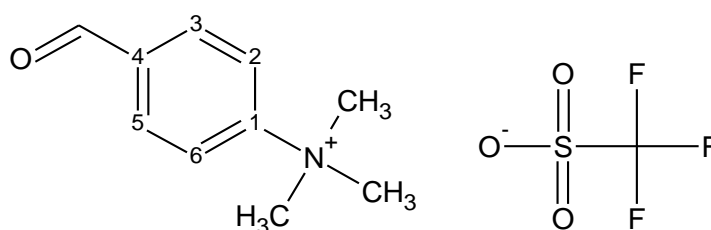
^{1}H-NMR (400.16 MHz, DMSO-D$_6$):

δ 10.1 (1H, s, CHO), 7.67 (2H$_{3,5}$, d, $^3J_{2,3}$ = 8 Hz, Ph), 6.78 (2H$_{2,6}$, d, $^3J_{5,6}$ = 8.8 Hz, Ph), 3.03 (9H, s, Me).

^{13}C-NMR (100.63 MHz, DMSO-D$_6$):

δ 192.1 (C-CHO), 151.1 (C-1), 136.8 (C-4), 130.9 (C-3, 5), 121.7 (C-2, 6), 56.4 (C-8, 9, 10).

IR $\bar{\nu}$/cm^{-1}(T%):

3046 (93%), 2941 (93%), 2835 (98%), 2298 (98%), 1701 (97%), 1609 (96%), 1497 (80%), 1483 (84%), 1474 (84%), 1457 (88%), 1416 (88%), 1368 (86%), 1317 (91%), 1252 (28%), 1223 (41%), 1195 (63%), 1160 (48%), 1119 (71%), 1099 (52%), 1078 (56%), 1051 (51%), 1025 (29%), 984 (53%), 958 (67%), 940 (69%), 909 (70%), 890 (85%), 848 (64%), 818 (65%), 757 (77%), 744 (92%), 710 (89%).

MS-FAB (70 eV) *m/z:*

164.1 (100%) [M-CF$_3$COO]$^+$.

m.p.: 109°C

5.2.4.2 4-Formyl-N,N,N,2-tetramethylbenzenaminium trifluoromethanesulfonate (2)
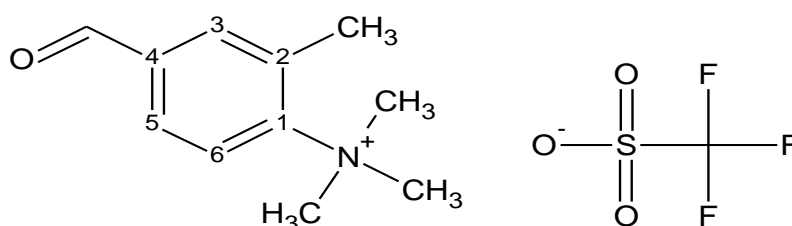
^{1}H-NMR (400.16 MHz, DMSO-D$_6$):

δ 10.1(1H, s, CHO), 8.85(1H$_5$, d, $^3J_{5,6}$ = 8.36 Hz, Ph), 8.49(1H$_3$, s, Ph), 7.56 (1H$_6$, d, $^3J_{5,6}$ = 8.85 Hz, Ph), 2.7 (9H, s, 3CH$_3$).

^{13}C-NMR (100.63 MHz, DMSO-D$_6$):

δ 192.1 (C-CHO), 149.05 (C-1), 137(C-4), 136 (C-5), 132 (C-3), 128.4 (C-2), 122.7 (C-6), 56.61 (C-3CH$_3$), 22.7 (C-CH$_3$).

IR $\bar{\nu}$/cm^{-1}(T%):

3052 (93%), 2296 (98%), 1691 (60%), 1609 (93%), 1584 (88%), 1496 (76%), 1480 (81%), 1389 (90%), 1376 (90%), 1315 (92%), 1255 (26%), 1223 (30%), 1197 (76%), 1147 (33%), 1092 (78%), 1067 (60%), 1026 (20%), 962 (80%), 947 (58%), 820 (73%), 777 (65%), 756 (72%), 739 (90%), 679 (86%).

MS-FAB (70 eV) *m/z:*

178.1 (100%) [M]$^+$, 163.1 (16%) [M-CH$_3$]$^+$, 136 (27%) [M-CH$_3$-CO]$^+$.

m.p.:115°C

5.2.4.3 2-Formyl-4-methoxy-N,N,N-trimethylbenzenaminiumtrifluoromethanesulfonate (3)
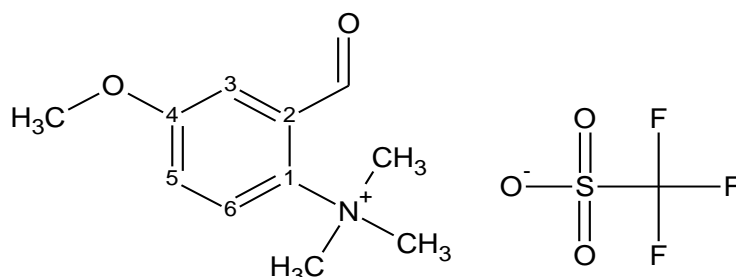
^{1}H-NMR (DMSO-D$_6$, 400.16 MHz):

δ 10.19 (1H, s, CHO), 8.00 (1H$_3$, s, Ph), 7.87 (1H$_5$, d, $^3J_{5,6}$ = 8.8 Hz, Ph), 7.46 (1H$_6$, dd, $^3J_{6,5}$ = 8.5 Hz, Ph), 4.00 (3H, s, OCH$_3$), 3.71 (9H, s, 3CH$_3$).

.^{13}C-NMR (DMSO-D$_6$, 100.63 MHz):

δ 193.0 (C-CHO), 160.1 (C-4), 137.0 (C-1), 131.1 (C-2), 126.0 (C-6), 124.3 (C-5), 118.7 (C-3), 57.0 (C-3CH$_3$), 56.3 (C-OCH$_3$).

IR $\bar{\nu}$/cm^{-1}(T%):

3085 (93%), 3045 (92%), 2985 (94%), 2951 (94%), 2851 (95%), 2287 (96%), 1700 (67%), 1686 (62%), 1609 (89%), 1585 (61%), 1493 (77%), 1462 (82%), 1447 (82%), 1407 (86%), 1309 (83%), 1255 (17%), 1221 (37%), 1203 (70%), 1146 (31%), 1082 (86%), 1029 (18%), 956 (72%), 942 (75%), 922 (52%), 901 (64%), 830 (51%), 770 (69%), 754 (65%), 690 (84%), 660 (83%).

MS-FAB (70 eV) *m/z:*

194 (100 %) [M]$^+$, 179 (14 %) [M-CH$_3$]$^+$, ,164 (8 %) [M-CH$_3$-CH$_3$]$^+$, 150 (6 %) [M-CH$_3$-CH$_2$]$^+$, 136 (8 %) [M-CH$_3$-CH$_2$ -CH$_2$]$^+$.

m.p.: 112°C

5.2.4.4 2-Formyl-6-methoxy-N,N,N-trimethylbenzenaminiumtrifluoromethanesulfonate (4)
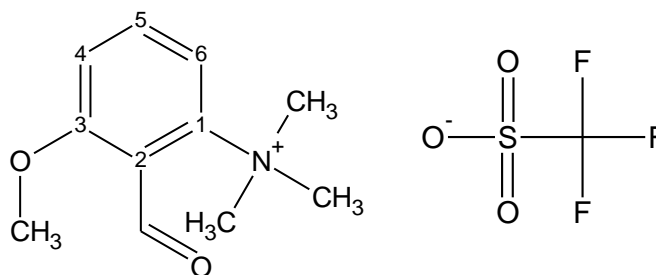
^{1}H-NMR (DMSO-D$_6$, 400.16 MHz):

δ 10.3 (1H, s, CHO), 7.35 (1H$_6$, s, Ph), 7.31 (1H$_5$, d, $^3J_{5,6}$ = 8.22 Hz, Ph), 6.91 (1H$_4$, d, $^3J_{4,5}$ = 8.11 Hz, Ph), 3.83 (3H, s, OCH$_3$), 3.60 (9H, s, 3CH$_3$).

^{13}C-NMR (DMSO-D$_6$, 100.63 MHz):

δ 183 (C-CHO), 164 (C-3), 149 (C-1), 134 (C-5), 119 (C-4), 116 (C-6, 2), 56 (C-OCH$_3$), 51 (C-3CH$_3$)

IR $\bar{\nu}$/cm^{-1}(T%):

3085 (93%), 3045 (92%), 2985 (94%), 2951 (94%), 2851 (95%), 2287 (96%), 1700 (67%), 1686 (62%), 1609 (89%), 1585 (61%), 1493 (77%), 1462 (82%), 1447 (82%), 1407 (86%), 1309 (83%), 1255 (17%), 1221 (37%), 1203 (70%), 1146 (31%), 1082 (86%), 1029 (18%), 956 (72%), 942 (75%), 922 (52%), 901 (64%), 830 (51%), 770 (69%), 754 (65%), 690 (84%), 660 (83%).

MS-FAB (70 eV) m/z:

194 (100 %) [M]$^+$, 179 (14 %) [M-CH$_3$]$^+$, 164 (8 %) [M-CH$_3$-CH$_3$]$^+$, 150 (6 %) [M-CH$_3$-CH$_2$]$^+$, 136 (8 %) [M-CH$_3$-CH$_2$ -CH$_2$]$^+$.

m.p.: 109°C

5.2.4.5 2-Formyl-3,4-dimethoxy-N,N,N trimethylbenzenaminiumtrifluoromethanesulfonate (5)
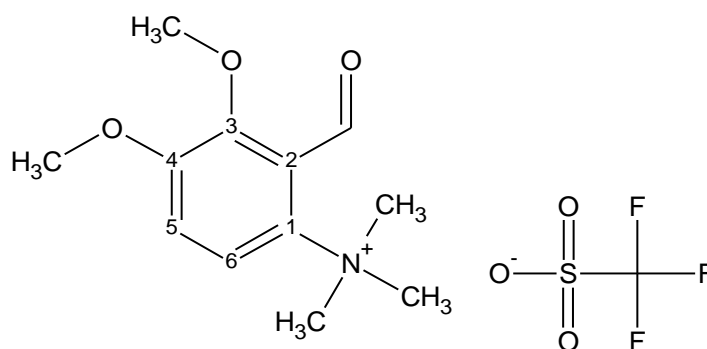
^{1}H-NMR (400.16 MHz, DMSO-D$_6$):

δ 10.1(1H, s, CHO), 8.01(1H$_5$, d, $^3J_{5,6}$ = 8.35 Hz, Ph), 6.93 (1H$_6$, d, $^3J_{6,5}$ = 8.5 Hz, Ph), 3.7(3H, s, OCH$_3$) 3.85(3H, s, OCH$_3$) 3.6(9H, s, 3CH$_3$).

^{13}C-NMR (100.63 MHz, DMSO-D$_6$):

δ 183 (C-CHO), 153.8 (C-3), 151 (C-4), 143 (C-1), 121 (C-5), 118 (C-6), 115 (C-2), 61 (C-OCH$_3$), 57 (C-3CH$_3$), 56 (C-OCH$_3$).

IR $\bar{\nu}$/cm^{-1}(T%):

3056 (95%), 2952 (94%), 1699 (77%), 1586 (84%), 1499 (81%), 1484 (69%), 1466 (76%), 1433 (90%), 1400 (82%), 1370 (91%), 1325 (87%), 1258 (31%), 1226 (41%), 1153 (44%), 1066 (75%), 1028 (36%), 982 (81%), 945 (68%), 934 (71%), 894 (88%) , 848 (85%), 833 (84%), 808 (72%), 781 (79%) 756 (80%), 704 (92%), 689 (89%), 675 (90%).

MS-FAB (70 eV) *m/z:*

224.1 (100%) [M]$^+$, 210.1 (62%) [M-N]$^+$, 194.1 (16%) [M-CH$_2$O]$^+$, 147.1 (24%) [M-C$_6$H$_5$]$^+$.

m.p.: 138°C

5.2.4.6 N,N,N,2-tetramethylbenzenaminium trifluoromethanesulfonate (6)
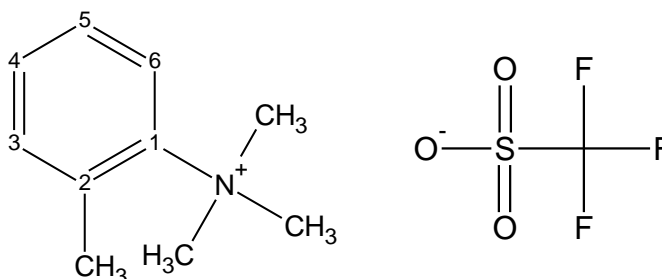
^{1}H-NMR (DMSO-D$_6$, 400.16 MHz):

δ 7.83 (1H$_3$, d, $^3J_{3,4}$ = 7.84 Hz, Ph), 7.49 (1H$_{5,6}$, m, Ph), 7.31 (1H$_4$, d, $^3J_{4,5}$ = 7.67 Hz, Ph), 3.66 (9H, s, 3CH$_3$), 2.72 (3H, s, CH$_3$).

^{13}C-NMR (DMSO-D$_6$, 100.63 MHz):

δ 146 (C-1), 139 (C-4), 134 (C-3), 130 (C-2), 129 (C-5), 121 (C-6), 56 (C-3CH$_3$), 22 (C-CH$_3$).

IR $\bar{\nu}$/cm^{-1}(T%):

3040 (94%), 1742 (96%), 1492 (71%), 1419 (89%), 1392 (94%), 1256 (16%), 1223 (29%), 1147 (23%), 1080 (79%), 1062 (69%), 1027 (20%), 944 (59%), 853 (67%), 785 (62%), 762 (61%), 718 (81%), 710 (78%), 683 (91%)

MS-FAB (70 eV) *m/z:*

150 (100 %) [M]$^+$, 135 (20 %) [M-CH$_3$]$^+$.

m.p.:82°C

5.2.4.7 N,N,N,2,6-pentamethylbenzenaminium trifluoromethanesulfonate (7)
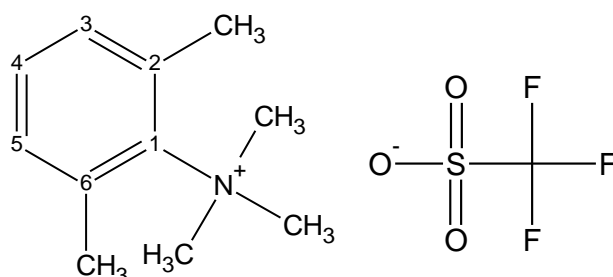
¹H-NMR (DMSO-D₆, 400.16 MHz):

δ = 7.91 (1H$_5$, s, Ph), 7.89 (1H$_3$, d, $^3J_{3,4}$ = 7.84 Hz, Ph), 7.06 (1H$_4$, d, $^3J_{4,5}$ = 7.84 Hz, Ph), 3.51 (9H, s, 3CH$_3$), 2.15 (6H, s, 2CH$_3$).

¹³C-NMR (DMSO-D₆, 100.63 MHz):

δ = 147 (C-1), 135 (C-3,5), 133 (C-2,6), 132 (C-4), 57 (C-3CH$_3$), 18 (C-2CH$_3$).

IR $\bar{\nu}$/cm⁻¹(T%):

3094 (94%), 1738 (94%), 1482 (75%), 1421 (86%) 1394 (90%), 1255 (18%), 1223 (30%), 1153 (24%), 1058 (67%), 1029 (16%), 943 (65%), 840 (64%), 792 (53%), 756 (73%).

MS-FAB (70 eV) *m/z:*

164 (100 %) [M]⁺, 149(27 %) [M-CH$_3$]⁺.

m.p.:131°C

5.2.5 2-Amino-3-hydroxymethyl toluene (8a)

30 mL of lithium aluminium hydride (LiAlH$_4$, 30 mmol) (1.5 eq) was added dropwise using dropping funnel to the flask containing 2-amino-3-methyl benzoic acid (3 g, 20 mmol) dissolved in 40 mL of THF at 0°C under argon. When bubble formation stopped, ice bath was removed and it was kept stirring at room temperature for 2 h. Afterwards, it was refluxed at 70°C for 20 min. Then, the reaction was stopped and reaction mixture was quenched with THF/H$_2$O (1:1, 50 mL) at 0°C. Reaction mixture was filtered, extracted by DCM (250 mL), washed by water, dried over anhyd.Na$_2$SO$_4$, filtered, solvent was evaporated. 2.65 g (19.3 mmol) of product was obtained as pinkish white solid (%yield: 97%).
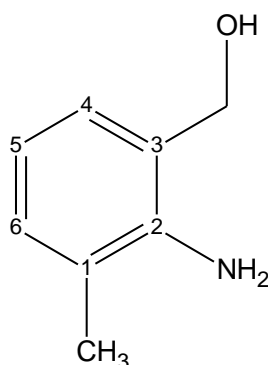
^{1}H-NMR (400.16 MHz, DMSO-D$_6$):

δ 7.29(1H$_4$, t, $^{3}J_{4,5}$ = 7.60 Hz, Ph), 6.89(1H$_5$, t, $^{3}J_{5,4}$ = 7.57 Hz, Ph), 6.74 (1H$_6$, m,Ph), 4.10 (2H, s, CH$_2$), 3.77 (3H, s, OH, NH$_2$), 2.09 (3H, s, CH$_3$).

^{13}C-NMR (100.63 MHz, DMSO-D$_6$):

δ 142 (C-2), 133 (C-3), 130 (C-5), 127 (C-6), 125 (C-4), 120 (C-1), 61 (C-CH$_2$), 17 (C-CH$_3$).

IR $\overline{\nu}$/cm^{-1}(T%):

3404 (62%), 3322 (54%), 3026 (80%), 2961 (76%), 2935 (75%), 2913 (75%), 2862 (69%), 1897 (90%), 1729 (90%) 1629 (61%), 1598 (68%), 1470 (40%), 1433 (59%), 1349 (77%), 1320 (66%), 1268 (61%), 1235 (59%), 1203 (73%), 1169 (68%), 1142 (79%), 1089 (67%), 1014 (24%), 971 (61%), 949 (68%), 887 (65%), 750 (34%), 683 (19%).

MS-EI (70 eV) *m/z:*

138 (100%) [M+1]$^+$, 120 (80%) [M-H$_2$O]$^+$, 106 (60%) [M-CH$_3$O]$^+$, 91 (40%) [C$_7$H$_7$]$^+$.

m.p.:83°C. **R$_f$:** 0.42 (PE/EtOAc 1:1).

5.2.6 *2-Dimethylamino-3-hydroxymethyl toluene (9a)*

3.1 g (23 mmol) of 2-amino-3-hydroxymethyl toluene **(8a)** and 6 g (158 mmol, 7 eq) of sodium borohydride (NaBH$_4$) dissolved in 7 mL of THF were added to the flask containing 1mL of 37% formaldehyde (HCHO, 0.158 moles) and 0.05 mL of sulfuric acid (H$_2$SO$_4$), under argon at 10-20°C using acetone/NaCl in an ice bath. At the end of reaction, solid sodium hydroxide (NaOH) was added and supernatant was separated, residue was washed by water, extracted by DEE (300 mL). Then, both organic layers were combined, and were washed by brine, dried over anhyd.Na$_2$SO$_4$, filtered and solvent was evaporated. Crude product was cleaned by MPLC using PE/EtAc (2:1) at a flow rate of 6mL/ min. 2 g (14.8 mmol) of cleaned product was obtained as oil (%yield: 65%).
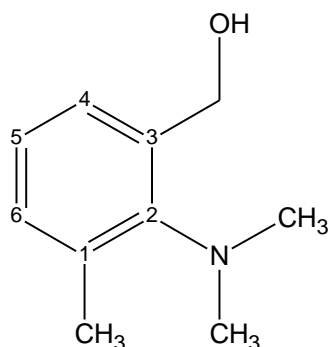
^{1}H-NMR (400.16 MHz, DMSO-D$_6$):

δ 7.27 (1H$_4$, t, $^{3}J_{4,5}$ = 7.50 Hz, Ph), 7.19 (1H$_5$, d, $^{3}J_{5,4}$ = 7.57 Hz, Ph), 7.08 (1H$_6$, s, Ph), 5.30 (1H, s, OH), 3.96 (2H, s, CH$_2$), 2.93 (6H, s, 2CH$_3$), 2.36 (3H, s, CH$_3$).

^{13}C-NMR (100.63 MHz, DMSO-D$_6$):

δ 148 (C-2), 133 (C-1), 131 (C-6), 129 (C-4), 126 (C-3), 122 (C-5), 63 (C-CH$_2$), 42 (C-2CH$_3$), 18(C-CH$_3$).

IR $\bar{\nu}$/cm^{-1}(T%):

3545 (72%), 3422 (64%), 3126 (81%), 2876 (76%), 2845 (65%), 2713 (55%), 2762 (79%), 1989 (90%), 1841 (87%) 1731 (71%), 1698 (58%), 1467 (60%), 1429 (69%), 1343 (71%), 1326 (56%), 1270 (51%), 1239 (69%), 1213 (83%), 1149 (58%), 1132 (69%), 1100 (57%), 1009 (21%), 956 (59%), 934 (48%), 819 (55%), 770 (44%), 643 (10%).

MS-EI (70 eV) *m/z:*

165 (100%) [M]$^+$, 150 (80%) [M-CH$_3$]$^+$, 122 (60%) [M-CH$_3$-CO]$^+$.

R$_f$: 0.72 (PE/EtOAc 1:1).

5.2.7 General Procedure for Oxidation (8b, 9b)

Substituted benzaldehyde **(8a, 9a)** dissolved in 20 mL of DCM was added into the flask containing oxidizing reagent (pyridinium chlorochromate, PCC, 2 eq) at RT. After 2 h, reaction was stopped and reaction mixture was extracted by DEE (250 mL), washed by water, dried over anhyd.Na$_2$SO$_4$, filtered and solvent was evaporated. Crude products were cleaned by MPLC using PE/EtOAc (4:1) solvent system at a flow rate of 5-6 mL/min. Compound **(8b)** was obtained as oil whereas compound **(9b)** was obtained as white solid (%yield: 60%).

5.2.7.1 2-Amino-3-methyl benzaldehyde (8a)
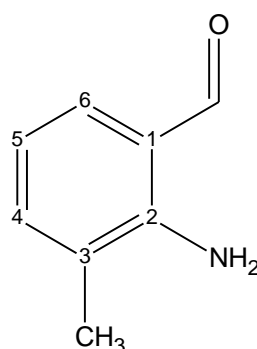
^{1}H-NMR (400.16 MHz, DMSO-D$_6$):

δ 9.81 (1H, s, CHO), 7.51 (1H$_6$, d, $^3J_{6,5}$ = 7.83 Hz, Ph), 7.07 (1H$_4$, d, $^3J_{4,5}$ = 7.57 Hz, Ph), 6.79 (1H$_5$, m,Ph), 3.11 (2H, s, NH$_2$), 2.10 (3H, s, CH$_3$).

^{13}C-NMR (100.63 MHz, DMSO-D$_6$):

δ 193 (C-CHO), 149 (C-2), 144 (C-4), 135 (C-6), 131 (C-1), 129 (C-5), 124 (C-3), 18 (C-CH$_3$).

IR $\bar{\nu}$/cm^{-1}(T%):

3460 (85%), 3345 (70%), 3041 (95%), 2855 (91%), 2741 (95%), 1656 (51%), 1612 (30%), 1562 (40%), 1466 (56%) 1434 (57%), 1380 (71%), 1343 (80%), 1272 (69%), 1219 (41%), 1134 (83%), 1087 (65%), 1001 (63%), 920 (73%), 850 (88%), 767 (59%), 740 (47%), 694 (49%)

MS-EI (70 eV) *m/z:*

135 (80%) [M]$^+$, 120 (100%) [M-CH$_3$]$^+$, 106 (60%) [M-CHO]$^+$, 92 (40%) [M-CH$_3$CO]$^+$.

R$_f$: 0.82 (PE/EtOAc 1:1).

5.2.7.2 1,8-Dimethyl-2,4-dihydro-1H-3,1-benzoxazine (9b)
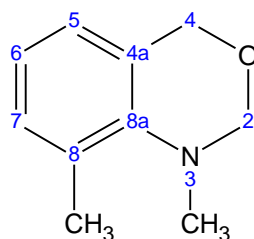
^{1}H-NMR (400.16 MHz, DMSO-D$_6$):

δ 7.34 (1H$_5$, s, Ph), 7.1 (2H$_{6,7}$, d, $^3J_{7,6}$ = 7.83 Hz, Ph), 4.82 (4H$_{4,2}$, m, 2CH$_2$), 3.03 (3H, s, N-CH$_3$), 2.10 (3H, s, CH$_3$).

^{13}C-NMR (100.63 MHz, DMSO-D$_6$):

δ 147 (C-8a), 131 (C-7), 129 (C-8), 125 (C-4a), 123 (C-6), 85 (C-CH$_2$), 67 (C-CH$_2$), 40 (C-NCH$_3$)., 18 (C-CH$_3$)

IR $\bar{\nu}$/cm^{-1}(T%):

3341 (54%), 3005 (85%), 2890 (81%), 2835 (75%), 2778 (88%), 1920 (90%), 1741 (91%), 1595 (70%), 1471 (36%), 1445 (59%), 1397 (64%), 1377 (69%), 1346 (74%), 1319 (78%), 1296 (74%), 1262 (66%), 1252 (57%), 1232 (52%), 1163 (86%), 1132 (65%), 1092 (57%), 1063 (53%), 1040 (38%), 1009 (55%), 963 (76%), 942 (58%), 913 (26%), 894 (60%), 828 (71%), 770 (33%), 745 (30%), 693 (42%), 675 (59%).

MS-EI (70 eV) *m/z:*

163 (80%) [M]$^+$, 148 (100%) [M-CH$_3$]$^+$, 133 (60%) [M-C$_2$H$_6$]$^+$, 103 (40%) [M-C$_8$H$_7$NO]$^+$, 91 (31%) [C$_7$H$_7$]$^+$.

R$_f$: 0.53 (PE/EtOAc 4:1).

5.2.8 2-Nitropyridine (10a)

1.0 g (10.6 mmol) of 2-aminopyridine was dissolved in 10 mL of concentrated H$_2$SO$_4$ and the resulting solution was cooled to 0°C using an ice bath. To this solution, a cooled (5°C) mixture of 30% aqueous hydrogen peroxide (H$_2$O$_2$, 15 mL) in 30 mL of concentrated H$_2$SO$_4$was added dropwise, while maintaining the temperature below 15°C. The colour of the solution changed from yellow to green. It was kept stirring at room temperature overnight and then, carefully basified with 3M aqueous KOH. The resulting mixture was then filtered, extracted with EtOAc (250 mL), washed with water and brine, and dried over anhydrous Na$_2$SO$_4$. The solvent was evaporated and the residue was separated by MPLC using PE/EtOAc (1:1) as mobile phase at a flow rate of 20 mL/min. 910 mg of 2-nitropyridine was obtained as yellow solid (%yield: 69%).
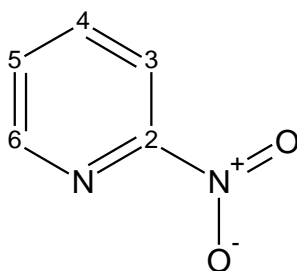
¹H-NMR (DMSO-D₆, 400.16 MHz):

δ 9.07 (1H₆, bdd, J_{app}= 0.91, 4.5 Hz, Py), 8.69 (1H₃, dd, $^3J_{3,4}$ = 8.24 Hz, Py), 8.62 (1H₄, td, $^3J_{4,5}$ = 7.02 Hz, Py), 8.3 (1H₅, ddd, $^3J_{5,6}$ = 5.28 Hz, Py).

¹³C-NMR (DMSO-D₆, 100.63 MHz):

δ 158 (C-2), 150 (C-6), 141 (C-4), 130 (C-5), 118.5 (C-3).

IR $\bar{\nu}$/cm⁻¹(T%):

3113 (90%), 3089 (90%), 2880 (92%), 1727 (93%), 1562 (89%), 1545 (70%), 1531 (62%), 1464 (80%), 1429 (70%), 1383 (84%), 1353 (58%), 1313 (76%), 1251 (78%), 1145 (80%), 1087 (80%), 1040 (79%), 994 (69%), 856 (66%), 813 (61%), 740 (60%), 700 (67%), 688 (56%).

MS-EI (70 eV) *m/z:*

124 (10%) [M]⁺, 94.1 (18%) [M-NO]⁺, 78.1 (100%) [M-NO₂]⁺.

m.p.:73°C. **R_f:** 0.45 (PE/EtAc 1:1).

5.2.9 *General Procedure for –OH Protection (12d, 13a, 13c, 15, 16, 17, 18, 19)*

Solution of sodium methoxide of MeONa (1.2 eq) in DMF (5 mL) was added dropwise to a stirred solution of hydroxyl substituted pyridines in DMF (20 mL) under argon. Afterwards, the mixture was stirred for 30 min. Thereafter, the reaction mixture was cooled to 4 °C and the respective MeI (1.2 eq) or benzyl halogenide (1.2 eq) was added. The reaction mixture was allowed to stir at RT for 10 h. Then the mixture was diluted with water (75 mL) and extracted with ethylacetate (200 mL). The organic phase was separated, washed with water, dried over anhydrous Na₂SO₄, filtered and concentrated under reduced pressure. The crude product was purified either by MPLC at a flow rate of 15 mL/min or by flash chromatography using PE/EtOAc (1:1) as mobile phase and then recrystallized from pentane. All compounds were obtained as white solids except compound (**14**, yellow solid) (%yield: 80-85%).

5.2.9.1 *3-Methoxy-2-chloropyridine (12d)*
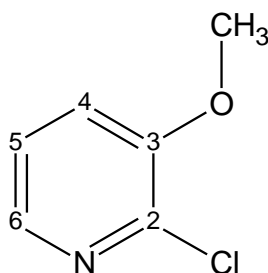
^{1}H-NMR (DMSO-D$_6$, 400.16 MHz):

δ 7.96 (1H$_6$, m, Py), 8.01 (1H$_5$, dd, $^3J_{5,6}$ = 8.2 Hz, Py), 7.81 (1H$_4$, dd, $^3J_{4,5}$ =0.91, & 8.37 Hz,), 3.67 (3H, s, OCH$_3$).

^{13}C-NMR (DMSO-D$_6$, 100.63 MHz):

δ 151 (C-3), 141 (C-6), 139 (C-2), 124 (C-5), 122 (C-4), 57 (C- OCH$_3$).

IR $\bar{\nu}$/cm^{-1}(T%):

3063 (84%), 3051 (83%), 2988 (86%), 2953 (89%), 2575 (89%), 2099 (90%), 1927 (90%), 1871 (91%), 1816 (92%), 1707 (92%), 1564 (48%), 1466 (54%), 1437 (74%), 1413 (47%), 1300 (52%), 1287 (36%), 1276 (49%), 1208 (53%), 1186 (59%), 1125 (63%), 1084 (44%), 1058 (45%), 1009 (47%), 964 (70%), 908 (66%), 791 (30%), 731 (46%), 689 (27%).

MS-EI (70 eV) *m/z:*

143 (100%) [M]$^+$, 100 (32%) [M-CH$_3$CO]$^+$, 93.1 (36%) [M-CH$_3$Cl]$^+$.

m.p.: 51°C. **R$_f$:** 0.69 (DCM/DEE 19:1).

5.2.9.2 3-Methoxy-6-methyl-2-nitropyridine (13a)
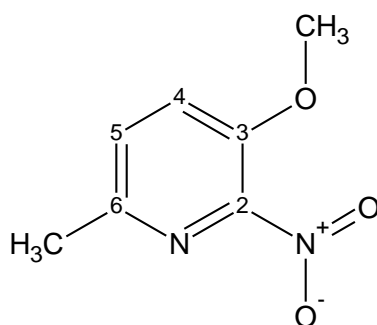
^{1}H-NMR (DMSO-D$_6$, 400.16 MHz):

δ 7.84 (1H$_4$, d, $^3J_{4,5}$ = 8.54 Hz, Py), 7.56 (1H$_5$, d, $^3J_{5,4}$ = 8.85 Hz, Py), 3.91 (3H, s, OCH$_3$), 2.42 (3H, s, CH$_3$).

^{13}C-NMR (DMSO-D$_6$, 100.63 MHz):

δ 148.2 (C-3), 147.3 (C-6), 145 (C-2), 129 (C-5), 125 (C-4), 57 (C-OMe), 22 (C-Me).

IR $\bar{\nu}$/cm^{-1}(T%):

3031 (89%), 2952 (90%), 2852 (90%), 1923 (94%), 1738 (95%), 1618 (88%), 1536 (40%), 1487 (42%), 1455 (61%), 1442.94 (60%), 1374 (45%), 1304 (44%), 1288 (43%), 1267 (59%), 1240 (58%), 1182 (76%), 1153 (73%), 1120 (43%), 1013 (63%), 995 (60%), 915 (71%), 830 (36%), 811 (57%), 767 (56%), 717 (57%), 666 (52%).

MS-EI (70 eV) *m/z:*

168.1 (16%) [M]$^+$, 122.1 (60%) [M-NO$_2$]$^+$, 92.1 (100%) [M-NO$_2$-CH$_2$O]$^+$, 65 (24%) [M-C$_2$H$_3$N$_2$O$_3$]$^+$.

m.p.: 84°C. **R$_f$:** 0.08 (PE/EtAc 5:1)

5.2.9.3 2-Bromo-3-methoxy-6-methylpyridine (13c)
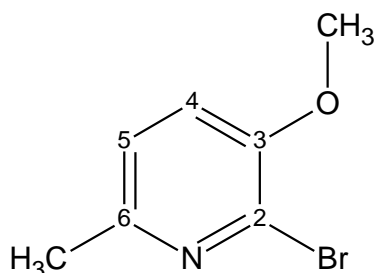
^{1}H-NMR (DMSO-D$_6$, 400.16 MHz):

δ 7.35 (1H$_5$, d,$^3J_{5,4}$ = 8.24 Hz, Py), 7.23 (1H$_4$, d, $^3J_{4,5}$ = 8.24 Hz, Py), 3.83 (3H, s, OCH$_3$), 2.36 (3H, s, CH$_3$).

^{13}C-NMR (DMSO-D$_6$, 100.63 MHz):

δ 150 (C-3), 149.7 (C-6), 130 (C-2), 123 (C-5), 121 (C-4), 56 (C-OCH$_3$), 23 (C-CH$_3$).

IR $\bar{\nu}$/cm^{-1}(T%):

2994 (85%), 2940 (86%), 2837 (86%), 1558 (72%), 1524 (89%), 1452 (65%), 1432 (63%), 1362 (67%), 1281 (63%), 1260 (65%), 1222 (70%), 1177 (79%), 1147 (74%), 1078 (57%), 1014 (70%), 994 (69%), 859 (73%), 825 (55%), 738 (60%), 666.23 (68%).

MS-EI (70 eV) m/z:

201 (100%) [M-1]$^+$, 158 (15%) [M-CH$_3$CO]$^+$, 122.1 (37%) [M-Br]$^+$, 92.1 (86%) [M-CH$_2$BrO]$^+$.

m.p.: 58°C. **R$_f$:** 0.3 (DCM/DEE 19:1).

5.2.9.4 3-Benzyloxy-6-methyl-2-nitropyridine (15)

^{1}H-NMR (DMSO-D$_6$, 400.16 MHz):

δ 7.93 (1H$_4$, d, $^3J_{4,5}$ = 8.59 Hz, Py), 7.59 (1H$_5$, d, $^3J_{5,4}$ = 8.59 Hz, Py), 7.44 (5H, m, J = 8.5 Hz, Ph), 5.32 (2H, s, CH$_2$), 2.42 (3H, s, CH$_3$).

^{13}C-NMR (DMSO-D$_6$, 100.63 MHz):

δ 149 (C-3), 147 (C-6), 144 (C-2), 135 (C-8), 129 (C-5), 128 (C-10, 12), 127 (C-9, 13), 126 (C-4), 71 (C-CH$_2$), 22.2 (C-CH$_3$).

IR $\bar{\nu}$/cm^{-1}(T%):

2911 (89%), 1771 (80%), 1606 (81%), 1584 (87%), 1526 (42%), 1479 (66%), 1469 (62%), 1460 (54%), 1376 (66%), 1366 (55%), 1284 (49%), 1271 (56%), 1162 (59%), 1143 (60%), 1115 (45%), 1025 (65%), 912 (68%), 899 (79%), 823 (39%), 768 (31%), 749 (78%), 689 (45%), 656 (48%).

MS-EI (70 eV): *m/z:*

216 (6%) [M-C$_2$H$_4$]$^+$, 164 (21%) [M-C$_5$H$_6$N]$^+$, 105 (100%) [C$_7$H$_5$O]$^+$, 77 (19%) [C$_6$H$_5$]$^+$, 43 (30%) [C$_2$H$_3$O]$^+$.

m.p.: 97 °C. **R$_f$:** 0.66 (PE/EtOAc 2:1).

5.2.9.5 6-Methyl-3-(3´-methylbenzyloxy)-2-nitropyridine (16)
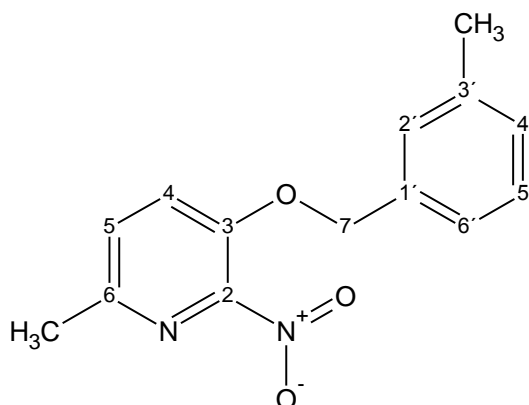
^{1}H-NMR (DMSO-D$_6$, 400.16 MHz):

δ 7.92 (1H$_4$, d, $^3J_{4,5}$ = 8.59 Hz, Py), 7.59 (1H$_5$, d, $^3J_{5,4}$ = 8.59 Hz, Py), 7.29 (1H$_{6´}$, t, $^3J_{6´,5´}$ = 7.58 Hz, Ph), 7.20 (2H$_{2´,5´}$, m, Ph), 7.15 (1H$_{4´}$, d, $^3J_{4´,5´}$ = 7.08 Hz, H$_{14}$), 5.27 (2H, s, CH$_2$), 2.42 (3H, s, CH$_3$), 2.30 (3H, s, CH$_3$).

^{13}C-NMR (DMSO-D$_6$, 100.63 MHz):

δ 149 (C-3), 147 (C-6), 145 (C-2), 141 (C-1´), 129 (C-3´), 128 (C-5), 127 (C-5´, 4´), 126 (C-2´), 125 (C-6´), 119 (C-4), 71 (C-CH$_2$), 22 (C-CH$_3$), 21 (C-CH$_3$).

IR $\bar{\nu}$/cm^{-1}(T%):

2921 (84%), 1781 (90%), 1610 (78%), 1594 (85%), 1530 (42%), 1489 (63%), 1479 (62%), 1455 (54%), 1376 (62%), 1359 (57%), 1284 (44%), 1256 (47%), 1163 (61%), 1150 (61%), 1115.23 (55%), 1025 (55%), 912 (58%), 894 (69%), 823 (42%), 779 (31%), 740 (77%), 690 (45%), 666 (58%).

MS-EI (70 eV): *m/z:*

230 (4%) [M-C$_2$H$_4$]$^+$, 178 (24%) [M-C$_5$H$_6$N]$^+$, 105 (100%) [C$_7$H$_5$O]$^+$, 77 (12%) [C$_6$H$_5$]$^+$, 43 (32%) [C$_2$H$_3$O]$^+$.

m.p.: 125 °C. **R$_f$:** 0.39 (PE/EtOAc 2:1).

5.2.9.6 3-(3´,5´-Dimethylbenzyloxy)-6-methyl-2-nitropyridine (17)
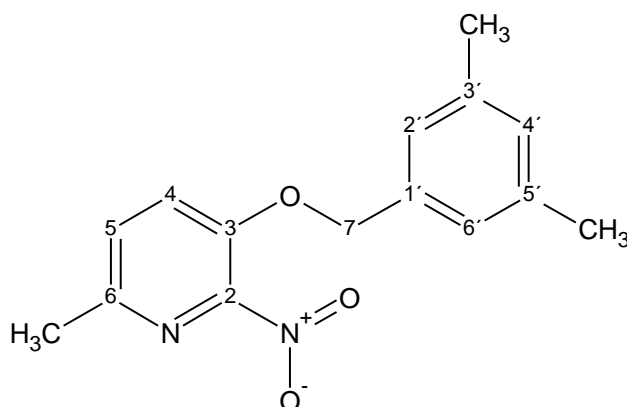
^{1}H-NMR (DMSO-D$_6$, 400.16 MHz):

δ 7.90 (1H$_4$, d, $^3J_{4,5}$ = 8.59 Hz, Py), 7.58 (1H$_5$, d, $^3J_{5,4}$ = 8.59 Hz, Py), 7.01 (2H$_{2´,6´}$, s, Ph), 6.96 (1H$_{4´}$, s, Ph), 5.22 (2H, s, CH$_2$), 2.42 (3H, s, CH$_3$), 2.25 (6H, s, 2CH$_3$).

^{13}C-NMR (DMSO-D$_6$, 100.63 MHz):

δ 148 (C-3), 147 (C-6), 145 (C-2), 143 (C-1´), 137 (C-3´, 5´), 135 (C-5), 129 (C-4´), 128 (C-2´, 6´), 125 (C-4), 71 (C-CH$_2$), 22 (C-CH$_3$), 21 (C-2CH$_3$).

IR $\bar{\nu}$/cm^{-1}(T%):

2916 (87%), 1610 (82%), 1559 (78%), 1529 (50%), 1481 (67%), 1455 (68%), 1369 (57%), 1299 (71%), 1282.81 (54%), 1261.28 (64%), 1246 (68%), 1162 (77%), 1150 (81%), 1116 (62%), 1045 (71%), 914 (75%), 888 (85%), 837 (49%), 816 (58%), 788 (58%), 720 (84%), 685 (56%), 667 (77%).

MS-EI (70 eV): *m/z:*

230 (8%) [M-C$_3$H$_6$]$^+$, 178 (22%) [M-C$_6$H$_6$O]$^+$, 119 (40%) [C$_8$H$_7$O]$^+$, 105 (100%) [C$_7$H$_5$O]$^+$, 77 (22%) [C$_6$H$_5$]$^+$, 43 (28%) [C$_2$H$_3$O]$^+$.

m.p.: 107°C. **R$_f$:** 0.45 (PE/EtOAc 2:1).

5.2.9.7 6-Methyl-3-(4´-methylbenzyloxy)- 2-nitropyridine (18)
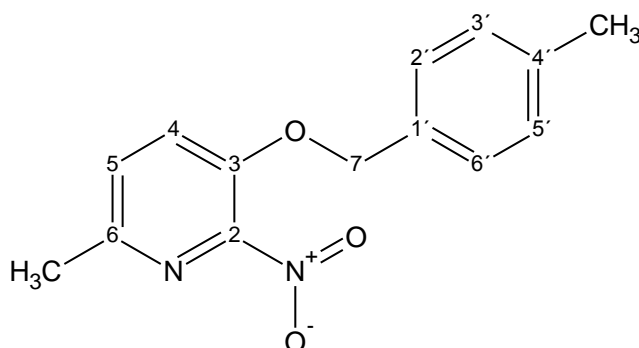
^{1}H-NMR (DMSO-D$_6$, 400.16 MHz):

δ 7.93 (1H$_4$, d, $^3J_{4,5}$ = 8.59 Hz, Py), 7.57 (1H$_5$, d, $^3J_{5,4}$ = 8.09 Hz, Py), 7.29 (2H$_{2´,6´}$, d, $^3J_{6´,5´}$ = 8.08 Hz, Ph), 7.19 (2H$_{3´,5´}$, d, $^3J_{3´,2´}$ = 7.58 Hz, Ph), 5.26 (2H, s, CH$_2$), 2.41 (3H, s, CH$_3$), 2.28 (3H, s, CH$_3$).

^{13}C-NMR (DMSO-D$_6$, 100.63 MHz):

δ 148 (C-3), 147 (C-6), 145 (C-2), 140 (C-1´), 137 (C-4´), 133 (C-5), 129 (C-3´, 5´), 127 (C-2´, 6´), 126 (C-4), 71 (C-CH$_2$), 22 (C-CH$_3$), 21 (C-CH$_3$).

IR $\bar{\nu}$/cm^{-1}(T%):

2922 (89%), 1905 (94%), 1640 (95%), 1618 (89%), 1559 (74%), 1529 (47%), 1520 (46%), 1482 (64%), 1455 (60%), 1416 (86%), 1374 (50%), 1315 (75%), 1280 (46%), 1248 (62%), 1185 (80%), 1152 (74%), 1118 (55%), 1032 (67%), 1020 (66%), 916 (73%), 850 (88%), 819 (48%), 799 (45 %), 787 (48%), 715 (83%), 666 (60%).

MS-EI (70 eV): *m/z:*

230 (6%) [M-C$_2$H$_4$]$^+$, 178 (24%) [M-C$_5$H$_6$N]$^+$, 105 (100%) [C$_7$H$_5$O]$^+$, 77 (18%) [C$_6$H$_5$]$^+$, 43 (8%) [C$_2$H$_3$O]$^+$.

m.p.: 130 °C. **R$_f$:** 0.56 (PE/EtOAc 2:1).

5.2.9.8 3-(2´,4´-Dimethylbenzyloxy)-6-methyl-2-nitropyridine (19)
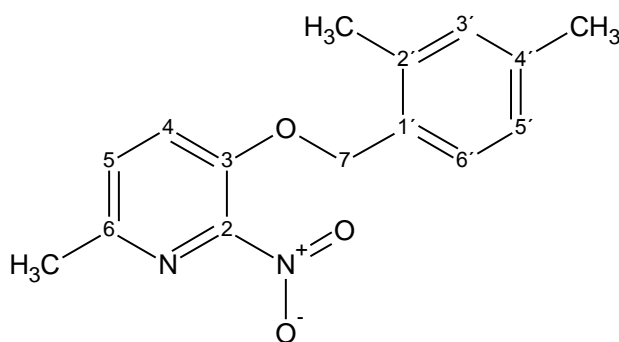
^{1}H-NMR (DMSO-D$_6$, 400.16 MHz):

δ 7.98 (1H$_4$, d, $^3J_{4,5}$ = 8.59 Hz, Py), 7.60 (1H$_5$, d, $^3J_{5,4}$ = 8.58 Hz, Py), 7.26 (1H$_{6´}$, d, $^3J_{6´,5´}$ = 7.58 Hz, Ph), 7.03 (1H$_{3´}$, s, Ph), 6.99 (1H$_{5´}$, d, $^3J_{5´,6´}$ = 8.08 Hz, Ph), 5.24 (2H, s, CH$_2$), 2.42 (3H, s, CH$_3$), 2.31 (3H, s, CH$_3$), 2.25 (3H, s, CH$_3$).

^{13}C-NMR (DMSO-D$_6$, 100.63 MHz):

δ 148 (C-3), 147 (C-6), 144 (C-2), 138 (C-1´), 137 (C-4´), 131 (C-5), 129 (C-3´), 127 (C-5´), 125 (C-4´), 69 (C-CH$_2$), 22 (C-CH$_3$), 21 (C-CH$_3$), 19 (C-CH$_3$).

IR $\bar{\nu}$/cm^{-1}(T%):

2918 (83%), 1723 (90%), 1613 (81%), 1534 (43%), 1508 (56%), 1482 (64%), 1450 (54%), 1374 (60%), 1354 (59%), 1283 (43%), 1248 (42%), 1214 (66%), 1154 (54%), 1110 (53%), 1042 (72%), 1008 (58%), 975 (71%), 912 (58%), 896 (69%), 826 (34%), 801 (55%), 777 (58%), 767 (63%), 734 (74%), 717 (74%), 705 (66%), 665 (50%).

MS-EI (70 eV): *m/z:*

230 (6%) [M-C$_3$H$_6$]$^+$, 178 (22%) [M-C$_6$H$_6$O]$^+$, 119 (76%) [C$_8$H$_7$O]$^+$, 105 (100%) [C$_7$H$_5$O]$^+$, 43 (44%) [C$_2$H$_3$O]$^+$.

m.p.: 110 °C. **R$_f$:** 0.49 (PE/EtOAc 2:1).

5.2.10 General Procedure for Synthesis of Standards (12b, 13b)

A mixture of potassium fluoride (KF, 12 mmol, spray-dried) and kryptofix-222 (K222, 3 eq) was heated at 140°C under argon for 20 min, then, substituted 2-nitropyridine in 20 mL of DMF was added and the reaction solution was heated for 20 min. Afterwards, reaction mixture was poured into water (25 mL), extracted with DEE (250 mL), washed with 25 mL of 1N NaOH, water and with brine. Thereafter, it was dried over anhyd. Na_2SO_4 and the solvent was evaporated. Crude product was cleaned by MPLC using PE/EtOAc (3:1) as mobile phase at a flow rate of 20 ml/min. Cleaned products were obtained as oils (%yield: 60%).

5.2.10.1 2-Fluoro-3-methoxypyridine (12b)
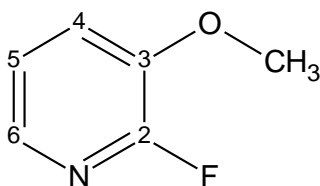
^{1}H-NMR (DMSO-D$_6$, 400.16 MHz):

δ 7.70 (1H$_6$, m, Py), 7.62 (1H$_5$, ddd, $^3J_{5,6}$ = 6.41 Hz, Py), 7.27 (1H$_4$, m, Py), 3.86 (3H, s, OCH$_3$).

^{13}C-NMR (DMSO-D$_6$, 100.63 MHz):

δ 154 (C-2), 151 (C-2), 142 (C-3, d, $^3J_{C-F}$ = 26 Hz), 136 (C-6, d, J_{C-F} = 13.4 Hz), 123(C-4, d, $^4J_{C-F}$ = 3.82 Hz), 117 (C-5), 56 (C- OCH$_3$).

IR $\overline{\nu}$/cm^{-1}(T%):

3053 (74%), 3043 (83%), 2990 (86%), 2953 (89%), 2575 (89%), 2099 (90%), 1927 (90%), 1871 (91%), 1820 (92%), 1710 (92%), 1564 (48%), 1468 (54%), 1439 (74%), 1413 (47%), 1300 (52%), 1287 (36%), 1276 (49%), 1208 (53%), 1186 (59%), 1125 (63%), 1084 (44%), 1058 (45%), 1009 (47%), 964 (70%), 808 (66%), 691 (30%), 631 (46%), 589 (37%).

MS-EI (70 eV) *m/z:*

127.1 (100%) [M]$^+$, 84.1 (43%) [M-CH$_3$CO]$^+$.

R$_f$: (PE/EtAc 3:1) : 0.36

5.2.10.2 2-Fluoro-3-methoxy-6-methylpyridine (13b)
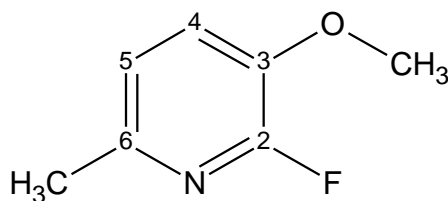
^{1}H-NMR (DMSO-D$_6$, 400.16 MHz):

δ 7.15(1H$_5$, d, $^3J_{5,4}$ = 8.1Hz, Py), 7.10(1 H$_4$, d, $^3J_{4,5}$ = 7.99 Hz, Py), 3.87 (3H, s, OCH$_3$), 2.56(3H, s, CH$_3$).

^{13}C-NMR (DMSO-D$_6$, 100.63 MHz):

δ 159 (C-2), 153 (C-2), 149 (C-6, d, J_{C-F} = 9.8 Hz), 141 (C-3, d, J_{C-F} = 26 Hz), 121 (C-5), 120 (C-4, d, J_{C-F} = 3.82 Hz), 56.6 (C- OCH$_3$), 24.5 (C-CH$_3$).
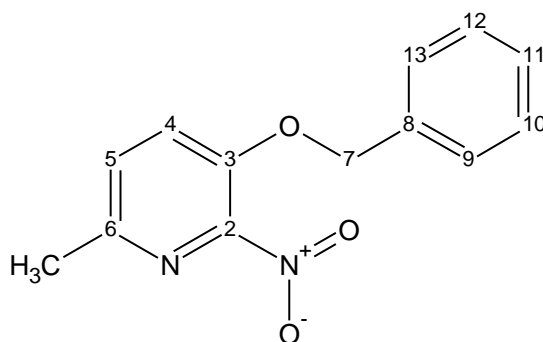
IR $\bar{\nu}$/cm^{-1}(T%):

2994 (85%), 2940 (86%), 2837 (86%), 1658 (72%), 1524 (89%), 1452 (65%), 1432 (63%), 1362 (67%), 1281 (73%), 1260 (55%), 1219 (70%), 1177 (79%), 1147 (74%), 1078 (57%), 1014 (70%), 994 (79%), 869 (73%), 825 (55%), 718 (60%), 660 (68%).

MS-EI (70 eV) *m/z:*

141.1 (100%) [M]$^+$, 126.1 (43%) [M-CH$_3$]$^+$, 98.1 (24%) [M-CH$_3$CO]$^+$.

R$_f$: 0.32 (PE/EtOAc 5:1)

5.3 Radiofluorination of Model Compounds (1-19)

General procedure for [^{18}F]-labelling of all model compounds **(1-19)** is shown in Fig 5.1 and is described as under.

5.3.1 Production of [^{18}F]fluoride

No-carrier-added (n.c.a.) [^{18}F] fluoride was produced at the cyclotron (PET trace, GE Medical Systems, Uppsala) of the PET-Center in Ulm *via* the ^{18}O (p,n) ^{18}F nuclear reaction by irradiation of > 95% enriched [^{18}O] water with 16.5 MeV protons.

5.3.2 [^{18}F]-Labelling

Aqueous [^{18}F]fluoride (40-50 MBq) was added into a 5 mL sealed vial containing 100 μL of 3.5% aqueous K$_2$CO$_3$ and 15 mg K222. The [^{18}F]fluoride solution was dried for 20 min under argon flow (ca. 2 mL/min) at 140°C by azeotropic distillation with acetonitrile (2 × 1 mL). Afterwards, 10 mg of precursor dissolved in 1 mL of DMF was added into the reaction vial containing the [^{18}F]KF-K222 complex and the reaction mixture was heated to the labelling temperature (140°C, 120°C, 100°C, 60°C, 30°C). After some time (1, 3, 7, 10, 20, 30 min), sample was withdrawn from reaction mixture for further analysis by radio-TLC and radio-HPLC. For 2-substituted pyridines **(10a, 10b, 10c, 10d)**, samples were withdrawn for analysis (20 min) after cooling down the reaction mixture to 0°C because of high volatility of 2-[^{18}F]fluoropyridine (b.p.: 126°C).

5.3.3 Cartridge Purification

After 30 min of labelling of compounds **(13a, 15, 16, 17, 18, 19)** at 140°C, reaction mixture was diluted with water upto 20 mL and passed through the combination of Alumina N and C18 cartridges. Free [^{18}F]fluoride retained on the alumina phase. Subsequently, the labelled product was eluted with 3 mL of dichloromethane (DCM) from the C18 cartridge. DCM was evaporated at room temperature under flow of argon. The residue was subjected to hydrolysis.

In case of catalytic hydrogenation, the [^{18}F]-labelled intermediate [2-[^{18}F]fluoro-6-methyl-3-(4-methylbenzyloxy)pyridine, **(v)**] was eluted from the C18 cartridge with 3 mL of acetonitrile (MeCN). Solvent was evaporated and the residue was dissolved in 500 µL of dry MeOH.

5.3.4 Acidic Hydrolysis

1 mL of acid was added to the labelled intermediate. Afterwards, the reaction mixtures were heated at 150°C for 10 min. HI (10 mg of NaI in 1 mL of 48% HBr), 48% HBr, 32% HCl, and 70% TFA were used for hydrolysis.

For 3-(2,4-dimethylbenzyloxy)-2-[^{18}F]fluoro-6-methylpyridine **(v)** and 2-[^{18}F]fluoro-6-methyl-3-(4-methylbenzyloxy)pyridine **(vi)**, time dependence experiments were additionally performed at temperatures of 25°C (RT), 60°C, and 120°C. At every time point (1, 3, 5, 7, and 10 min), quenching of the reaction mixture was carried out by addition of 500 µL to 1 mL of 5% KHCO$_3$ till pH 8 was achieved. Aliquots of the reaction mixture (5 µL) were taken and analyzed by radio-HPLC and radio-TLC.

5.3.5 Transfer Hydrogenation

Dried 2-[^{18}F]fluoro-6-methyl-3-(4-methylbenzyloxy)pyridine **(v)** was dissolved in 500 µL of MeOH and transferred into a vial containing 20 mg of 10% Pd/C. Hydrogenating reagent, 1,4-cyclohexadiene (1,4-CHD, 147 µL, 1.55 mmoles) or ammonium formate (HCOONH$_4$, 49 mg, 0.77 mmoles), dissolved in 500 µL of dry MeOH was added to the mixture. Afterwards, the reaction mixture was heated at 70°C (reflux temperature). Aliquots (5 µL) were taken from the reaction mixture at 1, 3, 5, 7, 10, 20 and 30 min and filtered using Millipore filters (Millex®-GV, 0.22 µm). The resulting filtrates were analyzed by radio-TLC and radio-HPLC.

5.3.6 Radio-TLC Analysis

Silica gel plates were used as stationary phase while mobile phase was mixture of PE/EtOAc (v/v). Visualization and quantification was carried out by phosphor imager. The R$_f$ values in PE/EtOAc (3:1) were as follows: 0.69 for *p*-[^{18}F]fluorobenzaldehyde, 0.68 for 2-[^{18}F]fluoro-5-methoxybenzaldehyde, 0.65 for 2-[^{18}F]fluoro-6-methoxybenzaldehyde, 0.67 for 2-[^{18}F]fluoro-3-methylbenzaldehyde, 0.66 for 6-[^{18}F]fluoro-2,3-dimethoxybenzaldehyde, 0.64 for 2-[^{18}F]fluoropyridine, 0.22 for 2-[^{18}F]fluoro-3-methoxypyridine, 0.48 for 2-[^{18}F]fluoro-3-methylpyridine, 0.38 for 2-[^{18}F]fluoro-3-methoxy-6-methylpyridine for 2-[^{18}F]fluoro-3-methoxy-6-methylpyridine. The R$_f$ value for 2-[^{18}F]fluoro-3-hydroxy-6-methylpyridine was 0.59 in PE/EtOAc (1:1).

5.3.7 Radio-HPLC Analysis

HPLC analysis was performed using reversed phase column (Phenomenex Luna, 5 µ, C18, 250 x 10 mm) and eluents comprising of mixture of MeCN/water (0.1%TFA) at a flow rate of 1 mL/min. The *k´* values in 30% MeCN with 0.1% TFA were as follows: 3.6 for 2-[^{18}F]fluoro-3-

hydroxy-6-methylpyridine, 0.95 for 2-[^{18}F]fluoro-3-methylpyridine, 0.98 for 2-[^{18}F]fluoro-3-methoxy-6-methylpyridine. However, the *k´* values in 20% MeCN (0.1% TFA) were 0.72 for 2-[^{18}F]fluoropyridine and 0.81 for 2-[^{18}F]fluoro-3-methoxypyridine.

In case of analysis by radio-HPLC, the fraction of the [^{18}F]-labelled product was collected and measured by means of a γ-counter. The radiochemical yield (RCY) was calculated by relating the radioactivity of the product peak to the total amount of radioactivity injected onto the column.

Precursor
10 mg

1) [^{18}F]fluoride sol, K222 (15 mg), K$_2$CO$_3$
(3.5 mg), MeCN, **140°C**, 20 min
2) Precursor in DMF (1 mL),
140°C, 30 min

[^{18}F]-Labelled Product

Aliquotes for TLC/HPLC analysis
Except *O*-protected
6-methyl-2-nitropyridines that
were subjected further for
hydrolysis

Alumina N

Free ^{18}F$^-$ trapped here,
goes to waste

Alumina N (Plus),
C18 (Light)

Product eluted from
C18 by 3 mL DCM

C18

Evaporation at RT
under argon

1 mL of acid,
150°C-RT,
10 min

Acidic Hydrolysis

Residue

Catalytic Hydrolysis
500 μL MeOH

20 mg 10%Pd/C,
1,4-CHD (147μL, 1.55 mmol) or
HCOONH$_4$ (49 mg, 0.77 mmol)
in 500 μL MeOH,
70°C, 1, 3, 5, 7, 10, 20, 30 min

Aliquotes for
TLC/HPLC analysis

Acids: HI (10 mg NaI in 48%HBr),
48%HBr, 32%HCl, 70%TFA

TLC/HPLC analysis

Aliquotes flitered
by Millipore
filters (0.22 μm)

Fig 5.1 Radiofluorinations of model precursors (1-19) *via* **S$_N$Ar by [^{18}F]fluoride**

5.4 Synthesis of *O*-[2-[¹⁸F]Fluoro-3-(2-Nitroimidazol)propyl]tyrosine ([¹⁸F]FNT])

5.4.1 Organic Synthesis

Organic synthesis of precursor (**e**) was carried out according to the scheme-10 as described in results and discussion. Detailed description of each step is presented in the following:

5.4.1.2 Methyl N-[(benzyloxy)carbonyl]-O-[(2,2-dimethyl-1,3-dioxane-4-yl)methyl] tyrosinate (a)

[IUPAC: Methyl 2-(benzyloxycarbonylamino)-3-(4-((2,2-dimethyl-1,3-dioxane-4-yl)methoxy)phenyl) propanoate]

1.2 g (4.6 mmol, 1.5 eq) of triphenylphosphine (PPh₃) and 0.5 mL (3.6 mmol, 1.2 eq) of dioxolane were added to the solution of 1g (3.17 mmol) of Z-L-tyorsine methyl ester in 20 mL of tetrahydrofuran (THF). Afterwards, 1.65 mL (3.7 mmol) of diethyl azodicarboxylate (DEAD, 2.25 M, 40%) was added into it and the reaction mixture was heated at 60°C for 3 h. Later, solvent was evaporated and residue was cleaned by flash chromatography using dry silica 60 as stationary phase and PE/EOtAc 2:1 as mobile phase. 1.0 g (2.33 mmol, 74%) of product was obtained as oil.
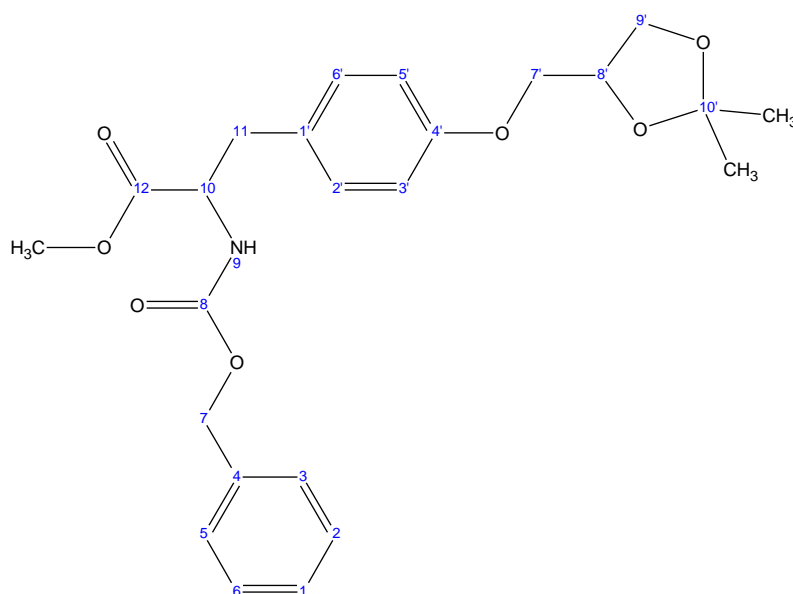
¹H-NMR (DMSO-D₆, 400.16 MHz):

δ 7.33 (1H₆, d, $^3J_{6,1}$ = 7.15 Hz, Ph), 7.31 (1H₅, m, Ph), 7.28 (1H₃, d, $^3J_{3,2}$ = 7.30 Hz, Ph), 7.21 (1H₂, d, $^3J_{2,1}$ = 7.15 Hz, Ph), 7.09 (1H₆·, m, Ph), 6.97 (1H₅·, d, $^3J_{5·,6·}$ = 8.39 Hz, Ph), 6.95 (1H₃·, d, $^3J_{3·2·}$= 8.40 Hz, Ph), 5.26 (1H, s, NH), 5.12 (1H₇, s, CH₂), 4.66 (1H₁₀, s, CH), 4.15 (5H₇·,₈·,₉·, m, CH₂, CH), 3.95 (2H₇·, m, CH₂), 3.71 (3H, s, OCH₃), 2.94 (2H₁₁, m, CH₂), 1.40 (3H, s, CH₃), 1.37 (3H, s, CH₃).

¹³C-NMR (DMSO-D₆, 100.63 MHz):

δ 172.1 (C-12), 156.2 (C-8,4'), 136.1 (C-4), 130.3 (C-2',6'), 128.1 (C-2,6), 126.3 (C-3,5), 125.2 (C-1), 115.1 (C-3',5'), 110.1 (C-10'), 74.3 (C-8'), 69.1 (C-CH₂), 67.3 (C-CH₂), 65.2 (C-CH₂), 55.1 (C-10), 52.3 (C-CH₃), 38.6 (C-CH₂), 27.4 (C-CH₃), 25.3 (C-CH₃).

IR $\bar{\nu}$/cm^{-1}(T%):

3335 (93%), 3033 (95%), 2986 (91%), 2951 (91%), 1719 (55%), 1612 (85%), 1585 (91%), 1511 (49%), 1454 (75%), 1371 (73%), 1351 (78%), 1239 (46%), 1209 (38%), 1178 (56%), 1157 (64%), 1111 (77%), 1081 (67%), 1048 (43%), 1025 (51%), 910 (85%), 839 (61%), 775 (77%), 738 (62%), 697 (53%).

MS-EI (70 eV) *m/z:*

443.1(28%) [M]$^+$, 428.1 (55%) [M-CH$_3$]$^+$, 384.2 (38%) [M-C$_2$H$_3$O$_2$]$^+$, 367.1 (58%) [M-C$_6$H$_4$]$^+$, 340.1(85%) [M-C$_8$H$_7$]$^+$, 324.1 (71%) [M-C$_8$H$_7$O]$^+$, 307.1(100%) [M-C$_8$H$_8$O$_2$]$^+$.

HRMS (EI) m/z measured: 443.196 [M]$^+$, **m/z calculated:** 443.194

R$_f$: 0.73 (PE/EtOAc 2:1).

5.4.1.3 *Methyl N-[(benzyloxy)carbonyl]-O-[2,3-dihydroxypropyl]tyrosinate (b)* *[IUPAC: Methyl 2-(benzyloxycarbonylamino)-3-(4-(2,3-dihydroxypropoxy) phenyl)propanoate]*

20 mL of acetic acid (AcOH) was added to the solution of 2 g (4.66 mmol) of compound **(a)** in water (15 mL)/methanol (10 mL) and then, the reaction mixture was kept stirring at room temperature overnight. Next day, reaction mixture was poured into ice-cold water and afterwards, solid sodium bicarbonate (NaHCO$_3$) was added slowly to it till the formation of carbon dioxide (CO$_2$) was ceased. Then, it was extracted by diethylether (DEE, 250 mL), washed by saturated solution of sodium bicarbonate (250 mL), dried over anhydrous sodium sulfate (Na$_2$SO$_4$), filtered, and solvent was evaporated. Crude product was cleaned by MPLC by gradient elution by using first PE/EtOAc 1:1 at a flow rate of 10 mL /min and later 100% EtOAc at a flow rate of 40 mL/min. 1.4 g (3.6 mmol, 77%) of product was obtained as oil.
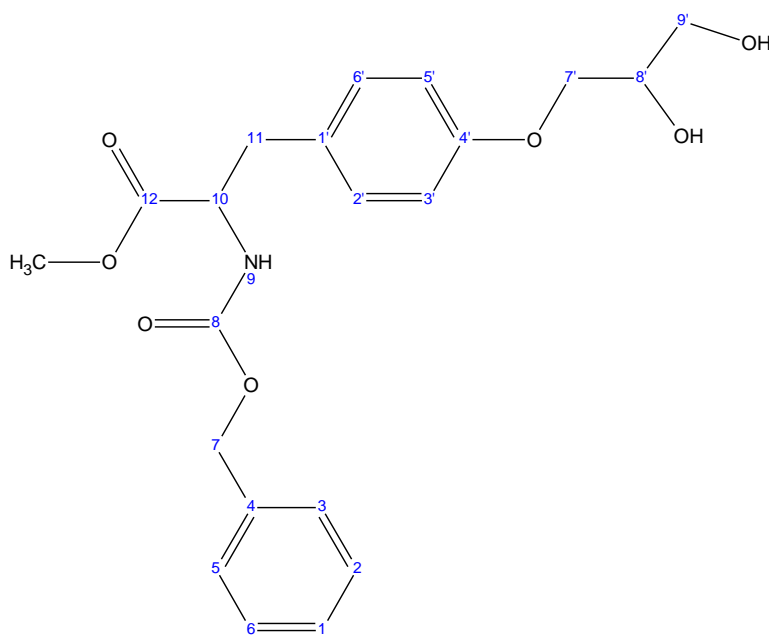
^{1}H-NMR (DMSO-D$_6$, 400.16 MHz):

δ 7.33 (1H$_6$, d, $^3J_{6,1}$ = 7.15 Hz, Ph), 7.31 (1H$_5$, m, Ph), 7.28 (1H$_3$, d, $^3J_{3,2}$ = 7.30 Hz, Ph), 7.21 (1H$_2$, m, Ph), 7.06 (1H$_{6'}$, m, Ph), 6.97 (1H$_{5'}$, d, $^3J_{5',6'}$ = 8.39 Hz, Ph), 6.95 (1H$_{3'}$, d, $^3J_{3'2'}$= 8.40 Hz, Ph), 5.12 (1H$_7$, s, CH$_2$), 4.70 (1H$_{10}$, s, CH), 4.04 (2H$_{7'}$, dd, $^3J_{7',8}$= 8.00 Hz, CH$_2$), 3.75 (1H$_{8'}$, ddd, $^3J_{8',9}$ = 8.00 Hz, CH), 3.71 (3H, s, OCH$_3$), 3.56 (2H$_{9'}$, m, CH$_2$), 2.94 (2H$_{11}$, d, $^3J_{11,10}$ = 6.67 Hz, CH$_2$), 3.22 (3H, s, 2OH, NH).

^{13}C-NMR (DMSO-D$_6$, 100.63 MHz):

δ 171.2 (C-12), 155.5 (C-8,4'), 136.1 (C-4), 131.3 (C-2',6'), 129.3 (C-2,6), 128.2 (C-3,5), 126.1 (C-1), 124.1 (C-1'), 116.4 (C-3',5'), 71 (C-8'), 69.1 (C-CH$_2$), 67.2 (C-CH$_2$), 64.5 (C-CH$_2$), 55.6 (C-10), 52.1 (C-OCH$_3$), 37.3 (C-CH$_2$).

IR $\bar{\nu}$/cm^{-1}(T%):

3348 (88%), 3034 (94%), 2951 (90%), 1702 (46%), 1611 (84%), 1584 (90%), 1511 (49%), 1454 (75%), 1440 (74%), 1355 (70%), 1243 (44%), 1215 (42%), 1178 (56%), 1111 (70%), 1041 (46%), 930 (81%), 878 (83%), 825 (72%), 802 (77%), 775 (76%), 740 (64%), 697 (56%).

MS-EI (70 eV) *m/z:*

404.2 (20%) [M+1]$^+$, 360.1 (81%) [M-C$_2$H$_3$O]$^+$, 343.1 (44%) [M-C$_2$H$_4$O$_2$]$^+$, 252.1 (56%) [C$_{13}$H$_{18}$NO$_4$]$^+$, 181 (68%)[M-C$_{13}$H$_{18}$O$_3$]$^+$, 154.1(80%) [C$_8$H$_{12}$NO$_2$]$^+$, 136.1 (85%) [C$_8$H$_8$O$_2$]$^+$, 107.1 (100%) [C$_7$H$_7$O]$^+$.

HRMS (EI) m/z measured: 404.176 [M+1]$^+$, **m/z calculated:** 404.171

R$_f$: 0.13 (PE/EtOAc 1:1).

5.4.1.4 General Procedure for Tosylation

p-Tosylchloride (OTsCl, 1.1 eq for monotosylation; 2.2 eq for ditosylation) was added to the solution of 3.34 mmol of compound (**b**) in 15 mL of pyridine as a solvent under inert conditions of argon. It was kept stirring at room temperature for 3 h. Afterwards, reaction mixture was added into 300 mL of DEE and then, it was washed by 250 mL of 5% HCl, afterwards by 300 mL of sat.NaHCO$_3$, and then by brine (250 mL). It was dried over anhyd.Na$_2$SO$_4$ and after that, solvent was evaporated. Crude product was cleaned by MPLC by using PE/EtOAc 1:1 at flow rate of 6 mL/min. 1.1 g (2.02 mmol, 60%) of monotosylated product (**c**) and 1 g (1.43 mmol, 45%) of ditosylated product (**d**) were produced as oils.

5.4.1.4.1 Methyl N-[(benzyloxy)carbonyl]-O-[2-hydroxy-3-{[(4-methylphenyl)sulfonyl]oxy}propyl]tyrosinate (c)

[IUPAC: Methyl 2-(benzyloxycarbonylamino)-3-(4-(2-hydroxy-3-(tosyloxy)propoxy)phenyl) propanoate]
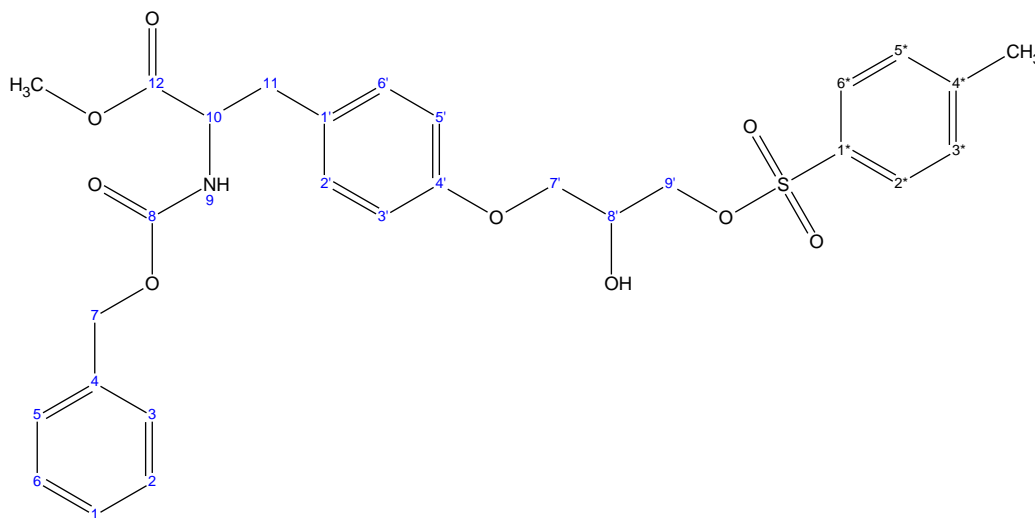
^{1}H-NMR (DMSO-D$_6$, 400.16 MHz):

δ 7.78 (2H$_{2*,6*}$, m, Ph), 7.35 (2H$_{3*,5*}$, m, Ph), 7.33 (2H$_{2,6}$, m, Ph), 7.31 (2H$_{3,5}$, m, Ph), 7.28 (1H$_1$, m, Ph), 7.07 (2H$_{2',6'}$, m, Ph), 6.95 (2H$_{3',5'}$, m, Ph), 5.12 (2H$_7$, s, CH$_2$), 4.66 (1H$_{10'}$, m, CH), 4.59 (2H, s, OH, NH), 4.09 (5H$_{7',8'9'}$, m, CH$_2$, CH), 3.71 (3H, s, OCH$_3$), 3.13 (2H$_{11}$, d, $^3J_{11,10}$ = 6.67 Hz, CH$_2$), 2.41 (3H, s, CH$_3$).

^{13}C-NMR (DMSO-D$_6$, 100.63 MHz):

δ 171.2 (C-12), 157.2 (C-8), 154.3 (C-4'), 145.1 (C-4*), 136.3 (C-4), 130.2 (C-5*,3*), 129.1 (C-2,6), 128.2 (C-2*,6*), 127.3 (C-3,5), 125.3 (C-1), 115.1 (C-3',5'), 73.2 (C-CH$_2$), 70 (C-CH$_2$), 67 (C-CH$_2$), 68.3 (C-8'), 55 (C-10), 52.1 (C-CH$_3$), 37 (C-CH$_2$), 21.1 (C-CH$_3$).

IR $\overline{\nu}$/cm^{-1}(T%):

3314 (92%), 3034 (94%), 2932 (90%), 1719 (70%), 1659 (37%), 1612 (85%), 1598 (90%), 1511 (65%), 1438 (80%), 1387 (75%), 1355 (65%), 1245 (55%), 1189 (35%), 1095 (60%), 1049 (70%), 978 (68%), 939 (77%), 814 (65%), 742 (77%), 698 (73%), 664 (53%).

MS-EI (70 eV) *m/z:*

558 (40%) [M+1]$^+$, 460.1 (100%) [M-C$_4$H$_3$NO$_2$]$^+$, 443.1 (44%) [M-C$_4$H$_4$NO$_3$]$^+$, 352.1 (56%) [M-C$_{11}$H$_{12}$NO$_3$]$^+$, 298 (68%) [C$_{17}$H$_{16}$NO$_4$]$^+$, 245.1 (80%) [C$_{10}$H$_{13}$SO$_5$]$^+$, 136.1 (85%) [C$_8$H$_8$O$_2$]$^+$, 107.1 (100%) [C$_7$H$_7$O]$^+$.

HRMS (EI) m/z measured: 558.41 [M+1]$^+$, **m/z calculated:** 558.376

R$_f$: 0.47 (PE/EtOAc 1:1).

5.4.1.4.2 *Methyl N-[(benzyloxy)carbonyl]-O-[2,3-{di[(4-methylphenyl)sulfonyl]oxy} propyl]tyrosinate (d)*

[IUPAC: Methyl 2-(benzyloxycarbonylamino)-3-(4-(2,3-bis(tosyloxy)propoxy)phenyl) propanoate]
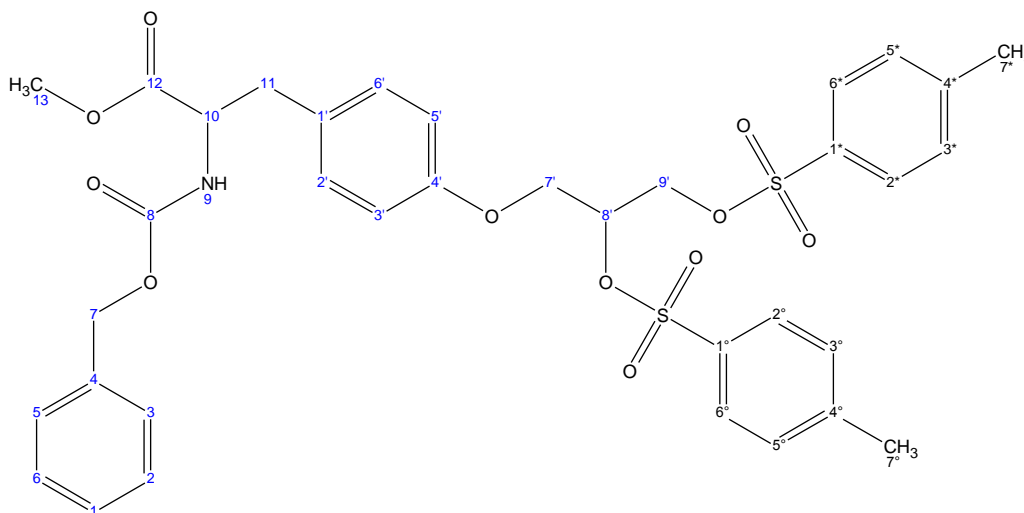
^{1}H-NMR (DMSO-D_6, 400.16 MHz):

δ 7.76 (4H$_{2*,6*2°,6°}$, m, Ph), 7.35 (4H$_{3*,5*3°,5°}$, m, Ph), 7.33 (2H$_{2,6}$, m, Ph), 7.29 (4H$_{3,5,3´,5´}$, m, Ph), 7.07 (2H$_{2´,6´}$, m, Ph), 5.26 (1H, s, NH), 5.12 (2H$_7$, s, CH$_2$), 5.02 (1H$_{8´}$, ddd, $^3J_{8´,9}$= 8.24 Hz, CH), 4.66 (1H$_{10}$, m, CH), 4.21 (2H$_{7´}$, dd, $^3J_{7´,8}$= 8.24 Hz, CH$_2$), 4.42 (2H$_{9´}$, m, CH$_2$), 3.71 (3H, s, OCH$_3$), 2.95 (2H$_{11}$, d, $^3J_{11,10}$ = 6.67 Hz, CH$_2$), 2.44 (3H, s, CH$_3$), 2.39 (3H, s, CH$_3$).

^{13}C-NMR (DMSO-D_6, 100.63 MHz):

δ 172 (C-12), 156.1 (C-8), 154.3 (C-4'), 146 (C-4°), 145.3 (C-4*), 136.1 (C-4), 130.2 (C-6´,2´), 129.3 (C-2°,6°), 128.3 (C-5*,3*), 127.2 (C-2,6), 126.8 (C-2°,6°), 126 (C-2*,6*), 125 (C-3,5), 124.3 (C-1'), 114.1 (C-3',5'), 75 (C-8'), 71 (C-CH$_2$), 69 (C-CH$_2$), 67 (C-7), 55 (C-10), 52.6 (C-CH$_3$), 22.6 (C-2CH$_3$).

IR $\bar{\nu}$/cm^{-1}(T%):

3384 (96%), 3033 (95%), 2953 (93%), 1720 (59%), 1611 (89%), 1597 (84%), 1511 (59%), 1453 (79%), 1400 (86%), 1364 (53%), 1293 (76%), 1242 (52%), 1212 (58%), 1189 (43%), 1174 (21%), 1111 (79%), 1096 (69%), 1043 (59%), 1018 (60%), 1001 (60%), 930 (52%), 813 (45%), 755 (53%), 695 (62%), 664 (38%).

MS-EI (70 eV) *m/z:*

712 (36%) [M+1]$^+$, 668 (92%) [M-C$_2$H$_3$O]$^+$, 560 (32%) [M-C$_9$H$_{11}$O$_2$]$^+$, 489 (60%) [M-C$_{13}$H$_{18}$O$_3$]$^+$, 383 (68%) [C$_{17}$H$_{19}$O$_6$S$_2$]$^+$, 307 (100%) [M-C$_{26}$H$_{28}$O$_4$]$^+$, 289 (44%) [M-C$_{26}$H$_{30}$O$_5$]$^+$, 165 (40%) [M-C$_{33}$H$_{37}$O$_7$]$^+$.

HRMS (EI) m/z measured: 712.655 [M+1]$^+$, **m/z calculated:** 712.549

R$_f$: 0.57 (PE/EtOAc 1:1).

5.4.1.5 General Procedure for 2-Nitroimidazole Coupling

Triethylamine (1.5 eq) was added to the solution of compound (**c** or **d** = 1 eq) in *N,N´*-dimethylformaide (DMF). Afterwards, 2-nitroimidazole (1 eq) was added into the reaction mixture and it was heated at 60°C for 1-2 days. Then, reaction mixture was poured into toluene and was concentrated under vacuum in order to get rid of DMF. After evaporation, residue was dissolved in EtOAc (250 mL), washed by sat.$NaHCO_3$ (250 mL), brine (300 mL) and dried over anhyd.Na_2SO_4. After drying, it was filtered and solvent was evaporated. Crude product was cleaned by MPLC by gradient elution by using first PE/EtOAc 1:1 at a flow rate of 15 mL/min and later 100% EtOAc at a flow rate of 20 mL/min. 1.0 g (1.53 mmol, 65%) of compound (**e**) and 1.31 (2.61 mmol, 69%) of compound (**f**) were obtained as white solids.

5.4.1.5.1 *Methyl N-[(benzyloxy)carbonyl]-O-[2-{[(4-methylphenyl)sulfonyl]oxy}-3-(2-nitro-1H-imidazol-1-yl)propyl]tyrosine (e)*
[IUPAC: Methyl 2-(benzyloxycarbonylamino)-3-(4-(3-(2-nitro-1H-imidazole-1-yl)-2-(tosyloxy)propoxy)phenyl)propanoate]
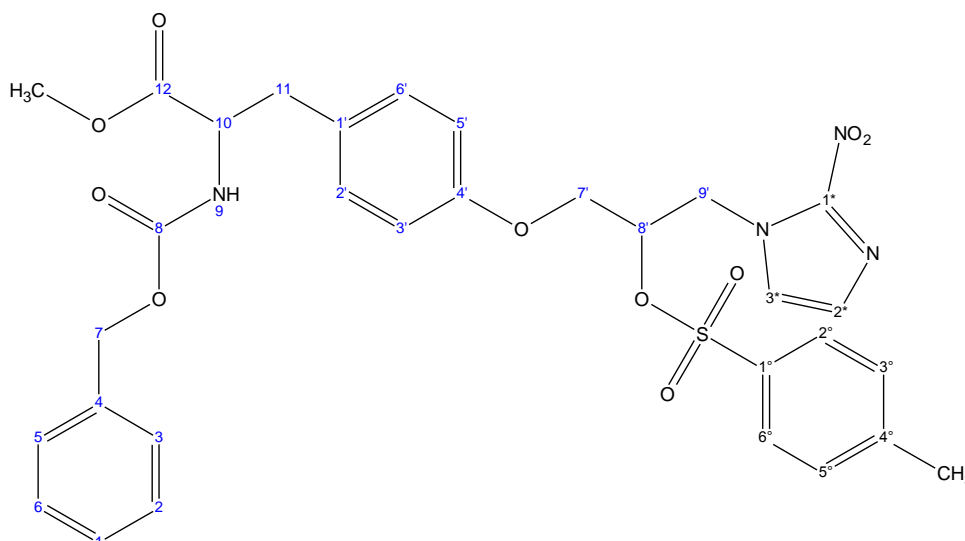
^{1}H-NMR (DMSO-D$_6$, 400.16 MHz):

δ 7.84 (1H$_{3*}$, $^3J_{3*,2*}$ = 2.00 Hz, CH), 7.63 (2H$_{2°,6°}$, m, Ph), 7.46 (1H$_{2*}$, m, CH), 7.28 (5H$_{1,2,3,4,5,6}$, m, Ph), 7.27 (4H$_{3´,5´,3°,5°}$, m, Ph), 6.99 (2H$_{2´,6´}$, m, Ph), 5.26 (1H, s, NH), 5.12 (2H$_7$, s, CH$_2$), 4.70 (1H$_{10}$, m, CH), 4.62 (2H$_{9´}$, m, CH$_2$), 4.54 (1H$_{8´}$, ddd, $^3J_{8´,9}$ = 9.30 Hz, CH), 4.37 (2H$_{7´}$, dd, $^3J_{7´,8}$ = 7.67 Hz, CH$_2$, 3.71 (3H, s, OCH$_3$), 2.95 (2H$_{11}$, d, $^3J_{11,10}$ = 6.67 Hz, CH$_2$).

^{13}C-NMR (DMSO-D$_6$, 100.63 MHz):

δ 172.1 (C-12), 162.3 (C-4'), 156.3 (C-8), 146.3 (C-1*), 145.6 (C-4°), 136.5 (C-4), 133.2 (C-3°,5°), 132.3 (C-6´,2´), 130.5 (C-2,6), 129.1 (C-3,5,2°,6°), 114.3 (C-3',5'), 75.1 (C-8'), 71 (C-CH$_2$), 67 (C-CH$_2$), 55.5 (C-10), 52.3 (C-OCH$_3$), 49.1 (C-9'), 37.5 (C-CH$_2$), 22.1 (C-CH$_3$).

IR $\bar{\nu}$/cm^{-1}(T%):

3385 (95%), 3034 (95%), 2954 (93%), 1715 (60%), 1611 (89%), 1597 (84%), 1511 (59%), 1486 (55%), 1439 (80%), 1359 (43%), 1238 (56%), 1189 (52%), 1175 (38%), 1052(63%), 1017 (59%), 913 (56%), 897 (50%), 856 (75%), 837 (58%), 814 (56%), 742 (48%), 698 (56%), 663 (42%).

MS-EI (70 eV) *m/z:*

653 (100%) [M+1]$^+$, 609 (24%) [M-C$_2$H$_3$O]$^+$, 549 (20%) [M-C$_4$H$_7$O$_3$]$^+$, 501 (21%) [M-C$_4$H$_{11}$O$_2$]$^+$, 324 (56%) [C$_{13}$H$_{14}$N$_3$O$_5$S]$^+$.

HRMS (EI) m/z measured: 653.18107 [M+1]$^+$, **m/z calculated:** 653.191666

m.p.: 115°C. **R$_f$:** 0.37 (PE/EtOAc 1:1).

5.4.1.5.2 *Methyl N-[(benzyloxy)carbonyl]-O-[2-{[(4-methylphenyl)sulfonyl]oxy}-3-(2-nitro-1H-imidazol-1-yl)propyl]tyrosine (f)*

[IUPAC: Methyl 2-(benzyloxycarbonylamino)-3-(4-(2-hydroxy-3-(2-nitro-1H-imidazole-1-yl)propoxy)phenyl)propanoate]
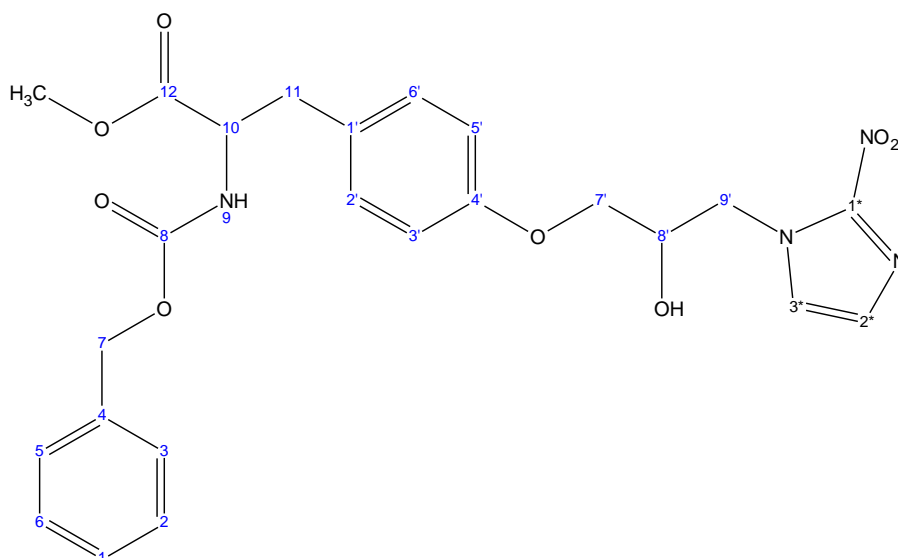
^{1}H-NMR (DMSO-D$_6$, 400.16 MHz):

δ 7.53 (1H$_{3*}$, $^3J_{3*,2*}$ = 2.00 Hz, CH), 7.43 (1H$_{2*}$, m, CH), 7.33 (1H$_6$, d, $^3J_{6,1}$ = 7.15 Hz, Ph), 7.31 (1H5, d, $^3J_{5,6}$ = 7.30 Hz, Ph), 7.28 (1H$_3$, d, $^3J_{3,2}$ = 7.30 Hz, Ph), 7.24 (1H$_2$, d, $^3J_{2,1}$ = 7.15 Hz, Ph), 6.97 (2H$_{2',6'}$, m, Ph), 6.90 (2H$_{3',5'}$, m, Ph), 5.12 (2H$_7$, s, CH$_2$), 4.79 (1H$_{8'}$, ddd, $^3J_{8',9}$ = 9.00 Hz, CH), 4.69 (2H$_{9'}$, m, CH$_2$), 4.66 (1H$_{10}$, m, CH), 4.24 (2H$_{7'}$, dd, $^3J_{7',8}$ = 7.40 Hz, CH$_2$) , 4.16 (2H, s, OH, NH), 3.71 (3H, s, OCH$_3$), 2.95 (2H$_{11}$, d, $^3J_{11,10}$ = 6.67 Hz, CH$_2$).

^{13}C-NMR (DMSO-D$_6$, 100.63 MHz):

δ 172.3 (C-12), 160.4 (C-4'), 156.5 (C-8), 146.7 (C-1*), 136.5 (C-4), 131.3 (C-6´,2´), 129.2 (C-2,6), 128.3 (C-3*), 127.5 (C-3,5), 125.3 (C-2*), 116.1 (C-3',5'), 70 (C-CH$_2$), 67 (C-CH$_2$), 64 (C-8'), 55.6 (C-10), 52.4 (C-CH$_3$), 49.4 (C-9'), 37 (C-CH$_2$).

IR $\bar{\nu}$/cm⁻¹(T%):

3345 (93%), 3029 (91%), 2951 (89%), 1711 (56%), 1610 (81%), 1521 (66%), 1506 (49%), 1489 (56%), 1440 (65%), 1360 (30%), 1225 (39%), 1171 (51%), 1160 (57%), 1108 (50%), 1043 (46%), 955 (76%), 920 (60%), 834 (61%), 776 (65%), 730 (59%), 677 (49%), 640 (60%).

MS-EI (70 eV) *m/z:*

499 (10%) [M+1]⁺, 382 (15%) [M-C₉H₈]⁺, 301 (34%) [M-C₁₄H₁₅N]⁺, 230 (60%) [M-C₁₈H₂₂NO]⁺, 124 (65%) [C₇H₈O₂]⁺, 107 (100%) [C₇H₇O]⁺, 91 (94%) [C₇H₇]⁺, 79.2 (40%) [C₆H₇]⁺.

HRMS (EI) m/z measured: 499.151 [M+1]⁺, **m/z calculated:** 499.067

m.p.: 112°C. **R$_f$:** 0.14 (PE/EtOAc 1:1).

5.4.1.6 *Methyl N-[(benzyloxy)carbonyl]-O-[2-fluoro-3-(2-nitro-1H-imidazol-1-yl)propyl] tyrosine (g)*

[IUPAC: Methyl 2-(benzyloxycarbonylamino)-3-(4-(2-fluoro-3-(2-nitro-1H-imidazole-1-yl)propoxy) phenyl)propanoate]

0.12 mL (0.9 mmol, 1 eq) of diethylaminosulfur trifluoride (DAST) was added slowly to the solution of 440 mg (0.9 mmol) of compound **(c)** in 10 mL of dichloromethane (DCM) at -78°C under argon. It was kept stirring for 6 h. Afterwards, the temperature of reaction mixture was increased slowly and at -20°C, it was quenched by addition of 5 mL of water. Then, the organic layer was washed by brine (250 mL), dried over anhyd.Na₂SO₄. It was filtered and solvent was evaporated. Residue was dissolved in PE/EtOAc 1:1, precipitates so formed were removed by filtration and filtrate was cleaned by MPLC by gradient elution by using first PE/EtOAc 1:1 and later 100% EtOAc at a flow rate of 20 mL/min. 0.250 g (0.514 mmol, 57%) of white solid was obtained as a final product.
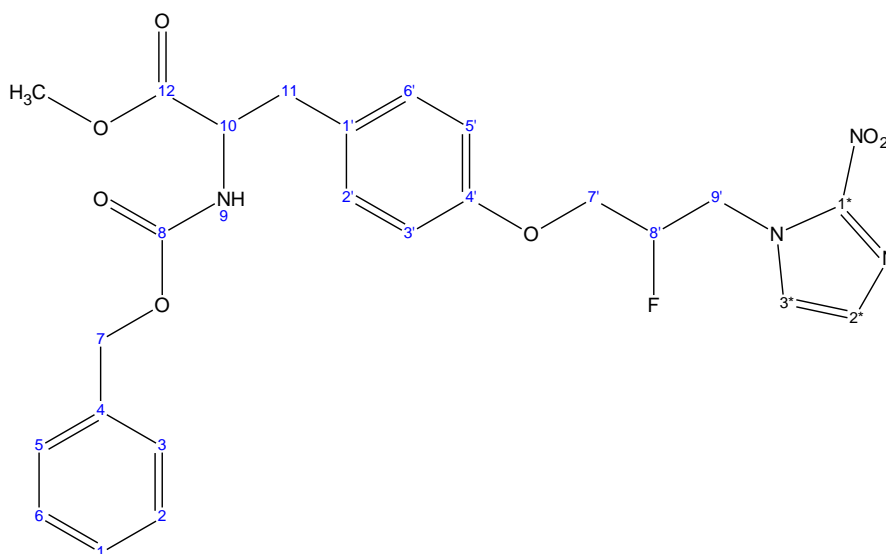
^{1}H-NMR (DMSO-D$_6$, 400.16 MHz):

δ 7.89 (1H$_{3*}$, $^3J_{3*,2*}$ = 2.00 Hz, CH), 7.28 (5H$_{1,2,3,5,6}$, m, Ph), 7.17 (1H$_{2*}$, m, CH), 7.02 (4H$_{2',3',5',6'}$, m, Ph), 5.26 (1H, s, NH), 5.12 (2H$_7$, s, CH$_2$), 4.84 (3H$_{8',9'}$, m, CH$_2$, CH), 4.69 (1H$_{10}$, m, CH), 4.43 (2H$_{7'}$, dd, $^3J_{7',8}$ = 5.73 Hz, CH$_2$), 3.71 (3H, s, OCH$_3$), 2.95 (2H$_{11}$, d, $^3J_{11,10}$ = 6.04 Hz, CH$_2$)

^{13}C-NMR (DMSO-D$_6$, 100.63 MHz):

δ 172.4 (C-12), 159.5 (C-4'), 155.3 (C-8), 143.2 (C-1*), 136.6 (C-4), 131.4 (C-2',6'), 129.5 (C-2,6), 128.7 (C-3,5), 127.2 (C-2*,3*), 116.3 (C-3',5'), 75 (d, $^3J_{C-F}$ = 15 Hz C-8'), 69 (d, $^1J_{C-F}$ = 156 Hz C-CH$_2$), 66.6 (C-CH$_2$), 55 (C-10), 52 (C-OCH$_3$), 50 (d, $^1J_{C-F}$ = 163 Hz C-9'), 37 (C-CH$_2$).

IR $\bar{\nu}$/cm^{-1}(T%):

3340 (95%), 3034 (97%), 2954 (93%), 1708 (51%), 1611 (85%), 1537 (67%), 1510 (49%), 1486 (55%), 1438 (75%), 1359 (40%), 1240 (41%), 1179 (60%), 1161 (57%), 1111 (70%), 1047 (56%), 950 (86%), 912 (80%), 836 (63%), 776 (65%), 740 (60%), 697 (59%), 640 (70%).

MS-EI (70 eV) m/z: 483 (12%) [M-H$_2$O]$^+$, 349 (36%) [M-C$_9$H$_{12}$O$_2$]$^+$, 303 (20%) [M-C$_{11}$H$_{18}$O$_3$]$^+$, 278 (16%) [M-C$_{13}$H$_{18}$O$_3$]$^+$, 172 (100%) [C$_6$H$_7$FN$_3$O$_2$]$^+$, 107 (36%) [C$_7$H$_7$O]$^+$, 91.1 (72%) [C$_7$H$_7$]$^+$.

HRMS (EI) m/z measured: 483.16928 [M+1]$^+$, **m/z calculated:** 483.167941

R$_f$: 0.28 (PE/EtOAc 1:1).

5.4.2 Radiosynthesis of [^{18}F]FNT

Radiosynthesis for [^{18}F]FNT is shown in Fig 5.2 and is described as below.

5.4.2.1 [^{18}F]-Labelling

No-carrier-added (n.c.a.) [^{18}F] fluoride was produced at the cyclotron (PET trace, GE Medical Systems, Uppsala) at the PET-Center, Ulm, *via* the ^{18}O (p,n) ^{18}F reaction by irradiating > 95% enriched [^{18}O] water with 16.5 MeV protons. The [^{18}F]fluoride activity (200±1 MBq) was introduced into a vial containing 3 mg of potassium carbonate (K$_2$CO$_3$) and 7 mg of kryptofix-222 (K222). Afterwards, the [^{18}F] fluoride solution was dried for 10 min under a mild stream of argon (ca. 2 mL/min) at 140°C by azeotropic distillation with acetonitrile (2 x 0.8 mL). Then, 5 mg of precursor dissolved in 1 mL of dimethylsulfoxide (DMSO) was added to the reaction vial containing the [^{18}F]KF-K222. Labelling reaction was performed at 140°C. After 3 min, reaction mixture was diluted upto 10 mL of water and was passed through the combination of Alumina N and C18 cartridges. Free fluoride [^{18}F] was trapped in Alumina while product was eluted from C18 cartridge by 1 mL of 70%TFA into a vial for hydrolysis. Hydrolysis was performed at 120°C. After 20 min, reaction mixture was quenched by 750 µL of 6N NaOH untill pH 8 was obtained. Then, reaction mixture was passed through Alumina N and was injected into HPLC for preparative synthesis. Product peak so collected was diluted by 20 mL of water and was passed through preconditioned Strata-X cartridge. [^{18}F]FNT was eluted by 500 µL of ethanol (EtOH). 80±1.1 MBq of [^{18}F]FNT (40±1%, decay uncorrected, n = 3) were obtained within 90 min at EOS.

5.4.2.2 Radio-TLC Analysis

Samples (5 μL) were withdrawn at 1, 2, 3, 5, 7, 10, 15, and 20 min directly from reaction reaction after labelling step for radio-TLC analysis of [^{18}F]-labelled intermediate (**h**). PE/EtOAc 1:1 was used as mobile phase. For reference, standard spot was visualized under UV-lamp (254 nm) and was marked by radioactive spot. Quantitative assay of radioactive spots was carried out by phosphor imager. The R$_f$ value of [^{18}F]-labelled intermediate (methyl *N*-[(benzyloxy)carbonyl]-*O*-[2-[^{18}F]fluoro-3-(2-nitro-1*H*-imidazol-1-yl)propyl] tyrosine, **h**) was found to be 0.3.

5.4.2.3 LC/MS Analysis

For the purpose of identification of hydrolysed product, radiosynthesis of [^{18}F]FNT was carried out as a carrier-added (c.a.) synthesis in order to get MS-compatible amounts of the desired compounds. The experiments were performed in order to check the mass of product [^{18}F]FNT by LC/MS. The [^{18}F]fluoride solution was introduced into a 5 mL sealed vial containing 50 μL of 1% aqueous K^{19}F, 100 μL of 3.5% aqueous K$_2$CO$_3$ and 15 mg K222, the following steps were the same as in case of no-carrier added (n.c.a.) [^{18}F]-fluorinations. After hydrolysis, 20 μL samples were injected into HPLC and the peaks showing signals in radioactive detector were separated. The fraction (50 μL) from each peak was injected into the LC/MS system. A HP ODS (100 x 2.1 mm, 5μ) column was used. Eluents were methanol/water (20/80, v/v) buffered with ammonium acetate (144 mg/L) and flow rate was 0.3 mL/min. The mass peak [ACPI (+) mode] 353 (100%) [M+1]$^+$ for [^{18}F]FNT confirmed R$_t$ of the product on HPLC system.

5.4.2.4 Radio-HPLC Analysis

Analytical assay by high pressure liquid chromatography (HPLC) was performed for both of the labelling and the hydrolysis steps. After labelling reaction, 20 μL from reaction mixture were analysed by HPLC having reversed-phase column (Phenomenex Luna, 5 μ, C 18, 250 x 4.6 mm) using isocratic elution (MeCN/H$_2$O with 0.1%TFA; 50:50) at a flow rate of 2 mL/min. [^{18}F]-labelled intermediate showed R$_t$ value of 7.9 min and its peak was collected and was measured by a γ-counter. The RCYs were calculated by relating the radioactivity of the product peak to the amount of the radioactivity injected into HPLC.

For preparative step after hydrolysis, 1 mL of reaction mixture was injected into HPLC having reversed-phase preparative column (Phenomenex Luna, 5 μ, C 18, 250 x 10 mm) using gradient elution of solvent A (water with 2 mM NH$_4$OAc) and solvent B (MeOH with 2 mM NH$_4$OAc), at a flow rate of 5 mL/min for 10 min (A: 100 to 0%; B: 0 to 100%). [^{18}F]FNT peak (R$_t$: 6.7 min) was collected. However, analytical assay for quality control was carried out using same column as for labelling step and under gradient elution conditions as for preparative step but at a flow rate of 1 mL/min. R$_t$ value of [^{18}F]FNT (radiochemical purity ≥ 98%) under quality control conditions was 8.9 min.
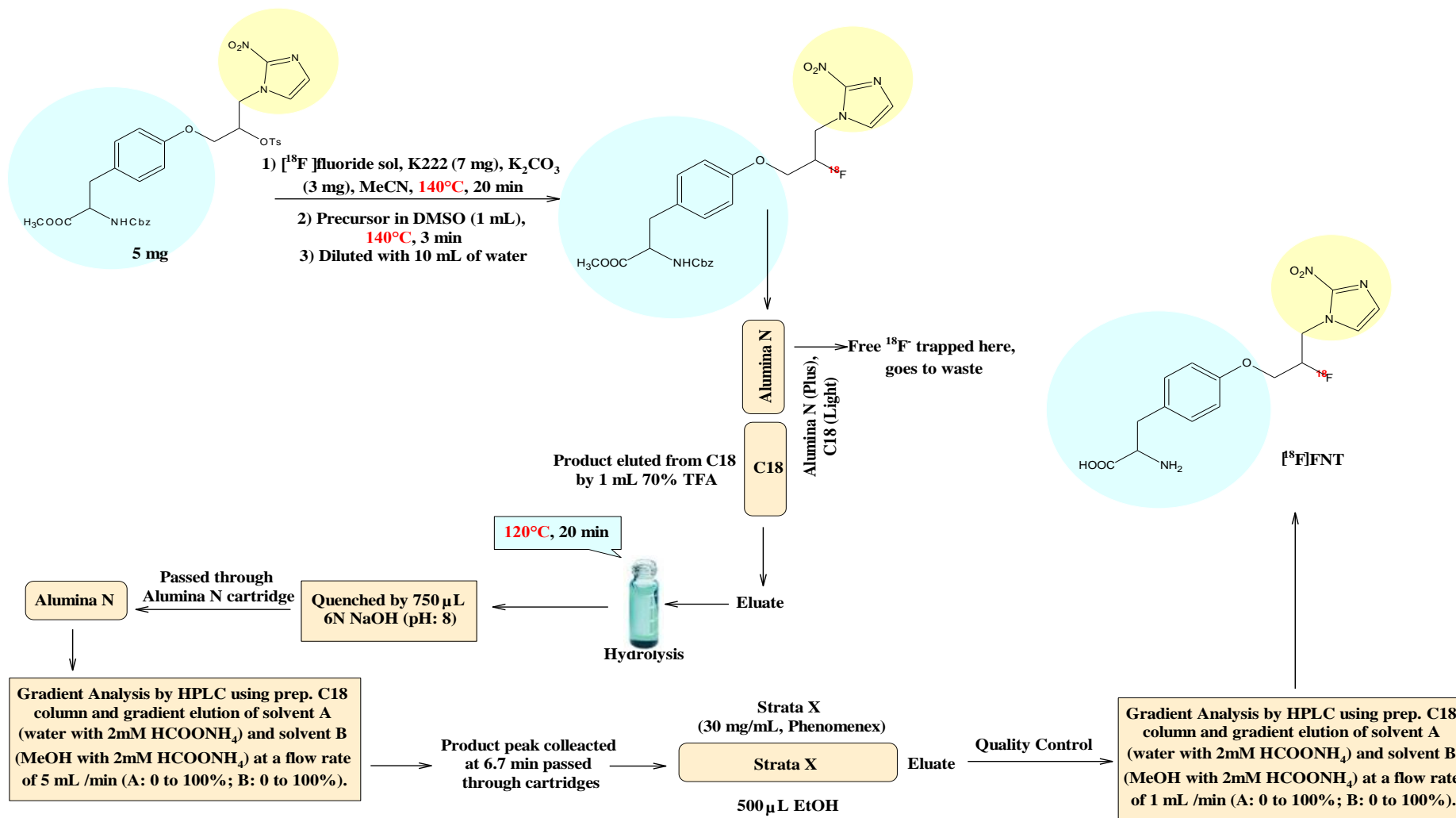
Fig 5.2 Radiosynthesis of [^{18}F]FNT: A new hypoxia tracer for PET-Imaging

5.5 Synthesis of New PSMA Targeting Ligand ([^{18}F]FPy-DUPA-Pep])

5.5.1 Organic Synthesis

5.5.1.1 6-Chloronicotinic acid 2,3,5,6-tetrafluorophenylester (j)

It was synthesized according to Lit[80]. To the solution of 6-chloronicotinic acid (2 g, 13 mmol) and tetrafluorophenol (2.2 g, 13 mmol) in dioxane (80 mL), 2.6 g (12.5 mmol) of *N,N'*-dicyclohexylcarbodimide (DCC) were added under argon and the reaction mixture was stirred at room temperature overnight. Afterwards, reaction mixture was filtered and solvent was removed under vacuum. The residue was dissolved in hot hexane (30 mL) and was filtered immediately. After a short period of time, white crystals began to form in the filtrate. Later, the filtrate was put in a freezer overnight. Next day, crystals were filtered and washed by ice-cold hexane (2 x 65 mL). 3.2 g (10.3 mmol) of product **(j)** was obtained as white solid (%yield: 80%).
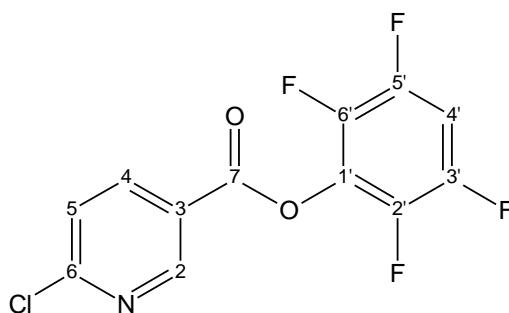
^{1}H-NMR (DMSO-D$_6$, 400.16 MHz):

δ 9.19 (1H$_2$, s, Py), 8.37 (1H$_4$, d, $^3J_{4,5}$ = 8.27 Hz, Py), 8.07 (1H$_5$, dd, $^5J_{2,5}$ = 0.8 Hz, $^3J_{4,5}$ = 8.7 Hz, Py), 7.09 (1H$_4'$, tt, $^4J_{H,F}$ = 6.5 Hz, $^3J_{H,F}$ = 9.26 Hz, Ph).

^{13}C-NMR (DMSO-D$_6$, 100.63 MHz):

δ 161 (C-CO), 155 (C-6), 152 (C-3',5'), 150 (C-3',5'), 150 (C-2), 146 (C-2´,6´), 145 (C-2',6'), 137 (C-4), 129 (C-3), 119 (m, C-1'), 116 (C-5), 101 (m, C-4').

MS-EI (70 eV) *m/z:* 306.1 (30%) [M+H]$^+$, 157 (100%) [M-C$_6$H$_2$F$_4$]$^+$, 107 (36%) [C$_7$H$_7$O]$^+$, 91.1 (61%) [C$_7$H$_7$]$^+$.

HRMS (EI) m/z measured: 305.9985 [M+1]$^+$, **m/z calculated:** 305.9940

R$_f$: 0.65 (PE/EtOAc 5:1).

5.5.1.2 N,N,N-Trimethyl-5-((2,3,5,6-tetrafluorophenoxy)-carbonyl)pyridin-2-aminium trifluoromethanesulfonate (k)

It was also synthesized according to the procedure as described earlier[80]. The solution of compound (**j**, 1.0 g, 3.3 mmol) in 15 mL of tetrahydrofuran (THF) was filtered into a 35 mL vial capped with a rubber septum. A steady stream of trimethylamine gas at room temperature was passed through the filtrate under vigorous stirring. After 5 min, a white precipitate started to form and the reaction was allowed to proceed for 3 h under trimethylamine flow. The solid material was filtered off

and washed with DEE (150 mL) and DCM (100 mL). 0.53 g (1.5 mmol) of *N,N,N*-trimethyl-5-((2,3,5,6-tetrafluorophenoxy) carbonyl)pyridin-2-aminium chloride was suspended in DCM (100 mL) under an argon by ultrasonification. To the vigorously stirred suspension, trimethylsilyl trifluoromethanesulfonate (0.78mL, 4.4 mmol) was added over 10 min. The solution was filtered, and volatile components were removed under reduced pressure. The dry residue was washed with DEE (3 x 50 mL), dried under vacuum, affording 0.5 g of *N,N,N*-trimethyl-5-((2,3,5,6-tetrafluorophenoxy) carbonyl)pyridin-2-aminium trifluoromethanesulfonate **(k)** as a white fluffy solid (%yield: 32%).
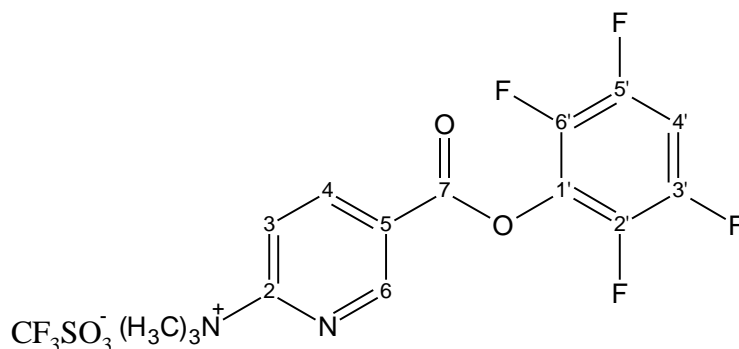
¹H-NMR (DMSO-D₆, 400.16 MHz):

δ 10.2 ($1H_6$, s, Py), 9.37 ($1H_4$, d, $^3J_{4,3} = 8.14$ Hz, Py), 7.27 ($1H_3$, d, $^3J_{3,4} = 8.5$ Hz, Py), 7.14 ($1H_{4'}$, m, Ph), 3.67 (9H, s, N(CH₃)₃).

¹³C-NMR (DMSO-D₆, 100.63 MHz):

δ 162 (C-CO), 155 (C-2), 152 (C-3',5'), 146 (C-2',6'), 144 (C-6), 142 (C-4), 128 (C-5), 117 (m, C-1'), 114 (C-3), 98 (m, C-4').

MS-EI (70 eV) *m/z:* 329.1 (100%) [M]⁺, 314.1 (30%) [M-CH₃]⁺.

HRMS (EI) m/z measured: 329.1253 [M]⁺, **m/z calculated:** 329.0913

5.5.1.3 6-Fluoronicotinic acid 2,3,5,6-tetrafluorophenyl ester (l)

A mixture of spray dried potassium fluoride (KF, 7.3 mg, 0.12 mmol) and K222 (59 mg, 0.16 mmol) in dry MeCN (1.0mL) was stirred for 5 min. To this mixture, a solution of 50 mg (0.10 mmol) of compund **(k)** in 0.5 mL of dry MeCN was added and the resulting mixture was stirred for 15 min at room temperature. Afterwards, the reaction mixture was diluted with 2.0 mL water/0.1% TFA, filtered, and purified by reversed-phase preparative chromatography using C18 column (Phenomenex Luna, 250 mm x 21.2 mm, 5 μm) at a flow rate of 10 mL/min with a gradient of 40-80% MeCN/0.1% TFA over 30 min. From the collected fractions, MeCN was removed under reduced pressure and the aqueous phase was extracted with DCM (3 x 25mL). The combined organic phases were washed with water (20 mL), brine (20 mL), dried over anhydrous Na₂SO₄, filtered and the organic phase was removed in vacuum affording 10 mg of 6-fluoronicotinic acid 2,3,5,6-tetrafluorophenyl ester **(l)** as a waxy off-white solid (%yield: 37%).
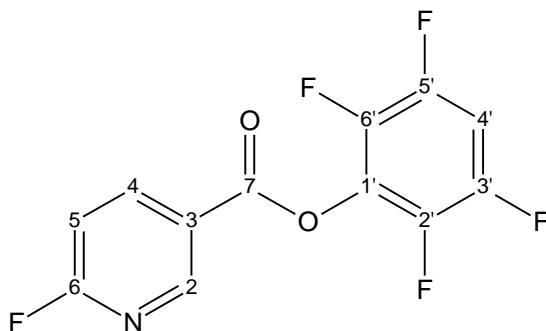
¹H-NMR (DMSO-D₆, 400.16 MHz):

δ 9.02 (1H₂, dd, $^4J_{2,4}$ = 2.49 Hz, $^5J_{2,5}$ = 0.81 Hz, Py), 7.55 (1H₄, d, $^3J_{3,5}$ = 8.76 Hz, Py), 7.10 (1H₅, m, Py), 7.07 (1H_{4'}, m, Ph).

¹³C-NMR (DMSO-D₆, 100.63 MHz):

δ 173 (C-6), 166 (C-6), 160 (C-CO), 152 (C-2), 151 (C-3',5'), 145 (C-2',6'), 143 (C-3',5'), 137 (C-4), 123 (C-3), 118 (m, C-1'), 108 (C-5), 106 (C-5), 97 (m, C-4').

MS-EI (70 eV) *m/z:* 290.2 (12%) [M+H]$^+$, 141.2 (100%) [M-C$_6$H$_2$F$_4$]$^+$, 107 (41%) [C$_7$H$_7$O]$^+$, 91.1 (52%) [C$_7$H$_7$]$^+$.

HRMS (EI) m/z measured: 290.0249 [M+1]$^+$, **m/z calculated:** 290.0235

R$_f$: 0.58 (PE/EtOAc 7:1).

5.5.1.4 2-[3-(3-Benzyloxycarbonyl-1-tert-butoxycarbonyl-propyl) ureido]pentanedioic acid ditert-butyl ester (m)

Triethylamine (TEA, 2.3 mL, 16.4 mmol) was added slowly to the solution of L-glutamate di-*tert*-butyl ester hydrochloride (2.0 g, 6.76 mmol) and triphosgene (329.8 mg, 1.12 mmol) in DCM (25.0 mL) at -78 °C under argon. After stirring for 2 h at -78 °C, the solution of L-Glu(OBn)-OtBu (2.4 g, 8.2 mmol) and TEA (1.4 mL, 9.82 mmol) in DCM (5.0 mL) was added. Afterwards, the reaction mixture was stirred at RT overnight. Next day, the reaction mixture was quenched with 1 M HCl (till the pH 3-4) and the organic layer was separated, washed with brine and dried over anhyd. Na$_2$SO$_4$. After evaporation, the crude product was purified by flash chromatography using hexane/EtOAc 1:1 to yield 2.5 g of product **(m)** (%yield: 82%) as a colourless oil.

(m)
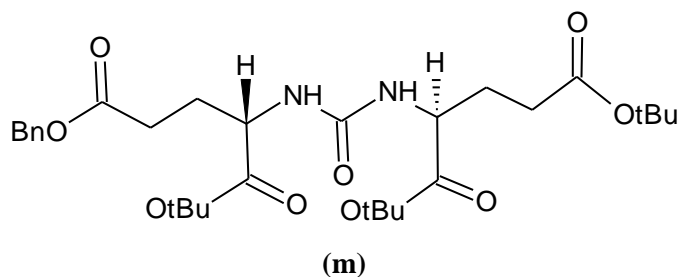
^{1}H-NMR (DMSO-D$_6$, 400.16 MHz):

δ 7.3 (5H, m, Ph), 5.3 (2H, s, NH), 5.08 (2H, s, Ph-CH$_2$), 4.5 (1H, s, CH), 4.3 (1H, s, CH), 2.5 (2H, m, Glu-H), 2.4 (2H, m, Glu-H), 2.1 (1H, m, Glu-H), 2.05 (1H, m, Glu-H), 1.9 (1H, m, Glu-H), 1.87 (1H, m, Glu-H), 1.5 (9H, s, CH$_3$tBu), 1.4 (9H, s, CH$_3$tBu), 1.39 (9H, s, CH$_3$tBu).

^{13}C-NMR (DMSO-D$_6$, 100.63 MHz):

δ 176 (C-CO), 174 (C-CO), 173 (C-CO), 158 (C-urea-CO), 136 (C-Ph-C), 128.7 (C-Ph-2CH), 128.4 (C-Ph-2CH), 84 (C-2C-tBu), 79 (C-C-tBu), 67 (C-CH$_2$), 55 (C-Glu-2CH), 32 (C-Glu-2CH$_2$), 30 (C-Glu-2CH$_2$), 28 (C-9C-tBu), 27 (C-3C-tBu).

MS-EI (70 eV):

Positive mode m/z: 579.32 [M+H] $^+$, **Negative mode m/z:** 577.33 [M-H] $^+$.

HRMS (EI) m/z measured: 579.2879 [C$_{30}$H$_{47}$N$_2$O$_9$]$^+$, **m/z calculated:** 579.3179

R$_f$: 0.71 (Hexane/EtOAc 1:1).

5.5.1.5   2-[3-(1,3-Bis-tert-butoxycarbonyl-propyl)-ureido]pentanedioic acid 1-tert-butyl ester [DUPA(OtBu)$_3$-OH] (n)

2-[3-(3-benzyloxycarbonyl-1-*tert*-butoxycarbonyl-propyl)-ureido]pentanedioic acid tri-*tert*-butyl ester [DUPA(O*t*Bu)$_3$-OBn] (1.2 g, 1.78 mmol) was hydrogenated over 10% Pd/C (0.2 g) in 25 mL of EtOAc at atmospheric pressure of hydrogen for 16 h. The reaction mixture was filtered through a pad of celite and concentrated under reduced pressure. The residue was recrystallized from EtOAc/hexane to give 0.96 g of compound (**n**) (%yield: 93%) as a colourless solid.

(n)
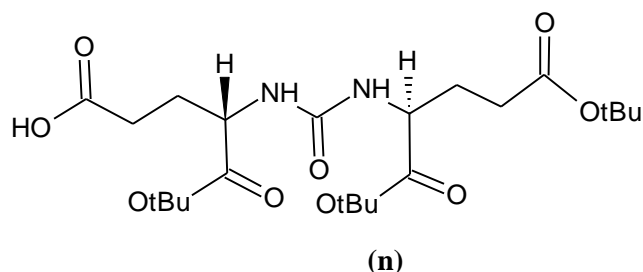
^{1}H-NMR (DMSO-D$_6$, 400.16 MHz):

δ 5.1 (2H, s, NH), 4.4 (1H, s, CH), 4.3 (1H, s, CH), 2.6 (2H, m, Glu-H), 2.3 (2H, m, Glu-H), 2.2 (1H, m, Glu-H), 2.1 (1H, m, Glu-H), 1.9 (2H, m, Glu-H), 1.5 (27H, m, CH$_3$tBu).

^{13}C-NMR (DMSO-D$_6$, 100.63 MHz):

δ 179 (C-CO), 176 (C-CO), 173 (C-CO), 158 (C-urea-CO), 84 (C-2C-tBu), 79 (C-C-tBu), 55 (C-Glu-CH), 54 (C-Glu-CH), 34 (C-Glu-2CH$_2$), 32 (C-Glu-2CH$_2$), 28 (C-12C-tBu).

MS-EI (70 eV):

Positive mode m/z: 489.31 [M+H] $^+$, **Negative mode m/z:** 487.3 [M-H] $^+$.

HRMS (EI) m/z measured: 489.2814 [C$_{23}$H$_{41}$N$_2$O$_9$]$^+$, **m/z calculated:** 489.2833

R$_f$: 0.66 (Hexane/EtOAc 2:3).

### 5.5.1.6 DUPA-Aoc-Phe-Phe-NH(CH$_2$)$_2$NH$_3^+$·TFA (DUPA-Pep) (o)

Solid phase peptide synthesis was performed on the 1,2-diaminoethane preloaded trityl resin (Novabiochem, cat. nr. 856084) in syringes equipped with polytetrafluoroethylene (PTFE) frites.

Washings after couplings and deprotections (pro 1 mL of resin): *N,N*-dimethylformamide (DMF, 3 × 5 mL), isopropanol (*i*PrOH, 3 × 5 mL), DMF (3 × 5 mL).

Coupling: diisopropylcarbodiimide (DIC, 4 eq) was added to a stirred ice-cold solution of the *N*-Fmoc protected amino acid (4 eq) and hydroxybenzotriazole (HOBt, 4 eq) in DMF (4 mL/mL of resin). After 2 min, the solution was added to the deprotected and DMF-preswollen peptidyl resin and the mixture was gently shaken for 3 h. As in case of peptide synthesis on the diamines preloaded trityl resins, the coupling efficiency could not be exactly assessed by the Kaiser test, as it was not carried out. For attachment of the *N*-terminal urea unit, 2-[3-(1,3-bis-*tert*-butoxycarbonyl-propyl)-ureido]pentanedioic acid 1-*tert*-butyl ester [DUPA(O*t*Bu)$_3$-OH], a double coupling with 1,5-fold excess of the DUPA(O*t*Bu)$_3$ was used.

Fmoc-Deprotection: A solution of DMF/piperidine (4:1) was added to the Fmoc-protected peptidyl resin and the mixture was shaken for 1 min. Thereafter, the resin was drained, a fresh solution of DMF/piperidine (4:1) was added to the resin and shaking was continued for a further 2 min. Finally, the resin was drained, a fresh solution of DMF/piperidine (4:1) was added to the resin and shaking was continued for a further 18 min.

Cleavage from resin and removal of *t*-Bu-groups: After the final coupling the peptidyl resin was additionally washed with dichloromethane (DCM, × 3), drained and treated with trifluoroacetic acid/triisopropylsilane/water (TFA/TIS/H$_2$O, 95/2.5/2.5) for 1 min (3 × 5 mL/mL of resin). The combined TFA fractions were incubated at ambient temperature for 45 min and concentrated under reduced pressure at the bath temperature < 30 °C. The residue was dissolved in TFA (10 mL/mL resin) and incubated at ambient temperature for further 3 h. The mixture was concentrated under reduced pressure at the bath temperature < 30 °C and the residue was carefully triturated first with Et$_2$O and, thereafter, with EtOAc to give the crude depsipeptide which was further purified as a colorless solid by preparative HPLC using reversed phase column with eluents of 29% MeCN in H$_2$O (0.1% TFA) at a flow rate of 9 mL/min with detection under UV and after lyophilization DUPA-Pep (%yield: 56–67%) was obtained as white solid.
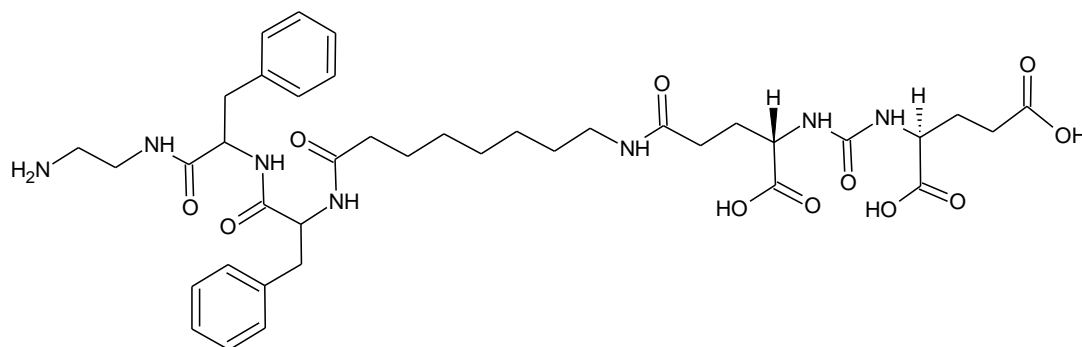
(o)

Analytic HPLC:

Column: Nucleosil-100-5 C18 HD (4.6 mm × 250 mm, Macherey-Nagel); Gradient: 0–15 min – 29% MeCN (0.1% TFA), 15–18 min – 29 to 99% MeCN (0.1% TFA), 18–25 min – 99% MeCN (0.1% TFA); Flow rate: 1.2 mL/min; Detection: UV: λ = 210, 254 nm; R_t = 6.5 min; Purity > 98%.

MS-EI (70 eV):

Positive mode m/z: 798.4 [M+H]$^+$, **Negative mode m/z:** 796.4 [M-H]$^+$.

HRMS (EI) m/z measured: 798.4028 [$C_{39}H_{56}N_7O_{11}$]$^+$, **m/z calculated:** 798.4032; **m/z measured:** 796.3883 [$C_{39}H_{54}N_7O_{11}$]$^-$, **m/z calculated:** 796.3887

5.5.1.7 *DUPA-Aoc-Phe-Phe-NH(CH₂)₂NH₂-6-F-Nic (p)*

2,3,5,6-tetrafluorophenyl 6-fluoronicotinate (4.8 mg, 16.45 µmol) was added to a solution of DUPA-Pep (5.14 mg, 5.64 µmol) in 0.15 M sodium bicarbonate (NaHCO₃, 400 µL; pH = 8.30) and acetonitrile (MeCN, 500 µL). The resulting colorless solution was incubated at ambient temperature for 3 h. The reaction was quenched by addition of TFA (40 µL) and the product **(p)** (4.0 mg, 77%) was isolated as a colorless solid by semipreparative HPLC using gradient elution at a flow rate of 1.2 mL/min with detection under UV.
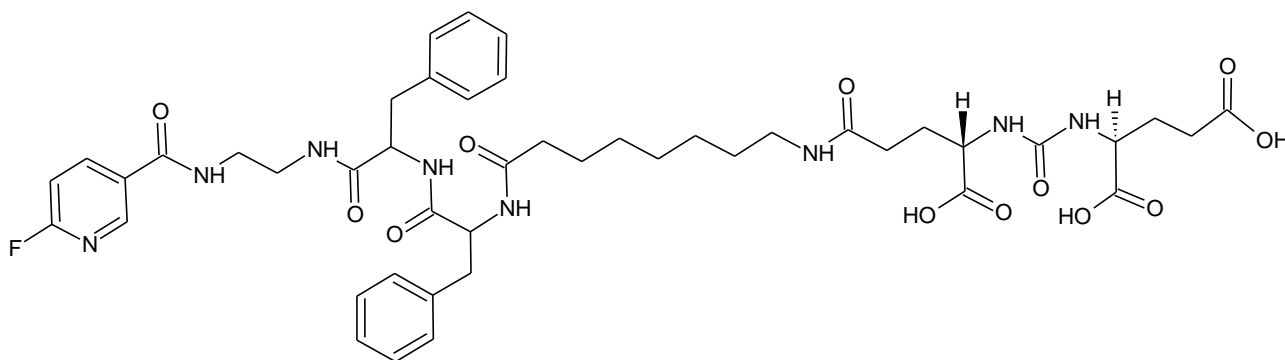
(p)

Analytic HPLC:

Column: Nucleosil-100-5 C18 HD (4.6 mm × 250 mm, Macherey-Nagel); Gradient: 0–1 min – 25% MeCN (0.1% TFA), 1–18 min – 25 to 75% MeCN (0.1% TFA), 18–24 min – 75% MeCN (0.1% TFA); Flow rate: 1.2 mL/min; Detection: UV: λ = 210, 220, 254, 280 nm; R_t = 8-10 min; Purity > 98%.

MS-EI (70 eV):

Positive mode m/z: 943.4 [M+Na]$^+$, 921.4 [M+H]$^+$.

HRMS (EI) m/z measured: 943.3970 [$C_{45}H_{57}FN_8O_{12}Na$]$^+$, m/z **calculated:** 943.3972; m/z measured: 921.4151 [$C_{45}H_{58}FN_8O_{12}$]$^+$, m/z calculated: 921.4153.

5.5.2 Radiosynthesis

Radiosynthesis for [^{18}F]FPyDUPA-Pep is shown in Fig 5.3 and is described as below.

5.5.2.1 [^{18}F]FPy-TFP

The activity (800±1.1 MBq) was introduced into a 5 mL sealed vial containing 2 mg KHCO$_3$ and 2 mg kryptofix-222. The [^{18}F] fluoride solution was dried for 10 min under a mild stream of argon (ca. 2 mL/min) at 140°C by azeotropic distillation with acetonitrile (2 x 0.8 mL). Then, the reaction vial containing the [^{18}F]KF-K222 complex was put in ice-cold water to lower down its temperature to 20°C and afterwards, 8 mg of precursor **(k)** dissolved in 1 mL of MeCN/tBuOH (1:4) was added. Labelling reaction was performed at 40°C. After 10 min, reaction mixture was quenched by addition of few drops of TFA till pH 4 was obtained. Reaction mixture was diluted with water up to 20 mL was passed through the combination of two preconditioned oasis cartridges (Oasis MCX Plus, extraction cartridge, Sep-Pak$^©$, Waters). Product was eluted using 2.1 mL of 65% MeCN.

5.5.2.2 [^{18}F]FPy-DUPA-Pep

Product fraction was passed through two preconditioned Strata-x cartridges (33µ, polymeric reversed phase, 30 mg/ mL, Phenomenex) and product was eluted by 500 µL of 80% MeCN directly into a vial containing 1 mg of peptide, 5.5 mg NaHCO$_3$, and 300 µL of water. Coupling reaction was carried out at 60°C for 10 min. Afterwards, 800 µL of reaction mixture were injected into HPLC (P680 Dionex) equipped with NaI (TI)-scintillation detector (GABI, Raytest, Gemany) and coupled with a UV detector (GY-400, 254 nm). Reversed-phase preparative column (Phenomenex Luna, 5 µ, C18, 250 x 10 mm) was used. Isocratic analysis was carried out by using 28% MeCN as mobile phase at a flow rate of 6.5 mL/min for 10 min. Peak of labelled peptide (6.5 min) was collected from system and was passed through preconditioned Strata-X cartridge after diluting it up to 40 mL with water. [^{18}F]-labelled peptide was eluted by 200 µL of EtOH. [^{18}F]FPy-DUPA-Pep (380±1 MBq, 48±0.9% RCY, decay uncorrected) was obtained with purity of > 98%.

5.5.2.3 Radio-TLC Analysis

Samples (5 µL) were withdrawn 10, 15 and 20 min directly from reaction reaction for radio-TLC analysis of [^{18}F]FPy-TFP. Silica gel plates were used as stationary phase and PE/EtOAc (7:1) was used as mobile phase. Standard spot was visualized under UV-lamp (254 nm) and was marked by radioactive spot. Quantitative assay of radioactive spots was carried out by phosphor imager (Raytest, FLA3000). The R$_f$ value of [^{18}F]FPy-TFP was found to be 0.6.

5.5.2.4 Radio-HPLC Analysis

Analytical assay by high pressure liquid chromatography (HPLC) was performed using gradient elution of solvent A (water with 0.1%TFA) and solvent B (MeCN with 0.1%TFA), started with 90% of solvent A at 1 min, then went down to 20% of solvent A at 14 min and continued with

20% of solvent A till 20 min at a flow rate of 1.5 mL/min. Column so used for analytical purpose and quality control was reversed-phase column (Phenomenex Luna, 5 μ, C18, 250 x 4.6 mm). The R_t values for [^{18}F]FPy-TFP and [^{18}F]FPy-DUPA-Pep are 15.7 min and 10.3 min, respectively.

Product fractions comprising of [^{18}F]FPy-TFP and [^{18}F]FPy-DUPA-Pep were collected from HPLC and were measured by a γ-counter. The RCYs were calculated by relating the radioactivity of the product peak to the amount of the radioactivity injected into HPLC.
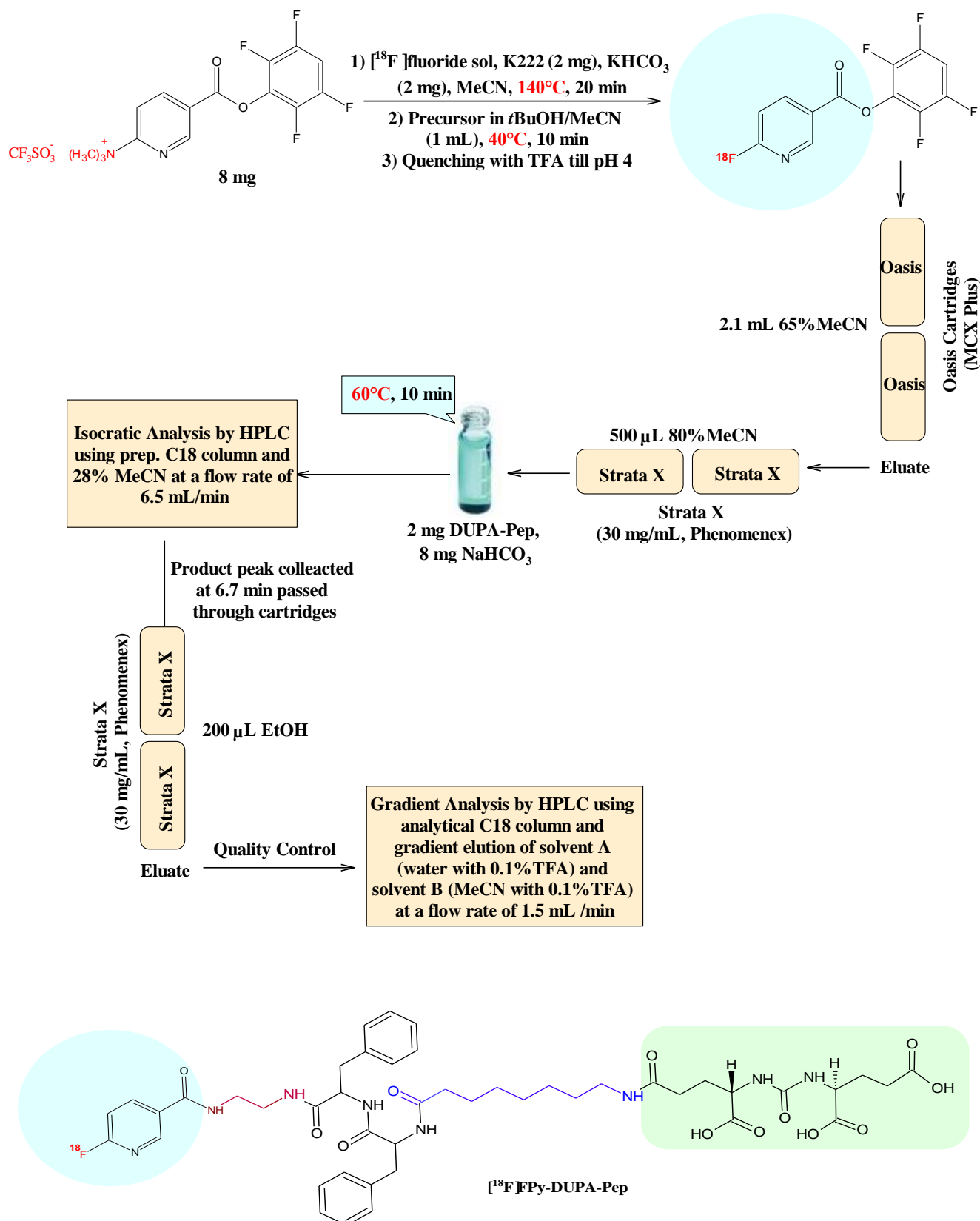
Fig 5.3 Radiosynthesis of [¹⁸F]FPy-DUPA-Pep: A new PSMA targeting ligand

6. REFERENCES

1. Christiansen I.A, Hevesy G, Lomholt S. Radiochemical method of studying the circulation of bismuth in the body. *C.A.Acad.Sci.*, *Paris*, 1924; 178: 1324-1326.

2. Pichler B.J, Kolb A, Nägele T, and Schlemmer H-P. PET/MRI: Paving the way for the next generation of clinical multimodality imaging applications. *J.Nucl.Med.*, 2010; 51 (3): 333-336.

3. Qaim S.M. Nuclear data relevant to the production and application of diagnostic radionuclides. *Radiochim.Acta*, 2001; 89: 223-232.

4. Coenen H.H. Radiopharmazeutische Chemie: Grundlagen zur in vivo Untersuchung molekularer Vorgänge mit PET. *Der Nuklearmediziner*, 1994; 17: 203-214.

5. Ache H.J. Chemistry of the positron and of positronium. *Angew.Chem.*, 1972; 11 (3): 179-199.

6. Miller P.W, Long N.J, Vilar R, and Gee A.D. Synthesis of ^{11}C, ^{18}F, ^{15}O, and ^{13}N radiolabels for poritron emission tomography. *Angew.Chem.Int.Ed.*, 2008; 47: 8998-9033.

7. Elsinga P.H. Radiopharmaceutical chemistry for positron emission tomography. *Methods*, 2002; 27 (13):208-217.

8. Ganguly B.N, Mondal N.N, Nandy M, and Roesch F. Some physical aspects of positron annihilation tomography: A critical review. *J.Radioanal.Chem.*, 2009; 279 (2): 685-698.

9. Van D.M.E, Rehemtulla A, Ross B.D. PET and SPECT imaging of tumor biology: new approaches towards oncology drug discovery and development. *Current Computer-Aided Drug Design*, 2008; 4 (1): 46-53.

10. Machulla H-J. Basics of radiopharmacy. *Lectures in radiopharmacy*, 2010.

11. Judenhofer M.S, Wehrl H.F, Newport D.F, Catana C, Siegel S.B, Becker M., Thielscher A, Kneilling M, Lichy M.P, Eichner M., Klingel K, Reischl G, Widmaier S, Roecken M, Nutt R.E, Machulla H-J, Uludag K, Cherry S.R, Claussen C.D, and Pichler B.J. Simultaneous PET-MRI: a new approach for functional and morphological imaging. *Nat.Med.* (New York, NY, U.S.), 2008; 14 (4): 459-465.

12. Bars D.L. Fluorine-18 and medical imaging: radiopharmaceuticals for positron emission tomography. *J.Fluor.Chem.*, 2006; 127 (11): 1488-1493.

13. McQuade P, McCarthy D.W, and Welch M.J. Metal radionuclides for PET imaging. *Positron Emission Tomography*, 2005; 237-250: DOI: 10.1007/1-84628-007-9_11

14. Vallabhajosula S. ^{18}F-Labeled Positron Emission Tomographic Radiopharmaceuticals in Oncology: An Overview of Radiochemistry and Mechanisms of Tumor Localization. *Semin.Nucl.Med.*, 2007; 37 (6): 400-419.

15. Cai L, Lu S, and Pike V.W. Chemistry with [18F]fluoride Ion. *Eur.J.Org.Chem.*, 2008; 2008 (17): 2853-2873.

16. Machulla H-J. PET-Diagnostika in der Onkologie. *Pharm.Unserer Zeit*, 2005; 34 (6): 490-497.

17. Gallagher B.M, Fowler J.S, Gutterson N.I, McGregor R.R, Wan C.N, and Wolf A.P. Metabolic trapping as a principle of radiopharmaceutical design– some factors responsible for biodistribution of [18F]2-deoxy-2-fluoro-dglucose. *J.Nucl.Med.*, 1978; 19 (10):1154–1161.

18. Reivich M, Kuhl D, Wolf A, Greenberg J, Phelps M, Ido T, Casella V, Fowler J, Hoffman E, Alavi A, Som P, and Sokoloff L. The [18F]fluorodeoxyglucose method for the measurement of local cerebral glucose-utilization in man. *Circ.Res.*, 1979; 44 (1):127–137.

19. Levy S, Elmaleh D.R, and Livni E. A new method using anhydrous [18F]fluoride to radiolabel 2-[18F]fluoro-2-deoxy-D-glucose. *J.Nucl.Med.*, 1982; 23 (10): 918-922.

20. Ehrenkaufer R.E, Potocki J.F, and Jewett D.M. Simple synthesis of F-18-labelled 2-fluoro-2-deoxy-D-glucose: concise communication. *J.Nucl.Med.*, 1984; 25 (3): 333-337.

21. Namavari M, Bishop A, Satyamurthy N, Bida G, and Barrio J.R. Regioselective radiofluorodestannylation with [18F]F₂ and [18F]CH₃COOF: a high yield synthesis of 6-[18F]fluoro-L-DOPA. *Appl.Radiat.Isot.*, 1992; 43 (8): 989–996.

22. Lemaire C, Damhaut P, Plenevaux A, and Comar D. Enantioselective synthesis of 6-[Fluorine-18]-fluoro-L-DOPA from no-carrier-added fluorine-18-fluoride. *J.Nucl.Med.*, 1994; 35 (12): 1996–2002.

23. Wester H-J, Herz M, Weber W, Heiss P, Senekowitsch-Schmidtke R, Schwaiger M, and Stöcklin G. Synthesis and radiopharmacology of *O*-(2-[18F]fluoroethyl)-L-tyrosine for tumor imaging. *J.Nucl.Med.*, 1999; 40 (1): 205–212.

24. Mineura K, Kowada M, and Shishido F. Brain tumor imaging with synthesized [18F]fluorophenylalanine and positron emission tomography. *Surg.Neurol.*, 1989; 31(6): 468-469.

25. Hamacher K, and Coenen H.H. Efficient routine production of the [18F]labelled amino acid O-(2-[18F]fluoroehtyl)-L-tyrosine. *Appl.Radiat.Isot.*, 2002; 57 (6): 853–856.

26. Couturier O, Luxen A, Chatal J-F, Vuillez J-P, Rigo P, and Hustinx R. Fluorinated tracers for imaging cancer with positron emission tomography. *Eur.J.Nucl.Med.Mol.Imaging.*, 2004; 31 (8): 1182–1206.

27. Shiue C-Y, Watanabe M, Wolf A.P, Fowler J.S, and Salvadori P. Application of the nucleophilic substitution reaction to the synthesis of no-carrieradded [18F]fluorobenzene and other 18F-labelled aryl fluorides. *J.Label.Compd.Radiopharm.*, 1984; 21 (6): 533–547.

28. Morrish P.K, Rakshi J.S, Bailey D.L, Sawle G.V, and Brooks D.J. Measuring the rate of progression and estimating the preclinical period of Parkinson's disease with [18F]DOPA PET. *J.Neurol .Neurosurg.Psychiatry*, 1998; 64 (3): 314–319.

29. Hess E, Sichler S, Kluge A, and Coenen H.H. Synthesis of 2-[18F]fluoro-L-tyrosine via regiospecific fluoro-de-stannylation. *Appl.Radiat.Isot.*, 2002; 57 (2): 185-191.

30. Wienhard K, Herholz K, Coenen H, Rudolf J, Kling P, Stöcklin G, and Heiss W-D. Increased amino acid transport into brain tumors measured by PET of L-2-[18F]fluorotyrosine. *J.Nucl.Med.*, 1991; 32 (7): 1338-1346.

31. Murakami M, Takahashi K, Kondo Y, Mizusawa S, Nakamichi H, Sasaki H, Hagami E, Iida H, Kanno I, Miura S, and Uemura K. 2-[18F]phenylalanine and 3-[18F]-tyrosine — synthesis and preliminary data of tracer kinetics. *J.Label.Comp.Radiopharm.*, 1988; 25 (7): 773–782.

32. Tang G, Wang M, Tang X, Luo L, and Gan M. Pharmacokinetics and radiation dosimetry estimation of *O*-(2-[18F]fluoroethyl)-L-tyrosine as oncologic PET tracer. *Appl.Radiat.Isot.*, 2003; 58 (2): 219–225.

33. Dejesus O.T, Murali D, Kitchen R, Endres C, Oakes T.R, Shelton S.E, Freund L, Houser D, Uno H, Holden JE, and Nickles R.J. Evaluation of 3-[18F]fluoro-α-fluoromethyl-*p*-tyrosine as a tracer for striatal tyrosine hydroxylase activity. *Nucl.Med.Biology*, 1994; 21 (4), 663-667.

34. Weber W.A, Wester H-J, Grosu A.L, Herz M, Dzewas B, Feldmann H-J, Molls M, Stöcklin and G, Schwaiger M. *O*-(2-[18F]fluoroethyl)-L-tyrosine and L-[methyl-11C]methionine uptake

in brain tumours: initial results of a comparative study. *Eur.J.Nucl.Med.*, 2000; 27 (5): 542-549.

35. Hideomi W, Tomio I, Tetsuya S, Takashi Y, Adel R.A, Katsumi T, Noboru O, Mari T, Jun A, Keigo E, and Kenji T. PET imaging of musculoskeletal tumours with fluorine-18 α-methyltyrosine: comparison with fluorine-18 fluorodeoxyglucose PET. *Eur.J.Nucl.Med.*, 2000; 27 (10):1509-1517.

36. Qaim S.M, Clark J.C, Crouzel C, Guillaume M, Helmeke H-J, Nebeling B, Pike V.W, and Stöcklin G. PET radionuclide production. *Radiopharmaceuticals for Positron Emission Tomography, Methodological Aspects,* 1993; 1-43; Ed: Stöcklin G, and Pike V.W; Publ: Kluwer Academic, Dordrecht.

37. Hess E, Blessing G, Coenen H.H, and Qaim S.M. Improved target system for production of high purity [^{18}F]fluorine via the ^{18}O(p,n)^{18}F reaction. *Appl.Radiat.Isot.*, 2000; 52 (6): 1431–1440.

38. Hess E, Takács S, Scholten B, Tárkányi F, Coenen H.H, and Qaim S.M. Excitation function of the ^{18}O(p,n)^{18}F nuclear reaction from threshold up to 30 MeV. *Radiochim.Acta*, 2001; 89 (6): 357–362.

39. Bergman J, and Solin O. Fluorine-18-labelled fluorine gas for synthesis of tracer molecules. *Nucl.Med.Biol.*, 1997; 24 (7):677–683.

40. Kim D.W, Jeong H-J, Lim S.T, Sohn M-H, A. Katzenellenbogen J, and Chi D.Y. Facile nucleophilic fluorination reactions using *tert*-alcohols as a reaction medium: significantly enhanced reactivity of alkali metal fluorides and improved selectivity. *J.Org.Chem.*, 2008; 73 (3): 957–962.

41. Kim H.W, Jeong J.M, Lee Y-S, Chi D.Y, Chung K-H, Lee D.S, Chung J-K, and Lee M.C. Rapid synthesis of [^{18}F]FDG without an evaporation step using an ionic liquid. *Appl.Radiat.Isot.*, 2004; 61 (6): 1241–1246.

42. Lee S.J, Oh S.J, Chi D.Y, Lee B.S, Ryu J.S, and Moon D.H. Comparison of synthesis yields of 3'-deoxy-3'-[^{18}F]fluorothymidine by nucleophilic fluorination in various alcohol solvents. *J.Label.Compd.Radiopharm.*, 2008; 51 (1): 80–82.

43. Shen B, Löffler D, Zeller K-P, Übele M, Reischl G, and Machulla H-J. Decarbonylation of multi-substituted [^{18}F]benzaldehydes for modelling syntheses of ^{18}F-labelled aromatic amino acids. *Appl.Radiat.Isot.*, 2007; 65, (11):1227-1231.

44. Shen B, Löffler D, Übele M, Reischl G, Zeller K-P, and Machulla H-J. Decarbonylation of highly substituted model compounds aiming at direct nucleophilic ^{18}F-labelling of [18F]FDOPA. *J.Nucl.Med..,* 2007; 48 (Suppl-2): 317P.

45. Shen B, Löffler D, Reischl G, Machulla H-J, and Zeller K-P. Nucleophilic substitution of nitro groups by [18F]fluoride in methoxy-substituted *ortho*-nitrobenzaldehydes—A systematic study. *J.Fluor.Chem.*, 2009; 130 (2): 216-224.

46. Guo N, Alagille D, Tamagnan G, Price R.R, and Baldwin R.M. Microwave-induced nucleophilic [18F]fluorination on aromatic rings: Synthesis and effect of halogen on [18F]fluoride substitution of *meta*-halo (F, Cl, Br, I)-benzonitrile derivatives. *Appl.Radiat.Isot.*, 2008; 66 (10): 1396-1402.

47. Ndiokwere C.L. Fluorine-18 labelling of *ortho*-fluorohippuric acid by isotope exchange reaction. *J.Label.Compd.Radiopharm.*, 1978; 14 (5): 705–712.

48. Baptista M.J.V.de O, and Widdowson D.A. The relative nucleophilicities of fluoride and aryloxy ions towards acyl and nitroaryl groups. *J.Chem.Soc.Perkin 1*, 1978; 1978 (3): 295-298.

49. Cacace F, Speranza M, Wolf A.P, and Fowler J.S. Labelling of fluorinated aromatics by isotopic exchange with [18F]fluoride. *J.Labelled.Compd.Radiopharm.*, 1981; 18 (12): 1721-1730.

50. Tsuji J, and Ohno K. Decarboylation reactions using transition metal compounds. *Synthesis*, 1969; 1969 (04): 157-169.

51. Pike V.W, and Aigbirhio F.I. Reactions of [18F]fluoride with aryliodonium salts – a novel route to no-carrier-added aryl [18F]fluorides. *J.Label.Compd.Radiopharm*, 1995; 37: 120–122.

52. Gail R, Hocke C, and Coenen H.H. Direct n.c.a. ^{18}F-fluorination of halo and alkylarenes via corresponding diphenyliodonium salts. *J.Label.Compd.Radiopharm.*, 1997; 40 (1): 50–52.

53. Wust F.R, and Kniess T. Synthesis of 4-[18F]fluoroiodobenzene and its application in sonogashira cross-coupling reactions. *J.Label.Compd.Radiopharm.*, 2003; 46 (8): 699–713.

54. Ross T.L, Ermert J, Hocke C, and Coenen H.H. Nucleophilic [18F]-fluorination of heteroaromatic iodonium salts with no-carrier-added [18F]fluoride. *J.Am.Chem.Soc.*, 2007; 129 (25): 8018–8025.

55. Shen B, Löffler D, Reischl G, Machulla H-J, Zeller K-P. Nucleophilic substitution of nitro groups by [¹⁸F]fluoride in methoxy-substituted ortho-nitrobenzaldehydes - A systematic study. *J.Fluor.Chem.*, 2009; 130 (2): 216-224.

56. Irie T, Fukushi K, and Ido T. Synthesis of ¹⁸F-6-fluoropurine and ¹⁸F-6- fluoro-9-ß-D-ribofuranosylpurine. *Int.J.Appl.Radiat.Isot.*, 1982; 33 (6): 445–448.

57. Knust E.J, Müller-Platz C, and Schüller M. Synthesis, quality control and tissue distribution of 2-[¹⁸F]-nicotinic acid diethylamide, a potential agent for regional cerebral function studies. *J.Radioanal.Chem.*, 1982; 74 (1-2): 283–291.

58. Dollé F. Fluorine-18-labelled fluoropyridines: advances in radiopharmaceutical design. *Current Pharmaceutical Design*, 2005; 11 (25): 3221–3235.

59. Dolci L, Dollé F, Jubeau S, Vaufrey F, and Crouzel C. 2-[¹⁸F]fluoropyridines by no-carrier-added nucleophilic aromatic substitution with [¹⁸F]FK-K222- a comparative study. *J.Label.Compd.Radiopharm.*, 1999; 42 (10): 975-985.

60. Carroll M.A, Nairne J, and Woodcraft J.L. Diaryliodonium salts: a solution to 3-[¹⁸F]fluoropyridine. *J.Label.Compd.Radiopharm.*, 2007; 50 (5-6): 452–454.

61. Shai Y, Kirk K.L, Channing M.A, Dunn B.B, Lesniak M.A, Eastman R.C, Finn R.D, Roth J, and Jacobson K.A. ¹⁸F-labelled insulin: A prosthetic group methodology for incorporation of a positron emitter into peptides and proteins. *Biochem.*, 1989; 28 (11): 4801–4806.

62. Coenen H.H. Fluorine-18 labeling methods: Features and possibilities of basic reactions. *Ernst.Schering.Res.Found.Workshop.*, 2007; (62): 15-50.

63. Krohn K.A, Link .M, and Mason R.P. Molecular Imaging of Hypoxia. *J.Nucl.Med.*, 2008; 49 (Suppl-2):129S–148S.

64. Chapman J.D. Hypoxic sensitizers: implications for radiation therapy. *N.Engl.J.Med.*, 1979; 301: 1429-1432.

65. Chapman J.D, Franko A.J, Sharplin J. A marker for hypoxic cells in tumours with potential clinical applicability. Br.J.Cancer., 1981; 43: 546–550.

66. Rasey J.S, Martin G.V, Krohn K.A. Quantifying hypoxia with radiolabeled fluoromisonidazole: pre-clinical and clinical studies. in: Machulla H-J, ed. The Imaging of Hypoxia. *Dordrecht, The Netherlands: Kluwer Academic Publishers;* 1999 Vol. 33: 85-117.

67. Reischl G, Ehrlichman W, Bieg C, Solbach C, Kumar P, Wiebe L.I, and Machulla H-J. Preparation of the hypoxia imaging PET tracer [^{18}F]FAZA: reaction parameters and automation. *Appl.Radiat.Isot.*, 2005; 62 (6): 897-701.

68. Reischl G, Sabbah A, and Machulla H-J. [^{18}F]FAZA and [^{18}F]FMISO: In vitro comparison in hypoxic human tumor cells. *J.Nucl.Med.*, 2007; 48 (Supplement 2): 325P.

69. Jain-Vakkalagadda B, Dey S, Pal D, and Mitra A.K. Identification and functional characterization of a Na$^+$-independent large neutral amino acid transporter, LAT1, in human and rabbit cornea. *Investigative Ophthalmology and Visual Science*, 2003; 44 (7): 2919-2927.

70. Meier C, Ristic Z, Klauser S, and Verrey F. Activation of system L heterodimeric amino acid exchangers by intracellular substrates. *The EMBO Journal*, 2002; 21 (4): 580-589.

71. Rajasekaran, A.K, Anilkumar G, and Christiansen J.J. Is prostate-specific membrane antigen a multifunctional protein? *Am.J.Physiol.Cell.Physiol.*, 2005; 288 (5): 975-981.

72. Ikeda M, Ochi R, Wada A, Hamachi I. Supramolecular hydrogel capsule showing prostate specific antigen-responsive function for sensing and targeting prostate cancer cells. *Chem.Sci.*, 2010; 1: 491-498.

73. Kularatne A.S, Zhou Z, Yang J, Post C.B, and Low P.S. Design, synthesis, and preclinical evaluation of prostate-specific membrane antigen targeted ^{99m}Tc-radioimaging agents. *Mol.Pharmaceutics*, 2009; 6 (3): 790–800.

74. Kularatne S.A, Wang K, Santhapuram H-K.R, and Low P.S. Prostate-specific membrane antigen targeted imaging and therapy of prostate cancer using a PSMA inhibitor as a homing ligand. *Mol.Pharmaceutics*, 2009; 6 (3): 780–789.

75. Tang G, Zeng W, Yu M, and Kabalka G. Facile synthesis of *N*-succinimidyl 4-[^{18}F]fluorobenzoate [^{18}F]SFB for protein labelling. *J.Label.Compd.Radiopharm.*, 2008; 51 (1): 68-71.

76. Glaser M, Årstad E, Luthra S.K, and Robins E.G. Two-step radiosynthesis of [^{18}F]-*N*-succinimidyl-4-fluorobenzoate ([^{18}F]SFB). *J.Label.Compd.Radiopharm.*, 2009; 52 (8): 327–330.

77. Scott P.J.H, and Shao X. Fully automated, high yielding production of *N*-succinimidyl 4-[^{18}F]fluorobenzoate ([^{18}F]SFB), and its use in microwave-enhanced radiochemical coupling reactions. *J.Label.Compd.Radiopharm.*, 2010; 53 (9): 586–591.

78. Laverman P, McBride W.J, Sharkey R.M, Eek A, Joosten L, Oyen W.J, Goldenberg D.M, and Boerman O.C. A novel facile method of labelling octreotide with ^{18}F-fluorine. *J.Nucl.Med.*, 2010; 51 (3): 454-61.

79. Becaud J, Mu L, Karramkam M, Schubiger P.A, Ametamey S.M, Graham K, Stellfeld T, Lehmann L, Borkowski S, Berndorff D, Dinkelborg L, Srinivasan A, Smits R, Koksch B. Direct one-step ^{18}F-labeling of peptides via nucleophilic aromatic substitution. *Bioconj.Chem.*, 2009; 20 (12): 2254-2261.

80. Olberg D.E, Arukwe J.M, Grace D, Hjelstuen O.K, Solbakken M, Kindberg G.M, and Cuthbertson A. One step radiosynthesis of 6-[^{18}F]fluoronicotinic acid 2,3,5,6-tetrafluorophenyl ester ([^{18}F]F-Py-TFP): a new prosthetic group for efficient labelling of biomolecules with fluorine-18. *J.Med.Chem.*, 2010; 53 (4): 1732–1740.

81. Leo A, Hansch C, and Elkins D. Partition coefficients and their uses. *Chem.Rev.*, 1971; 71 (6): 525–616.

82. ACD/LogP Freeware. http://www.acdlabs.com/resources/freeware/chemsketch/logp/

83. Ishiwata K, Monma M, Iwata R, and Ido T. Automated photosynthesis of ^{11}C-glucose. *J.Label.Compd.Radiopharm.*, 1982; 19 (11-12): 1347-1349.

84. Padgett H.C, Barrio J.R, MacDonald N.S, and Phelps M.E. The unit operations approach applied to the synthesis of [1-^{11}C]-2-deoxy-D-glucose for routine clinical applications. *J.Nucl.Med.*, 1982; 23 (8): 739-744.

85. Ido T, Iwata R. Fully automated synthesis of [13]NH$_3$. *J.Label.Compd.Radiopharm.*, 1981; 18 (1-2): 244-246.

86. Suzuki K, Tamate K, Nakayama T, Yamazaki T, Kasida Y, Fukushi K, Maruyama Y, Maekawa H, and Nakaoko H. Development of an equipment for the automatic production of [13]NH$_3$ and L-(^{13}N)- glutamate. *J.Label.Compd.Radiopharm.*, 1982; 19 (11-12): 1374-1375.

87. Blessing G, Coenen H.H, Hennes M, and Lipperts H. A computer-controlled automatic apparatus for radiochemical separation of [75]Br and synthesis of [75]Br-labelled radiopharmaceuticals. *J.Label.Compd.Radiopharm.*, 1982; 19 (11-12): 1333-1335.

88. Hamacher K, Coenen H.H, and Stöckling G. Efficient stereospecific synthesis of no-carrier-added 2-[^{18}F]-fluoro-2-deoxy-D-glucose using amino polyether supported nucleophilic substitution. *J.Nucl.Med.*, 1986; 27 (2): 235-238.

89. Kilbourn M.R, Hood J.T, and Welch M..J. A simple ^{18}O water target for ^{18}F production. *Int.J.Appl.Radiat.Isot.*, 1984; 35 (7): 599-602.

90. Vries E.F.J.de , Luurtsema G, Brüssermann M, Elsinga P.H, and Vaalburg W. Fully automated synthesis module for the high yield one-pot preparation of 6-[^{18}F]fluoro-L-DOPA. *Appl.Radiat.Isot.*, 1999; 51 (4): 389-394.

91. Krasikova R, Fedorova O, Korsakov M, Nagren K, Maziere B, and Halldin C. A fast and convenient method for robotic preparation of [11C]flumazenil avoiding HPLC purification. *Appl.Radiat.Isot.*, 2000; 43: 613-621.

92. Crouzel C., Clark J.C, Brihaye C, Langstrom B, Lamaire C, Meyer G.J, Nebeling B, and Stone-Elander S. Radiochemistry automation for PET. In *Radiopharmaceuticals for Positron Emission Tomography Methodological Aspects*, 1993; 45-89; Ed: Stöcklin G, and Pike V.W; Publ: Kluwer Academic, Dordrecht.

93. Palmer B.M, and Sajjad M, Rottenberg D.A. An automated [^{15}O]H$_2$O production and injection system for PET imaging. *Nucl.Med.Biol.*, 1995; 22 (2): 241-249.

94. Plascjak P.S, Kim K, Meyer Jr W, Divel J, Der M and Eckelman W.C. An automated radiopharmaceutical dispenser. *Appl.Radiat.Isot.*, 1997; 48 (3): 345-348.

95. Dembowski B, and Gonzalez-Lepera C. Control of radioactive material pneumatic transport system using an inexpensive programmable logic controller. *In Proceeding of the 5th workshop on target and Target Chemistry,* 1994; 323-329.

96. Jewwet D.M, and Kilbourn M.R. High performance extraction disks for the preparation of a PET agent: a fast synthesis of [^{11}C]carfentanil. *J.Label.Compd.Radiopharm.*, 1999; 42: S873-S874.

97. Shen B. Dissertation, 2008. Studies on the nucleophilic aromatic ^{18}F-fluorination - From model compounds to aromatic amino acids - http://tobias-lib.ub.uni-tuebingen.de/volltexte/2008/3666/pdf/doktorarbeit_final_081219.pdf

98. Sun H, and DiMagno S.G. Competitive demethylation and substitution in *N,N,N*-trimethylanilinium fluorides. *J.Fluor.Chem.*, 2007; 128 (7): 806-812.

99. Al-Labadi A.G.M, 2006. Nucleophilic aromatic substitution by [^{18}F]fluoride and its applications to the synthesis of model precursors for the multi-step synthesis of the PET-tracer 6-[^{18}F]Fluoro-L-DOPA. http://tobias-lib.uni-tuebingen.de/volltexte/2006/2333/pdf/Dissertation_Al-Labadi_2006.pdf

100. Wagner F, Ermert J, and Coenen H.H. New nucleophilic three-step synthesis of 6-[^{18}F]fluoro-L-DOPA. *J.Nucl.Med.*, 2008; 49 (Suppl): 142p.

101. Tierling T, Hamacher K, and Coenen H.H. A new nucleophilic asymmetric synthesis of 6-[^{18}F]fluoro-DOPA. *J.Label.Compd.Radiopharm.*, 2001; 44 (Suppl): S146-S148.

102. Shen B, Ehrlichmann W, Übele M, Machulla H-J, and Reischl G. Automated synthesis of n.c.a. [^{18}F]FDOPA via nucleophilic aromatic substitution with [^{18}F]fluoride. *Appl Radiat Isot*, 2009; 67 (9): 1650-1653.

103. Rengan R, Chakraborty P.K, and Kilbourn M.R. Can we predict reactivity for aromatic nucleophilic substitution with [^{18}F]fluoride Ion. *J.Label.Compd.Radiopharm.*, 1993; 33 (7): 563-572.

104. Ding Y.S, Shiue C-Y, Fowler J.S, Wolf A.P, and Plenevaux A. No-carrier-added (n.c.a.) aryl [^{18}F]fluorides via the nucleophilic aromatic substitution of electron-rich aromatic rings. *J.Fluor.Chem.*, 1990; 48 (2): 189-206.

7. APPENDICES

Appendix-1: RCY at different temperatures and different times of substituted 2-nitropyridines of following pattern:
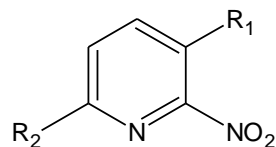
Nr.	Substituent		Temp. (°C)	n	%RCY±SD (TLC)						n	%RCY±SD (HPLC)	
	R_1	R_2			1 min	3 min	7 min	10 min	20 min	30 min		20	30
10a	-H	-H	140°C	4	69±1.2	73±0.9	76±1.1	79±0.5	83.5±3	88±1	3	90±3	-
			120°C	4	52±3	56±0.5	60±2.4	77±0.8	89±0.3	91±2.3	-	-	-
			60°C	3	3.8±1.6	19±3	52±7	65±2	79±2	80±3	-	.-	-
			30°C	3	1±0.3	13±0.5	39±1	48±0.5	59±1	63±0.8	-	-	-
11a	-CH₃	-H	140°C	5	72±2	76±1.6	84±2	87±1.5	88±1	89±1	2	-	87±3
			120°C	5	18±1	40±2	56±3	65±1.2	68±2	72±3	-	-	-
			60°C	4	4.9±0.3	11±0.6	18±0.8	32±2.4	42±1.6	51±1.4	-	-	-
			30°C	3	1±0.1	2.7±0.5	5±0.1	7.1±0.2	9.5±0.5	13±0.5	-	-	-
12a	-OCH₃	-H	140°C	5	88±1	89±1	90±0.1	90±0.3	90±0.4	91±0.4	2	-	87±1.4
			120°C	3	33±4.5	57±4.5	70±1	86±1	88.7±1	90±0.6	-	-	-
			60°C	5	14.6±3	34.5±3	70.5±3	77±1.5	83.5±4	88±2	2	-	78.5±1
			30°C	3	5±1	11±1.3	26±1.2	49±0.9	57±0.7	66±1.1	-	-	-
13a	-OCH₃	-CH₃	140°C	4	57±3	68±0.7	79±1.6	80±0.7	81±0.6	81±1	2	-	79±0.4
			120°C	5	14.4±1	48±2	78.5±1	79±1.3	80±0.6	81±0.6	-	-	-
			60°C	3	5±0.2	12±1	30±1.6	37±2	62±2	70±1	-	-	-
			30°C	3	1.6±1	2.3±0.2	5.6±0.6	7±0.3	14±1	22±1	-	-	-

Labelling conditions (for all compounds): Precursor (10 mg), DMF (1 mL), Kryptofix 222 (15 mg), 3.5 % K_2CO_3 (100 μL)

Appendix-2: RCY at different temperatures and different times of substituted 2-fluoropyridines of following pattern:
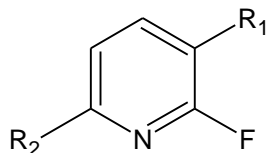
Nr.	Substituent		Temp. (°C)	n	%RCY±SD (TLC)						n	%RCY±SD (HPLC)	
	R_1	R_2			1 min	3 min	7 min	10 min	20 min	30 min		20	30
10b	**-H**	**-H**	140°C	4	-	-	-	-	83±1.5	-	4	90±2	-
			120°C	4	7±2	43±3	59±2	63±3	68±0.8	71±2	-	-	-
			60°C	3	1±0.3	3±0.3	4±0.4	9±0.3	13±0.8	19±1.6	-	.-	-
11b	**-CH₃**	**-H**	140°C	4	30±4	51±3	69±3.5	71±4	78±1.3	80±1	-	-	-
			120°C	3	1.9±0.1	14.5±2	36±0.3	46±1.6	56±0.4	59±2	-	-	-
12b	**-OCH₃**	**-H**	140°C	5	31±3	56±4	73±1	74±0.8	76±0	78±0.6	-	-	-
			120°C	3	1.5±0.5	6±0.5	17±1.3	22±0.5	40±4	48.5±1	-	-	-
13b	**-OCH₃**	**-CH₃**	140°C	4	10±1.5	28±1	41.5±1	46±1.6	53±1.8	55±3	-	-	-
			120°C	3	1.5±0.5	2.8±0.3	9.3±1	19±0.3	36±0.6	46±2	-	-	-
14a	**-CHO**	**-H**	140°C	3	77±1.3	70±3.5	60±3.4	48±3.5	17±3.5	8±1.5	-	-	-
			60°C	3	70±2.5	75±0.6	68±3	64±1.5	57±3	54±3	-	-	-

Labelling conditions (for all compounds): Precursor (10 mg), DMF (1 mL), Kryptofix 222 (15 mg), 3.5 % K_2CO_3 (100 μL)

Appendix-3: RCY at different temperatures and different times of substituted 2-bromopyridines of following pattern:

Labelling conditions (for all compounds): Precursor (10 mg), DMF (1 mL), Kryptofix 222 (15 mg), 3.5 % K_2CO_3 (100 µL)
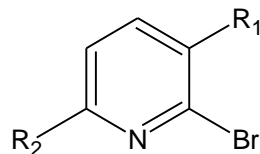
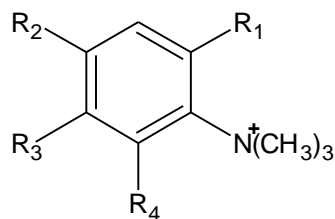| Nr.	Substituent		Temp. (°C)	n	%RCY±SD (TLC)						n	%RCY±SD (HPLC)	
	R_1	R_2			1 min	3 min	7 min	10 min	20 min	30 min		20	30
10c	-H	-H	140°C	3	-	-	-	-	56±3	-	3	66±3	-
			120°C	3	3.1±1	9±1	11±0.7	12±0.7	14±0.7	16±0.4	-	-	-
			60°C	3	0.4±0.1	0.8±0.3	2±0.4	2.6±0.2	3±0.4	3.1±0.3	-	.-	-
11c	-CH$_3$	-H	140°C	4	9±0.1	14±2.6	18.7±1	27.5±1	40±1	47±1.6	-	-	-
			120°C	3	2.2±0.4	3.5±0.3	4.7±0.1	9.9±1	15±0.6	19±0.8	-	-	-
12c	-OCH$_3$	-H	140°C	4	10±1.3	20±2	28±1	32±1	39±1.3	41±3	2	-	39±1.4
			120°C	5	2.2±0.5	6±0.5	13±1.2	16±1	24±0.8	28±1.1	-	-	-
13c	-OCH$_3$	-CH$_3$	140°C	3	3.7±0.5	7±1.6	11.5±2	12±3	14±3	20±0.6	-	-	-
			120°C	3	1.3±0.4	5±0.3	10±0.5	11±0.8	12±0.3	16.5±3	-	-	-
14b	-CHO	-H	140°C	5	81±3.6	84±4	80±3	76±2	61±3	49±3	-	-	-
			100°C	4	78±4	85±1	83.5±1	81±2	72±4	60±6	-	-	-
			60°C	3	59±3	71±3	75±2	78±1	79.5±1	76±1	-	-	-
			30°C	3	27±8	39±3	43±7	45±7	49±6	50±7	-	-	-

Appendix-4: RCY at different temperatures and different times of substituted 2-chloropyridines of following pattern:
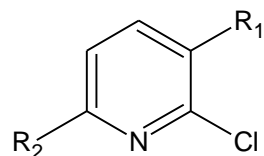
| Nr.	Substituent		Temp. (°C)	n	%RCY±SD (TLC)						n	%RCY±SD (HPLC)	
	R_1	R_2			1 min	3 min	7 min	10 min	20 min	30 min		20	30
10d	-H	-H	140°C	3	-	-	-	-	57±3	-	3	61±2	-
			120°C	3	2.3±0.2	5.2±0.2	7±0.3	8±1	12±1.5	12.4±1	-	-	-
			100°C	3	1.6±0.2	3.5±0.4	5±0.5	9±1.1	10±1.1	11±1	-	-	-
			60°C	3	0.6±0.1	1±0.4	1.3±0.4	1.7±0.1	1.9±0.1	2±0.1	-	.-	-
11d	-CH₃	-H	140°C	4	1.8±1.3	5±1	7.2±0.6	9±1	12±1	13.6±1	-	-	-
			120°C	5	3.1±2	5.1±3.5	6±2.6	7.3±3	9±3	10±3.6	-	-	-
12d	-OCH₃	-H	140°C	3	1.7±0.3	9±1.3	12±1.2	13±1	16±1.2	20±0.7	2	-	25±3
			120°C	4	1.9±0.3	3±0.5	4.5±1	5.3±0.6	12.5±2	16.5±3	-	-	-
14c	-CHO	-H	140°C	4	75±5	67±3	42±4	11±2	3.5±0.9	2±0.6	-	-	-
			100°C	3	70±2.5	63±1.5	51±2	40±2.8	3±1	1.5±0.4	-	-	-
			60°C	5	24±3	50.5±2	65±1.4	69±2.2	74±3.5	75±2.4	-	-	-
			30°C	4	8±1.5	26±3	31±6	22±3	14±3	8±2	-	-	-

Labelling conditions (for all compounds): Precursor (10 mg), DMF (1 mL), Kryptofix 222 (15 mg), 3.5 % K_2CO_3 (100 μL)

**Appendix-5: RCY (n = 3) at 140°C at different times of substituted benzenaminium salts of following pattern:**

Nr	Substituent				%RCY±SD (TLC)						%RCY±SD (HPLC)	
	R$_1$	**R$_2$**	**R$_3$**	**R$_4$**	**1 min**	**3 min**	**7 min**	**10 min**	**20 min**	**30 min**	**3 min**	**10 min**
1	**-H**	**-CHO**	**-H**	**-H**	79±1.1	80±1	86±0.9	89±0.6	82±1.2	81±1	-	88±1
2	**-CH$_3$**	**-CHO**	**-H**	**-H**	58±1.7	69±1	64±1.3	63±2	55±0.9	53±1.1	73±0.6	-
3	**-H**	**-OCH$_3$**	**-H**	**-CHO**	31±1	36±1.5	27±1.2	22±0.5	19±0.8	15±1.4	38±1.7	-
4	**-H**	**-H**	**-OCH$_3$**	**-CHO**	43±0.7	51±0.4	37±0.6	26±1.9	23±1.7	18±1	55±1	-
5	**-H**	**-OCH$_3$**	**-OCH$_3$**	**-CHO**	33±1.5	41±1.4	39±1.1	35±0.9	27±1.2	11±1	43±1.2	-
6	**-CH$_3$**	**-H**	**-H**	**-H**	0.2±0.1	1.2±1.1	0.6±0.1	0.2±0.1	0.1±0	0.0±0	-	-
7	**-CH$_3$**	**-H**	**-H**	**-CH$_3$**	0.5±0.3	1.7±1	1.4±0.4	1.3±0.5	0.4±0.1	0.3±0.2	-	-

Labelling conditions (for all compounds): Precursor (10 mg), DMF (1 mL), Kryptofix 222 (15 mg), 3.5 % K$_2$CO$_3$ (100 μL)
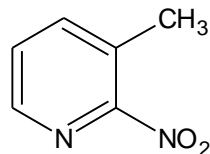
Appendix-6: ln (1-RCY) values at different times and temperatures for calculation of rate constants (k') graphically for 2-nitropyridine
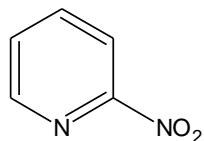
Time (min)	ln (1-RCY)			
	140°C	**120°C**	**60°C**	**30°C**
1	-1.171	-0.734	-0.039	-0.0101
3	-1.309	-0.821	-0.211	-0.139
7	-1.427	-0.916	-0.734	-0.494
10	-1.561	-1.47	-1.05	-0.654
20	-1.802	-2.207	-1.561	-0.892
30	-2.12	-2.408	-1.61	-0.994

Appendix-7: k' values at different temperatures calculated graphically for plotting against reciprocal of temperature in Arrhenius plot for 2-nitropyridine
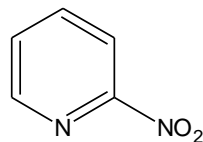
T [K]	$1/T * 10^{-3}$	k	lnk
413	2.42	0.033	-3.47
393	2.54	0.055	-2.75
333	3.00	0.064	-2.90
303	3.3	0.031	-3.41

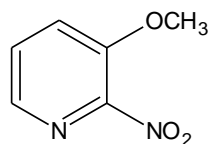**Appendix-8: ln (1-RCY) values at different times and temperatures for calculation of rate constants (k') graphically for 3-methyl-2-nitropyridine**

| Time	ln (1-RCY)			
(min)	140°C	120°C	60°C	30°C
1	-1.273	-0.1985	-0.05	-0.0101
3	-1.427	-0.511	-0.116	-0.0274
7	-1.833	-0.821	-0.1985	-0.0513
10	-2.04	-1.05	-0.386	-0.074
20	-2.12	-1.14	-0.545	-0.0998
30	-2.21	-1.273	-0.713	-0.14

Appendix-9: k' values at different temperatures calculated graphically for plotting against reciprocal of temperature in Arrhenius plot for 3-methyl-2-nitropyridine
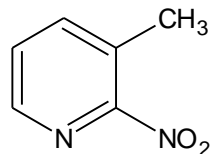
| T [K]	$1/T * 10^{-3}$	k'	lnk'
413	2.42	0.03	-3.51
393	2.54	0.032	-3.44
333	3.00	0.023	-3.77
303	3.3	0.0027	-5.91

Appendix-10: ln (1-RCY) values at different times and temperatures for calculation of rate constants (k') graphically for 3-methoxy-2-nitropyridine

Time	ln (1-RCY)			
(min)	140°C	120°C	60°C	30°C
1	-1.171	-0.734	-0.039	-0.0101
3	-1.309	-0.821	-0.211	-0.139
7	-1.427	-0.916	-0.734	-0.494
10	-1.561	-1.47	-1.05	-0.654
20	-1.802	-2.207	-1.561	-0.892
30	-2.12	-2.408	-1.61	-0.994

Appendix-11: ln (1-RCY) values at different times and temperatures for calculation of rate constants (k') graphically for 3-methoxy-2-nitropyridine
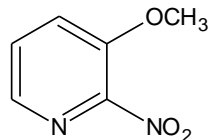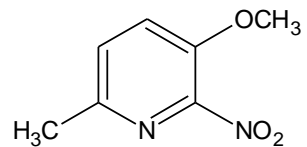

T [K]	$1 / T \, * \, 10^{-3}$	k	lnk
413	2.42	0.033	-3.47
393	2.54	0.055	-2.75
333	3.00	0.064	-2.90
303	3.3	0.031	-3.41

Appendix-12: ln (1-RCY) values at different times and temperatures for calculation of rate constants (k') graphically for 3-methoxy-6-methyl-2-nitropyridine
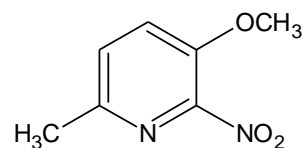
Time (min)	ln (1-RCY)			
	140°C	**120°C**	**60°C**	**30°C**
1	-0.844	-0.1555	-0.0513	-0.016
3	-1.14	-0.654	-0.128	-0.0233
7	-1.561	-1.537	-0.357	-0.058
10	-1.61	-1.561	-0.462	-0.0726
20	-1.661	-1.61	-0.968	-0.151
30	-1.661	-1.661	-1.204	-0.248

Appendix-13: k' values at different temperatures calculated graphically for plotting against reciprocal of temperature in Arrhenius plot for 3-methoxy-6-methyl-2-nitropyridine

T [K]	$1/T^* \cdot 10^{-3}$	k'	lnk'
413	2.42	0.023	-3.77
393	2.54	0.04	-3.22
333	3.00	0.04	-3.22
303	3.3	0.009	-4.71

Appendix-14: RCY after hydrolysis of intermediates (v, vi) at different temperatures and at different reaction times (n=3)

Nr.	Acid/ Reagent	Temp (°C)	%RCY±SD (TLC)										%RCY±SD (HPLC)
			1 min		3 min		5 min		7 min		10 min		10 min
			P	I	P	I	P	I	P	I	P	I	
(v)	32% HCl	150°C	50±1	34±0.7	56±1.5	0	66±2	0	67±0.5	0	69±0.9	0	79±1.6
		120°C	46±1.1	50±1.3	57±0.3	0	61±1	0	65±1.7	0	68±0.4	0	73±1
		60°C	29±1.4	59±0.5	33±0.9	40±1	37±1.8	27±1.6	40±1.3	15±0.7	47±0.5	5±0.2	49.5±1.2
		RT	25±1	65±0.8	29±1.5	59±0.6	34±0.7	50±1	36±1.1	49±1	39±1	45±1	41±0.7
	70% TFA	150°C	39±1.3	40±1	41±1.7	17±1.1	43±1.5	9±0.7	44.2±0.5	0	46±1.6	0	50±1.5
		120°C	30±0.5	65±1	35±1.3	51±1	39±1.5	45±1	41±0.3	37±1.3	43±1.4	5±0.4	48±1
		60°C	17±0.7	75±1.6	19±0.6	71±0.9	21±1.6	69±1	26±1.4	67±1	29±1.9	55±1.3	31±1.2
		RT	9±1	80±1.1	10±0.1	79±1	14±1.1	75±1	17±1	71±1.1	21±0.5	70±1	23±0.2
	1,4-CHD	70°C	1±0.2	82±0.6	3±0.5	77±1.1	31±1	28±0.5	45±0.7	22±0.3	57±1	13±0.9	61±1.4
	HCOONH$_4$	70°C	60±1	5±0.4	63±1.2	3±0.8	65±1.1	1.7±1	67±1.4	0	75±1.3	0	79±1.5
(vi)	32% HCl	150°C	59±0.4	3±1	61±1.2	0	63±0.5	0	75±1.4	0	77±1.8	0	82±1.1
		120°C	50±1.1	7±1.5	53±1	0	57±1	0	69±0.9	0	72±0.7	0	75±1.3
		60°C	38±1.3	9.5±1	41±1.7	4±0.4	47±0.5	0	51±0.8	0	55±0.5	0	58±1.2
		RT	27±1	15±1.3	29±0.4	8.3±1	31±0.7	0	33±1.4	0	35±0.1	0	39±0.5
	70% TFA	150°C	51±0.5	46±0.7	54±0.8	24±1.6	66±1.3	0	77.7±0.1	0	78±0.1	0	80±0.3
		120°C	39±0.3	50±1	43±0.7	20±1	49±1.1	0	51±1.7	0	57±0.8	0	63±1.5
		60°C	25±0.7	48±0.6	27±1	18±1.2	31±0.1	0	33±1.3	0	37±1.1	0	41±0.9
		RT	11±0.1	60±1.7	17±1.1	33±1	22±0.5	0	27±0.1	0	29±0.7	0	34±1

Appendix-15: RCY after labelling (n = 2) of hypoxia precursor (e) by using 5 mg of precursor under different sets of experimental conditions

Time (min)	%RCY±SD (TLC)				
	Label Cond.[1]	Label Cond.[2]	Label Cond.[3]	Label Cond.[4]	Label Cond.[5]
1	27.1±1	22.4±0.7	38±0.6	19.7±0.9	1.1±0.5
2	29±0.9	37.1±1.3	42.4±1.5	25.6±0.5	3.7±0.6
3	25.7±0.6	39±1	21.6±1.1	37.2±0.6	5.2±0.8
5	21.4±1.2	21.1±0.5	13.9±1.3	34±1.1	11.6±1
7	16.7±1.5	19.1±0.8	7.4±1.7	30.4±1	19±1.1
10	11.2±1	10.8±1	3.7±1	24.7±1.3	29.3±1.6
15	9.8±1	6±1.3	1.5±0.9	12.1±1.8	33.4±1.7
20	7.2±0.8	3.5±1.4	0.8±0.6	9.3±1	37±1.5

Labelling conditions:

[1] MeCN; 90°C; 3.5mg K_2CO_3; 15mg K222

[2] MeCN; 100°C; 3.5mg K_2CO_3; 15mg K222

[3] DMF; 120°C; 3.5mg K_2CO_3; 15mg K222

[4] MeCN:DMSO (1:1); 120°C; 3.5mg K_2CO_3; 15mg K222

[5] MeCN:2-Methyl-1-butanol (1:9); 100°C; 3.5mg Cs_2CO_3; 15mg K222

Appendix-16: RCY after labelling (n = 3) of hypoxia precursor (e) by using 5 mg of precursor and 1mL of DMSO under different sets of experimental conditions

Time (min)	%RCY±SD (TLC)					
	Label Cond.[1]	Label Cond.[2]	Label Cond.[3]	Label Cond.[4]	Label Cond.[5]	Label Cond.[6]
1	42.3±1.5	20±0.8	15±0.5	63±0.9	5±0.5	29±0.9
2	48.9±1.4	44.5±0.6	30±0.6	79±1.8	9±0.6	38±0.8
3	41.4±1.3	47±1	36±1	81±0.9	14±0.7	56±1.5
5	37.4±0.6	58±1.3	45±1.3	68±1.6	21±0.6	47±1.3
7	22.5±0.8	49±1.1	31±1.5	39±1	27±0.5	23±1.3
10	10.8±0.6	35±1.5	25±1.6	25±1.1	37±1	11±1
15	8.3±0.9	23.1±1.6	17.3±0.9	11±1.2	51±0.9	9±0.6
20	4.2±1	11.9±0.9	13.5±0.7	6±1	21±0.3	4±0.5

Labelling conditions:
[1]120°C; 3.5mg K_2CO_3; 15mg K222
[2]120°C; 1.8mg K_2CO_3; 15mg K222
[3]110°C; 3.5mg K_2CO_3; 15mg K222
[4]140°C; 3mg K_2CO_3; 7mg K222
[5]140°C; 2mg $KHCO_3$; 2mg K222
[6]120°C; 3.5mg K_2CO_3; 10mg K222

Appendix-17: RCY after lhydrolysis (n = 3) of [^{18}F]-labelled hypoxia intermediate (h) under different sets of experimental conditions
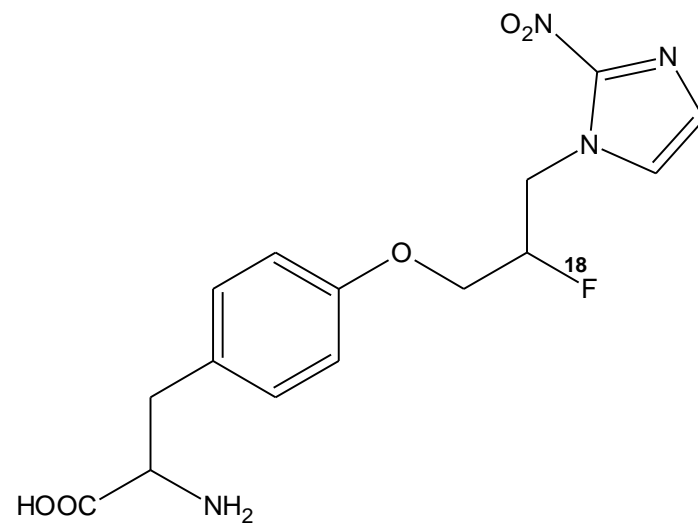
Acid	Temp (°C)	%RCY±SD (HPLC)					
		10 min	15 min	20 min	30 min	60 min	120 min
70% TFA	**90°C**	1±0.6	5±0.8	11±1	20±1	31±1.1	53±0.9
	120°C	29±1	39±1.3	56±1.5	-	-	-
	140°C	5±0.9	16±1.1	36±0.7	-	-	-
32% HCl	**90°C**	1±0.9	3±1	9±1.3	-	-	-
	120°C	4±1	11±0.7	20±0.8	-	-	-

Appendix-18: RCY (n = 3) after coupling of [¹⁸F]FPy-TFP with DUPA-Pep at different temperatures and different times.
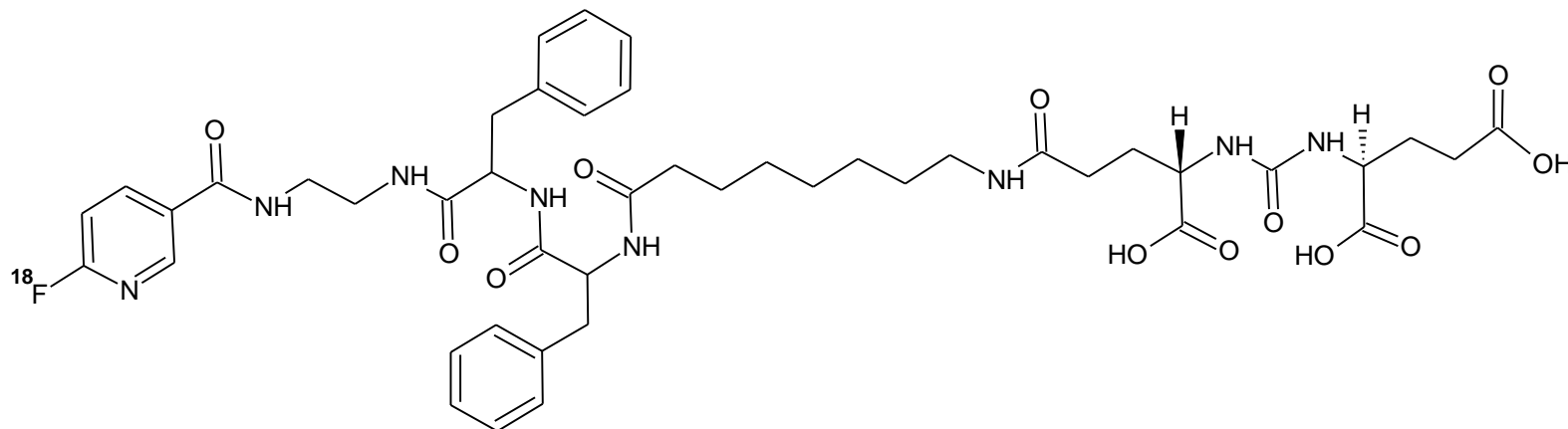
Temp	%RCY±SD (HPLC)				
(°C)	3 min	7 min	10 min	20 min	30 min
40°C	9±0.1	20±0.5	44±0.3	81±1	88±1.1
50°C	25±0.5	70±0.6	92±1.1	86±1.2	82±1
60°C	26±0.3	75±0.6	95±1.2	58±1	40±0.9

Lebenslauf

Noeen Malik

24. Februar. 1982	Geboren in Sargodha, Punjab, Pakistan

Akademisch

1996-1998	Grundschule in Pakistan
1998-2000	Abitur in Pakistan
2000-2002	B.Sc Studium an der Punjab University, Lahore, Pakistan
2002-2004	M.Sc. in Organische Chemie an der University of Agriculture, Faisalabad, Pakistan
2003-2005	B.Ed. Studium an der Allama Iqbal Open University, Islamabad, Pakistan
2004-2006	M.Phil. in Organische Chemie mit dem Thema *"Study of biokinetics of Pyrazinamide in blood after oral Administration of test tablet in Male humanbeings"* an der University of Agriculture, Faisalabad, Pakistan
2007-2008	Training Projekt auf *"Syntheses of [^{18}F]-labelled model compounds for aromatic amino acids via S_NAr"* and *"Synthesis of [^{18}F]DOPA via isotopic exchange by S_NAr"* in der Radiopharmazie, Universitätsklinikum, Eberhard-Karls Universität, Tübingen
April 2008-May 2011	Ph.D-Dissertation in der Radiopharmazie in Tübingen und Ulm mit dem Thema *"Radiofluorinations in Homo- and Heteroaromatic Systems with Application in Two New Types of Metabolic PET-Tracers ([^{18}F]FNT, [^{18}F]FPy-DUPA-Pep "*.
Sept-2011	Mündliche-Prüfung von Ph.D